The role of prohibitin and miR-27a in prostate cancer progression and therapy response

A Thesis Submitted in Accordance with the Requirements of Imperial College London for the Degree of Doctor of Philosophy

Ailsa Sita-Lumsden

Supervisor: Professor Charlotte Bevan
Co-Supervisor: Dr Alwyn Dart
Co-Supervisor: Professor Jonathan Waxman

Department of Oncology,
Division of Surgery and Cancer

Date of Submission July 2016

Statement of Originality

Unless otherwise stated in the text, this thesis is the result of my own work. Some of the work described In this theiss has been previously published: Fletcher C.E., Dart D. A., Sita-Lumsden A., Cheung H., Rennie P. S., Bevan C. L. (2012). *Androgen–regulated processing of the oncomir miR-27a, which targets Prohibitin in prostate cancer.* Hum. Mol. Genet. **21**(14): 3112-3127.

Copyright Declaration

Acknowledgements

I would like to thank Cancer Research UK for the financial support of this research, through a studentship from the Imperial Cancer Research UK Centre.

I would like to express my sincere gratitude to my supervisor Professor Charlotte Bevan for the continuous support of my Ph.D study and related research, for her immense patience, motivation and knowledge. I can't imagine having a better advisor and mentor. I consider myself incredibly lucky to have had this opportunity to learn from her and my colleagues in the androgen signalling lab.

In addition I would like to thank my co-supervisors Professor Jonathan Waxman and Dr Alwyn Dart for their insightful comments, encouragement and support.

Besides my supervisors, I would like to thank the rest of my colleagues in the androgen signalling lab. Their good humour and immense knowledge has made the last five years a pleasure.

I would also like to thank my family, without whom I would not have been able to complete this work. My Father for pushing me to pursue a higher degree and being my inspiration. My Mother for all her love, encouragement and understanding. Both my parents and my parents-in-law for the many hours of babysitting that freed me up to finish my work. My amazing husband who has supported me emotionally through this work. Last but not least, Arthur and Stella, my two little rays of sunshine, they extended my Ph.D experience, but they taught me the importance of time management and efficiency, and above all, they make every day a joy.

Table of Contents

List of Figures

List of Tables

Abreviations

AR	Androgen receptor	MAR	Membrane androgen receptors
ACTH	Adrenocorticotropic hormone	MDR1	Multi-Drug Resistance 1
Ago2	Argonaute-2	Mib	Mibolerone
AREs	Androgen Response Element	miRNA	microRNA
ASO	Antisense OligomiR	mtDNA	mitochondrial DNA
ATCC	American Type Culture Collection	PBS	Phosphate-buffered saline
Bic	Bicalutamide	PCA3	Prostate Cancer gene 3
BPH	Benign Prostatic Hypertrophy	PHB	Prohibitin
BSA	Bovine Serum Albumin	PIN	prostatic intraepithelial neoplasia
CRH	Corticotropin-releasing hormone	PSA	Prostate Specific Antigen
CRPC	Castrate Resistant Prostate Cancer	qRT-PCR	Reverse transcription polymerase chain reaction
CYP17	Cytochrome P450 17A1,	REV	Reverse
DHEA	Dehydroepiandrosterone	RISC	RNA-induced silencing complex
DHT	Dihydrotestosterone	RNA	Ribonucleic Acid
DNA	Deoxyribonucleic acid	RNAseq	RNA sequencing
EC	Extraction coefficient	ROS	Reactive oxygen species
EGFR	epidermal growth factor receptor	RPMI	Roswell Park Memorial Institute medium
ER	Oestrogen Receptor	RT	Reverse Transcription
FBS	Fetal Bovine Serum	SCID	Severe combined immunodeficiency
FDR	False Discovery Rate	SDS	sodium dodecyl sulfate
FGF	Fibroblast Growth Factor	SEM	Standard Error of the Mean
FOR	Forward	siRNA	Silencing RNA
GnRH	gondaotrophin releasing hormone	SNP	single nucleotide polymorphism
HCV	Hepatitis C Virus	SRB	sulforhodamine B
HDACs	Histone deacetylases	TCA	Trichloroacetic acid
HDL	High-density lipoprotein	TEMED	Tetramethylethylenediamine
HIF-1alpha	Hypoxia-inducible factor 1-alpha	TET-R	Tetracycline-Controlled Transcriptional Activation
HIPK2	Homeodomain Interacting Protein Kinase 2	tk	thymidine kinase
ICGC	International Cancer Genome Consortium	TRE	Tetracycline Response Elements
IP	IntraPeritoneal	UV	Ultra Violet
LH	Luteinizing hormone	VEGF	Vascular endothelial growth factor
LHRH	luteinizing hormone–releasing hormone	wt	wild type
LNA	Locked Nucleic Acid		

Abstract

Introduction: Prostate cancer is the most commonly diagnosed male cancer in the Western world, with more than 40,000 cases in the UK diagnosed annually. The androgen receptor (AR) is required for the survival and proliferation of the prostate cancer cell and is key to prostate cancer treatment. The levels of both AR itself and its cofactors are in turn modulated by specific microRNAs, hence manipulating key microRNAs that affect androgen signaling is a potential therapeutic strategy for prostate cancer. One such key microRNA is miR-27a, which has a confirmed oncogenic role in gastric cancer and we previously showed to target the AR corepressor Prohibitin. In addition, circulating microRNAs (miRNAs) have been a source of hope as potential new biomarkers for cancer.

Results: There is evidence that prohibitin is decreased in the more aggressive prostate cancer cell lines and also in metastatic deposits in clinical cases of prostate cancer. Conversely miR-27a is increased in the more aggressive cell lines and in the metastatic deposits in clinical cases of prostate cancer. Treatment of LNCaP cells with an anti-sense oligomiR inhibitor of miR-27a (ASO-27a) resulted in a decrease in miR-27a levels, an increase in prohibitin levels, and a decrease in cell growth. Conversely when LNCaP cells were induced to express high levels of miR-27a (via stable transfection with a doxycycline-inducible miR-27a expression vector) there was a significant increase in growth. These findings, suggestive of tumour-promoting properties of miR-27a, were supported in an *in vi*vo xenograft model. Mice bearing human prostate tumours and treated systemically with ASO-27a had significantly less tumour growth when compared to those treated with control oligomiR. Surprisingly, we did not observe a direct effect on prohibitin levels in the treated tumours. The genes showing significant differential expression following treatment with ASO-27a were compared with published data sets of gene expression at different clinical stages of prostate cancer tissue. Multiple genes of interest were identified, that were both significantly raised following treatment with ASO-27a and expressed at significantly lower levels in cases of metastatic prostate cancer.

In the circulation of men with metastatic prostate cancer I found that miR-27a is generally higher when compared to men with healthy prostates. A targeted panel of

miRs was screened in this context, and a subset consisting of miR-21, miR-10b, miR-126, miR-150, miR-378 and miR-93 could differentiate benign from metastatic disease; it would be interesting to explore this 6 miR signature further as potential diagnostic or predictive biomarker test.

Conclusion: We have shown that using an anti-sense oligomiR to miR-27a reduces prostate cancer growth both *in vitro* and *in vivo*, at least in part via increasing apoptosis, and thus warrants further investigation as a potential future therapy. In addition circulating levels of miRNAs, including miR-27a, may provide clinically useful biomarker information regarding diagnosis, prognosis, or prediction of response to treatment.

Chapter 1 Introduction

1.1 The Prostate Gland

The prostate is a walnut sized gland found between the bladder and the penis and in front of the rectum in men. The urethra runs through the prostate carrying urine from the bladder and then out of the body via the penis. The prostate is an exocrine gland that produces and secretes 30% of the ejaculate fluid that protects and nourishes sperm in semen. During ejaculation the prostate expels this fluid into the urethra and it combines with sperm, carried from the testes by the *vas deferentia*, and fluid secreted by the seminal vesicles to become semen.

The prostate gland can pathologically be divided into three different zones (Figure 1.1A). These zones encircle the urethra; the innermost zone that surrounds the urethra is called the transition zone and this makes up around 10% of the gland. This area of tissue is enlarged in old age, a condition termed benign prostatic hypertrophy (BPH). The central zone surrounds the transition zone and makes up about 20% of the gland. This is where the ejaculatory duct is found. The peripheral zone makes up around 70% of the bulk of the prostate gland and this is the most common zone for prostate cancer to develop.

The prostate develops in the embryo from a protrusion of the urethra, the glandular epithelium develops from endodermic cells and the stroma and smooth muscle from the mesoderm. This development process starts when the leydig cells in the fetal testes begin secreting testosterone.

1.2 The hypothalamic-pituitary-testicular axis and steroidal synthesis

Androgens such as testosterone were first discovered in 1936. The production of testosterone in the embryo is key for male sexual differentiation and the development of the male sexual organs including the prostate. Circulating testosterone levels are low in male children, aside from during embryogenesis, until puberty. At puberty the hypothalamic-pituitary-testicular axis (Figure 1.1B) becomes increasingly active and testosterone production stimulates target organs, including the prostate, to mature to adult size. Testosterone is produced principally in the testes following stimulation of

the steroidal synthesis pathway by leutenising hormone (LH), but also to a lesser extent in the adrenal gland.

Figure 1.1: Anatomy and Physiology of the Hypothalamic-Pituitary-Testicular Axis

(A) The prostate gland is located under the bladder and it has the urethra running through it carrying urine from the bladder to the outside world. The prostate is divided into zones pathologically from the transitional zone that wraps around the urethra, then the central zone and finally the peripheral zone on the outside. (B) The prostate develops in response to testosterone signalling that arises from the testes. The testes produce testosterone after stimulation by leuteinising hormone (LH) produced in the pituitary gland. High serum levels of testosterone serve to negatively regulate this hormonal signal by decreasing the production of LH and gonadotrophin releasing hormone (GnRH) from the hypothalamus.

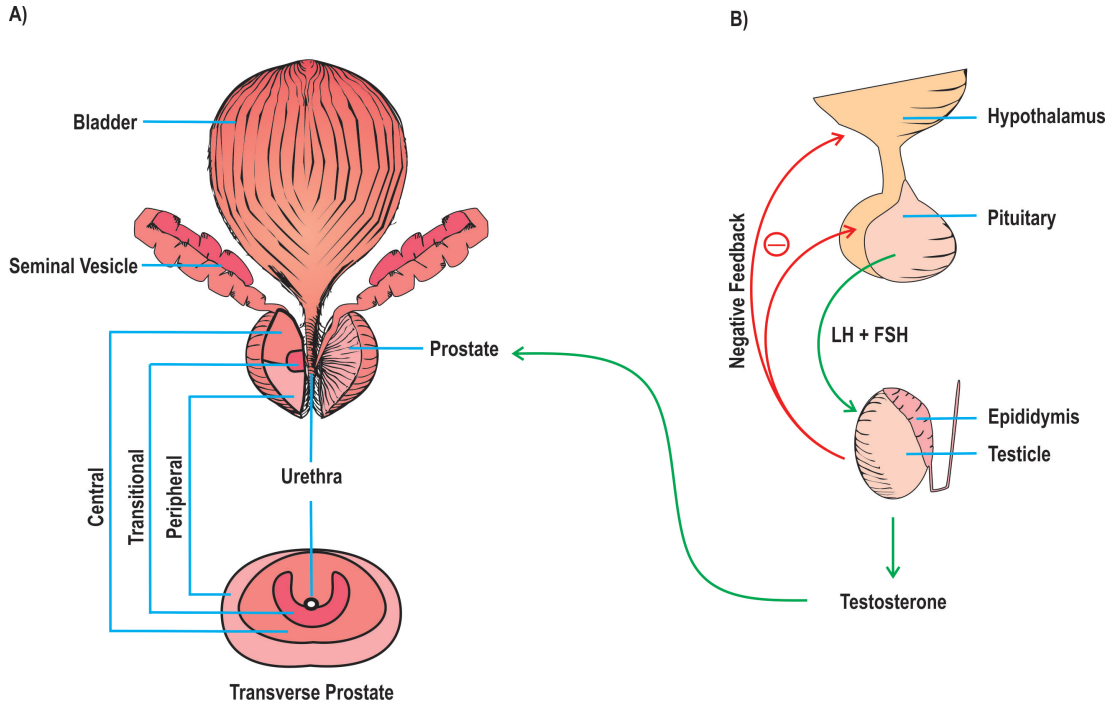

1.3 Prostate Cancer

Prostate cancer is the most commonly diagnosed male cancer in the Western world, with over 40,000 cases in the UK diagnosed each year leading to a substantial public health burden (CRUK 2012). Prostate cancer largely affects older men, with a median age at diagnosis of 72 years. Age is an important risk factor for prostate cancer as it is rarely seen in men under 40 years of age but then the risk rapidly increases with every decade of life from 1 in 298 for men of 49 years and younger to 1 in 9 for men aged 70 and over. A man's overall lifetime risk of developing prostate cancer is one in seven, according to data taken from the United States National Cancer Institute Surveillance Epidemiology and End results (SEER) database

(Howlader N 2014). Prostate cancer exhibits tremendous differences in incidence among worldwide populations. The lowest incidence is found in men in Asia, with northern European men having a generally high incidence rate but it is African American men, with a 60% higher incidence then Caucasian American men, who have the highest incidence in the world (McIntosh 1997). These differences are likely due to the interplay between genetic, social and environmental factors. Familial clustering of prostate cancer has been reported frequently and from 5%-10% of prostate cancer cases are linked to inheritance of high-risk susceptibility genes. The most well known of these genes is the BRCA gene, mutation in which confers an increased lifetime risk of prostate cancer to 15-25%.

Almost all prostate cancers are dependent on androgens at the initial diagnosis (Heinlein and Chang 2004). This is unsurprising as within the normal prostate gland, tissue growth and differentiation are androgen dependent. The androgen-signalling pathway is pivotal both to initial prostate cancer growth and to disease progression, and androgen responses are mediated via the AR, a ligand-activated transcription factor (Shen and Abate-Shen 2010).

1.4 Prostate cancer diagnosis and treatment

Prostate cancer and other prostate diseases often present with similar symptoms. The symptoms largely result from constriction of the urethra causing urinary outflow obstruction. The development of symptoms related to outflow is dependent on the location within the gland of the cancer and the extent of the disease. The initial diagnosis of prostate cancer is generally made by the detection of a raised level of Prostate Specific Antigen (PSA) in the blood as well as a digital rectal examination that may detect an enlarged or abnormal prostate when the patient is asymptomatic. PSA is a protein, also known as kallikrein-3, made and secreted by normal cells of the prostate as well as cancerous cells. Its function is to liquefy semen and help the propagation of sperm and to aid their entrance into the womb by dissolving cervical mucus. It is normal for men to have a low level of circulating PSA in their blood, however, a rising or especially high level of PSA can be indicative of a prostate malignancy.

If there is a suspicion of prostate cancer following these tests, then a patient is sent to see a Urologist for a trans rectal ultrasound-guided prostate needle biopsy, which takes 10-12 small prostate samples, for a definitive tissue diagnosis. The disease is then evaluated on a microscopic level by a histopathologist to determine the Gleason grade, which is indicative of how active the cancer, is and each sample is given a score between 1 and 5. Grade 1 represents normal looking prostate tissue, meaning that the cancer is well differentiated, and is currently very rarely reported. Grade 5, conversely, has few recognizable glands or features of normal prostate tissue and is thus is representative of anaplastic neoplasia. The grades of the two most common patterns found in the patient samples are then combined to give an overall Gleason score, which can range from 2-10, with 2 representing the most well-differentiated tumors and 10 the least-differentiated tumors. Gleason scores have often been categorized into groups that show similar biologic behavior: low-grade (well-differentiated), intermediate-grade, moderate to poorly differentiated or high-grade.

An investigation of the Johns Hopkins Radical Prostatectomy Database (1982-2011) led to the proposed reporting of Gleason grades and prognostic grade groups as: Gleason score ≤ 6 (prognostic grade group I); Gleason score 3+4=7 (prognostic grade group II); Gleason score 4+3=7 (prognostic grade group III); Gleason score 4+4=8 (prognostic grade group IV); Gleason scores 9-10 (prognostic grade group V) (Pierorazio, Walsh et al. 2013). Prostate cancers with a Gleason score ≤ 6 usually have rather good prognoses with a relapse rate at 5 years post radical prostatectomy of only 5%. This can be compared to a relapse rate of 76% for the Gleason 9-10 cancers, the prognostic group V (Grossfeld, Latini et al. 2002).

Depending on the PSA and the Gleason score patients may then be evaluated for extent of spread of disease at diagnosis with a combination of bone scans, CT and MRI. Information from these imaging modalities will allow the physicians to determine if the cancer has spread outside of the prostate and in turn outside of the pelvis. Based on all of this information the disease is staged I-IV and this determines the treatment algorithm the patient will follow. Patients diagnosed with the disease at stages I-III receive treatment that includes any of the following; surveillance,

prostatectomy, hormonal therapies and radiotherapy the choice of which is determined by the individual and the characteristics of their cancer.

The mainstay of treatment for patients whose disease at diagnosis is too advanced or spread to be treated radically is to control the growth of the cancer by lowering circulating androgens, so called 'chemical castration'. A summary of androgen production and therapeutic manipulation can be seen in Figure 1.2. For the majority of patients this is achieved by reducing testosterone levels through interference with its normal regulatory mechanism, via an endocrine pituitary feedback loop, using luteinising hormone-releasing hormone (LHRH) agonists or LHRH antagonists. Anti-androgens such as Flutamide (Shering-Plough), Enzalutamide (Xantandi; Medivation/Astellas) and Bicalutamide (AstraZeneca) may also be used to competitively inhibit the binding of the androgens to the AR; these do not activate transcription so are used to block the initial flare of testosterone at initiation of LHRH agonist therapy or later when the LHRH agonists are failing to control the prostate cancer growth (Perlmutter and Lepor 2007). As the effects of single agent treatment tend to be less significant than LHRH agonist treatment they are rarely used on their own.

Hormonal treatment is initially effective in over 80% of prostate cancers (Khorasanizadeh and Rastinejad 2001, Heinlein and Chang 2004). The exact mechanisms of anti-androgen action are not completely understood, but they appear to function at least in part via promoting the recruitment of corepressors to the regulatory regions of target genes, for example the corepressors NCoR and SMRT were shown by Shang *et al.* to be recruited to the promoter region of the *PSA* gene following treatment with the anti-androgen Bicalutamide (Shang, Myers et al. 2002).

Figure 1.2: The production of androgens in the human body, their stimulation of Prostate cancer and the ability to manipulate them with therapeutics.

The hypothalamus produces gonadotrophin releasing hormone (GnRH) and cortisol releasing hormone (CRH) that act upon the anterior pituitary gland to stimulate the release of adrenocorticotropic hormone (ACTH). The ACTH stimulates the adrenal production of dehydroepiandrosterone (DHEA) which is converted to testosterone and dihydrotestosterone by cytochrome P450 17 (CYP17) in the Prostate. Testosterone is also produced by the testes and in the adrenals from cholesterol. Modified with permission from the original published by Yin et al. (2013) CYP17 inhibitors—abiraterone, C17,20-lyase inhibitors and multi-targeting agents. *Nat. Rev. Urol (Yin and Hu 2014).*

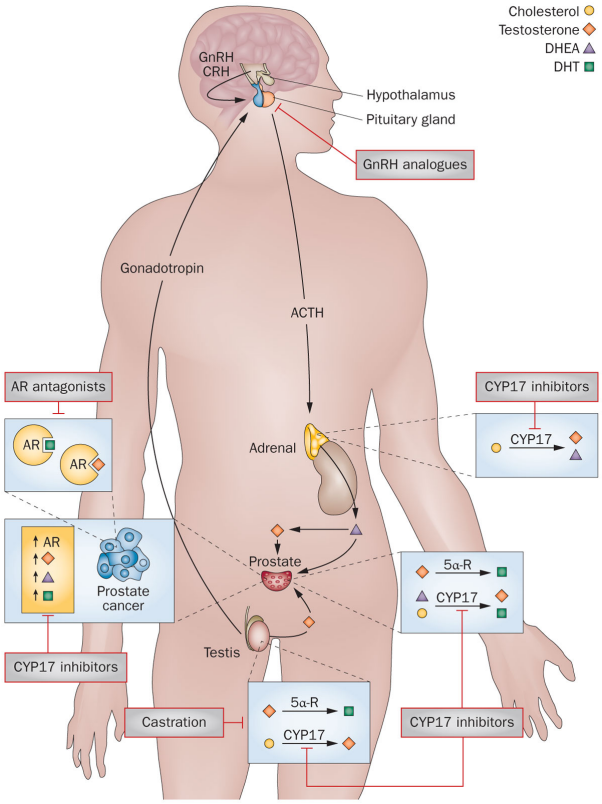

Low levels of other circulating androgens, such as androstenedione and Dehydroepiandrosterone (DHEA) are still present in circulation and are metabolised peripherally to testosterone and 5-α-dihydrotestosterone (DHT). Therefore, androgen synthesis inhibitors have been developed, which work by inhibiting testosterone production from cholesterol by blocking the enzyme CYP17, which is found in testicular, adrenal and prostate tumour tissue. One such androgen synthesis inhibitor, Abiraterone acetate (Zytiga; Janssen), has recently been approved for use in metastatic castration-resistant Prostate cancer.

The natural history of tumour response to anti-androgens and LHRH agonists is that

they will inevitably fail. PSA progression is seen after a median of 13 months and the patients will relapse with symptomatic disease one year later, at which point the prognosis is poor. One of the proposed reasons for failure is that the AR develops ligand binding site mutations that allow it to be activated by noncanonical ligands (Gottlieb, Trifiro et al. 1997), allowing antagonists such as Bicalutamide and Flutamide to act as agonists of the AR. This has been documented in the clinical setting with as many as 30% of patients achieving a 50% reduction in PSA upon withdrawal of anti-androgen (Oh 2002). Another proposed mechanism for escape from hormonal control is the loss or reduction of corepressors, such as prohibitin, needed for functional activity of the anti-androgens (see section 1.6). The loss of prohibitin can drive castrate resistant prostate cancer in a mouse model as shown by Dart *et a,* 2009 (Dart, Spencer-Dene et al. 2009).

The historical standard treatment for castration-resistant Prostate cancer (CRPC) is Docetaxel, an anti-mitotic chemotherapy agent that compared with androgen deprivation therapy (ADT) alone significantly improved overall survival by around 10–15 months in two recent randomized control trials (James, Sydes et al. 2015, Sweeney, Chen et al. 2015). In recent years, several new products have come to the market; Abiraterone and Enzalutamide, approved in 2011 and 2012 respectively, both target AR signaling (Scher, Fizazi et al. 2012, Ryan, Smith et al. 2015). Enzalutamide functions by preventing translocation of the AR from cytoplasm to the nucleus. In 2011, a cancer vaccine, Sipuleucel-T (Provenge; Dendreon) was approved for first line usage in minimally symptomatic CRPC. This agent acts by stimulating a generalized immune response against the tumour (Kantoff, Higano et al. 2010). In 2013, the radioactive calcium mimetic radium-223 dichloride (Xofigo; Bayer) was approved, this specifically targets bone metastases (Hoskin, Sartor et al. 2014). Another medication specifically targeting bone metastases is the receptor activator NF-kB (RANK) ligand inhibitor, Denosumab (Xgeva; Amgen) (Smith, Saad et al. 2012). Lastly, a new taxane chemotherapy, Cabazitaxel (Jevtana; Sanofi), has also been added to the oncologist's therapeutic arsenal. Despite all these recent improvements there is still an unmet need for products that provide a greater survival benefit than current treatment regimens (de Bono, Oudard et al. 2010, Smith, Saad et al. 2012).

In theory prostate cancer can spread to any part of the body but most cases follow a specific pattern of spread, predominantly to the bones, lymph nodes but also to the lungs, the liver and rarely the brain. Bone metastasis contributes significantly to the morbidity associated with advanced prostate cancer, leading to pain, pathological fractures, metastatic spinal cord compression that can if untreated lead to paralysis as well as hypercalcaemia and the haematological effects of bone marrow infiltration such as anaemia and thrombocytopenia. Unlike other epithelial tumours, metastatic prostate cancer is characterized by osteoblastic rather than osteolytic lesions but both types of metastasis may be present (Krutzfeldt, Rajewsky et al. 2005).

1.5 The three major clinical challenges in Prostate cancer

1.5.1 Distinguishing indolent from aggressive disease

As will be discussed later, there has been a dramatic increase in the number of men diagnosed with prostate cancer in the last 20 years since the introduction of PSA testing. It is argued whether or not PSA population screening testing saves lives. In a recent Cochrane meta-analysis of over 350,000 men in screening trials analysis no benfit was found to screening It is also argued that PSA screening leads to over diagnosis and overtreatment of indolent prostate cancer, as PSA is unable to differentiate between latent and aggressive prostate tumours. Information on prognosis for an individual faced with making a decision as to whether or not to proceed with active treatment, is limited to disease stage and Gleason score It can be seen that there is, therefore, a great need for new biomarkers to differentiate tumours of an aggressive nature and mark them for a more interventional treatment algorithm and in turn mark the more indolent ones for minimal treatment.

1.5.2 Tropism of bone metastasis

Prostate cancer has a propensity to metastasise to the bone which causes marked morbidity and mortality. It is still not well understood why prostate cancer displays such tropism or why it forms such characteristic osteoblastic lesions. Trying to understand the molecular changes underlying these features is a major research challenge that is made particularly difficult by the challenges of acquiring metastatic human bone tissue and by the lack of robust animal models that reliably generate bone metastasis at an appreciable frequency.

1.5.3 The treatment of castrate resistant Prostate cancer

The third major clinical challenge in prostate cancer is finding new targets for treatment of CRPC. As already discussed men with advanced prostate cancer inevitably have a recurrence of their prostate cancer after the initial androgen depletion therapy. Although there has been a recent surge in new treatments approved for CRPC this remains an area that could be significantly improved by basic research.

1.6 The development of Prostate cancer and the relevant genetic changes

It has been suggested that prostatic intraepithelial neoplasia (PIN) is a precursor to prostate cancer (Bostwick, Montironi et al. 2000). PIN is characterized histologically by luminal hyperplasia, enlarged and atypical nuclei and a reduction but not absence of basal cells. Prostate cancer also has a luminal phenotype but on staining for p63 and cytokeratin 5/14 is characterized by a complete absence of basal cells (Nana-Sinkam and Croce 2011).

Greater than 95% of cases of prostate cancer are classified as adenocarcinoma and the remaining 5% of prostate cancer are made up of mucinous, signet ring and neuroendocrine tumours, of which neuroendocrine is the most clinically significant. This lack of distinguishable histological subtypes that differ in prognosis and treatment response is unusual for epithelial cancers. Breast cancer by comparison is subdivided by histology into distinct groups that require different treatments and have differing prognoses. Significant progress has been made in recent years in establishing the genomic and epigenetic changes associated with prostate cancer progression using array-base technology and a next generation sequencing approach. What is clear is that the molecular complexity of the disease is high with high levels of intra and inter-tumoural heterogeneity.

Primary prostate cancer is multifocal containing multiple independent histologic foci of cancer that are genetically distinct (Hyun, Jeong et al. 2003, Ren, Wang et al. 2010). In contrast metastatic prostate cancer is regarded as monoclonal on molecular analysis with phenotypically distinct metastases showing significant clonal similarity (Dijkstra, Hamid et al. 2012). In addition, although prostate cancer is largely a

disease of older men, studies of prostate specimens from a younger cohort of men (<40 years old) have found foci of prostate cancer (Hsiao, Wong et al. 2008). These findings indicate that there is a significant chain of molecular events that give rise to the development of metastatic and clinically relevant prostate cancer. However, it should be noted that there is little clinical evidence that PIN develops into invasive cancer. A summary diagram of the proposed chain of molecular events can be seen in Figure 3.

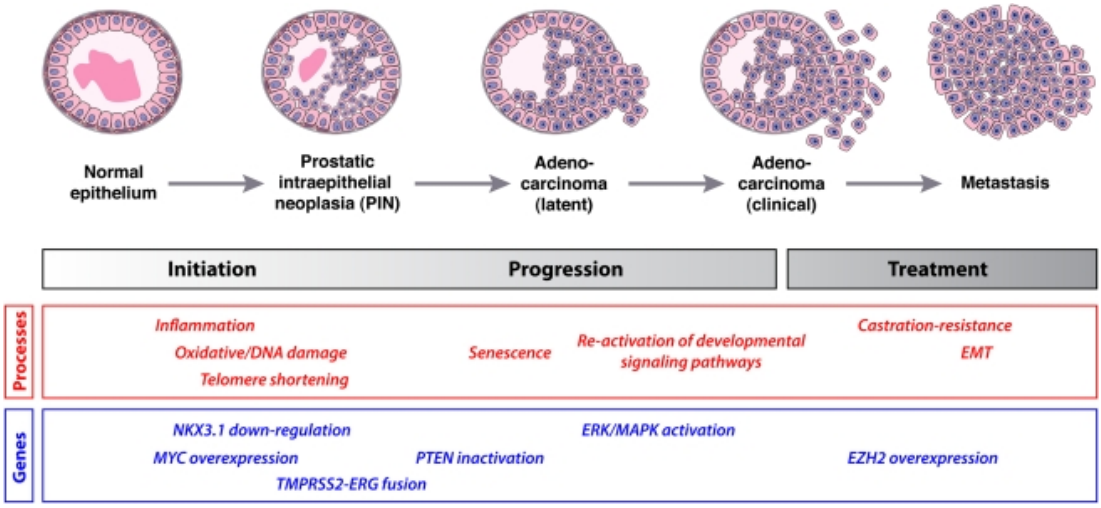

Figure 1.3: The pathway of Prostate cancer progression.

The genes highlighted in blue are likely to be significant at each stage. Adapted from Abate-Shen and Shen 2010 with permission (Shen and Abate-Shen 2010).

Regardless whether this model of progression, is accepted there are several molecular events that are now known to play a key role in the initiation and progression of prostate cancer. One such critical event found in 85% of PIN and prostate cancer is the down-regulation of the homeobox gene NKX3.1 (Li, Mertens-Talcott et al. 2010). Mouse models have shown that NKX3.1 is a critical regulator of prostate epithelial differentiation (Zhang, Liu et al. 2011) (Tardif, Hum et al. 2009) and stem cell function (Chandra, Heinze et al. 2007) and the evidence demonstrates a reduction, but not loss, of NKX3.1 expression throughout prostate cancer progression (Feng, Iwama et al. 2009).

Amplification of the MYC oncogene has been associated with a subset of advanced prostate cancer for some time but it also has a role in cancer initiation as transgenic mice over-expressing human MYC rapidly develop PIN that progresses to invasive prostate cancer (Kelavkar, Harya et al. 2007).

Chromosomal rearrangements that activate transcription factors in prostate, such as the *TMPRSS2-ERG* fusion gene, have also been found with some regularity in prostate cancer, in the case of the *TMPRSS2-ERG* fusion gene this occurs at a frequency of around 50% in localised prostate cancer (Hyun, Jeong et al. 2003) (Lu, Zhang et al. 2004). It is suggested that these gene rearrangements are selected for their ability to promote prostate cancer progression through cooperation with other transforming events such as the loss of *Pten* (Liu, Kirschenbaum et al. 2005).

Pten is a tumour suppresser gene frequently mutated or deleted in a wide range of cancers (Montironi, Cheng et al. 2009). It was found that it was frequently reduced or lost in prostate tumours and that its chromosomal location 10q23 frequently undergoes allelic loss in prostate cancer. *Pten* acts as a tumour suppressor via negative regulation of the cell cycle through the Akt/mTOR signaling pathway. Genetically engineered mouse models have shown that *Pten* deletion acts cooperatively with the inactivation of other key genes, such as those recently discussed, and in addition can increase AR acuity and output (Liu, Kirschenbaum et al. 2005, Bartel 2009, Chen, Chi et al. 2013). In addition, *Pten* reduction predisposes to the emergence of CRPC (O'Hair, Villagran et al. 2003, Paez, Janne et al. 2004). As already noted *Pten* loss results in up regulation of the AKT/mTOR pathway, chiefly through the activation of Akt1 (Paez, Janne et al. 2004). However, this pathway can also be up regulated through activation of PI3K (Raoul, Van Laethem et al. 2009). In addition Erk/MAPK signalling is also frequently activated in prostate cancer together with AKT (Mitry, Lievre et al. 2009, Mok, Wu et al. 2009) signalling leading to promotion of tumour progression and castration resistance in both cell lines and mouse models (Mok, Wu et al. 2009).

EZH2 is associated with aggressive tumours and is frequently up regulated in advanced prostate cancer. Finally *EZH2* encodes a histone lysine methyltransferase, among the targets of which is *NKX3.1* (Di Lorenzo, Tortora et al. 2002) as well as

(Italiano, Ortholan et al. 2009) and *DAB21P (Gilbert, Sanda et al. 2014)* both of which are associated with metastatic ability.

There are two models proposed to explain the development of CRPC. The traditional "adaptation" model proposes that previously androgen dependent cells undergo genetic and epigenetic changes during the conditions of androgen depletion. The alternative "clonal selection" model suggests CRPC emerges as a reflection of the proliferation of a population of castrate resistant cells within an otherwise androgen dependent population.

1.7 The role of Androgen Signalling

Progression to androgen insensitivity is frequently signalled by a rise in serum levels of PSA whilst under endocrine treatment (referred to as biochemical recurrence, BCR) and definitively confirmed by progression to metastatic disease. However, despite appearing 'insensitive' to normal therapy, the AR still plays a pivotal role in tumour growth and in many cases signalling pathways develop that circumvent the need for high circulating levels of androgens. CRPC tumours express AR as well as AR target genes such as *PSA* indicating the pathway remains intact. It appears that androgen signalling switches from a paracrine mechanism reliant on the stroma in androgen dependent prostate cancer to an autocrine mechanism in CRPC for example with the androgen signalling coming from the adrenal glands (Eisenberg, Karnes et al. 2013). There are seven proposed mechanisms identified that can explain progression to apparent androgen independence, five of which are dependent on the AR (Schroder 2008). These mechanisms (outlined in Table 1-1) are chiefly pre-existing clonal populations of androgen insensitive stem cells, the amplification of oncogenic pathways promoting survival, ligand-independent AR activation, AR mutation, increasing ligand responsiveness and receptor amplification (Brinkmann and Trapman 2000, Schroder 2008). One part of this complex interaction of mechanisms is the role of repressive protein complexes, or co-repressors of the AR. Down regulation of co-repressors of the androgen receptor may lead to hypersensitivity of the androgen receptor to low levels of androgens. Corepressors also play a role in the mechanism of action of antiandrogens and thus their loss may be involved in the development of resistance to such therapies.

Table 1-1 Mechanisms of progression of Prostate cancer to androgen insensitivity

Cause of androgen insensitivity	AR dependent change	Examples of mechanisms
1. Genetic change in Prostate cancer cells	No	Malignant epithelial stem cells
2. Bypassing the AR	No	Parallel survival pathways (e.g. inhibition of apoptosis via up-regulating bcl)
3. Ligand-independent AR activation	Yes	Growth factors function as ligands (e.g. IGF-1)
4. AR hypersensitivity	Yes	Modification of co-repressors
5. Change of AR specificity by mutations	Yes	Stimulation by non-androgens (e.g. flutamide)
6. Gene fusions	Yes	Between androgen dependent promoters and oncogenes (e.g. TMPRSS2 and ERG)
7. Androgen synthesis in Prostate cancer tissue	Yes	Increase in androgen synthesis enzyme genes

1.8 Androgen Receptor regulation and the role of Corepressors

The AR is a nuclear receptor activated by binding androgenic hormones in the cytoplasm. Activated AR translocates to the nucleus, where it binds as a homodimer to specific DNA elements in promotor or enhancer regions called androgen response elements (AREs) and functions as a transcription factor (Shen and Abate-Shen 2010). AR recruits regulatory protein complexes to the promoters of these genes. The AR target genes include those involved in cell proliferation e.g. cyclin D1, and differentiated function e.g. members of the kallikrein family of serine proteases such as *PSA* (Khorasanizadeh and Rastinejad 2001). The main circulating androgen in males is testosterone, which is predominantly produced by the testes with a smaller fraction being produced indirectly by the adrenal gland. Testosterone is converted to

DHT by the nuclear membrane enzyme 5-alpha-reductase in several target tissues including prostate. Testosterone and DHT are both hydrophobic ligands that interact directly with the cytoplasmic AR; DHT is the most potent binding agonist and is the main androgen responsible for Prostate growth (Heinlein and Chang 2004). Once the AR is bound to the ARE, a range of coregulators are recruited. These molecules are required for efficient function of nuclear receptors and either repress or induce transcription of hormone responsive genes. Coactivators, such as SRC1, p300, CBP and pCAF, induce functional activity of the receptor by re-arranging nucleosomes, by acetylating histones, to increase accessibility, themselves or by recruiting histone acetylases, allowing transcription factors to bind promotor regions of target genes (McKenna, Lanz et al. 1999). They can also initiate transcription by interacting directly with components of the pre-initiation complex or by acting as bridging molecules for the steroid receptor and the pre-initiation complex. Corepressors such as NCoR and SMRT, conversely, suppress ligand-independent nuclear receptor-mediated transcription by compacting and condensing the chromatin in a tight structure making it inaccessible to transcription factors and inhibiting gene expression; repressors may recruit histone deacetylases (HDACs), a class of enzymes that remove acetyl groups from an ε-N-acetyl lysine amino acid on a histone, thus converting transcriptionally active hyperacetylated chromatin to silent hypoacetylated chromatin (McKenna, Lanz et al. 1999, McKenna, Xu et al. 1999).

1.9 Prohibitin

Prohibitin is a 32kDa evolutionarily conserved, ubiquitously expressed protein named for its anti-proliferative activity in human diploid fibroblast cells and encoded by a gene at chromosome 17q21 (Wang, Nath et al. 1999). The first role to be identified was that of a putative tumour suppressor gene as the prohibitin mRNA was found to inhibit DNA synthesis and cell cycle progression (McClung, King et al. 1992, Lu, Darne et al. 2013). Prohibitin has a vital role in embryonic development with the complete deletion of prohibitin in mice resulting in embryonic lethality (He, Feng et al. 2008).

Prohibitin appears to have several distinct roles in all cell types dependent on its subcellular localization. It was initially identified via microscopy to be localized to

the inner mitochondrial membrane, where it acts a chaperone protein (Coates, Jamieson et al. 1997). Prohibitin has also been observed in the nuclei of breast and Prostate cancer cells (Fusaro, Wang et al. 2002, Robinson, Creed et al. 2010). It has also been found in the vasculature of white adipose tissue (Kolonin, Saha et al. 2004). In addition it is known to associate with the IgM receptor of lymphocytes (Terashima, Kim et al. 1994) and with lipid rafts in cell plasma membranes (Mishra, Moulik et al. 2007).

The prohibitin family of proteins consists of two members that together form a high molecular weight complex in mitochondria. The second member, prohibitin2 otherwise known as B-cell-receptor-associated protein 37 (BAP 37) was originally identified by its ability to bind the IgM receptor of B-lymphocytes. BAP 37 is also known as repressor of estrogen activity (REA) as it was identified as a corepressor of the oestrogen receptor (ER) (Delage-Mourroux, Martini et al. 2000). Prohibitin is known to co-localise with BAP 37/REA to the inner mitochondrial membrane where they form a holdase complex and work as a chaperone to prevent degradation of mitochondrial proteins (reviewed in (Nijtmans, Artal et al. 2002)). Both components are needed for formation of this supercomplex, which has been identified in yeast, *C. elegans* and mammals (Artal-Sanz and Tavernarakis 2009). Disruption of either gene leads to complete loss of the other protein, despite being able to detect the mRNA, implying that the proteins individually are unstable in the mitochondria when not coupled in the supercomplex (Rastinejad, Perlmann et al. 1995). Nijtmans *et al.* established the role of the prohibitin supercomplex within the mitochondria; firstly they found that in the absence of the complex there was a decrease in the stability of the mitochondrial subunits indicating that the complex protected the subunits from protease activity. Secondly co-immunisation experiments showed Cox3p interacting with prohibitin, confirming the interaction between the complex and mitochondrial translation products. Thirdly upon increased mitochondrial stress prohibitin mRNA levels were increased 2.5-fold. The authors concluded that the complex functions as a chaperone protein at the inner mitochondrial membrane, protecting the newly-synthesised subunits from protease degradation (Nijtmans, de Jong et al. 2000). However, both prohibitin and BAP 37/REA function individually as monomers

outside of the mitochondria, for example they both have transcriptional roles in the nucleus as described in detail below.

Prohibitin has also been found to be important for structural maintenance of the mitochondria through preservation of nucleoid activity. Kasashima *et al.* showed that mitochondrial DNA (mtDNA), which forms structures with nucleoids to regulate DNA stability, replication and translation, was released into the soluble fraction upon silencing of prohibitin in Hela cells. This implies that prohibitin regulates organization and stability of mitochondrial nucleoids (Kasashima, Sumitani et al. 2008). The mitochondrial form of prohibitin has also been found to be important in maintaining angiogenic potential. Schleicher *et al.* showed that in SCID mice bearing subcutaneous matrigel mixed with FGF and VEGF, prohibitin silencing led to reduced formation of functional blood vessels (Schleicher, Shepherd et al. 2008). It was also shown that prohibitin silencing in HUVEC cells increased the production of reactive oxygen species (ROS) in the mitochondria, leading to cellular senescence (Schleicher, Shepherd et al. 2008).

Prohibitin has been visualized and plays a key role at the cell plasma membrane (Rajalingam, Wunder et al. 2005). In prohibitin deficient cells the adhesion complex proteins cadherin and beta-catenin relocalise to the plasma membrane and stabilize adhesion junctions and therefore reduce cell motility (de la Taille, Irani et al. 2011). In addition it has been shown that prohibitin is required for Ras-induced Raf-MEK-ERK activation in epithelial cells (Rajalingam, Wunder et al. 2005). This has an enhancing role in tumourigenesis, as activation of this pathway initiates signalling via the MAPK cascade, leading to cell growth and enhanced cell survival (Tomlins, Aubin et al. 2011). This tumourigenic role of prohibitin has been further tested in several cancer cell lines (prostate and breast cancer cell lines were not included) and the silencing of prohibitin lead to reduced DNA synthesis, decreased cell proliferation and reduced anchorage-independent growth (Molife, Attard et al. 2010).

However, prohibitin is also located in the nucleus of the cell where it has a role as a cell cycle regulatory protein, binding the transcription factor E2F and regulating transcription of E2F target genes by recruiting the response proteins Rb, HDAC1 and NCoR, thus condensing chromatin and silencing gene activation (Wang, Nath et al.

1999). It has been shown that over expression of the RNA encoded by the prohibitin 3' untranslated region (3'UTR) results in G1/S arrest and inhibition of E2F-mediated apoptosis (Fusaro, Wang et al. 2002).

Thus the roles of prohibitin within the cell are complex and conflicting depending on the subcellular location. It appears that prohibitin at the plasma cell membrane plays a pro-tumourigenic role in conflict to the apparent tumour suppressive activity of nuclear based prohibitin. The various roles of prohibitin are summarised in Figure 1.4 (modified from Mishra *et al*, 2005) (Mishra, Murphy et al. 2005).

Figure 1.4: Proposed subcellular locations and a potential roles of prohibitin

Prohibitin is required at the cell membrane for Ras mediated Raf activation. Mitochondrial prohibitin has a role in stabilization of mitochondrial respiratory enzymes. In the nucleus prohibitin functions as a modulator of transcription via localization with E2F, Rb and p53. Modified from the original published by Mishra *et al. TRENDS in Molecular Medicine* 11, 192-197 (2005) (Mishra, Murphy et al. 2005)

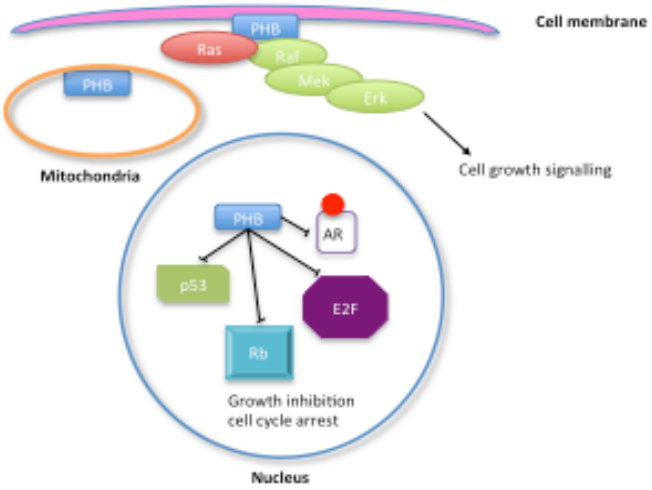

1.10 The role of prohibitin in disease

The observed effect of an increase in reactive oxygen species (ROS) in response to decreased prohibitin levels led to the proposal that prohibitin protects against oxidant-induced damage in ROS-related diseases of the intestine such as ulcerative colitis and Crohn's disease, known collectively as inflammatory bowel disease. Theiss *et al.* showed that levels of prohibitin were decreased in colonic mucosal biopsies of Crohn's disease patients when compared to healthy controls and also in two mouse models of intestinal inflammation (Theiss, Idell et al. 2007). Indeed, using a mouse model of intestinal inflammation, treatment with an adenovirus expressing prohibitin resulted in reduced inflammation severity, indicating that re-expression of prohibitin may represent a therapeutic approach for treatment of inflammatory bowel disease.

Prohibitin has also been proposed to have a complex role in adipogenesis and obesity. It may act initially to promote adipogenesis but then have a different role in mature adipocytes, acting to regulate lipid metabolism and induce apoptosis to prevent unrestrained adipogenesis (Vessal, Mishra et al. 2006, Theiss and Sitaraman 2011, Zhang, Ambati et al. 2011, Liu, Lin et al. 2012).

1.11 The role of prohibitin in cancer

There has been conflicting evidence to date as to whether prohibitin is a tumour suppressor protein, as originally proposed, or in fact the opposite. As already discussed the original definition of prohibitin as a tumour suppressor was called into question when it was discovered that it was actually the 3'UTR that was acting to halt the cell cycle (McGrath, Binge et al. 2013). The levels of prohibitin have been reported to be decreased in glioma (Chumbalkar, Subhashini et al. 2005) and in gastric cancer (Liu, Tang et al. 2009). However, they have also been reported to be increased in a variety of different cancers including gastric (Ryu, Kim et al. 2003, Kang, Zhang et al. 2008), bladder (Wu, Wu et al. 2007), oesophageal (Ren, Wang et al. 2010), thyroid (Franzoni, Dima et al. 2009), cervical (Tsai, Chow et al. 2006), breast (Molife, Attard et al. 2010), ovarian (Dijkstra, Hamid et al. 2012) and even prostate (Salami, Schmidt et al. 2013). Ummanni *et al.* demonstrated prohibitin levels were higher in prostate cancer specimens when compared to BPH samples

(Salami, Schmidt et al. 2013). This study is small with only 23 patients in total and in fact only 4 prostate cancer samples demonstrated dramatically increased prohibitin levels when compared to the BPH. Larger studies need to be conducted and ideally the proportion of mitochondrial, cell membrane and nuclear prohibitin distinguished. Prohibitin, as discussed before, is found in the mitochondria of cells and the increased levels may be explained by the increased number of mitochondria in cancer cells to fuel their relatively increased growth pattern. In addition, the prohibitin promoter has been found to contain a putative binding site for *c-Myc*, which may contribute to the increased levels in some of the cancer types (Coates, Nenutil et al. 2001). There is some evidence to link increased prohibitin levels with chemotherapy resistance in ovarian cancer cells, whilst silencing prohibitin partially restored sensitivity of the resistant cell line to chemotherapy (Osborne, Green et al. 2014) and rendered such cells more sensitive to activation of apoptotic pathways (Dijkstra, Hamid et al. 2012). Ultimately, the functional significance of increased total prohibitin expression in cancer is unclear.

Mutations in prohibitin appear to be relatively rare events. Figure 1.5 shows analysis from cBioportal of data from 9 prostate cancer sequencing projects, mutations were only found at all in 5 of the 9 studies and then at a low rate, 3% and below (de Bono, Oudard et al. 2010, Farmer, Frenk et al. 2010, Gupta 2010, Connock, Hyde et al. 2011, Smith, Saad et al. 2012, Ganeswaran, Sweeney et al. 2014). Interestingly the genetic mutations observed in the clinical samples result in amplification of prohibitin protein. The maximum frequency with which the mutations appeared was 3%. This low mutational rate is corroborated by data from the International Cancer Genome Consortium (ICGC) reporting 132 mutations, in 113 donors from 6,368 participants across 31 projects, see table 1-2.

Figure 1.5: Histogram of mutational frequency of Prohibitin across 5 studies

Data from cBioportal (cBioportal.org) (Fusaro, Dasgupta et al. 2003) . The columns represent the alteration frequency, the red colour indicates that the mutation results in amplification of the gene. The blue circle indicates that all samples were adenocarcinoma of the prostate.

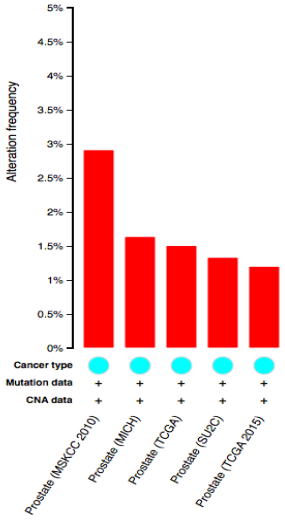

Table 1-2: ICGC summary of somatic mutations in prohibitin

Project - Country	Tumour Type	Number of donors with simple somatic mutations in PROHIBITIN	Number of tested donors
Bladder Urothelial Cancer - TGCA, US	Bladder cancer	1	128
Pediatric Brain Cancer - DE	Pediatric brain tumours	1	248
Liver Cancer - RIKEN, JP	Liver cancer	7	208
Lung Squamous Cell Carcinoma - TCGA, US	Lung cancer	2	178
Liver Cancer - FR	Liver cancer	1	54
Brain Lower Grade Gliona - TCGA, US	Brain cancer	1	268
Gastric Adenocarcinoma - TCGA, US	Gastric cancer	3	289
Oesophageal Adenocarcinoma - UK	Oesophageal cancer	1	16
Renal Cell Cancer - EU/FR	Renal cancer	1	95
Pancreatic Cancer - AU	Pancreatic cancer	5	338
Liver Cancer - NCC, JP	Liver cancer	2	244
Early Onset Prostate Cancer - DE	Prostate cancer	1	11
Kidney Renal Papillary Cell Carcinoma - TCGA, US	Renal cancer	1	146
Pancreatic Cancer - CA	Pancreatic cancer	1	112
Malignant Lymphoma - DE	Malignant lymphoma	1	44
Breast Triple Negative/Lobular Cancer - UK	Breast cancer	1	117
Skin Cutaneous melanoma - TCGA, US	Skin cancer	2	319
Uterine Corpus Endometrial Carcinoma-TCGA, US	Endometrial cancer	10	246
Acute Myeloid Leukemia - KR	Blood cancer	2	78
Ovarian Cancer - AU	Ovarian cancer	3	93
Breast Cancer - TCGA, US	Breast cancer	2	943
Lung Cancer - KR	Lung cancer	1	111
Colon Adenocarcinoma - TCGA, US	Colon cancer	1	216

1.12 Prohibitin in prostate cancer

As discussed prohibitin has been described in the literature as being a pro-proliferative cancer gene or a tumour suppressor depending on the type of tumour examined. In steroid regulated cancers, breast and prostate for example, the evidence to date suggests prohibitin has a tumour suppressor role. As already mentioned the 3'UTR of prohibitin was needed for tumour suppression as opposed to just the prohibitin coding region (McClung, King et al. 1992, Beck, Robinson et al. 2013, McGrath, Binge et al. 2013, Parr, Mills et al. 2013). Furthermore, prohibitin has been shown to interact with the tumour suppressors Rb and p53 in breast and prostate cancer cells and the binding of prohibitin increases p53 transcriptional activity through enhanced DNA binding (Wang, Zhang et al. 2002, Robinson, Creed et al. 2010).

It has been shown in prior work in our lab that prohibitin is important in modulating cell cycle transition in androgen-stimulated prostate cancer cells. Knockdown of prohibitin resulted in an increase in androgen-induced cell cycle entry, whilst overexpression of cDNA (coding region only) had the opposite effect (Gamble, Odontiadis et al. 2004). Prohibitin inhibits AR activity and represses androgen target gene expression thus making it a co-repressor of the AR (Gamble, Chotai et al. 2007); additionally prohibitin is down regulated in prostate cancer cells in response to androgens (Gamble, Odontiadis et al. 2004). Similarly prohibitin has been reported to inhibit ER activity in breast cancer cell lines, mediating the effects of anti-oestrogens (Wang, Zhang et al. 2004, He, Feng et al. 2008). Dai *et al*. have demonstrated that prohibitin is required for recruitment of the repressive chromatin-remodeling complex, containing BRG1, to the anti-androgen bound androgen receptor (Dai, Ngo et al. 2008). There are, therefore, several mechanisms by which prohibitin may exert its repressive effects, which are not mutually exclusive. This leads to the hypothesis that prohibitin is a key protein in prostate cancer therapy response and that a decrease in co-repressor levels is a possible mechanism by which tumours escape from anti-androgen therapy control.

Prohibitin manipulation in human prostate cancer cells revealed that over-expression of prohibitin in human prostate cancer xenografts reduced AR activity and led to

tumour growth arrest (Dart, Spencer-Dene et al. 2009). Conversely, prohibitin knockdown increased AR activity and accelerated tumour growth, in the presence of testosterone. In castrate conditions, prohibitin knockdown maintained tumour size with less shrinkage than normally seen in response to androgen withdrawal. This confirms that reduction of prohibitin promotes both androgen-dependent and androgen-independent tumour growth.

In summary, decreasing prohibitin levels leads to increased AR activity and enhanced growth of the cells as well as potentially decreased efficacy of anti-androgens. The mechanism for prohibitin down regulation by AR is not clear and may involve several mechanisms, including promoter silencing, post-translational modifications or by the binding of AR-induced microRNAs (miRNAs) to their 3'UTR, triggering degradation. Previous work in our lab demonstrated that the optimum siRNA oligo used to silence prohibitin shared considerable sequence homology to miR-27a, a published oncomiR targeting the prohibitin 3'UTR (Gamble, Odontiadis et al. 2004). Prohibitin has a large, highly conserved 3'UTR, with several binding sites for miRNAs, potentially indicating a predominant method of regulation. Prohibitin is a 32kD protein and therefore not ideal for a direct molecular therapy as it may be impossible to administer. However, since prohibitin has been shown to be degraded by miRNA-27a (Liu, Tang et al. 2009), interfering with this miRNA regulation may offer a potential mechanism for increasing prohibitin levels in vivo.

1.13 miRNAs

MiRNAs are short ribonucleic acid (RNA) molecules, on average 22 nucleotides long. The first described miRNA, Lin-4, was identified in the *Caenorhabidtis elegans* (*C. elegans*) nematode (Lee, Feinbaum et al. 1993). First discovered in 1993, they function as post transcriptional regulators that bind to complementary sequences on target messenger RNA (mRNA) (Lee, Feinbaum et al. 1993, Meltzer 2005). This usually results in translational repression or mRNA degradation, see Figure 1.6. MiRNA gene transcription is regulated by transcription factors, responding to multiple stimuli and leading to RNA polymerase II activation or recruitment, producing the primary transcripts (pri-miRNAs) in the nucleus. These are several

kilobases in length with a hairpin structure and are capped and polyadenylated. These pri-miRNAs are then processed by an RNaseIII enzyme called Drosha, to form one or more precursor-miRNAs (pre-miRNA). Pre-miRNAs are comprised of a short double stranded RNA stem with a base-paired 5' end and a protruding 3' end. These are then exported from the nucleus and processed by the cytoplasmic RNase III, Dicer, which cleaves the stem-loop to form the miRNA duplex. This duplex undergoes functional separation into the functional strand, which has complementary binding to its mRNA target and becomes the mature miRNA and the passenger strand, which is subsequently degraded. Mature miRNAs are incorporated into the RNA-induced silencing complex (RISC) and are guided to their mRNA target. The miRNA and RISC complex bind by imperfect base pairing to the 3'UTR of the target mRNA, inducing mRNA degradation or translational repression (miRNA processing reviewed in Winter *et al.* 2009 (Winter, Jung et al. 2009)). The system is complex: genes can be targeted by multiple miRNAs and each miRNA is able to target up to approximately two hundred transcripts either directly or indirectly (Lai 2004). The importance of miRNAs in gene regulation is highlighted by the observation that loss of Dicer, one of the RNase enzymes required for miRNA biogenesis, results in embryonic lethality in mice(Bernstein, Kim et al. 2003).

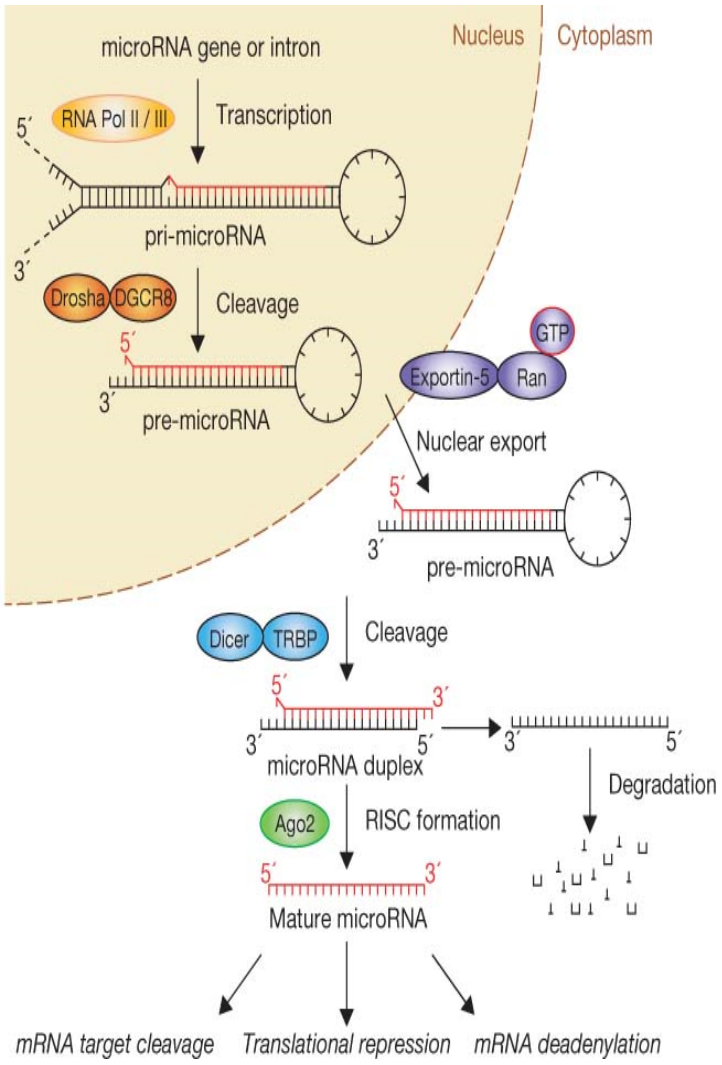

Figure 1.6: miRNA processing The primary miRNA transcript (pri-miRNA) is synthesised by RNA polymerase II or III.

Cleavage occurs in the nucleus by the microprocessor complex Drosha–DGCR8 the pre-miRNA. This is exported from the nucleus by Exportin-5–Ran-GTP where Dicer complexed with TRBP cleaves the pre-miRNA hairpin into its mature form. The functional strand of the miRNA/miRNA* duplex is loaded with Argonaute (Ago2) proteins into the RNA-induced silencing complex (RISC), and guides the RISC to silence target mRNAs through various mechanisms. The passenger strand (miRNA*) may be degraded or in some instances is functional. Reproduced with permission from Winter et al. *Nature Cell Biology* 11, 228 - 234 (2009) (Winter, Jung et al. 2009)

1.14 MiRNAs and cancer

Over 50% of miRNA encoding loci are found within chromosomal regions altered by tumourigenesis. There is a growing body of evidence that miRNAs can be overexpressed or down regulated in the malignant process and may, therefore, function as either oncomiRs or tumour suppressors. Indeed, there are reports of a given miRNA having both these effects, for example miRNA-125b has oncogenic activity in prostate cancer but acts as a tumour suppressor in ovarian and breast cancer (Cortez, Bueso-Ramos et al. 2011). This is likely due to the fact that miRNAs have pleiotrophic effects since each can potentially target hundreds of transcripts; hence the overall function of a given miRNA in a particular context is determined by the relative availability of the target mRNAs. MiRNAs circulate in a highly stable, cell free form and can be detected in both plasma and serum (Mitchell, Parkin et al. 2008). Furthermore tumour cells have been shown to release miRNAs into the circulation (Mitchell, Parkin et al. 2008) and profiles of miRNAs have been found to be altered in the plasma and/or serum of patients with cancer (Chen, Ba et al. 2008, Taylor and Gercel-Taylor 2008). Their discovery potentially explains some of the difference seen between tumour genotype and tumour phenotype, and has further increased our understanding of post-transcriptional regulation. The functional importance of miRNAs in both healthy and diseased tissue has led to the supposition that they have great potential as disease biomarkers and therapeutic targets.

1.15 MiR-27a

MiR-27a is transcribed as part of a cluster of three miRNAs miR-23a, miR-27a, miR-24-2 from chromosome 19p13.1 between 13804510 and 13808884. The individual members of the miR-23a-27a-24-2 cluster have few predicted overlapping targets, however, they show similar patterns of regulation in disease states indicating that their regulation may be by the same signalling cascades (Parekh, Ankerst et al. 2006). These signalling cascades are frequently dysregulated in cancer, examples include Wnt, TGF-β, MAPK and insulin signalling (Parekh, Ankerst et al. 2006). The miR-23a-27a-24-2 cluster has been shown to be androgen regulated, with increasing androgen levels leading to a steady increase in mature miR-27a levels as well as miR-23a and miR-24-2 levels although to differing degrees. This is due to

enhanced cluster transcription and increased primiR processing (Fletcher, Dart et al. 2012).

MiRNA-27a has been termed an oncomiR as it has been found to be up-regulated in a number of tumour types for example gastric adenocarcinoma (Liu, Tang et al. 2009) and pancreatic carcinoma (van den Bergh, Roemeling et al. 2009). It has also been shown to be highly expressed in a number of cancer cell lines across tumour types such as the breast cancer cell line MDA-MB-231 (Schroder 2009) and in SV40 ST-transformed human bronchial epithelial cells (HBERST) (Wang, Li et al. 2011). In this lung cancer cell line model, increased cell growth was observed when miR-27a was over expressed; conversely when miR-27a levels were suppressed there was a decrease in growth (Wang, Li et al. 2011). Inhibition of miR-27a in pancreatic cell lines (PANC-1 and MIA PaCa-2) suppresses growth, colony formation and migration (Thompson, Chi et al. 2006).

Bioinformatically, there are currently 5386 predicted targets for miR-27a based on complimentary seed regions in mRNA 3'UTRs, 1600 have conserved seed regions (Target Scan 7, 2015). A number of these have now been validated to various levels; a summary is given in Table 1-3. Interestingly, a number of key proteins that could confer a tumourigenic advantage, if suppressed, have now been validated as targets for miR-27a. Liu *et al.* demonstrated that miR-27a targets prohibitin, and subsequent work in our lab has demonstrated that overexpression of miR-27a leads to reduced prohibitin protein, RNA and 3'UTR levels, increased expression of AR target genes and increased prostate cancer cell growth (Kroh, Parkin et al. 2010). Mertens-Talcott *et al.* found that inhibiting miR-27a with an antagomiR in MDA-MB-231 cells decreased proliferation and also that it decreased the percentage of cells in S phase and increased the percentage of cells in the G2-M phase (Schroder 2009). They propose that this is through the regulation of Myt-1 and ZBTB10. ZBTB10 is a suppressor of the specificity protein (Sp) family of transcription factors, which have been shown to be enhanced in tumours and lead to increased proliferation (Thompson, Ankerst et al. 2006). Mertens-Talcott *et al.* showed upregulation of ZBTB10 and decreased expression of Sp1, 3, and 4 following the treatment of the breast cancer cell lines with an antagomiR to miR-27a (Alimirah, Chen et al. 2006).

Other targets within the cell cycle machinery have been validated as targets of miR-27a such as FBW7 and p44: miR-27a was shown to destabilize the p44 subunit of the TFIIH complex during the G2-M phase, thereby modulating the transcriptional shutdown observed during this transition (Jansen, Roobol et al. 2009, Portal 2011). Forkhead box protein O1 (FOXO1) also has regulatory functions in cell cycle progression and induction of apoptosis (Pyfferoen, Mestdagh et al. 2014). Treatment with the antagomiR to miR-27a in breast cancer cell lines led to an increase in FOXO1 expression and a decrease in cell number that could be reversed using FOXO1 siRNA (Torjesen and Sandnes 2004). Similar results were found on treatment of an endometrial cancer cell line with the miR-27a antagomiR (Sheedy and O'Neill 2008)

In ovarian cancer, miR-27a expression has been associated with chemotherapy resistance. Li *et al.* showed that levels of miR-27a are higher in the paclitaxel resistant cell line A2780/Taxol compared to the parental A2870 cell line as well as in multidrug resistant cell lines A2780DX5 and KB-V1 (Sato, Saito et al. 1992, Isakoff, Sansam et al. 2005). In addition they showed that inhibition of miR-27a in A2780/Taxol cells leads to paclitaxel induced apoptosis(Isakoff, Sansam et al. 2005). A potential mechanism is via the multi-drug resistance 1 gene (MDR1) that is involved in drug efflux in cells. MiR-27a is known to target homeodomain-interacting protein kinase 2 (HIPK2) - this leads to the derepression of hypoxia-inducible factor 1α (HIF-1α) and the induction of MDR1 (Subramanian, Tamayo et al. 2005). In oesophageal cancer cells a decrease in miR-27a levels increases sensitivity to chemotherapy agents, Vincristine, Adriamycin, 5-Fluorouracil and Cisplatin with increased apoptosis and decreased levels of MDR1 (Subramanian, Opipari et al. 2005). Similar findings were made by Zhao *et al.* in gastric cells (MKN45) (Ray, Mootha et al. 2003) .

Table 1-3 miR-27a targets include a panel of proteins with functions that provide an oncogenic advantage

Target	Cellular Role	Reporter Assay	Western	qPCR	Microarray	Reference

PROHIBITIN prohibitin	Mitochondrial chaperone AR corepressor Transcription factor	√	√	√		Liu *et al*, 2009 (Liu, Tang et al. 2009) Schaar *et al.* 2009 (Schaar, Medina et al. 2009) Fletcher *et al,* 2012 (Fletcher, Dart et al. 2012)
SPRY2 sprouty homolog 2	SPRY2 is a negative feedback regulator of multiple receptor tyrosine kinases including receptors for fibroblast growth factor, epidermal growth factor and hepatocyte growth factor. Antagonist of the Ras/MAPK signaling pathway	√	√	√	√	Ma *et al,* 2010
ZBTB10 zinc finger and BTB domain containing 10	Inhibits SP1 a transcription factor associated with proliferation and angiogenesis in cancer	√	√			Li *et al.,* 2010 (Li, Mertens-Talcott et al. 2010) Mertens-Talcott *et al.,* 2007
MYT1 myelin transcription factor 1	inhibits G_2-M through enhanced phosphorylation and inactivation of cdc2	√	√			Mertens-Talcott *et al.,* 2007
FOXO1 forkhead box O1	Transcription factor with an important roles in regulation of gluconeogenesis and glycogenolysis by insulin signaling, and central to the decision for a preadipocyte to commit to adipogenesis.	√	√	√		Guttilla et al., 2009 (Torjesen and Sandnes 2004) Myatt et al., 2010 Zhou 2012 et al., (Zhou, Yin et al. 2012)
THRB thyroid hormone receptor, beta	One of several receptors for thyroid hormone, and mediates the biological activities of thyroid hormone.	√	√			Nishi et al., 2011 (Nishi, Ono et al. 2011)
RunX1 runt-related transcription factor 1	Transcription factor that regulates the differentiation of hematopoietic stem cells into mature blood cells	√	√	√		Ben-Ami et al., 2009 (Ben-Ami, Pencovich et al. 2009) Feng et

						al., 2009 (Feng, Iwama et al. 2009)
APC adenomatous polyposis coli	A negative regulator that controls Beta-catenin concentrations and interacts with E-cadherin, which are involved in cell adhesion.	√	√			Zhang et al., 2011 (Zhang, Liu et al. 2011)
HIPK2 homeodomain interacting protein kinase 2	A conserved serine/threonine nuclear kinase that interacts with homeodomain transcription factors		√	√		Li et al., 2010
WEE1	A G2 checkpoint kinase	√		√		Mertens-Talcott et al., 2007 Wuchty et al., 2011
IGF1 insulin-like growth factor 1	Member of a family of proteins involved in mediating growth and development	√	√	√		McKinsey et al., 2011
EGFR Epidermal growth factor receptor	Transmembrane growth receptor. On binding of the ligand the receptor dimerises leading to cell proliferation	√				Li et al., 2010 Wang, 2103
MMP-13 matrix metallopeptidase 13	Involved in the breakdown of extracellular matrix by cleaving collagen			√		Tardif et al., 2009 (Tardif, Hum et al. 2009)

As miR-27a has been shown to function as an oncomiR in a number of cancers, several studies have sought to clarify the role of miR-27a mutations in cancer initiation, progression or treatment response. A single nucleotide polymorphism (SNP) in miR-27a reported to have a divergent role in breast and gastric cancer, the G-variant of rs895819, is located in the terminal loop of pre-miRNA-27a (Mootha, Lepage et al. 2003). Yang *et al*. found that the G allele of rs895819 is associated with decreased familial breast cancer risk, the authors propose that this SNP leads to delayed maturation of miR-27a and thus reduced levels of the mature miRNA

(Mootha, Lepage et al. 2003). The same SNP has been shown to be an important factor of gastric cancer susceptibility (Sun, Gu et al. 2010) - an A/G polymorphism in position 40 of miR-27a was found to be associated with gastric atrophy and metaplasia in males. This was studied in further detail by Sun *et al*. who found that subjects with the variant genotypes had a significantly increased risk of gastric cancer and a significant positive correlation with lymph node metastasis (Sun, Gu et al. 2010). Tumours with the variant genotype had increased expression of miR-27a when assessed by qPCR .

1.16 miR-27a and prohibitin

As discussed previously, miR-27a was found to function as an oncomiR in gastric cancer through targeting prohibitin (Liu, Tang et al. 2009). Liu *et al.* found increased expression in gastric adenocarcinoma compared to healthy gastric tissue and that suppression of miR-27a levels was able to inhibit gastric cancer cell growth *in vitro* through derepression of prohibitin levels (Liu, Tang et al. 2009). Interestingly, it has been noted that the most efficient siRNAs targeting prohibitin share sequence homology with miR-27a (Dart, Spencer-Dene et al. 2009). As discussed earlier mutations in the 3'UTR have been described by Jupe *et al.* and Jakubowska *et al (Davis and Waldor 2009, Beck, Robinson et al. 2013).* These mutations are in putative binding sites for multiple miRNAs, however, no mutations have been described in the miR-27a binding site of the prohibitin 3'UTR.

1.17 MiR-27a and prostate cancer

Contrasting results have been reported in the literature for miR-27a expression in prostate cancer. Three studies have showed no difference in miR-27a expression levels when comparing tumour samples to control samples (Calin and Croce 2006, Ambs, Prueitt et al. 2008, Tong, Fulgham et al. 2009). This contrasts with work of Volinia *et al.,* who found miR-27a expression to be increased in a similar study (Volinia, Calin et al. 2006). However, Porrka *et al*., found that miR-27a levels were downregulated in CRPC when compared to androgen responsive tumours (Porkka, Pfeiffer et al. 2007). Thus it is still unclear as to whether miR-27a may play a role in prostate cancer, specifically whether it has a role in development or androgen resistance.

1.18 Antisense OligomiRs as potential cancer therapeutics

With the growing evidence that miRNA expression is deregulated in cancer development and then progression, their role as potential therapeutic targets is supported. Targeting oncogenes by re-expression of tumour suppressive miRNAs, or encouraging re-expression of tumour suppressor genes by silencing an oncomiR could achieve this. However, a single miRNA targets many mRNAs thereby simultaneously modifying a number of genes and pathways within the tumour, thus leading to potentially significant off-target effects.

AntagomiRs are a novel class of chemically engineered oligonucleotides used to silence endogenous miRNA, believed to operate by irreversibly binding the miRNA of exact complementary sequence, thereby preventing interactions between the miRNA and its target mRNA. The most basic examples are anti-miRNA oligonucleotides (AMOs) a 'naked' single strand molecule, however, these are relatively unstable as they are easily degraded by endogenous RNases, limiting systemic administration. Adding a phosphorothioate backbone confers greater stability in cells and tissues. The substitution of sulphur for a non-bridging oxygen at each phosphorus in the chain conserves the charge and solubility as well as not interfering with the hybridisation of the target mRNA.

Nevertheless the result is a biologically active different chemical entity and though the specificity of AMOs comes from the Watson-Crick base pair interaction, there are concerns that the chemistry of these molecules themselves may be causing complex non-sequence specific events. Phosphorothioates are polyanions, and as such can bind to proteins such as bFGF, PDGF, VEGF, EGFR as well as others, and this binding affinity is length dependent (as reviewed in Stein, 2001 (Krutzfeldt, Rajewsky et al. 2005)). In addition the length of the phosphorothiate AMO must be carefully considered when designing the antagomir as ribonuclease H, the ubiquitous enzyme that recognizes the mRNA strand of an RNA-DNA duplex for cleaving, can recognize a duplex as small as 6mer and does not require full-length homology (Kane, Bassett et al. 2005). Thus with additional length comes the paradoxical drop in target specificity. Current opinion holds that the optimized length to minimize this effect is 16-20 nucleotides (Krutzfeldt, Rajewsky et al. 2005). Concentration of

AMO used also has a bearing on these non-sequence specific events and it is advised to avoid concentrations greater than 4-5 μM (Krutzfeldt, Rajewsky et al. 2005).

In addition to the phosphorothiate backbone other modifications have been trialled to improve stability and sensitivity. One is the addition of cholesterol conjugated 2'-O-methyl groups, this was successfully used by Krutzfelt *et al.* to design an antogomiR that targeted miR-122 in mice, resulting in prolonged miR-122 silencing and a significant decrease in serum cholesterol (Krutzfeldt, Rajewsky et al. 2005). This modification was also used in the systemic delivery of an antagomiR to miR-10b in a mouse mammary tumour model, which successfully prevented metastasis formation (Ma, Teruya-Feldstein et al. 2007). Another modification that has shown promise is 'locked nucleic acid' (LNA) oligmers, which contains a ribose moiety functionally locked into a C3'-endo conformation via the addition of a methylene bridge. This structure confers greater stability, increased miRNA-binding affinity and lower toxicity (Nana-Sinkam and Croce 2011). These modifications are summarized in figure 1.7.

Figure 1.7: Oligonucleotide configurations

Phosphorothioate backbones (PS), as well as 2′-*O*-methoxyethyl (2′-MOE) and 2′-*O*-methyl (2′-OMe) substituents, increase resistance to degradation and promote protein binding to target RNA. Locked nucleic acid (LNA) modification markedly increases the binding of the oligonucleotide to the targeted mRNA. Reproduced with permission from Kole *et al*, 2012

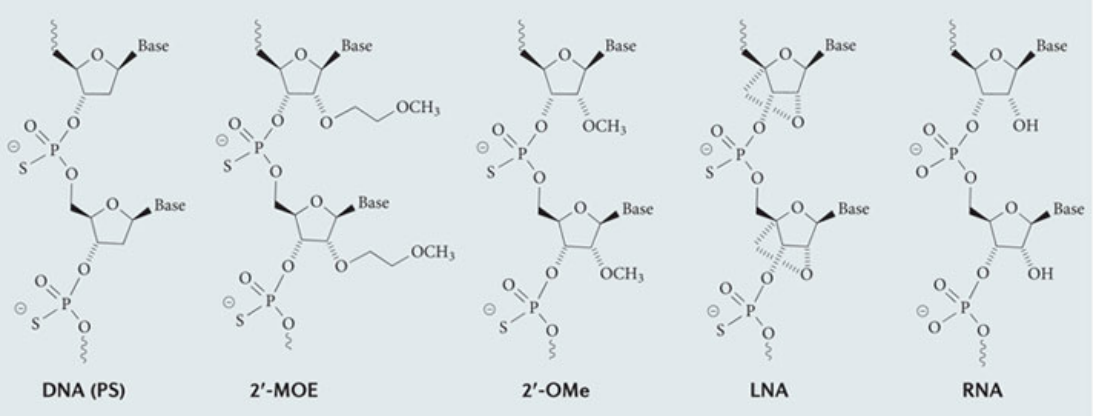

The antagomiR chemistry does appear to dictate the fate of the targeted miRNAs. The higher affinity antagomiRs, such as the LNA modified moieties, sequester the target miRNAs in a heteroduplex whereas the lower affinity molecules, such as 2'-

MOE modified antagomiRs, appear to promote miRNA degradation (Torres, Fabani et al. 2011).

An LNA antagomiR targeting miR-122 (Miravisen, SPC3649, Santaris Pharma) has been shown to suppress the Hepatitis C virus (HCV) RNA replication in HCV infected chimpanzees with a prolonged 300-fold suppression in viraemia (Haussecker and Kay 2010). It was shown to be safely tolerated in humans with limited toxicity and a clear-dose dependent pharmacology in the subsequent Phase I study, and now has entered Phase II trials (ClinicalTrials.gov NCT01200420) (Mahal, Aizer et al. 2014). This first miRNA mimic therapy, MRX34 (MiRNA Therapeutics), has started phase I clinical trials in patients with unresectable primary liver cancer or advanced metastatic cancer with liver involvement or haematological malignancies (ClinicalTrials.gov NCT01829971). It is administered as an intravenous agent twice a week for 3 weeks with one week off for a total of 28 days then continued until disease progression or intolerence. The liposomal formulation of the miR-34 mimic delivers a concentrated dose to the liver achieving a greater than 100-fold increase in miR-34 levels in liver cells. MiR-34 is a known tumour suppressor that is under expressed in a wide variety of cancers. Preliminary data was presented at the AACR annual meeting in San Diego, USA in April 2014. In the interim analysis, adverse events primarily consisted of infusion reactions, including fever, chills, fatigue, thrombocytopenia, diarrhoea, back and flank pain, nausea, and neutropenia. The addition of dexamethasone, a corticosteroid, premedication was found to ameliorate infusion reactions (Hahn, Yiannoutsos et al. 2014). A summary of current miRNA therapeutics in development can be seen in Figure 1.8.

Figure 1.8: Summary of current miRNA therapeutics in development

Red coloured miRNAs indicate replacement therapy with a drug mimicking the endogenous miRNA. Blue coloured miRNAs indicate inhibition therapy with drugs targeting the endogenous miRNA. Only one of the trials has published results thus far, NCT01200420 (Mahal, Aizer et al. 2014). Further details of the other trials can be found on the website clinicaltrials.gov and then entering the NCT number referenced below.

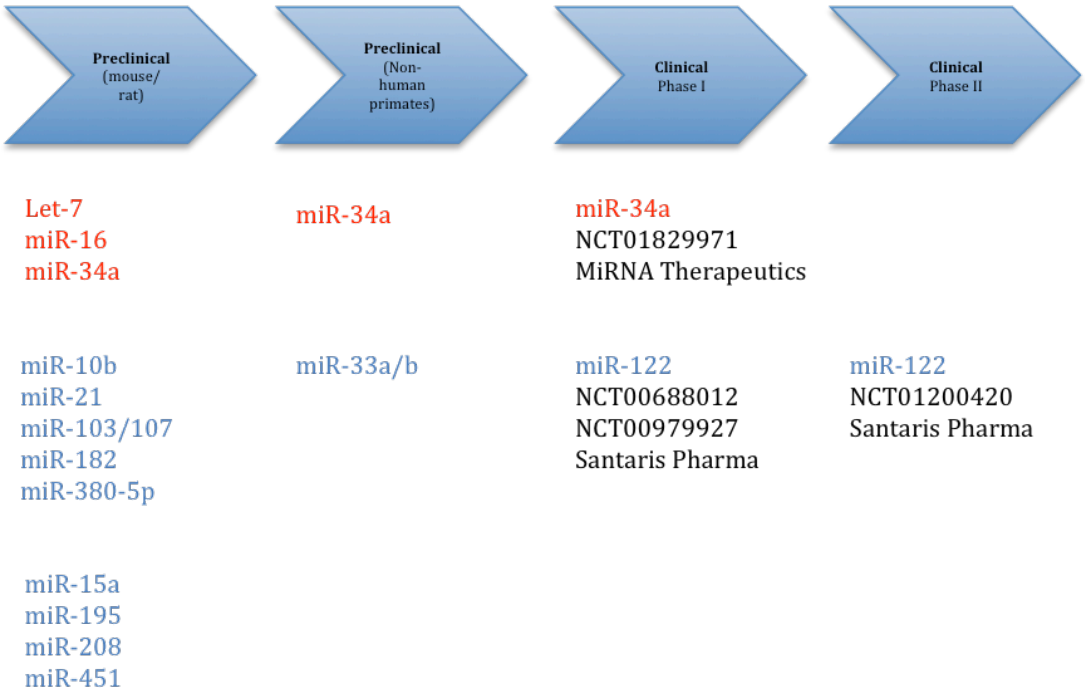

Research into this new class of therapeutics encompasses a wide range of mechanistic approaches as well as complex delivery and tissue targeting strategies. The hurdles posed by the human body's natural barriers have hampered the systemic delivery of these drugs but this is being overcome by innovative modifications. Increasingly novel delivery systems, such as nanoparticles are being designed to ensure tissue specific delivery (Davis, Zuckerman et al. 2010). Given their small size, specificity and low cost, antisense oligonucleotides targeting miR-27a are potentially viable therapeutic candidates requiring further investigation in Prostate cancer.

1.19 Prostate cancer needs new biomarkers

Whilst many men are diagnosed with prostate cancer far fewer will actually die of it. For men in the United States of America, overall lifetime risk of developing prostate cancer is one in seven however the mortality risk is markedly lower at one in thirty-six (Siegel, Naishadham et al. 2012). This creates a difficult paradigm whereby many

patients are diagnosed with prostate cancer yet many of them will have indolent disease. Without markers to predict which tumours will become aggressive, many patients will receive therapies, which have multiple deleterious side effects and for which little or no therapeutic benefit will be gained.

PSA detection in serum is the current gold standard biomarker for diagnosis of prostate cancer and response to treatment. The incidence of prostate cancer dramatically increased over the past two decades due in part to an ageing population, an increased awareness of prostate cancer and the use of PSA testing. At the same time over the last two decades prostate cancer survival rates have increased due to the overdiagnosis of indolent disease in part. PSA is a 33kDa serine protease (kallikrein-3) that is secreted by the epithelial cells of the prostate. When the basal-cell layer is disrupted, as is the case with prostate cancer, then PSA effectively "leaks" into the circulatory system and can be detected in the serum. There are well-known limitations to the use of PSA as a biomarker. Elevated serum PSA levels are not specific to prostate cancer and are frequently present in men with other diseases of the prostate, such as benign prostatic hypertrophy (BPH) and prostatitis. This results in a large false positive rate, with less than 50% of men who have a prostate biopsy following a raised PSA result actually being diagnosed with prostate cancer (Schroder and Roobol 2009). As prostate biopsy carries risks, especially of infection, this level of false positives is unacceptably high (Schroder and Roobol 2009). In addition, because of its lack of specificity, a very low PSA level does not completely rule out prostate cancer and there is also a false negative rate, of approximately 15%, where a negative PSA reading (0-4ng/ml) has not indicated the underlying presence of cancer (Jemal, Siegel et al. 2010). Furthermore, PSA does not distinguish between the different stages of prostate cancer with the specificity and sensitivity required to make therapeutic decisions. Recently there has been much discussion as to the actual benefit of PSA as a biomarker to screen populations. Two large multi-national randomised prospective control trials, the European Randomised Study of Screening in Prostate Cancer (ERSPC) and the Prostate, Lung, Colorectal and Ovarian Screening Trial (PLCO), were conducted (Andriole, Crawford et al. 2009, Schroder, Hugosson et al. 2009) and found that PSA screening did not provide any substantial benefit in overall patient survival (Schroder and Roobol 2009).

Following these results the United States Preventative Services Task Force (USPSTF) recommended that the population benefit of PSA screening is inconclusive and does not recommend it for men of any age (Lin, Lipsitz et al. 2008).

There is, therefore, a particular need for new, specific diagnostic biomarkers that define populations of men with prostate cancer needing treatment, rather than indolent cancer that can be monitored without treatment. There have been numerous strategies proposed to improve PSA diagnostic performance, such as free PSA, PSA velocity and age or race-specific PSA reference ranges. Although these have been used by clinicians and continue to be investigated there is no consensus on their use, as none of them have shown in clinical trials to decrease unnecessary biopsies or improve outcomes (Mitchell, Swindell et al. 2008).

The cost of over-diagnosis of prostate cancer - both on a personal health level and financially for healthcare systems - has driven a great deal of attention towards finding novel non-invasive markers. There are a number of other tests that have potential and are currently being trialled, for example raised urinary levels of Prostate Cancer Antigen 3 (PCA3) have been shown to correspond to a diagnosis of prostate cancer (Kane, Bassett et al. 2005). There are also ongoing trials looking at the expression of TMPRSS2:ERG fusion transcripts in cells discharged into the urine following a rectal exam, as this fusion gene is rarely found in cells of men without Prostate cancer (May, Knoll et al. 2007). See Table 1-4 for a summary of biomarkers in development currently.

Table 1-4: Prostate cancer biomarkers currently in research and development with pharmaceutical companies.

Name	Body Fluid	Methodology	Biomarker Type
Progens PCA3	Urine	Detects over-expression of PCA3 gene	Diagnostic
ERG Protein Marker	Biopsy tissue	Detects the ERG protein, indicative of cancer	Diagnostic
TMPRSS2:ERG	Urine	Detects TMPRSS2:ERG gene fusion	Prognostic
ERG Gene Marker	Biopsy tissue	Detects TMPRSS2:ERG gene fusion	Prognostic
ConfirmMDx	Negative biopsy tissue	Analyses genes associated with Prostate cancer	Predictive of future Prostate cancer risk
NADiA ProsVue	Blood	Determines rate of change of total PSA	Predictive of future Prostate cancer risk
Prostate Health Index	Blood	Level of p2PSA combined with PSA and free PSA	Diagnostic
OncoType testing for Prostate	Biopsy tissue	Analyses genes associated with Prostate cancer	Prognostic
Prolaris Diagnostic Test	Biopsy tissue	46 -RNA expression predicts 10 year survival	Prognostic
Phosphatase and tensin homolog (PTEN)	Blood	Detects PTEN gene	Diagnostic

Circulating miRNAs have the potential to be useful prognostic and predictive biomarkers. However, a prerequisite to developing circulating miRNA-based diagnostics is the ability to measure miRNAs from plasma and serum with sufficient sensitivity and precision. The measurement of these miRNAs has been associated with some special challenges, including those related to pre-analytic variation and data normalization (Kroh, Parkin et al. 2010).

1.20 Role and Transportation of Circulating miRNAs

Although it is clear that miRNAs function as a mechanism for posttranscriptional regulation, it has not been conclusively proven whether their presence in circulation is simply a by-product of cell degradation or whether they are being actively secreted into the body fluids to mediate intercellular gene regulation. The majority of

evidence supports the hypothesis that miRNAs can be actively and selectively secreted; for example, miR-1246 and miR-451 have been found to be released by the breast cancer cell line MCF-7 but not by the non-malignant mammary epithelial breast cell line MCF-10A (Pigati, Yaddanapudi et al. 2010). It is not just cancer cells that have the ability to secrete the miRNAs, it has also been demonstrated that miR-165 communicates radial position between cells in the root of plants via modulation of target gene expression (Carlsbecker, Lee et al. 2010).

Also in support of active secretion, is the appropriate packaging of miRNAs to facilitate circulation and protect them from degradation in body fluids. It has been shown that miRNAs in serum are resistant to circulating ribonucleases and severe conditions such as extended storage, freeze-thawing, extreme pH levels and boiling (Kroh, Parkin et al. 2010). There are three known methods by which miRNAs are packaged: in lipid vesicles, such as exosomes and apoptotic bodies; bound by RNA-binding proteins, such as nucleophosmin 1 and Argonaute 2; and associated with high-density lipoprotein (HDL). Such packaging of miRNAs also has a wider relevance as it facilitates the transfer of miRNAs between individuals, as exemplified by the example of immune related miRNAs in breast milk in the first six months of lactation, corresponding with the passive immunity gained from colostrum in the first six months (Zhou, Li et al. 2012). The implication of these findings for treatment is that miRNAs, when packaged appropriately, could be ingested and not digested (Iguchi, Kosaka et al. 2010). These structurally diverse extracellular miRNA-containing entities may also allow target enrichment and therefore improve the utility of miRNAs as biomarkers. For example, extraction of tissue-specific exosomes using protein surface markers could potentially enrich for a cancer specific miRNA population, as has been shown in ovarian cancer (Taylor and Gercel-Taylor 2008).

1.21 MiRs and Prostate cancer

The desirable properties of miRNAs in the context of circulating biomarkers include stability (they are stable even in archival samples) and availability (they have been isolated from most body fluids) (Cortez, Bueso-Ramos et al. 2011). Tumour cells release miRNAs into the blood and circulating expression profiles of miRNAs are altered in many tumour types, suggesting that the miRNA profile can be informative

about the disease (Taylor and Gercel-Taylor 2008, Heneghan, Miller et al. 2010). Further, detection and quantitation can be relatively easily achieved in low volumes of blood serum or plasma qRT-PCR, which is both specific and sensitive (Bassett, Cooperberg et al. 2005). Since the first publications about miRNAs relating to prostate cancer in 2007, there have been more than 100 articles on the subject reflecting the hope that miRNAs may be the future for biomarkers of this disease. Over the last decade, investigations into utility of circulating cell-free miRNAs as novel biomarkers have expanded dramatically.

1.21.1 MiRs as diagnostic biomarkers

Unfortunately cancers are still being diagnosed at a late stage and therefore often with a poorer prognosis. The discovery of tumour specific miRNA signatures that can be detected from a non-invasive blood test has led to the investigation of these molecules as early diagnostic biomarkers. The first report of miRNAs as potential diagnostic markers was in 2008. Mitchell *et al*. probed a panel of miRNAs in the serum of healthy men and those with advanced prostate cancer, and found that miR-141 was highly elevated in the cancer samples. Moreover, miR-141 was found to correlate significantly with serum PSA levels and could detect individuals with advanced prostate cancer with 60% sensitivity and 100% specificity (Mitchell, Parkin et al. 2008). By 2011 some miRNA species were clearly being identified across several studies, most notably miR-141. Yaman Agaoglu *et al.* tested the diagnostic utility of three miRNAs, miR-21, miR-141 and miR-221. They found miR-21 and miR-221 to be elevated in the serum of eighteen men with localised prostate cancer when compared to the twenty healthy controls. They also found that miR-141 could distinguish the men with bony metastases from those with localised disease (AUC= 0.755) (Yaman Agaoglu, Kovancilar et al. 2011).

1.21.2 MiRs as prognostic biomarkers

As already discussed, the limited ability to distinguish the small subgroup of prostate cancer patients who will relapse post ‘curative treatment’ with metastatic disease is based on an evaluation of a collection of markers, including PSA, Gleason score, and histological score. Profiling studies have demonstrated a number of correlations between differentially expressed miRNAs and prognosis. Brase *et al.* tried to

establish markers of micro metastasis in prostate cancer by comparing serum from men with primary prostate cancer to those with metastatic prostate cancer (Brase, Johannes et al. 2011). They found sixty-nine miRNAs to be elevated in men with metastatic disease; a subset of these was then measured in the men with localised prostate cancer. Three miRNAs - miR-141, miR-200b and miR-375, were found to be elevated with increasing tumour stage and Gleason score. The prognostic biomarker studies to date have consistently highlighted miR-141, miR-200b and miR-375 as significant disease correlates which could potentially be used as a test applied at the time of diagnosis to identify those patients with previously undetectable micro metastasis (Brase, Johannes et al. 2011, Moltzahn, Olshen et al. 2011, Bryant, Pawlowski et al. 2012).

1.21.3 MiRs as predictive biomarkers

Resistance to chemotherapy remains a major obstacle to effective treatment of CRPC. Recent studies postulate that aberrant miRNA expression might indicate tumour resistance to current therapy, suggesting a role for miRNAs as predictive biomarkers. Predicting a patient's response to treatment would allow tailoring of appropriate regimens and a reduction in treatment-induced morbidity. Zhang *et al.* looked specifically at levels of miR-21 in patients with localised prostate cancer, androgen dependent prostate cancer (ADPC), castrate resistant prostate cancer (CRPC) and BPH (Zhang, Yang et al. 2011). The levels of this miRNA were found to be significantly higher in CRPC and ADPC in those patients with a PSA>4ng/ml. Most interestingly, the four CRPC patients who were resistant to Docetaxel had significantly higher miR-21 levels than those six patients with responsive disease. Potentially, such miRNAs or miRNA profiles could be used to predict response to a given therapy, and further could give clues as to mechanisms of resistance.

1.22 Methodological challenges in measuring circulating miRNAs

A prerequisite to developing circulating miRNA-based diagnostics is the ability to quantify miRNAs from plasma and serum with sufficient sensitivity and precision. The accurate measurement of these miRNAs has been associated with many challenges, including those related to pre-analytic variation such as specimen collection, factors influencing RNA extraction efficiency and technical issues

involved in successful qRT-PCR and data analysis and normalization (Kroh, Parkin et al. 2010).

Body fluid choice of either plasma or serum, the collection tube used and the timings between collection and processing must be standardised across the study in question in order to reduce variability. The actual isolation of miRNAs from serum and plasma is relatively straightforward, using a guanidinium-phenol extraction followed by either precipitation of the miRNA-containing aqueous phase or column based purification (Kroh, Parkin et al. 2010).

The main issues that remain unresolved in the measuring of circulating miRNAs are normalisation, amplification and contamination. Quantitating the amount of total miRNA in body fluid specimens is not possible because of the extremely low concentrations eluted. In addition there is no consensus on suitable small RNA reference genes that could be used as an internal reference to control for biological variability; current protocol calls for samples to be processed from identical input volumes and then corrected for technical variability using a spiked-in quantity of synthetic non-human (*C. elegans*) miRNA to act as a normalising control for the technical variability's described above (Mitchell, Parkin et al. 2008, Kroh, Parkin et al. 2010). Some investigators have proposed the use of 'invariant' miRNAs as endogenous controls. Another area that requires standardisation across studies is the use of pre-amplification reagents to increase the sensitivity of the qRT-PCR, used in some studies but not in others. Lastly, the quantification of valid miRNAs in the serum can be grossly altered by contamination of leaked miRNAs from cellular blood components, either through haemolysis during sampling or processing or by the carry-over of whole cells in the serum/plasma. Until there is standardisation in phlebotomy protocol, sample processing and miRNA extraction methodology, the translatability of these studies will be limited (Kroh, Parkin et al. 2010).

Currently the use of miRNAs as biomarkers is limited by conflicting data between studies due to lack of standardisation in methodology and the lack of suitable reference genes for normalisation. It is unlikely that any one miRNA will achieve the desired level of diagnostic or prognostic accuracy, as evidence is increasing that in addition to prostate cancer many different tumour types can be associated with

increased levels of particular miRNAs. For example miR-21 is raised in a variety of other cancers such as lymphoma (Lawrie, Gal et al. 2008, Bao, Ali et al. 2011) and breast cancer (Asaga, Kuo et al. 2011). However, a miRNA-based diagnostic test has been described for pancreatic adenocarcinoma with results that showed better diagnostic ability then the current blood based biomarker for pancreatic cancer CA 19-9 (Szafranska-Schwarzbach, Adai et al. 2011).

Hypothesis and Aims

Hypothesis

Increasing the level of prohibitin protein by the use of an ASO to inhibit prohibitin mRNA degradation by an endogenous miRNA, will slow the growth of prostate cancer cells. In addition, circulating levels of miRNAs, including miR-27a, may provide clinically useful biomarker information regarding diagnosis, prognosis, or prediction of response to treatment.

Aims

The overall aim is to establish the role of prohibitin in prostate cancer progression and elucidate its potential as a novel therapeutic target. This has been broken down into four discrete aims. Firstly, characterisation of prohibitin in different prostate cancer cell lines to establish whether prohibitin levels are altered between them and whether there is any correlation with parameters of aggression. Secondly, the generation of cell lines stably transfected with expression vectors to artificially manipulate prohibitin. These cell lines facilitate the investigation of whether, by artificially increasing the wild type prohibitin levels, we can slow cell/tumour growth in a range of cell line models. Thirdly, to explore ASO-27a as a potential therapy, by establishing whether we can manipulate endogenous prohibitin using ASO to miR27a, and what effect this has on prostate cancer cell growth. Lastly, investigating circulating miRNAs as biomarkers for prostate cancer. This involves optimisation and standardisation of extraction of miRNAs from blood to establish whether circulating miR-27a found in the blood of prostate cancer patients is useful as a biomarker for diagnosing prostate cancer or as a biomarker of disease response or progression.

Chapter 2 Materials and Methods

2.1 Reagents, buffers and solutions

Preparation of reagents, buffers and solutions. dH_20 = distilled water, ddH_20 = MilliQ water (18 M**Ω**-cm).

2.1.1 Mammalian Cell Culture

Table 2-1 Cell Culture

Cell Type	Medium	Additives	Storage
LNCaP, VCaP, DuCaP, DU145, C4-2, C4-2-b	Normal Growth Medium RPMI (Roswell Park Memorial Institute) 1640	2mM glutamine, 100U/ml penicillin, 0.1mg/ml streptomycin, 10% fetal bovine serum (FBS)	4˚C
DU145/TR/MAR4/siRNAPHB C4-2/TR/MAR4/PHBflag C4-2/TR/MAR4/siRNAPHB	Selection Medium RPMI 1640	2mM glutamine, 100U/ml penicillin, 0.1mg/ml streptomycin, 10% tetracycline-free FBS, To flask: 1µl/ml of 12mg/ml blasticidin, 3 µl/ml of 100mg/ml zeocin, G418 5µl/ml of 100ng/ml For induction: Doxycycline added at 1-10µm final conc	4˚C
LNCaP, VcaP, DuCaP, DU145, C4-2, C4-2-b	Starvation Medium Phenol Red-free	2mM glutamine, 100U/ml penicillin, 0.1mg/ml streptomycin, 5% double charcoal-stripped FBS	4˚C

	RPMI		
All Cell Types	Freezing Medium 90% tetracycline-free FBS	10% dimethylsulphoxide	-20˚C
All Cell Types	Trypsin Solution	5ml 25g/L trypsin in 0.9% NaCl in 50ml 0.02% (w/v) EDTA	4˚C

Table 2-2 Antibiotics for Stable Cell Line Selection and Induction

Reagent	Procedure	Sterilisation	Storage
Blasticidin	Prepare to 12mg/ml in sterile ddH_2O (Melford Laboratories)	0.22µm filter	-20˚C
Zeocin	Supplied at 100mg/ml (Invitrogen)	-	-20˚C
Puromycin (G418)	Prepare to 4000µM in ddH_2O (Sigma-Aldrich)	-	-20˚C
Doxycycline	Supplied at 10mg/ml (Sigma-Aldrich)	0.22µm filter	-20˚C (in the dark)

Table 2-3 Media for Bacterial Culture

Reagent	Preparation	Sterilisation	Storage
LB (Luria-Bertani) Broth	10g LB broth mix in 500ml ddH_2O	Autoclave	4˚C
LB Agar	17.5g LB agar in 500ml ddH_2O	Autoclave	4˚C

Ampicillin (100mg/ml)	1g ampicillin in 10ml ddH_2O	0.22µm filter	-20˚C
Ampicillin resistance selection medium/agar	Ampicillin added at 1µl/ml to LB broth or molten LB agar to a final concentration of 100µg/ml	-	4˚C

Table 2-4 General Solutions

Reagent	Procedure	Sterilisation	Storage
1x Phosphate Buffered Saline (PBS)	1 tablet (Oxoid) dissolved in 100ml ddH_2O	Autoclave	4˚C
Proteinase inhibitor cocktail	Used at 5µl/ml	-	-20˚C
Phenylmethylsulfinyl Fluoride (PMSF)	Prepare to 100mM	-	-20˚C
1x Tris buffered saline (TBS)	Prepare from 20x stock (Severn Biotech) in ddH_2O	Autoclave	4˚C

Table 2-5 Hormones and Compounds used for the Treatment of Cells

Agonist/Antagonist	Preparation	Final Concentration	Storage
Mibolerone (Mib)	(Du Pont, NEN) prepared to 10mM in 100% Ethanol	0.01nM-10nM	-20˚C
Bicalutamide (Bic)	(Astra Zeneca) prepared to 1mM stock in 100% ethanol	1µM	-20˚C

Table 2-6 Gel Components for Polyacrylamide Gel Electrophoresis

Gel Component	8% (10ml)	10% (10ml)	12% (10ml)	Stacking (4%) (2ml)
ddH_2O	4.6ml	4.0ml	3.3ml	1.4ml
30% acrylamide	2.7ml	3.3ml	4.0ml	830µl
1.5M Tris-HCl (pH 8.8)	2.5ml	2.5ml	2.5ml	-
1.5M Tris-HCl (pH 6.8)	-	-	-	250µl
10% SDS	100µl	100µl	100µl	20µl
N,N,N',N'-tetramethyl-ethylenediamine (TEMED)	10µl	10µl	10µl	2µl

Table 2-7 SDS-PAGE Buffers

Reagent	Protocol	Sterilisation	Storage
1.5M Tris-HCl (pH6.8)	181.7g Tris dissolved in 800ml ddH_2O. HCl added to pH6.8. H_2O added to 1l	Autoclave	RT
1.5M Tris-HCl (pH8.8)	As above, HCl to pH 8.8	Autoclave	RT
10% sodium dodecyl sulphate (SDS)	50g SDS dissolved in 500ml ddH_2O	Autoclave	RT
10% ammonium	1g APS (Sigma) dissolved	-	-20˚C

persulphate (APS)	in 10ml ddH_2O		
H_2O-saturated butanol	200ml butan-2-ol and 200ml ddH_2O shaken vigorously. H_2O and butanol settle into two distinct phases. Butanol drawn from top phase	-	RT

Table 2-8 Western Blotting Buffers

Reagent	Protocol	Storage
5x SDS running buffer	144g glycine, 30g Tris, 10g SDS dissolved in 2l ddH_2O	4˚C
Semi-dry electro-transfer buffer	11.26g glycine, 2.44g Tris, 200ml methanol to 1l with ddH_2O	4˚C
Phosphate-buffered saline-Tween 20 (PBST wash buffer)	0.05% Tween 20 dissolved in 1xPBS	RT
Tris-buffered saline-Tween 20 (TBST wash buffer)	0.05% Tween 20 dissolved in 1xTBS	RT
Blocking/Probing Buffers		
5% dried skimmed milk powder blocking/probing buffer	5% dried skimmed milk powder dissolved in PBST wash buffer	Immediate use
5% bovine serum albumin (BSA) blocking/probing buffer	5% BSA dissolved in TBST wash buffer	Immediate use

Table 2-9 Radioimmunoprecipitation Buffer (RIPA)

Reagent	Procedure	Storage
RIPA lysis buffer	100mM NaCl, 0.5% NP40, 50mM Tris-HCl (pH8.0) made to volume with ddH_2O. PMSF to 0.2mM, 5µl/ml proteinase inhibitor cocktail and 10µl/ml phosphatase inhibitor cocktails 1 and 2 (Sigma) added immediately prior to use	4˚C

Table 2-10 Buffers for DNA Gel Electrophoresis

Reagent	Procedure	Storage
50x TAE (Tris acetate EDTA)	242g Tris, 57.1ml glacial acetic acid, 100ml 0.5M EDTA to pH8.0 and made to 1l with dH_2O	RT Diluted to 1x when required
DNA loading buffer	40g sucrose and 100mg Orange G made to 50ml with dH_2O	RT

Table 2-11 miRNA Northern Blotting Buffers

Reagent	Procedure	Storage
DEPC H_2O	1ml DEPC added to 1L ddH_2O and left overnight prior to autoclaving	RT
10xTBE	60.55g Tris, 25.68g Boric acid, 1.86g EDTA, 400ml ddH_2O, pH 8.0 made to 500ml with ddH_2O. 700µl DEPC added and left overnight prior to autoclaving.	RT
1xTBE	100ml 10xTBE, 900ml DEPC H_2O	RT

1mm non-denaturing urea/TBE 16% polyacrylamide gel	20g urea, 4ml 10xTBE and 20ml duracryl warmed briefly in microwave and made to 40ml with DEPC H_2O. Cooled on ice prior to additon of 240µl 10%APS and 16µl TEMED. Poured immediately into gel cast and allowed to polymerise for 1-2 hours.	Immediate use
RNA loading dye	50% glycerol. 0.03% xylene cyanol, 0.03% bromophenol blue, 1mM	4
20xSSC	87.7g NaCl, 44.1g sodium citrate, 400ml ddH_2O. 700µl DEPC added and left overnight prior to autoclaving.	RT
2xSSC, 0.1% SDS	50ml 20xSSC, 0.5g SDS made to 500ml with DEPC H_2O	RT
1xSSC, 0.1% SDS	25ml 20xSSC, 0.5g SDS made up to 500ml with DEPC H_2O	RT
0.1xSSC, 0.1%SDS	2.5ml 20xSSC, 0.5g SDS made to 500ml with DEPC H_2O	RT
1xSSC	25ml 20xSSC, 475ml DEPC H_2O	RT
Maleic Acid Buffer (0.1M Maleic Acid 0.15M NaCl, pH 7.5)	11.61g maleic acid, 8.77g NaCL, 900ml ddH_2O, pH 7.5, made up to 1000ml with ddH_2O. 700µl DEPC added and left overnight prior to autoclaving	RT
Dig Wash Buffer (0.1M Maleic acid, 0.15 M NaCl, 0.3% Tween 20, pH 7.5)	11.61g maleic acid, 8.77g NaCl, 900ml ddH_2O, pH 7.5, made up to 1000ml with ddH_2O. 700µl DEPC added and left overnight prior to autoclaving. 3ml Tween 20 added prior to use.	RT
10xDig Blocking Buffer (10%BSA in maleic acid buffer)	5g BSA made up to 50ml with maleic acid buffer and aliquoted (1ml).	-20˚C

Dig Blocking Buffer	1ml 10x dig blocking buffer, 9ml maleic acid buffer.	Immediate use.
Dig Detection Buffer (0.1M Tris-HCL, 0.1M NaCl, pH 9.5)	7.88g Tris-HCL, 2.92g NaCl, 400ml DEPC H_2O, pH 9.5 NaOH, made to 500ml with DEPC H_2O	RT

Table 2-12 Antibodies used for Western Blotting, Immunohistochemistry and Immunofluorescence

Protein	Species	Clone	Manufacturer	Application	Dilution
AR	Mouse (monoclonal)	AR441	Dako	Western Blot	1/400
PHB	Mouse (monoclonal)	Ab1-11-14-10	Neomarkers	Western Blot Immunohistochemistry	1/750-1/1000 1/50-1/75
PHB	Rabbit (monoclonal)	H80 sc28259	Santa Cruz	Immunofluorescence Western Blot	1/50 1/1000
β-Actin	Mouse (monoclonal)	AC-15	Abcam	Western Blot	1/3000
Flag	Mouse (monoclonal)	M2	Sigma	Western Blot	1/1000

Table 2-13 Oligonucleotide Primers for Sequencing

Oligonucleotide Name	Sequence
PROHIBITIN	5’ GCAAGATCTACCATGGCTGCCAAAGTGTTTGAGTCCATTGGC 3’

forward	
PROHIBITIN Reverse	5' TGCGAATTCTCACTGGGGCAGCTGGAGGAGCACGGACT 3'
PROHIBITIN 3'UTR forward	5' TAATCTAGAGGGCCCACCCTGCCTGCACCTCCGCGGG 3'
PROHIBITIN 3'UTR long reverse (Sal1)	5'-TTTGTCGACGGAAGGTCTGGGTGTCATTTATTGACAGCAGTTT-3'
PROHIBITIN (mid-coding sequence reverse) – midcodrev	5' ACCAGCTCTCTCTGGGTGAT 3'
PROHIBITIN UTR end for	5' AGTGAGAGAGGAGGCCTGGA 3'
PROHIBITIN UTR mid for	5' ATTGCCAAGTGCCTATGCAAACC 3'
PRO FOR	5' ATGGCTGCCAAAGTGTTTGAG 3'
UTR REV 2	5' TGTCACTGATGGAAGGTTTGCGGATGAG 3'
UTR REV 3	5' CAGGGTCCTAAAACTTGGATGGACTTGTAT 3'

2.2 Mammalian Cell Culture

LNCaP, C4-2, C4-2b, DU145, VcaP, DuCaP and PC3 cells were maintained in RPMI 1640 (Gibco) supplemented with FBS, antibiotics (100U/ml penicillin, 100mg/ml streptomycin) and L-glutamine (6.1.1). All cells were maintained at 37˚C in 5% CO_2. 24 to 72 hours prior to ligand treatment, media were replaced with

starvation media, supplemented with a minimal amount of 5% charcoal-stripped FBS, 100U/ml penicillin, 100mg/ml streptomycin and 2mM L-glutamine. Stably transfected DU145 and C4-2 cells (DU145/TR/MAR4Luc/siRNA-PHB and C4-2/TR/MAR4Luc/siRNAPHB, C4-2/TR/MAR4luc/PHBflag) were maintained in RPMI 1640 supplemented with 10% tetracycline-free FBS, 12µg/ml blasticidin, 300µg/ml zeocin and G418 500µg/µl (see 6.1.1).

2.3 Fugene HD Transfections

Cells were plated into 6-well plates and placed into starvation medium 24h prior to transfection. Fugene HD (Roche) transfections were performed according to the manufacturer's protocol. Briefly, serum-free medium (equal to the volume of DNA and Fugene reagent subtracted from 650µl) was added to a 1.5ml microcentrifuge tube and 3µl Fugene reagent was added per 1µg of DNA and incubated at room temperature for 5 minutes. 2µg DNA was then added, and following brief mixing, reactions were incubated at room temperature for 15 minutes. 30µl of the DNA mixture was added drop-wise to each well and incubated for 24h prior to hormone treatment.

2.4 Lipofectamine RNAiMAX-Mediated Transient Transfection

Ten thousand LNCaP or LNCaP/TR/MAR4 cells were plated per well in 96-well plates in antibiotic-free medium and incubated for 24 hours. Oligos were diluted in Optimem medium to give a concentration range of 5 to 70 nM in a volume of 10µl per well and RNAiMAX was diluted 0.3µl in Optimem in a volume of 10µl per well. 10µl diluted oligo was combined with 10µl diluted RNAiMAX per well and incubated at room temperature for 20 minutes. 20µl of the oligo/RNAiMAX complex was then added to each well. Cells were incubated at 37˚C for up to 7 days for analysis.

Table 2-14 Oligonucleotides for 96 well and 6-well Lipofectaine RNAiMAX-Mediated Cell Transfection

Name	Modifications	Sequence
miR-27a mimic (Dharmacon)	Unmodified Oligo	5'-TTCACAGTGGCTAAGTTCCGC-3'
miR-27a mimic scrambled (Dharmacon)	Unmodified Oligo	5'-TGACCGTATAGGCTAAGCGAC-3'
miR-27a ASO	LNA Modified	5'-ACTTAGCCACTGTGA-3'
miR-27a ASO scrambled	LNA modified	5'-ACGTCTATACGCCCA-3'

2.5 Luciferase Assay

Cells grown on 24 well plates had media removed and washed in PBS and were lysed in 60µl of lysis buffer, frozen (-80˚C) then thawed on ice. Luciferase assays were preformed using the Luclite assay (Packard, USA). 20µl of cell lysate from each well of the 24-well plate was added in duplicate to wells of a 96-well Optiplate (Packard). 20µl of 2x luclite substrate was added to each well and plates were incubated at room temperature in the dark for at least 15 minutes. Luminescence (counts per second) was assayed using a VICTOR Light luminescence counter (PerkinElmer). Luminescence values were normalised to β-galactosidase activity (see below).

2.6 β-Galactosidase Assay

Assays were performed using the β-galactosidase assay kit (Tropix, UK). Galacton substrate was diluted 100-fold in Galactolight reaction buffer diluent. 5µl of cell lysate was added in duplicate to wells of a 96-well Optiplate and 50µl of diluted galacton substrate was added to each well. Each plate was incubated for 60 minutes at room temperature in the dark. Following incubation, 75µl of Accelerator II (Tropix) was added to each well and plates were incubated for a further 15 minutes

at room temperature in the dark. β-galactosidase activity was measured using the VICTOR Light luminescence counter as described above.

2.7 Sulphorhodamine B (SRB) Assay

Cells grown in a 24 well plate were fixed by adding 500µl 40% trichloroacetic acid (TCA) and then incubated for 1h at room temperature. Plates were then gently washed with tap water and air-dried. 500µl of 0.4% (w/v) SRB in 1% acetic acid was added to each well and plates were incubated for 1h at room temperature. Plates were then washed 5 times in 1% acetic acid and air-dried. 400µl 10mM Tris-HCl pH8.0 was then added to each well and plates were incubated for 1h at room temperature with shaking. 200µl of the resulting solution from each well of the 24-well plate was then added in duplicate to wells of a 96-well plate and absorbance was read at 492nm on a spectrophotometer (Septra Max 190).

2.8 Cell Proliferation Assay – WST-1 Assay

10,000 cells in 100 µl of media were seeded in a 96 well plate and incubated for 24 hours. 10µl/well of cell proliferation agent WST-1 was added and the cells incubated for 30 minutes at 37°c and 5% CO_2. Following incubation the plate was shaken thoroughly for 1 minute on a shaker. The absorbance was then measured at 440nm on a spectrophotometer (Septra Max 190).

2.9 Immunofluorescent Staining of prostate cancer Cells

LNCaP,C4-2b, VcaP and DU145 cells were plated in individual growth chambers onto the same glass slide in full growth medium to 40% confluency. Cells were washed in 1xPBS then fixed with 1% formaldehyde in PBS for 10 minutes or in methanol acetate (50:50) for 10 minutes. Formaldehyde fixed cells were further permeabilised with 0.1% Triton X for 10 minutes at room temperature. Cells were washed x1 in PBS and then blocked with 10% goat serum in PBS for 1h. Primary antibody (Rabbit anti-prohibitin (Neomarkers)) was diluted 1/50 in 10% goat serum and added to cells for 1h at room temperature. Following washing with PBS, secondary antibody (goat anti-rabbit (Alexa Fluor-594)) was diluted 1/50 in 10% goat serum and added to cells for 1h at room temperature in the dark. Cells were washed briefly in PBS and coverslips were mounted onto glass slides using DAPI-

containing Vectashield mounting solution. Slides were visualised on a Zeiss Meta 512 confocal microscope.

2.10 Flow Cytometry

Cells were grown in 10cm dishes and treated according to the experimental plan. At harvest the medium was transferred from the dishes into separate 15ml falcon tubes. The cells were then washed with 1ml of PBS and the wash was added to the respective 15ml falcon tube. Trypsin (1ml) was added per plate and the plates were incubated and then the trypsin neutralised and cells harvested using the media from the respective falcon tube. The falcon tubes were centrifuged at 1200 rpm for 5 mins to pellet the cells. The media was poured away and the pellet resuspended in 10ml of 75% ethanol to fix the cells. The samples were stored at 4°C until completion of the experiment. Prior to analysing the samples with the flow cytometer the cells were pelleted by centrifugation at 1200 rpm for 5 mins and then washed twice with PBS. The cells were then treated with ribonuclease (50µl of 100µg/ml stock solution) to ensure only DNA and not RNA is stained by the addition of Propidium Iodide (200µl of 50µg/ml stock). Cells stained by PI were then analysed through fluorescence-activated cell sorting (FACS; BD FACSCanto A flowcytometer) using FACSDiva software v6.12. Linear scale representation of forward and side scatter was used during flow analysis, a total of 10 000 events were measured per sample. DNA Quality Control Particles (BDIS) were used to set the parameters for doublet discrimination and cell cycle profiles were measured.

2.11 SDS PAGE western blot analysis

2.1.2 Protein harvesting

Cells were washed twice in PBS, trypsinised and resuspended in 5-10ml minimal growth medium. Cells were pelleted by centrifugation at 1000 x*g* for 4 minutes and then washed in PBS and re-pelleted by centrifugation at 1000 *xg* for 4 minutes then supernatant removed and the pellet flash frozen in a dry ice and methanol bath. Pellets were stored at -80°C until required. Frozen cell pellets were thawed gently on ice. Immediately prior to use, 20µl 10mM PMSF, 5µl proteinase inhibitor cocktail and 10µl phosphatase inhibitor cocktails 1 and 2 (Sigma) were added per ml of RIPA

buffer (100mM NaCl, 0.5% NP40, 50mM Tris-HCl (pH8.0)). Cell were then lysed with 50-2000µl of RIPA added to cell pellets depending on cell number. Cells were incubated on ice for 15 minutes to ensure efficient lysis. Samples were then centrifuged for 7 minutes at 15,000x*g* at 4°C. The supernatant was removed into a pre-chilled microcentrifuge tube and aliquoted into further pre-chilled microcentrifuge tubes as appropriate to avoid repeated freeze-thawing of lysates. Protein concentration was determined by DC Protein assay and lysates were stored at -20°C until required.

2.1.3 DC Protein Assay (modified Lowry assay)

To determine the protein concentration of cell lysates, 5µl of known concentration (2.5, 5, 10, 20 µg/µl) of bovine serum Albumin (BSA) in appropriate lysis buffer or protein sample was used in the DC protein assay (Bio Rad). Assays were carried out in accordance with the manufacturer's instructions in a 96 well plate and read at a wavelength of 750nm on a spectrometer (Septra Max 190).

2.1.4 SDS PAGE and western blotting

Protein samples (10µg) were mixed with 2x SDS-PAGE loading buffer and incubated at 100˚C for 5 minutes. Proteins were separated on 8-12% SDS-polyacrylamide gel (Table 6.1.6) with 4% stacking polyacrylamide gel in 1x running buffer. Samples were transferred to PVDF membrane at 10V for 30 minutes by semi-dry electrotransfer using 1x semi-dry transfer buffer. PVDF membrane was blocked using blocking buffer (5% non-fat dried milk powder in 0.05% Tween-20 in 1x PBS (PBST)) with gentle shaking for 40 minutes at room temperature. Following blocking, the membrane was incubated with appropriate primary antibody diluted to appropriate concentration in blocking buffer for 1h with gentle shaking. After washing for 3 x 15 minutes in PBST with agitation, the membrane was incubated for 1h at room temperature with appropriate HRP-conjugated secondary antibody diluted 1 in 2000 in blocking buffer. The membrane was then washed 4x 15 minutes in PBST at room temperature with agitation, incubated with chemiluminescent substrate (GE Healthcare), and exposed to Kodak GRI autoradiography film.

2.12 DNA Agarose Gel Electrophoresis

1% agarose gels were prepared using agarose (Severn Biotech) dissolved in appropriate volume of 1x TAE buffer. The mixture was heated in a microwave until agarose was fully dissolved and allowed to cool prior to addition of ethidium bromide to a final concentration of 10µg/ml, and then poured into gel mould. DNA loading buffer was added to samples, which were run alongside a 1kb DNA ladder (GeneRuler, Bioline) to permit estimation of DNA size. Gels were run in 1xTAE at 90V and bands visualised under UV light.

2.13 DNA restriction enzyme digestion

1 µg of DNA was digested with the appropriate enzymes and the correct buffers, as shown in Table 4, for 1h at 37˚C. DNA was analysed by 1% agarose gel electrophoresis. DNA bands corresponding to size of desired insert were excised and gel extraction of DNA was performed using QIAquick Gel Extraction Kit (Qiagen). Vector DNA was then dephosphorylated using shrimp alkaline phosphatise (SAP) in 10x SAP buffer (both from Roche) to stop re-ligation of the vector. Samples were incubated at 37˚C for 1-2h, followed by incubation at 65˚C to heat inactivate the enzyme.

Table 2-15 Restriction Enzymes and Buffers for Restriction Digestion of DNA

Enzyme (Roche)	Buffer (Roche)	Incubation Temperature
*Bam*HI	A/B	37˚C
*Bgl*II	H/B/A	37˚C
*Eco*RI	H/B	37˚C
*Hind*III	B	37˚C
*Xho*1	H	37˚C

2.14 Ligation of plasmid DNA

Dephosphorylated vector and insert were ligated using the Rapid Ligation Kit (Roche) according to the manufacturer's instructions at 3:1, 2:1 and 1:1 molar ratios of insert to vector alongside no ligase, no insert controls. The mix was incubated at room temp for 30 minutes and then incubated for at least 2 hours at 4°C. The ligated DNA was then transformed into DH5α *E.coli* cells.

2.15 Transformation of plasmid DNA in competent DH5α *E.coli* cells (Invitrogen)

50µl competent DH5α cells were thawed on ice in sterile eppendorf tubes. Approximately 50ng of ligated vector from the ligation reaction was added to the bacterial aliquot and incubated on ice for 30 minutes. Following heat shock for 20s at 42˚C, they were incubated on ice for 2 minutes. 900µl SOC medium (Invitrogen) was then added and bacteria were cultured for 1h at 37˚C with shaking. 50 µl and 100µl of bacterial culture were then spread onto separate LB agar plates containing the appropriate antibiotic for selection of positive colonies under sterile conditions. LB agar plates were then incubated at 37˚C overnight.

2.16 Minipreps and Maxipreps

Transformed colonies were picked under sterile conditions, added to 5ml LB broth containing appropriate antibiotic and cultured overnight at 37˚C with shaking. DNA was prepared using the QIAgen Mini-prep kit, according to manufacturer's instructions. The concentration and purity of DNA was assessed by spectroscopy (ND-1000 Spectrophotometer (Labtech)) at 260nm. An aliquot of the resultant DNA was restriction digested to confirm successful insertion of DNA and results were analysed by agarose gel electrophoresis. 24h later, DNA was extracted from the 200ml bacterial culture using the QIAgen Maxi-prep kit. Vectors were then sequenced using appropriate primers to confirm successful subcloning. All DNA was sequenced at the MRC DNA core laboratory (Imperial College).

2.17 Serum Extraction from Blood

Whole blood samples of prostate cancer patients and healthy controls were collected at Charing Cross, Hammersmith and St Mary's Hospitals via venesection into red

topped, serum collection vacutainer tubes (BD) following written patient consent. The samples were allowed to stand at room temperature for 30 minutes to allow natural clotting to form (containing fibrin and cells) leaving the fluid phase containing the serum on top. The blood was then centrifuged at 1500xg for 10 minutes at room temperature. 1ml aliquots of the supernatant serum were stored at -80°C and recorded with the Imperial College Tissue Bank.

2.18 RNA Extraction from Cell Pellets and Flash-Frozen Tissues

For standard RNA extraction from cells for RT PCR the QIAshredder and Rneasy mini kits (Qiagen) were used, for total RNA extraction including short RNAs and micro RNAs TRIzol and TRIzol LS were used according to manufacturer's instructions. For tissue, the flash-frozen mouse or human xenograft tumours were homogenized using the Precelleys 24 Tissue Homogeniser in 1 ml TriZol. The concentration and purity was assessed by spectroscopy at 260nm (ND-1000 Spectrophotometer (Labtech)) and by gel electrophoresis.

2.19 TRIzol LS Extraction of miRNAs from Serum

Total RNA was extracted from serum using Trizol LS reagent according to manufacturer's instructions. Briefly, 1ml of Trizol was added to 400 µl of serum as well as 1µl (200 µg) of glycogen blue and mixed by repetitive pipetting and incubated at room temperature for 5 minutes. A mimic of *C. elegans* miRNA (cel-miR-39) was added (1µl of 1nM) as a spiked-in control to normalise for purification efficiency. 200µl chloroform was added per ml Trizol reagent used and samples were shaken vigorously for 15s, followed by incubation at room temperature for 2-3 minutes. Samples were centrifuged at 12,000x*g* for 15 minutes at 4°C and 500µl of the upper (aqueous) phase transferred to a fresh microcentrifuge tube. 500µl isopropanol was added per ml of Trizol used and samples were incubated at -20°C for 1 hour to allow RNA to precipitate. Samples were centrifuged at 12,000x*g* for 15 minutes at 4°C. The supernatant was removed and pellets were washed once with 500 µl 75% ice cold ethanol per ml Trizol used. Samples were mixed by vortexing and centrifuged at 7,500x*g* for 5 minutes at 4°C. RNA pellets were then air dried for

approximately 7 minutes and dissolved in 50 µl of Rnase-free ddH_2O by incubating at 55-60°C for 10 minutes. RNA samples were then stored at -80°C.

2.20 Reverse Transcription

500ng of total RNA was converted to cDNA using SuperScript First Strand Synthesis System for RT-PCR (Invitrogen) according to the manufacturer's protocol, using Oligo$(dT)_{12\text{-}18}$ primers for full-length cDNA or random hexamers for RT-PCR detection. For miRs MicroRNA-specific reverse transcription was performed using 10ng of RNA and the TaqMan microRNA Reverse Transcription Kit according to the manufacturer's instructions (Applied Bioscience).

2.21 Semi-Quantitative PCR

1µl of cDNA and 25pmoles of the appropriate forward and reverse primers were added to Ready Mix PCR Mastermix system (Abgene). Cycling conditions and primers are detailed in Table 2.15.

Table 2-16 PCR Primers and Conditions

Amplification Product	Primers	Primer Sequences	PCR Conditions
PHB	PHB F	5' GCAGAATTCATGGCTGCCAAAGTCTTTGA 3'	Denaturing: 94°C – 5min Denaturing: 94°C – 30 sec Annealing: 52°C – 30 sec 22 Cycles Extension: 70°C – 1 min Extension: 70°C – 10 min 4°C – forever
	PHB R	5' ACGCTCGAGTCACTGGGGCAGCTGGAGGA 3'	
PHB UTR	PHB F	5' GCAGAATTCATGGCTGCCAAAGTCTTTGA 3'	Denaturing: 94°C – 5min Denaturing: 94°C – 30 sec Annealing: 52°C – 30 sec 40 Cycles Extension: 70°C – 1 min Extension: 70°C – 10 min
	PHB UTR RevSal	5'TTTGTCGACGGAAGGTCTGGGTGTCATTTATTG ACAGCAGTTT-3'	

			4°C – forever

2.22 Gene expression analysis by quantitative real time PCR

Real-Time Quantitative PCR for each gene target was performed in triplicate on cDNA samples (technical replicates). The Taqman reaction consisted of: 2µl cDNA, 5µl Fast SYBR-green master mix and 2µl forward and reverse primers per reaction, reaction volume was adjusted to 10µl with ddH_20. Once all reagents were added to the wells, the 96-well optical plate was sealed with an adhesive cover (PE Applied Biosystems) and spun in a bench top centrifuge (Sorvall) at 2000rpm for 2 minutes. The qRT-PCR was performed using an ABI 900HT real time PCR machine (Applied Biosystems).

Table 2-17 Primer Sequences for SYBR Green qRT-PCR

Amplification Product	**Primer direction**	**Primer Sequences**
L19	For	5' GCAGCCGGCGCAAA 3'
	Rev	5' GCGGAAGGGTACAGCCAAT 3'
AR	For	5' CGCGACTACTACAACTTTCCACTGG 3'
	Rev	5' ACCACCACACGGTCCATACAACTGG 3'
KLK2	For	5' CCTCAGGTTCTGGCATCACTT 3'
	Rev	5' CGGCCAGGTGAGTTCCAA 3'
TMPRSS2	For	5'AATCGGTGTGTTCGCCTCTAC 3'
	Rev	5' GCGGCTGTCACGATCC 3'
DRG	For	5' GCAGCACACACTTCACAAAGC 3'

	Rev	5’ CCAGGCACCCGTTTGAAC 3’
PSA	For	5’ TTGTCTTCCTCACCCTGTCC 3’
	Rev	5’ AGCTGTGGCTGACCTGAAAT 3’
PROHIBITIN	For	5’ GGCTGAGCAACAGAAAAAGG 3’
	Rev	5’-GCTGGCAGGTAGGTGATGTT-3’
EGFR	For	5’-AGGACCCCCACAGCACTGCA-3’
	Rev	5’-CTTGCTGGGGCCATGAAGGC-3’
DICER	For	5’-TGCTATGTCGCCTTGAATGTT-3’
	Rev	5’-AATTTCTCGATAGGGGTGGTCTA-3’
FOXO1	For	5’-TGATAACTGGAGTACATT-3’
	Rev	5’-CGGTCATAATGGGTGAGAGTCT-3’
Caspase	For	5’-GGGACCGAGTGCCTACATATG-3’
	Rev	5’-CACCGATACCTGTCACTTTATCA-3’
RUNX1	For	5’-TCTTCACAAACCCACCGCAA-3’
	Rev	5’-CTGCCGATGTCTTCGAGGTTC-3’
TP53	For	5’-CAGCACATGACGGAGGTTGT-3’
	Rev	5’-TCATCCAAATACTCCACACGC-3’
ACLY	For	5’-ATCGGTTCAAGTATGCTCGGG-3’
	Rev	5’- GACCAAGTTTTCCACGACGTT-3’

HIPK2	For	5'-CCCGTGTACGAAGGTATGGC-3'
	Rev	5'-AGTTGGAACTCGGCTCTATTTTC-3'
APC	For	5'-AAAATGTCCCTCCGTTCTTATGG-3'
	Rev	5'-CTGAAGTTGAGCGTAATACCAGT-3'
THRB	For	5'-GGCGCAGCACGTTGAAAAAT-3'
	Rev	5'-CACATCATCATGGTCCAGATGG-3'
WEE1	For	5'-AGGGAATTTGATGTGCGACAG-3'
	Rev	5'-CTTCAAGCTCATAATCACTGGCT-3'
ARL2BP	For	5'-TATCATGGATGACGAGTT-3'
	Rev	5'-GGTGCTGTAATGTTGTGG-3'
YIPF7	For	5'-GTTCCATCAGAGATGCTC-3'
	Rev	5'-GCAAAGGAGGCTCTTCATCAAA-3'
YAP1	For	5'-TCATGCTTAGTCCACTGTCTGT-3'
	Rev	5'-TAGCCCTGCGTAGCCAGTTA-3'
MTRF1	For	5'-GGTCCAGGAGATATTGCCATCA-3'
	Rev	5'-ACATTGCTCAAGTGTTTGGTACT-3'
MTHFR	For	5'-GAGCGGCATGAGAGACTCC-3'
	Rev	5'-CCGGTCAAACCTTGAGATGAG-3'
HOXB13	For	5'-AGCTCCCGTGCCTTATGGTTA-3'

	Rev	5'-GGCTGGTAGGTTCCCGGATA-3'
NR4A1	For	5-'ATGCCCTGTATCCAAGCCC-3'
	Rev	5'-GTGTAGCCGTCCATGAAGGT-3'
TRIM13	For	5'-GTTTGCCTTGCTCCCACAAC-3'
	Rev	5'TCCTTACGGCATGTAGGACAC-3'
USP31	For	5'-CTGTGGCTTTTGGACCGAGTT-3'
	Rev	5'-CCTCAGGCATCATATCAGTCTCT-3'

2.23 RNA-seq Analysis

Two micrograms of total RNA from each *in vivo* tumour sample was used to produce cDNA libraries using the True-Seq Stranded mRNA preparation kit (Illumina Inc., San Diego, CA, USA) according to the manufacturer instructions. The samples were checked for quality using the Agilent Bioanalyser high sensitivity DNA assay. Paired end sequences (reads) 150 base pairs in length were then generated using a HiSeq 2000 instrument (Illumina). RNA-seq data from each sample in FASTQ file format were quality assessed using fastQC. Reads were mapped using BWA (Li and Durbin 2009) to the Homo sapiens version hg38 reference genome retrieved from UCSC (Kent, Sugnet et al. 2002). Read counts for each exon and gene were generated in R using the GenomicRanges and Samtools Bioconductor packages against the Homo sapiens version hg38 .gtf annotation file. The edger Bioconductor analysis package was used to determine differentially expressed genes using an FDR corrected p-value significance cutoff of 0.05 (Robinson, McCarthy et al. 2010).

Table 2-18: RNAseq data output

Sample ID	Index	Yield (Mbases)	Number of Reads	% of raw reads per lane	% of >= Q30 Bases (PF)
DL	CGATGT	4,811	48,112,286	18.39	96.91
ER	CAGATC	5,341	53,409,722	20.41	97.05
IL	CCGTCC	3,401	34,005,994	13	96.52
OL	TGACCA	6,052	60,523,524	23.13	97.06
TL	GTGAAA	2,077	20,768,750	7.94	95.88
WL	ACAGTG	4,110	41,101,766	15.71	97.01

2.24 microRNA Expression Analysis

MiRNA expression was quantified by quantitative real-time RT-PCR using the TaqMan microRNA assay for miR-27a with FAM probe (Applied Biosystems) and TaqMan Universal PCR Master Mix (Applied Biosystems) according to the manufacturer's protocol. PCR was performed using the ABI 900HT Real-Time PCR System under the 9600 Emulation mode. Cycling conditions were as follows: 95˚C – 10mins, 40 cycles of (95˚C – 15s, 60˚C – 60s). For both qRT-PCR protocols, the comparative C_T method was used for relative quantitation of samples.

Table 2-19 Primer/Probe Mixes Taqman miRNA quantitative PCR

Oligonucleotide	Sequence	Product Number	Cycling Mode
Syn-cel-miR-39	5'-UCACCGGGUGUAAAUCAGCUUG -3' 5'-PHO-UCACCGGGUGUAAAUCAGCUUG -3'	Probe TM:000200 (Life Technologies) Mimic (Eurofins MWG)	9600 Emulation
hsa-miR-27a	5'-UUCACAGUGGCUAAGUUCCC-3' 5'-PHO-UUC ACA GUG GCU AAG UUC CGC-3'	Probe TM: 000408 (Life Technologies) Mimic (Eurofins	9600 Emulation

		MWG)	
hsa-U18	Sequence details not available	Probe TM: 001204 (Life Technologies)	9600 Emulation
hsa-miR-1228	5'-UCACACCUGCCUCGCCCCCC-3'	Probe TM: 002919 (Life Technologies)	9600 Emulation
hsa-miR-195	5'-UAGCAGCACAGAAAUAUUGGC-3' 5'-PHOUAGCAGCACAGAAAUAUUGGC-3'	Probe TM: 000494 (Life Technologies) Mimic (Eurofins MWG)	9600 Emulation
hsa-miR-16	5'-UAGCAGCACGUAAAUAUUGGCG-3' 5'-PHOUAGCAGCACGUAAAUAUUGGCG-3'	Probe TM: 000391 (Life Technologies) Mimic (Eurofins MWG)	9600 Emulation
hsa-miR-141	5'-UAACACUGUCUGGUAAAGAUGG-3' 5'-PHO-UAA CAC UGU CUG GUA AAG AUG G-3'	Probe TM: 000463 (Life Technologies) Mimic (Eurofins MWG)	9600 Emulation
hsa-miR-21	5'-UAGCUUAUCAGACUGAUGUUGA-3' 5'-PHOUAGCUUAUCAGACUGAUGUUGA-3'	Mimic (Eurofins MWG)	
hsa-miR-423	5'-UGAGGGGCAGAGAGCGAGACUUU-3' 5'-PHOUGAGGGGCAGAGAGCGAGACUUU-3'	Mimic (Eurofins MWG)	
hsa-miR-146a	5'-UGAGAACUGAAUUCCAUGGGUU-3' 5'-PHOUGAGAACUGAAUUCCAUGGGUU-3'	Mimic (Eurofins MWG)	

2.25 Creation of Standard Curve of *C. elegans* miRNA-39 and miRNA-27a

Synthetic single-stranded RNA oligonucleotides corresponding to the mature miRNA sequence were purchased from Qiagen sequence information is provided in the table above. A standard curve was produced from an initial stock concentration of 30pM was taken and then 10 4-fold serial dilutions were made in water to a final concentration of 0.1125 fM and used for the RT reaction and then real time PCR was performed on an ABI Thermocycler (representative standard curves are provided in Fig. 4). A line was fit to data using Ct values within the linear range, from which an extraction coefficient (EC) was obtained according to the formula EC= Cel-miR-39initial conc/ Cel-miR-39final conc. The miRNA absolute level can then be derived from the equation miRNA absolute level = EC x (miRNA final conc). In general, the

lower limit of accurate quantification for each assay is designated based on the minimal number of copies input into an RT reaction that results in a Ct value within the linear range of the standard curve. Absolute copies of miRNA input into the RT reaction are converted to copies of miRNA per µl serum based on the knowledge that the material input into the RT reaction corresponds to RNA from 10% of the total starting volume of serum (i.e 5µl of the total RNA elute volume 50µl is input into the RT reaction).

2.26 Multiplex microRNA profiling using Abcam Firefly© technology

Serum samples were sent to the Firefly offices in the USA where they undertook multiplex miRNA assay. Their technology, unlike other approaches, allows the miRNA levels to be quantified in the serum without the need for reverse transcription, library preparation or amplification. The multiplexing is achieved by using encoded hydrogel particles; each bearing a unique barcode that identifies a miRNA species. Once the hydrogel particles are bound to the specific miRNA it is ligated to a universal adapter. After addition of a reporter species this binding event is detected via fluorescence. The level of fluorescence is quantified by a flow cytometer providing an accurate indication of the miRNA level in a given sample.

2.27 Non-Radioactive MicroRNA Northern Blotting

A 1mm non-denaturing urea-acrylamide gel was prepared by heating 20g urea, 4ml 10xTBE and 20ml duracryl in a microwave for 30 seconds. The solution was made up to 40ml with DEPC treated water and cooled to room temperature on ice prior to the addition of 240µl APS and 16µl TEMED. The gel was allowed to polymerise at 4°C for one hour. The gel was pre-run for one hour in 1xTBE. The RNA samples and the ASO-27a double digoxygenin labelled probe (acting as a positive control) were prepared by mixing 10µg of RNA with an equal volume of RNA loading buffer, then denatured at 65°C for 20 minutes. Samples were chilled on ice before being loaded into the pre-rinsed wells of the gel. The RNA was electrophoresed at 180V until the loading dye was seen to have reached 1 cm from the bottom of the gel. RNA bands were visualised by staining the gel with ethidium bromide in 1xTBE for 5 minutes, followed by rinsing with 1xTBE and visualisation of RNA bands on a UV Transilluminator. RNA was then transferred to a positive nylon membrane

(ROCHE) by semi-dry electrotransfer in 1xTBE for 1 hour at 10V. RNA was crosslinked to the membrane by UV crosslinking for 90 seconds. The membrane was then pre-hybridised in 10ml Ambion UltraHyb at 37°C with gentle shaking for 45 minutes. The ASO-27a double dig-labelled LNA-modified probe (Exiqon) was denatured at 95°C for 60 seconds and then added to the hybridisation buffer to a final concentration of 0.5nM. The membrane was then hybridised overnight at 37°C with slow shaking. Following probe hybridisation, the membrane was washed twice for 15 minutes in 2xSSC and 0.1%SDS. Then three times for 10 minutes in 0.1xSSC and 0.1% SDS and once for 10 minutes in 1xSSC. All washing steps were performed at 37°C with gentle shaking. The membrane was blocked by 3-hour incubation in blocking buffer. The membrane was incubated in the antibody solution (Anti-dig-AP (Fab fragment) centrifuged for 5 minutes at 10,000 rpm and diluted 1 in 50,000 in blocking buffer) for 30 minutes at room temperature. The membrane was washed four times for 15 minutes in dig wash buffer at room temperature and then incubated for 5 minutes in detection buffer. The membrane was placed RNA side up in a hybridisation bag and 7 drops of ready-to-use CDP star was added evenly across the membrane and incubated for 5 minutes. Excess CDP star was removed and the hybridisation bag sealed. The membrane was imaged using the Fusion Solo Chemiluminescence Imager (Peqlab).

2.28 Growth of Xenografts

Eight week old Male BALB/c strain nude mice (Harlan, Bicester, UK) were injected subcutaneously with 0.2ml LNCaP/MAR4 cells (1×10^6cells/ml) or PC3 cells (1×10^5cells/ml) suspended in Matrigel in each flank. Mice were monitored daily until tumours were confirmed (2-4 weeks after subcutaneous injection) and the biweekly tail vein injection treatments commenced. Animals received either the LNA modified antagomiR to 27a (ASO-27a), or the matching LNA modified Scram antagomiR, (at a dose of 20mg/kg suspended in 100µl of PBS) or PBS alone. Tumours were measured biweekly using callipers and volumes calculated using the formula width2×length/2 (Janik, Briand et al. 1975).The mice were imaged biweekly using the IVIS Imaging System 100 series (Xenogen Corporation). They were received an intra-peritoneal (IP) injection of the luciferase substrate luciferin at 150mg/kg, then anaesthetized (3% isoflurane, Abbott Animal Health UK) and placed

into a light-tight camera box. Light emission from luciferase was detected by the IVIS Imaging System 100 series at 10 minutes post IP injection (Xenogen Corporation), and overlaid as a pseudocolour image with reference scale, upon a greyscale optical image. Photon emission was later normalized either to tumour volume. Tumours were allowed to grow to 15mm diameter, when the animals were killed, tumours resected and then cut in half with half the tumour fixed in neutral-buffered formalin and the other half flash-frozen and then stored at -80 °C.

Animals received food and water *ad libitum* and were monitored for ill effects. All work was carried out in accordance with the provisions of the Animals (Scientific Procedures) Act 1986 of the United Kingdom (HMSO, London, UK, 1990) and with appropriate local ethical and Health and Safety approval (Workman, Aboagye et al. 2010). All procedures on mice were performed under an appropriate Home Office license.

2.29 Histology and immunochemistry

Dr Mahroukh Nohadani carried out the standard histology protocols. Antibodies used were Ki67 (DAKO M7249 at a concentration of 1:50); Caspase (cleaved caspase 3). Digital images were captured using the ACIS chromovision microscope. Ki67 and caspase positive cells were counted with five different areas within the tumour, containing approximately 200 cells each, for five tumours per group.

Chapter 3 Prohibitin and miR-27a characterisation across a panel of prostate cancer cell lines

Initial research in prostate cancer was undertaken on three cell lines LNCaP, DU145 and PC3, and these remain the most cited in the majority of published research; however, over the years a number of new cell lines have been developed (Sobel and Sadar 2005, Sobel and Sadar 2005). I have used a number of cell lines in the course of my research and have chosen those with differing characteristics that reflect the differing levels of aggression found in clinical prostate cancer and that mirror prostate cancer progression, summarized in Table 3.1. I have ranked these cell lines in order of phenotypic agression. The cell line with the least aggressive characteristics is the RWPE1 cell line. These cells are non-tumorigenic and were isolated from the peripheral zone of a non-neoplastic adult human prostate of a 54-year-old Caucasian man *(Rhim, Webber et al. 1994)*. They were immortalized using a human papillomavirus-18 (HPV-18) vector and are androgen-sensitive *(Bello, Webber et al. 1997)*. The AR was detectable in this cell line and they are slow-growing cells with a doubling time of 58 hours *(Sobel and Sadar 2005)*. These were used as a model of 'normal' prostate epithelium.

The next cell line in my order of aggressive characteristics is the LNCaP cell line, although it signifies a relatively large leap in aggressiveness compared to benign cells. This is a well-characterized androgen-sensitive human prostate cancer cell line (Horoszewicz, Leong et al. 1980). It was originally derived from a needle aspiration biopsy of a lymph node metastatic lesion from a 50-year-old Caucasian man (Horoszewicz, Leong et al. 1980). LNCaP cells grow slowly, with a mean doubling time of 60 hrs depending on the growth medium (Horoszewicz, Leong et al. 1983). The LNCaP cell line is widely used to study prostate cancer since LNCaP cells express stable levels of AR, although the AR is known to have a mutation that results in the T877A amino acid substitution, which in turn results in promiscuous activation of the receptor (Horoszewicz, Leong et al. 1980, Veldscholte, Ris-Stalpers et al. 1990). LNCaP cells are also known to express the oestrogen receptor (ER) (Horoszewicz, Leong et al. 1980). It does not normally metastasize when used in *in vivo* models.

Following on a scale of increasing aggression is the C4-2 cell line. This is a sub-line derived from the consequent tumour formed after co-injection of LNCaP cells together with human osteosarcoma cell line MS into castrated mice (Thalmann, Anezinis et al. 1994, Wu, Hsieh et al. 1994). This cell line is tumorigenic in an androgen-depleted environment, implying that C4-2 has a high growth potential (Thalmann, Anezinis et al. 1994). Moreover, C4-2 was shown to possess the capacity of metastasizing to lymph nodes and bone *in vivo* (Thalmann, Anezinis et al. 1994, Wu, Hsieh et al. 1994).

Table 3-1Cell line characteristics

Cell Lines	Source	Androgen Dependence	Receptor Status	Metastatic in nude mice	Doubling Time
RWPE1	Non-neoplastic adult prostate gland of a 54 yr old Caucasian male	Androgen Dependent	AR wild type PSA +ve	No	58 hrs
LNCaP	Lymph node met from 50 yr old Caucasian male	Androgen Dependent	AR mutant (T877A) PSA +ve	No	60 hrs
C42	Derived from LNCaP injected with human MS fibroblast cells into nude mice that were then castrated	Androgen Independent	AR mutant (T877A) PSA +ve	Yes	48 hrs
VCaP	Spinal cord met from male Caucasian with CRPC	Androgen Independent	AR wild type PSA +ve	Yes LN, bone, liver	53 hrs
DU145	Brain met from 69 yr old Caucasian male	Androgen Independent	AR null No PSA	Yes LN, lung, liver	30-40 hrs
PC3	Bone met from 62 yr old Caucasian male	Androgen Independent	AR null No PSA	Yes	30-40 hrs

Yr= year hrs=hours met=metastasis AR= Androgen receptor PSA=prostate specific antigen LN=Lymph node MS=osteosarcoma cell line CRPC=castrate resistant prostate cancer

The next cell line is VCaP, this is an androgen-sensitive prostate cancer cell line that is commonly used as a model to study the mechanisms of cancer progression and metastasis (Korenchuk, Lehr et al. 2001, Lee, Korenchuk et al. 2001). This cell line was derived from a 60-year-old Caucasian man diagnosed with hormone refractory

prostate cancer (Korenchuk, Lehr et al. 2001). The tissue was harvested at autopsy from a metastatic lesion to a lumbar vertebral body, and expresses AR. The cells are androgen-sensitive both *in vitro* and *in vivo* (Korenchuk, Lehr et al. 2001).

The penultimate cell line in my panel is the DU145, this was the first epithelial prostate cancer cell line to be established in tissue culture (Stone, Mickey et al. 1978). DU145 cells were derived from a tumour-mass excised from the brain of a 69-year-old Caucasian man diagnosed with prostate cancer and lymphocytic leukemia (Stone, Mickey et al. 1978). The mean doubling time of this androgen-independent cell line is about 34 hrs, this is higher due to the loss of AR and is tumerogenic in mice (Sobel and Sadar 2005).

Lastly on the aggression scale are the PC3 cell line, this is an androgen-independent prostate cancer cell line derived from a lumbar vertebral metastasis lesion from a 62-year-old Caucasian man (Kaighn, Lechner et al. 1978). PC3 cells grow relatively fast with a doubling time of approximately 33 hours (Sobel and Sadar 2005). This line has the highest metastatic potential in mice in comparison to the rest of prostate cancer cell lines studied in this project and is considered to be an essentially androgen-independent Prostate cancer cell line. In both PC3 and DU145, there is no detectable AR or PSA expression (Sobel and Sadar 2005).

Based on the previous work conducted in our lab, as outlined in the Introduction, I hypothesize that altered expression of the prohibitin gene results in a more aggressive and metastatic phenotype, see Figure 3.1. Furthermore, I hypothesise that the microRNA miR-27a may be one of the mechanisms by which alterations of the prohibitin transcript levels are achieved. To explore this further, I hypothesized that prohibitin and miR-27a expression may be altered at progressive stages of advancing prostate cancer cell lines. In this first results chapter I aim to investigate prohibitin and miR-27a in this panel of prostate cancer cell lines.

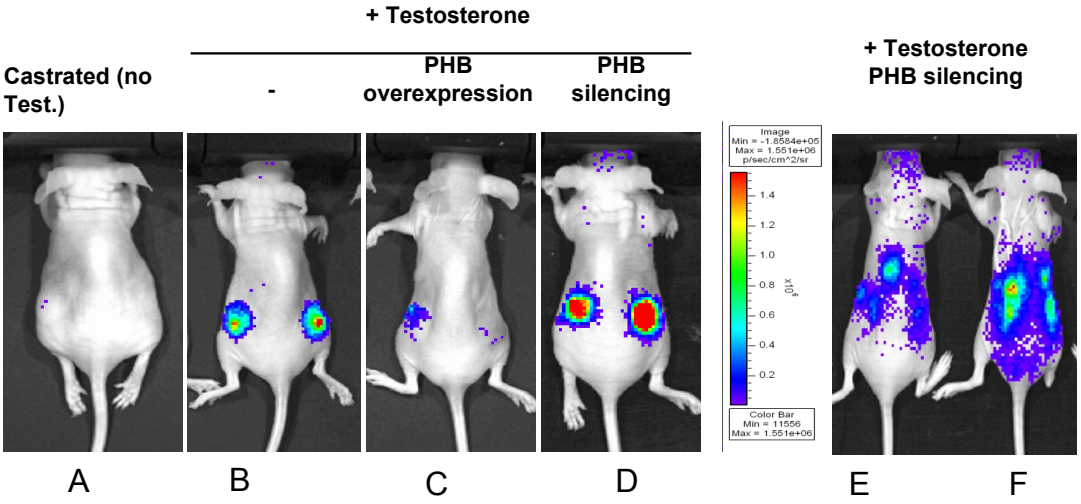

Figure 3.1: Prohibitin manipulation *in vivo*.

Mice carrying prostate cancer xenografts, visible by bioluminescent imaging. Increasing prohibitin levels in the tumours results in decreased tumour size (mouse C) while decreasing prohibitin results in increased tumour size and spread (mice D,E&F) Work by Dr DA Dart.

3.1 Results

3.1.1 Prohibitin transcript levels and protein levels across the cell line panel decrease with increasing aggressive phenotype

The cell lines have been arranged in order of their perceived aggression, as determined by their need for androgen for growth, their doubling times and their ability to metastasise *in vivo,* as seen in Table 3.1. Although this scale of cells is crude and over simplified it does serve to represent various clinical stages of prostate cancer in humans. As discussed in the introduction the cell lines include the RWPE1 cell line representing benign prostate disease, LNCaP cells representing early diagnosis and androgen responsive and dependent cells through to PC3 representing castrate resistant prosate cancer.

Relative prohibitin transcript levels were compared by RT-qPCR as shown in Figure 3.2A. The LNCaP cells had the highest level of prohibitin mRNA of all the cell lines and they are also the least aggressive of the cell lines in the panel, apart from

RWPE1. The lowest levels were found in the VCaP and PC3 cells, which are of the more aggressive cell lines able to metastasize in the xenograft model.

As RNA levels may not equate to functional protein the prohibitin protein levels were also analysed. To quantify the relative expression of prohibitin protein between the differing cell lines, the protein levels were analysed using western blotting. Again, the LNCaP cells were found to have the highest levels of prohibitin and the VCaP the lowest (Figure 3.2B). Figure 3.2D shows the densitometry from triplicate western blots. The lysates were also probed for AR (Figure 3.2C) to assess a potential correlation between AR and prohibitin expression, although there was no apparent correlation (Figure 3.2E and Figure 3.2F), the cell lines with no AR had the lowest levels of prohibitin.

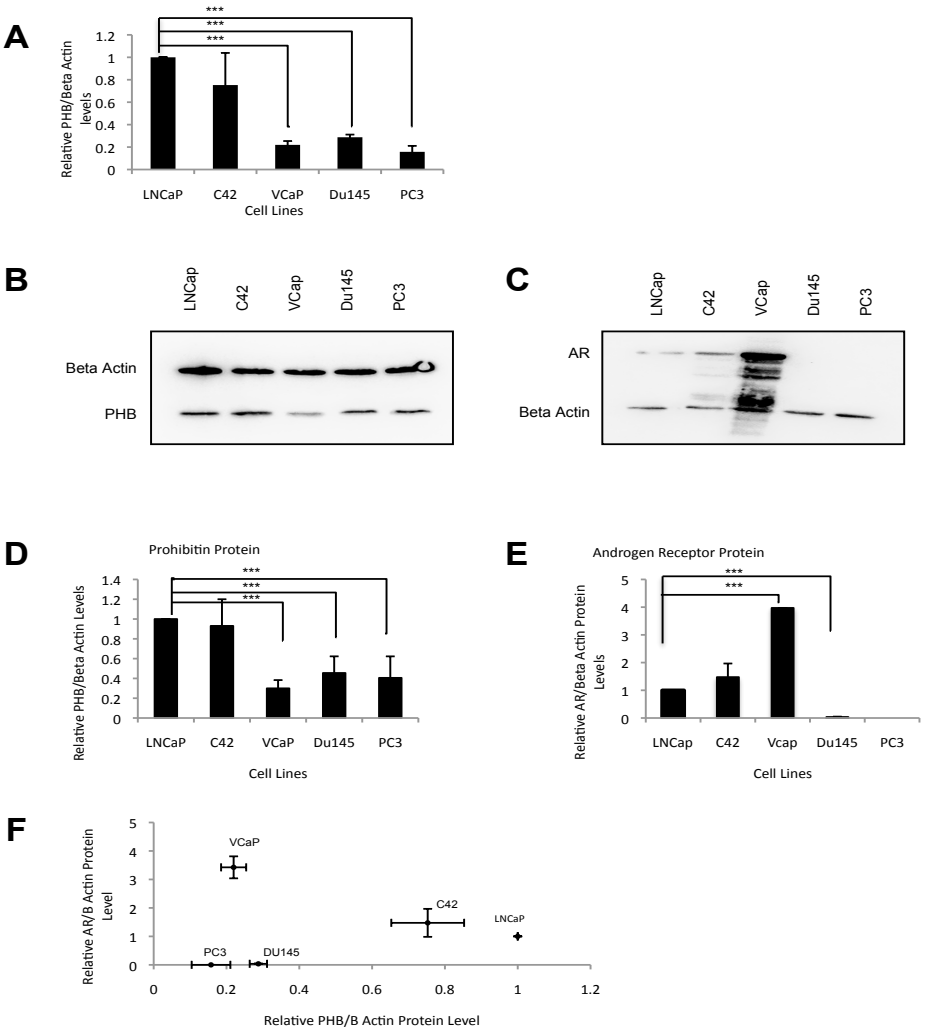

Figure 3.2: Analysis of Expression Levels of PHB in Prostate Cancer Cells

(A) qRTPCR analysis of relative PHB transcript levels from a panel of prostate cell lines that have been arranged in order of perceived aggression. The mean plotted is a result of three independent experiment and the value has been normalised to expression levels of Beta Actin as an endogenous control gene, the results were then made relative to LNCaP. The mean is represented +/- the standard error of the mean. (B) Representative western blot of Prohibitin (PHB) expression from the same panel of prostate cell lines, Beta Actin was used as a loading control. (C) Representative western blot of the Androgen Receptor (AR) expression from the same panel of prostate cell lines data, Beta Actin was used as a loading control. (D) Densitometry of the western blot data for PHB from three independent experiments. The mean is represented +/- the standard error of the mean. (E) Densitometry of the western blot data for PHB from three independent experiments. The mean is represented +/- the standard error of the mean. (F) Analysis of relationship between PHB protein levels and AR protein levels in a panel of prostate cell lines. PHB and AR protein levels were assayed by western blot. Data was normalised using Beta-Actin protein level, and represents the mean +/- SEM of 3 independent experiments. * indicates a P value <0.001 T-Test.**

3.1.2 miR-27a levels inversely correlate with prohibitin levels in the cell line panel

As discussed in the introduction, miR-27a was found to be an oncomiR that targets prohibitin. In order to further explore the relationship between miR-27a and prohibitin, miR-27a levels were assessed by qRT-PCR in the panel of prostate cell lines (Figure 3.3A). It was found that the levels were lowest in the LNCaP cell line, which is a moderately slow growing cell line that does not metastasise *in vivo*. In comparison, the more aggressive VCaP, DU145 and PC3 cell lines have much higher levels. These results were corroborated by examination of expression data from publically available data on www.ncbi.nlm.nih.gov/geo (GSE17317; Figure 3.3B) (Boll, Reiche et al. 2013). This data set did not contain C4-2 or VCaP prostate cancer cell lines.

In work done in collaboration with Dr Claire Fletcher in the lab, prohibitin levels were shown to inversely correlate with miR-27a expression (Figure 3.3C). The strength of the correlation was high, with a Pearson Correlation Coefficient value (r) of -0.881, and the association was highly significant (P=0.0088) (Fletcher, Dart et al. 2012).

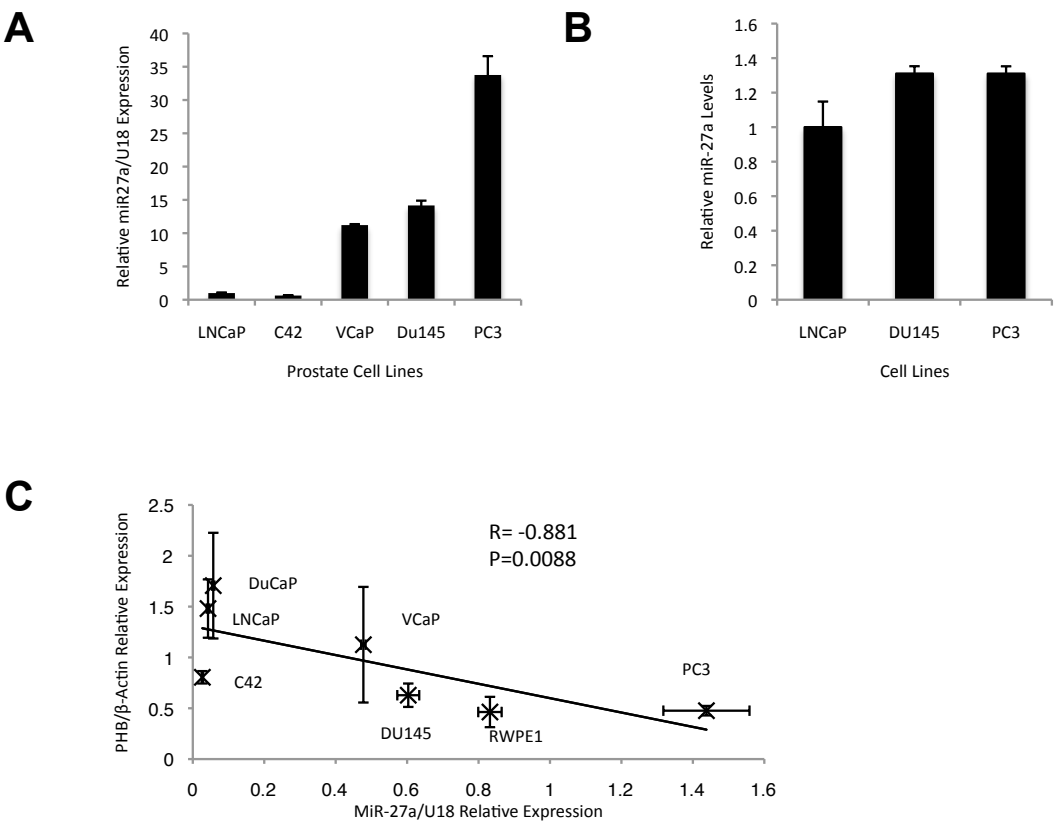

Figure 3.3: miR-27a levels *in vitro*

(A) qRT-PCR data measuring miR-27a from a panel of prostate cell lines, U18 was used as an endogenous control gene. Columns represent the mean gene expression across two independent experiments performed in triplicate +/- SEM (B) Data from a public array GSE17317. (C) Analysis of relationship between PHB protein levels and miR-27a levels in a panel of prostate cell lines. PHB protein levels were assayed by western blot and the miR-27a levels by qRT-PCR. Data was normalised using Beta-Actin protein level and U18 expression respectively, and represents the mean +/- SEM of 3 independent experiments. Pearson correlation coefficient (r) was calculated to assess correlation between PHB protein levels and miR-27a expression.

3.1.3 Prohibitin expression is lower in metastatic prostate tumours

It is very difficult to obtain metastatic tissue from prostate cancer patients as they rarely undergo biopsy or excision of the metastasis as part of the natural patient journey. In lieu of this, a publically available study was mined for data of expression levels of prohibitin and other potential miR-27a targets (GSE6919) (Yu, Landsittel et al. 2004, Chandran, Ma et al. 2007). As can be seen in Figure 3.4 A Prohibitin levels are highest in benign prostate tissue, and are subsequently lower in primary prostate cancer tissue and at the lowest in metastatic prostate tissue. This was a highly significant difference (p value of 3.14 E-06 T-test).

Using a database that records the experimentally valid miRNA-target interactions, I identified some of the most well validated targets of miR-27a as described in the introduction in Table 1.3. GSE6919 was mined for these targets and the results are displayed in Figure 3.4 B. Out of the ten targets examined eight of them had significant differences in expression between benign prostate tissue and metastatic prostate cancer tissue. As can be seen FOXO1, IGF1, and TP53 all showed significantly less expression in the metastatic deposits compared to benign prostate tissue, similar to prohibitin. Conversely EGFR, HIPK2, RUNX1, ACLY and Wee1 were all significantly increased in the metastatic tissue when compared to the benign tissue.

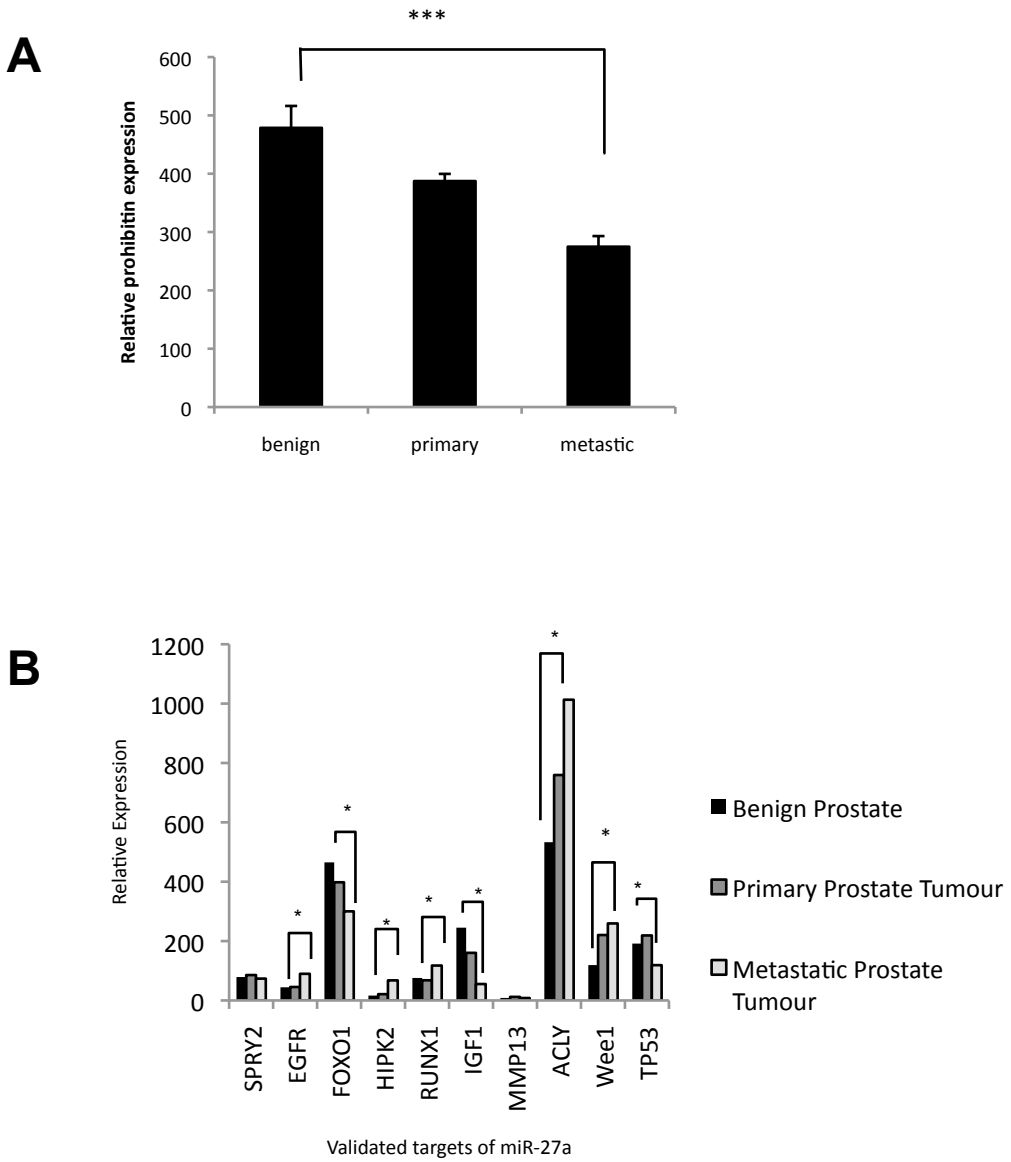

Figure 3.1: Gene expression across progressive human prostate cancer tissues.

Array data from GEO study GSE6919 (A) PHB gene expression levels in different prostate cancer tissues (* P value = 3.14 E-06 T-test) and (B) other validated targets of miR-27a**

3.1.4 Prohibitin is found in both the nucleus and the mitochondria of the prostate cancer cell line panel

Evidence is conflicting as to the cellular localization of prohibitin within cells. Initially prohibitin was reported to be confined to the mitochondria and the cell membrane but it has since been shown that there is nuclear localisation in some cells, particularly hormone sensitive cells such as breast and prostate (Gamble, Odontiadis et al. 2004). As these cell lines will be used for subsequent experiments in this study, and because it is possible that the nuclear pool of prohibitin would be more significant than total levels for the cell cycle and AR effects, I considered it important to confirm both mitochondrial and nuclear localization. In addition cells with a higher metabolic profile or doubling times may have higher levels of mitochondria and in turn higher levels of prohibitin. Immunofluorescence was used to determine cellular location of prohibitin. The cells were grown adjacent to each other in a divided glass chamber slide to ensure equal conditions, and then fixed and stained simultaneously with consistent levels of antibody. As can be seen in Figure 3.5, the prohibitin staining is found in the cytoplasm in all the cell lines as expected. In some of the cell lines notably, LNCaP, VCaP and PC3 the staining correlates well with DAPI staining, indicating nuclear location. The PC3 cell line shows very strong nuclear staining and little cytoplasmic staining in comparison to the other cell lines. However it should be noted, the staining of the PC3 cells was done at a different time and on a different microscope and is only a preliminary result.

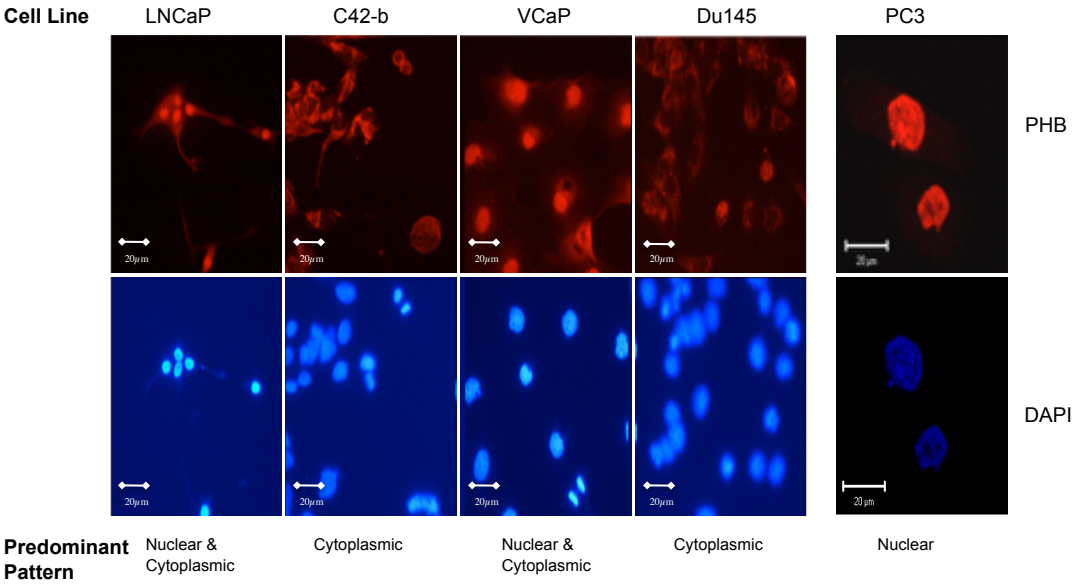

Figure 3.2: Confocal microscopy of PHB localisation in LNCaP, C42-b, VCaP, DU145 and PC3 cells

Cells were grown in full media in adjacent chambers on a single glass slide allowing the same conditions to be applied to all. The red staining (TRITC) is indicative of PHB and the blue is TOPORO/DAPI staining of the nucleus. Note the PC3 cells were imaged at a separate time point and to a higher magnification.

3.1.5 Prohibitin is wild type across the cell line panel

Since our overall aim is to increase functional cellular prohibitin levels we needed to know whether prohibitin was wild type in all our models. To date 12 prohibitin SNP mutations have been reported in prostate cancer cases (see Figure 1.3) but there are no prostate cancer cell line reported mutations, however, there are reported mutations in prohibitin in breast cancer cell lines and Hela the cervical cancer cell line (Sato, Saito et al. 1992, Jupe, Liu et al. 1996, Manjeshwar, Branam et al. 2003). RNA was extracted from pelleted cells and the prohibitin transcript was reverse transcribed to cDNA. The prohibitin coding region and 3' UTR were then amplified and the PCR product was then verified on a gel, extracted and sent for sequencing. In addition to enable sequencing of the complete 3'UTR, genomic DNA was extracted and then the relevant section was amplified by PCR before the product was sent for sequencing. From the regions sequenced I found that all of the prostate cancer cell lines

sequenced (LNCaP, C4-2, VCaP, DU145 and PC3) express wild type prohibitin (Figure 3.6 A). Hela cells were sequenced as a positive control for the methodology as there is a reported mutation at base 852 in the 3'UTR of PHB in these cells. Figure 3.6 B shows the single base change from a T to a C. Only 90-95% of the DNA has been covered in both directions thus far, due to the limitations of the primers and sequencing technology. Figure 3.7 demonstrates the prohibitin DNA sequence and highlights the position of the miR27a binding region on the 3'UTR.

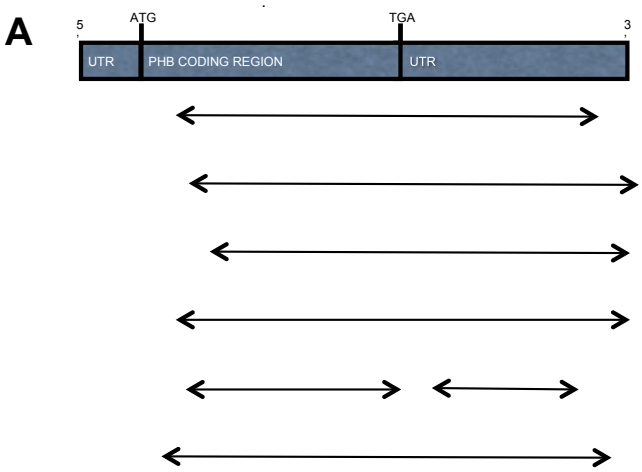

Cell Line	Percentage Coverage	Bases covered
LNCaP	88%	91→1701
C42	86%	144→1710
VCaP	77%	315 → 1724
Du145	90%	112→ 1750
PC3	75%	135→858 1025→ 1680
Hela	90%	84→1736

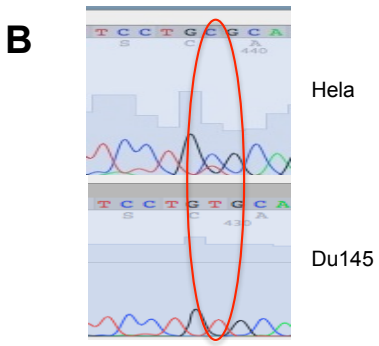

Figure 3.3: Amplification and sequencing of PHB cDNA coding region and 3' UTR.

(A) Schematic diagram indicating the sequencing coverage of prohibitin (B) Chromatogram from sequencing reaction of DU145 and Hela cell line created with 4Peaks software. Sequencing PHB the upper panel demonstrates a single nucleotide change (T →C) at position 729 in the PHB 3'UTR found in Hela cells the lower panel demonstrates wild type PHB sequenced from DU145 cells.

5′

```
     1 atgtggaggt cagagtggaa gcaggtgaga atggaggggg cggcaaaggc tcgtttctgg
    61 gcatctctgc agtcctcctc tgctccatga tgtgcacttt gggcgaggag agtgcgtgcg
   121 tgtgagaggg tccagcagaa ggaaacatgg ctgccaaagt gtttgagtcc attggcaagt
   181 ttggcctggc cttagctgtt gcaggaggcg tggtgaactc tgccttatat aatgtggatg
   241 ctgggcacag agctgtcatc tttgaccgat tccgtggagt gcaggacatt gtggtagggg
   301 aagggactca ttttctcatc ccgtgggtac agaaaccaat tatctttgac tgccgttctc
   361 gaccacgtaa tgtgccagtc atcactggta gcaaagattt acagaatgtc aacatcacac
   421 tgcgcatcct cttccggcct gtcgccagcc agcttcctcg catcttcacc agcatcggag
   481 aggactatga tgagcgtgtg ctgccgtcca tcacaactga gatcctcaag tcagtggtgg
   541 ctcgctttga tgctggagaa ctaatcaccc agagagagct ggtctccagg caggtgagcg
   601 acgaccttac agagcgagcc gccacctttg ggctcatcct ggatgacgtg tccttgacac
   661 atctgacctt cgggaaggag ttcacagaag cggtggaagc caaacaggtg gctcagcagg
   721 aagcagagag ggccagattt gtggtggaaa aggctgagca acagaaaaag gcggccatca
   781 tctctgctga gggcgactcc aaggcagctg agctgattgc caactcactg gccactgcag
   841 gggatggcct gatcgagctg cgcaagctgg aagctgcaga ggacatcgcg taccagctct
   901 cacgctctcg gaacatcacc tacctgccag cggggcagtc cgtgctcctc cagctgcccc
   961 agtgagggcc caccctgcct gcacctccgc gggctgactg ggccacagcc ccgatgattc
  1021 ttaacacagc cttccttctg ctcccacccc agaaatcact gtgaaatttc atgattggct
  1081 taaagtgaag gaaataaagg taaaatcact tcagatctct aattagtcta tcaaatgaaa
  1141 ctctttcatt cttctcacat ccatctactt ttttatccac ctccctacca aaaattgcca
  1201 agtgcctatg caaaccagct ttaggtccca attcggggcc tgctggagtt ccggcctggg
  1261 caccagcatt tggcagcacg caggcggggc agtatgtgat ggactgggga gcacaggtgt
  1321 ctgcctagat ccacgtgtgg cctccgtcct gtcactgatg gaaggtttgc ggatgagggc
  1381 atgtgcggct gaactgagaa ggcaggcctc cgtcttccca gcggttcctg tgcagatgct
  1441 gctgaagaga ggtgccgggg aggggcagag aggaagtggt ctgtctgtta ccataagtct
  1501 gattctcttt aactgtgtga ccagcggaaa caggtgtgtg tgaactgggc acagattgaa
  1561 gaatctgccc ctgttgaggt gggtgggcct gactgttgcc ccccagggtc ctaaaacttg
  1621 gatggacttg tatagtgaga gaggaggcct ggaccgagat gtgagtcctg ttgaagactt
  1681 cctctctacc ccccaccttg gtccctctca gatacccagt ggaattccaa cttgaaggat
  1741 tgcatcctgc tggggctgaa catgcctgcc aaagacgtgt ccgacctacg ttcctggccc
  1801 cctcgttcag agactgccct tctcacgggc tctatgcctg cactgggaag gaaacaaatg
  1861 tgtataaact gctgtcaata aatgacaccc agaccttccg gctcagccaa aaaaaaaaa
```

3′

Figure 3.4: Prohibitin DNA Sequence.

The underlined text corresponds to the coding region. The highlighted text (tcactgt) indicates the miR-27a binding site. NCBI Reference Sequence NG_023046.1

3.2 Discussion

3.2.1 Prohibitin transcript levels and protein levels inversely correlate with increasing aggressiveness of the cell lines

Prohibitin is a multifunctional protein, with diverse roles from mitochondrial respiration to regulation of gene transcription. It was important to establish baseline endogenous prohibitin levels in the cell lines that I will go on to work with in this study. In addition establishing endogenous levels in the prostate cancer cell line panel allows us to assess any potential correlation between protein levels and perceived aggression. When the data for the panel of cell lines is organized in order of increasing aggressiveness, the prohibitin transcript and protein levels are found to decrease. Although simplistic, and with a subset of cell lines (five cell lines from the 17 human prostate cancer cell lines described on the ATCC database), this demonstrates a possible correlation between increasing aggression and decreasing prohibitin levels. Supporting the hypothesis that decreasing prohibitin levels is one of the mechanism by which prostate cancer cells become more aggressive and ultimately evade hormonal control.

When the lysates were probed for AR there appears to be no correlation between prohibitin levels and AR levels. This evidence would indicate that there is not a direct effect on the protein level of AR when prohibitin levels are lowered and therefore this is not the mechanism by which we see a change in aggression of the prostate cancer cells. As a caveat; LNCaP, C4-2 and C4-2-b cells are all known to have a mutant AR and this may require less protein expression to achieve equivalent level of function as wild type AR or less ligand (Sobel and Sadar 2005).

3.2.2 miR-27a levels inversely correlate with prohibitin levels in the cell line panel

It has been shown that prohibitin protein levels are reduced by approximately 50% when treated with androgen (Gamble, Odontiadis et al. 2004). However, androgen treatment has been shown by Dr Claire Fletcher in our lab to only reduce prohibitin promoter activity by approximately 20% which led to the hypothesis that the inhibitory effect of AR signalling is mediated in part through miRNA binding of the 3'UTR, although it doesn't rule out sumoylation, phosphorylation or glycosylation as

these are mechanisms that could inactivate prohibitin (Fletcher, Dart et al. 2012). In order to investigate the potential correlation between miR-27a and prohibitin protein levels, Dr Fletcher and I investigated miR-27a expression across the same panel of prostate cancer cell lines with increasing *in vivo* aggressiveness. As shown, prohibitin transcript levels were highest in the least aggressive cell lines, such as LNCaP, and generally lower in the highly metastatic cell lines such as PC3s. An inverse correlation was seen in the profiling of miR-27a transcript levels. VCaP and DU145 cells had a twelve and fourteen fold higher transcript levels of miR-27a respectively then the less aggressive LNCaP cell lines and PC3 the most aggressive cell line had the highest levels approximately thirty-four times higher mature miRNA transcript levels. These data suggest that high levels of miR-27a could lead to low levels of prohibitin protein. Indeed there was a significant correlation between miR-27a levels and prohibitin protein levels across the panel of cell lines. In addition, Dr Fletcher's work on prohibitin UTR mutants prove that miR-27a does in fact reduce prohibitin levels (Fletcher, Dart et al. 2012). This is suggestive of the potential importance of miR-27a regulation of prohibitin levels and that the increased expression of miR-27a and attendant decrease in prohibitin may be aiding the progression of prostate cancer to a more aggressive phenotype.

3.2.3 Prohibitin expression is lower in metastatic prostate tumours

Dr Alwyn Dart showed that when prohibitin was silenced *in vivo* the normally non-metastatic cell line LNCaP was found to metastasize (Dart, Spencer-Dene et al. 2009). When looking at prostate cancer tissue specimens in a publically available data set the metastatic prostate tissue had significantly less prohibitin expression then the benign prostate tissue. This supports the hypothesis that lower prohibitin levels correlates with increasing aggressive metastatic ability of prostate cancer. This forms the basis for the next chapter of my thesis exploring the effects of manipulating prohibitin in the more aggressive cell lines with lower baseline endogenous levels of prohibitin. If we are able to increase the prohibitin levels in these cell lines we hypothesize that we will see less proliferation and cell cycle activity.

Within the same data set, looking at a further ten validated targets of miR-27a, in addition to prohibitin, showed a mixed pattern of changes in expression between

benign and metastatic tissue, *FOXO1, IGF1*, and *TP53* all showed significantly less expression in the metastatic deposits compared to benign prostate tissue in keeping with prohibitin. In contrast *EGFR, HIPK2, RUNX1, ACLY* and *Wee1* all showed increased expression in metastatic tissue when compared to the benign. Although we hypothesise that in the case of prohibitin its post transcriptional levels are modified extensively by miR-27a it does not mean that this is the predominant mechanism of control for these other genes and perhaps reflects the complex nature of genetic changes that take place in the progression of prostate cancer. Out of the ten genes analysed from the expression data eight were significantly altered at mRNA level indicating the importance of the targets that have been validated for miR-27a and indicating the potential for widespread effects of an antagomiR to miR-27a due to the large number of its targets. These changes were seen at the RNA level we would need to check the protein levels for further validation. However, this data provides some basis for the work I went onto do with the antagomiR to miR-27a.

3.2.4 Prohibitin is found in both the nucleus and the mitochondria of the prostate cancer cell line panel

Prohibitin is a protein with multiple roles that appear to be defined by its subcellular localization, from mitochondrial respiration to regulation of gene transcription. In initial studies prohibitin was reported as being exclusively cytoplasmic (Coates, Jamieson et al. 1997), however it has since been shown to also be located in the nucleus (Gamble, Odontiadis et al. 2004). In some locations, such as at the cell membrane as component of the Raf/Mek/ERK pathway, it is assumed to be tumorigenic, while in others it may be anti-tumorigenic. Prohibitins tumour repressor functions show some correlation with the nuclear localization of the protein as it is here that the cell cycle interactions and androgen receptor interactions occur (Wang, Nath et al. 1999, Gamble, Odontiadis et al. 2004, Gamble, Chotai et al. 2007). In order to establish endogenous prohibitin cellular localization in cell lines used for subsequent experiments in this study, immunofluorescence was performed on the panel of prostate cancer cell lines. Endogenous prohibitin was found to localize both cytoplasmically and to the nucleus of all of the prostate cancer cell lines. There was no decrease in nuclear localization in the more aggressive cell lines, the pattern was actually very variable in the different cell lines. Arguably the most aggressive cell

line PC3 had the most convincing nuclear staining with very little staining in the cytoplasm in contradiction to our initial hypothesis that the more aggressive phenotypic cell lines would have a cytoplasmic predominant pattern of staining. We might have expected the androgen responsive cell lines, LNCaP and C4-2-b to have the higher nuclear:cytoplasic prohibitin ratio as has previously found in hormonally responsive cell lines (Fusaro, Wang et al. 2002). However, as already mentioned this was a very preliminary result (n=1) and the PC3s were stained at a later date to the others and visualized on a different microscope.

3.2.5 Prohibitin is wild type across the cell line panel

On sequencing prohibitin, no mutations were found in any of the prostate cancer cell lines in this panel within the regions analysed. It is likely that the diminished protein levels observed in the more aggressive cell lines are most likely due to a mechanism other than gene alteration.

MiRNAs that bind at least 15 base pairs away from the coding stop site but still close to the coding mRNA section have been shown to confer optimal targeting (Grimson, Farh et al. 2007, Bartel 2009). The prohibitin 3'UTR contains the miR-27a binding site, approximately 100 base pairs from the coding region, thus an optimal targeting position (Figure 3.5). There were no mutations observed in the miR-27a binding sites across the panel of prostate cancer cell lines, which is important as this is our proposed method of increasing prohibitin levels *in vivo*. Any mutations within the binding site may negate any effects on prohibitin levels that we would expect when manipulating miR-27a levels with the anti-sense oligonucleotide to miR-27a. This is important as I used LNCaP cells and PC3 cells to form the xenograft tumours for my work with the antagomiR to miR-27a.

3.3 Summary of Chapter 3

In summary this chapter has demonstrated evidence that prohibitin is decreased in the more aggressive cell lines and also in metastatic deposits in clinical cases of prostate cancer. Conversely miR-27a is increased in the more aggressive cell lines and in the metastatic deposits in clinical cases of prostate cancer. There are no

mutations in prohibitin in this cell line panel and specifically there are no mutations in the miR-27a binding site.

Chapter 4 Generation of Cell Lines to artificially manipulate prohibitin

Prostate cancer is effectively treated by hormonal therapies that target the androgen signalling pathway. However, for each of these therapies the effect is only temporary and inevitably the tumours progress to an advanced stage that is termed castrate resistant. Despite the failure of these treatments, the androgen signalling pathway remains central to prostate cancer growth even in its advanced stages. We have been investigating whether one of the mechanisms by which these tumours escape hormonal control could be via altered levels of co-repressors of the AR such as prohibitin. In the previous chapter I established that prohibitin levels are lower in those prostate cancer cell lines with a more aggressive phenotype, both at a protein and mRNA transcript level. In addition, prohibitin gene expression is lower in metastatic prostate tissue, see Figure 3.4A (Yu, Landsittel et al. 2004, Chandran, Ma et al. 2007). It has already been established that overexpressing prohibitin in the LNCaP cell line arrests growth; conversely knocking it down leads to increased growth and also increased metastatic ability (Dart, Spencer-Dene et al. 2009). Thus, I aimed to elucidate the effects of altering prohibitin levels on the growth of further prostate cancer cell lines.

To analyse the effects of changing prohibitin levels, I aimed to create a panel of prostate cancer cell line pairs stably expressing either flag-tagged prohibitin or an siRNA to knock down prohibitin, respectively. LNCaP knockdown and overexpression lines have already been created by Dr A. Dart (Dart, Spencer-Dene et al. 2009). To explore whether these effects are common across other prostate cancer cell lines, I created similar overexpression and knockdown models in cell lines of differing aggressiveness and metastatic ability.

4.1 Results

4.1.1 The creation of C4-2 and DU145 cell lines that overexpress or knock down prohibitin

A schematic diagram outlining the Tetracycline-induced (Tet-on) expression system can be seen in Figure 4.1. In brief the cells were stably transfected in turn with a tetracycline repressor expression vector, an AR luciferase reporter and the tet-

regulated prohibitin expression vector. The presence of a tetracycline analogue, doxycycline, in the medium, triggers derepression of the CMV promotor in the prohibitin expression vector and expression of either the prohibitin cDNA or a small interfering RNA to prohibitin (siRNA PHB). The C4-2 cell line was chosen as it is derived from the LNCaP cell line but is able to metastasise *in vivo* to a limited extent and is more aggressive. In addition, the DU145 cell line was selected as it is androgen-independent, does not express the AR, and is highly aggressive *in vivo*. The use of an AR-negative cell line may help to determine if the anti-proliferative function of prohibitin is dependent on its roles and actions via the AR.

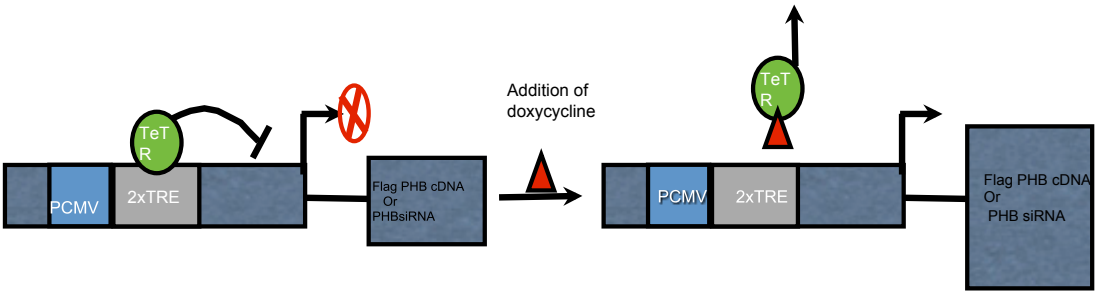

Figure 4.1: Tetracycline on system

Schematic demonstrating tetracycline (doxycycline) inducible PHB overexpression or PHB siRNA expression. Stably transfected tetracycline repressor (Tet-R) constitutively expressed from a stably transfected vector pcDNA6/TR (see Figure 4.2) binds the tet-response element (TRE) on the stably transfected pcDNA4/PHBflag (PHB cDNA promoter) or the pcDNA4/siRNAPHB promoter, leading to repression of PHB expression or siRNA PHB expression. Schematic demonstrating addition of doxycycline derepresses PHB cDNA or siRNA expression by binding the tet-R causing its removal from the promoter.

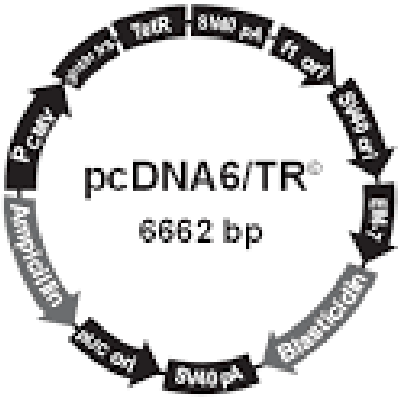

Figure 4.1: The pcDNA6/TR plasmid containing the blastocidin selection cassette, Invitrogen

The first component to be stably transfected into both cell lines was the tetracycline repressor expression vector pcDNA6TR, see Figure 4.2. The cells that had successfully incorporated the vector were able to survive in media containing the antibiotic blasticidin. Six C4-2 clones were harvested, however only 4 successfully grew to allow testing for response to tetracycline using a tetracycline driven luciferase plasmid pcDNA4/luc. This plasmid was transiently transfected into the cultured cells. This vector is similarly controlled i.e. it is repressed by tetracycline, so if luciferase is detected when cells are treated with doxycycline, it indicates the cells express functional tet repressor. The results of the luciferase assay can be seen in Figure 4.3A. The two most responsive clones were then re-tested, Figure 4.3B shows a clone that displayed an on/off response to tetracycline, whereas Figure 4.3C shows that C4-2/TR clone 4 has a dose-dependent response to the addition of tetracyclines C4-2/TR clone 4 was chosen to go forward for insertion of the AR reporter vector as the characteristic of having a dose-dependent response so being able to potentially control the amount of prohibitin being expressed at a later date was preferred. Figure 4.3D shows the testing of the DU145/TR of the 5 clones that survived being grown in blasticidin enriched media for tetracycline responsiveness. DU145/TR clone 2 and clone 5 were tested further as is shown in Figures 4.3E and 4.3F and DU145/TR clone 5 was taken forward for insertion of the AR reporter vector as it had a preferable response to tetracycline.

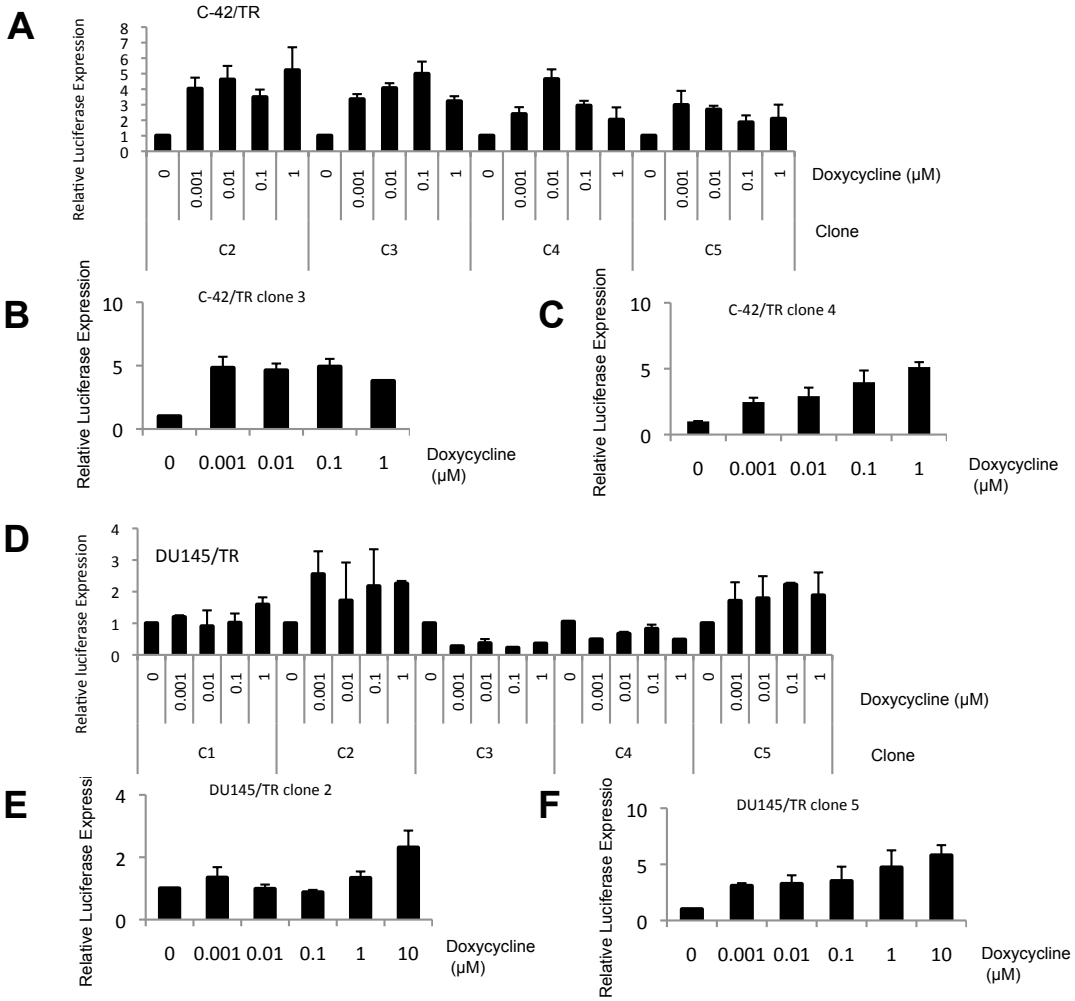

Figure 4.2: Confirming insertion of the Tetracycline Repressor Vector in the C42 and DU145 cell lines.

Clones of C-42 and DU145 cells that survived blastocidin selection treatment were tested for confirmation of insertion of pcDNA6/TR. The cells were transiently transfected with a tetracycline driven luciferase plasmid pCDNA4/luc, 24 hours later they were treated with doxycycline. After a further 48 hours the cells were treated with luciferin and a luciferase assay performed using a luminometer. Since the luciferase was tetracycline driven the activity of the luciferase can be directly corralated to successful integration of the pcDNA6/TR plasmid. Data shown are all representative of the mean ± SEM of n=3. (A) C-42 cells stably transfected with the p2TetR vector, repeated in duplicate. (B) Repeat luciferase assay in the successful clones, C-42/TR/ clone 3 and (C) C-42/TR/ clone 5 (D) DU145 cells transfected with the pcDNA6/TR vector (E) Repeat luciferase assay in the successful clones, DU145/TR clone 2 (F) DU145/TR clone 5

The second component to be stably transfected into the cell lines was the pMAR.ARE vector, a luciferase reporter vector that will inform us as to the activity of the AR as luciferase expression is under the control of a specific androgen response element (Dart, Spencer-Dene et al. 2009). The schematic plasmid map of the vector is shown in Figure 4.4. Matrix attachment regions were used in the plasmid as they have been shown to promote plasmid genomic integration and act as insulators to prevent silencing once the DNA is integrated into the genome (Puttini, van Zwieten et al. 2013). The thymidine kinase promoter was present to increase baseline luciferase signal that was not hormone inducible.

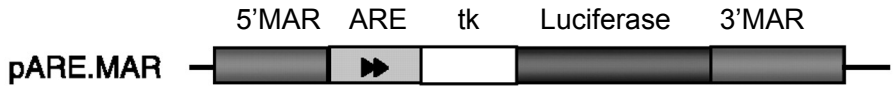

Figure 4.3: The pMAR.ARE Vector.

Picture courtesy of Dr D.A. Dart. MAR = Matrix Attachment Region, ARE = Androgen Response Element, tk = thymidine kinase promotor.

The C4-2/TR and DU145/TR cell lines were transfected with the pMAR.ARE vector and then grown in selection media containing Neomycin (G418). Six C4-2 clones were collected from the selection media and eight DU145, however in each case only 3 grew sufficiently well to be tested to verify insertion of the plasmid. The successful colonies were treated with mibolerone (a synthetic form of testosterone) to activate the androgen response element (ARE) in the plasmid and a luciferase assay was conducted to identify the clone that showed the clearest reporting of AR activity. Figure 4.5A shows that of the C4-2/TR/MAR4 clones, clone 5 showed the biggest response to mibolerone treatment with an almost doubling of luciferase expression. This clone was taken forward for the final stage of stable cell line creation. Of the DU145/TR/MAR4 clones only one showed a good luciferase response to increased AR activity as shown in Figure 4.4B. DU145/TR/MAR4 clone 4 was taken forward for insertion of the prohibitin cassette. By taking this clone forward I was assured

that the cassette was correctly integrated. The data displayed is relative so the fact that the clone responded to testosterone was not too much of a concern due to the negligible levels of AR in this cell line, see Figure 3.2 A. DU145 cells are described as being AR null, however there are reports in the literature of both DU145 and PC3 cells having very low level AR (Alimirah, Chen et al. 2006).

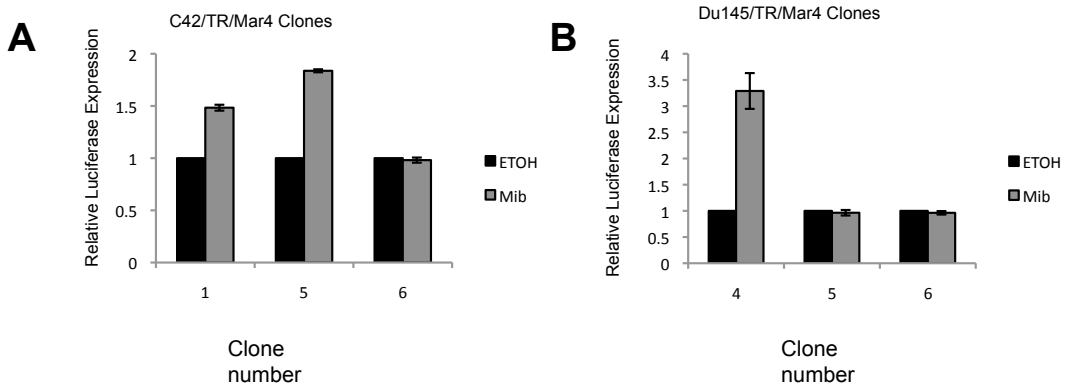

Figure 4.4: Confirming the stable integration of pMAR.ARE into the C42/TR and DU145/TR cell lines

(A) Clones that survived treatment with Luciferase assays from C42/TR/Mar 4 clones grown in starved medium for 72 hours and treated with 10nM of Mibolerone for 24 hours. Data presented relative to no Mibolerone for each clone. (B) Luciferase assays from the DU145/TR/MAR4 clones grown in starved medium for 72 hours and treated with 10nM of Mibolerone for 24 hours. Data shown is an average of three independent repeats, data represents mean +/- SEM.

4.1.2 Cloning of flag-tagged prohibitin and the prohibitin knockdown plasmid

As a means of identifying the over expression of prohibitin induced by our stable cell line we wanted to have a flag tag incorporated with the vector. For the lines ectopically (or exogenously) expressing prohibitin it was a means of discriminating between ectopically expressed and endogenous prohibitin. I fused the coding sequence for a Flag tag in frame within the prohibitin-encoding sequence, in the prohibitin expression vector created by Dr A. Dart in the lab, this was an N-terminal flag. The methodology for this is described in Figure 4.6. Using the plasmid pcDNA4/flagPQBP (donated by S Powell) a double digest was performed with *Eco*R1 and *Xho*1 to remove the PQBP DNA from the plasmid. The same restriction enzymes were then used to digest the plasmid pcDNA4/PHB (A Dart). The plasmid backbone pcDN4/flag and the insert prohibitin were then extracted from the gel and

ligated. The resulting product was then tested for successful insertion using an MSC digest.

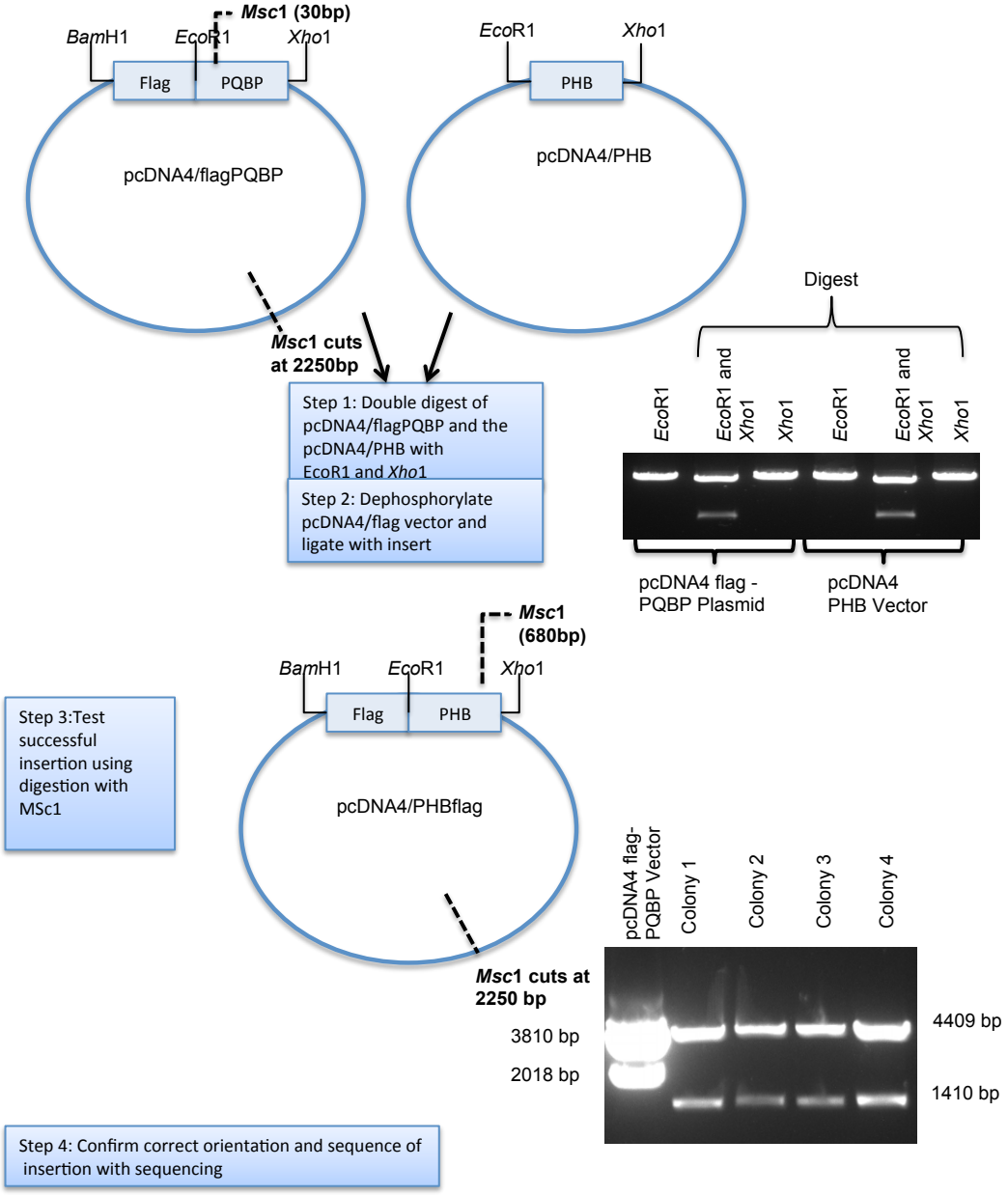

Figure 4.5: Schematic diagram demonstrating the creation of pcDNA4/PHBflag.

PHB = prohibitin. Predicted product size for the pcDNA4/PHBflag vector is 4409bp and 1410bp. This contrasts against the predicted product size for the pcDNA4flag-PQBP vector at 3810bp and 2018bp.

To confirm that the addition of the flag tag had not changed the ability of the plasmid to overexpress prohibitin and that the PHB-flag could still repress AR activity we conducted a repression assay, the results of which can be seen in figure 4.7 A & B. Increasing quantities of plasmid loaded into the transient transfection resulted in a steady increase in flag and in prohibitin. Additionally the response to mibolerone was similar between cells transfected with flag prohibitin or cells transfected with wild type prohibitin, as seen figure 4.7C

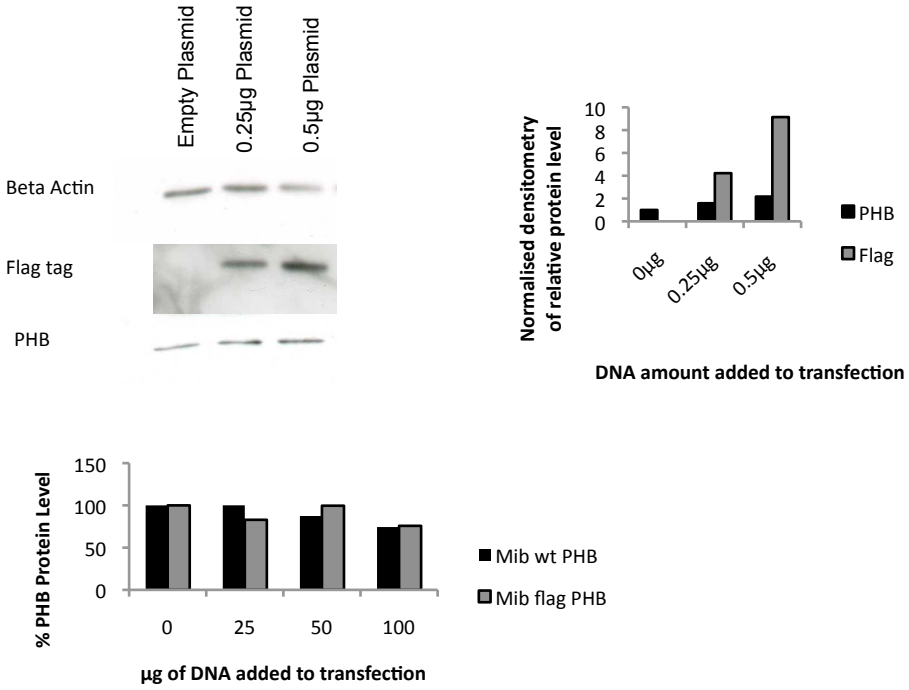

Figure 4.6: Flag tag repression assay. C-42 cells were transiently transfected with increasing quantities of the pcDNA4/PHBFlag plasmid

(A) Protein levels were assayed as shown in this representative western blot (B) Densitometry was conducted to quantify the protein levels of both the Flag tag and prohibitin (PHB) relative to Beta Actin (C) C-42 cells were transiently transfected with either the wild type PHB plasmid (wt PHB) or the Flag tagged plasmid (flag PHB) in increasing concentrations these cells were then treated for 48 hours with mibolorone (Mib) and protein levels of PHB assayed via qRT-PCR and made relative to baseline endogenous PHB levels.

The plasmid was then transfected into C4-2/TR/MAR4 clone 1 and 5, the clones that had successfully incorporated the vector were determined by selection with antibiotic Zeocin. They were then tested for the ability to overexpress prohibitin cDNA in response to treatment with Tetracycline. C4-2/TR/MAR4/PHBFlag clone 5 was chosen as prohibitin protein levels were increased in response to tetracycline (Figure 4.8 A & B) and the transcript was overexpressed approximately 5 fold at the RNA level (Figure 4.8C). Despite multiple attempts at transfection and selection I was unable to successfully achieve overexpression of prohibitin in the DU145/TR/MAR4/PHBFlag cell line. Clones were able to grow in the triple antibiotic selection media, but when tested for ability to express flag-tagged prohibitin they failed to demonstrate this trait (Figure 4.8D). For the characterization of effects of overexpression of prohibitin in this cell line I used transient transfections, as discussed later.

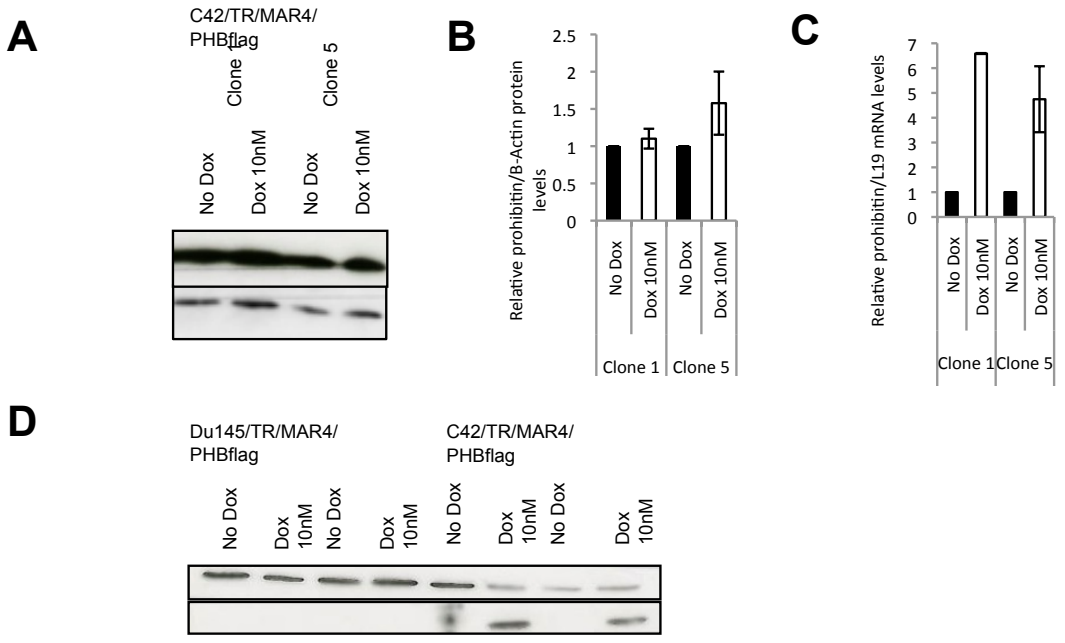

Figure 4.7: Confirmation of the stable integration of pcDNA/flagPHB to C42/TR/MAR4.

(A) Western blot analysis of the prohibitin protein expression levels in the C42/TR/MAR4/PHBflag clones relative to loading control B-Actin (B) Densitometry of the western blot of relative prohibitin levels to B-Actin, data represents the average of 3 individual experimental repeats (C) qRTPCR analysis of prohibitin transcript levels in the C42/TR/MAR4/PHBflag clones. The prohibitin is normalised to L19. Data shows the mean +/-SEM, n=3. (D) Western blot analysis of DU145/TR/MAR4/PHBflag and C42/TR/MAR4/PHBflag clones probed for flag and B-Actin as a loading control.

For the converse experiment – prohibitin knockdown cell lines - silencing of prohibitin expression was achieved using a complementary sequence oligonucleotide that binds to the coding region of prohibitin (Figure 4.9). In transient transfections, this achieved knockdown of prohibitin at the protein level of 95% as shown in figure 4.10A and B. This was then confirmed at the RNA level as shown in figure 4.10C. This oligonucleotide was cloned into the p2xTetR vector and used to stably transfect the C4-2/TR/MAR4 and DU145/TR/MAR4 cell lines to create C4-2/TR/MAR4/siRNAPHB and DU145/TR/MAR4/siRNAPHB.

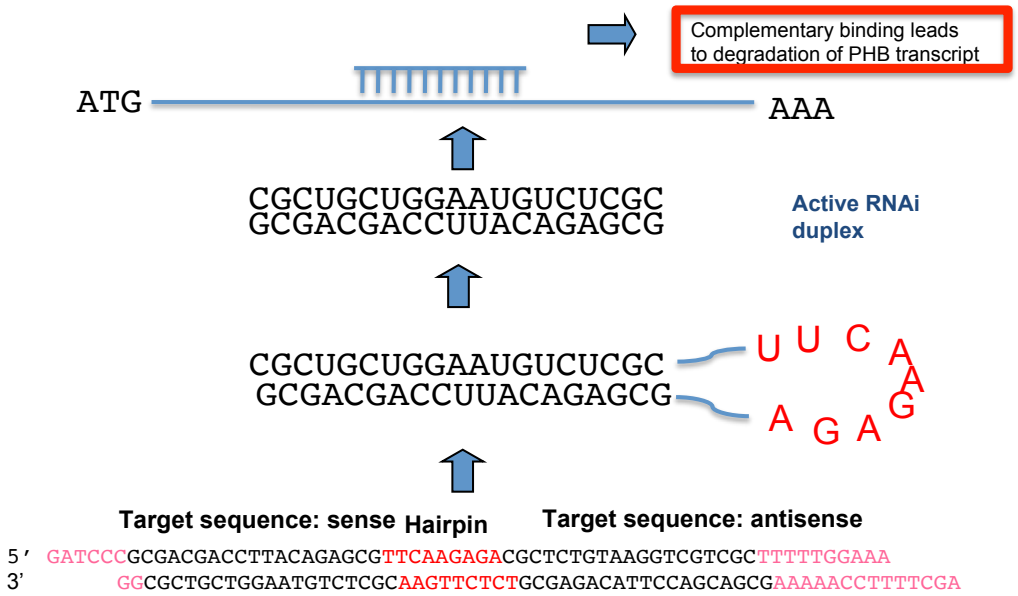

Figure 4.8: The design of an siRNA to target PHB

Schematic demonstrating the creation of the active RNAi duplex using hairpin technology. The active RNAi transcript then binds to its complementary sequence with the PHB transcript and this triggers it for degradation.

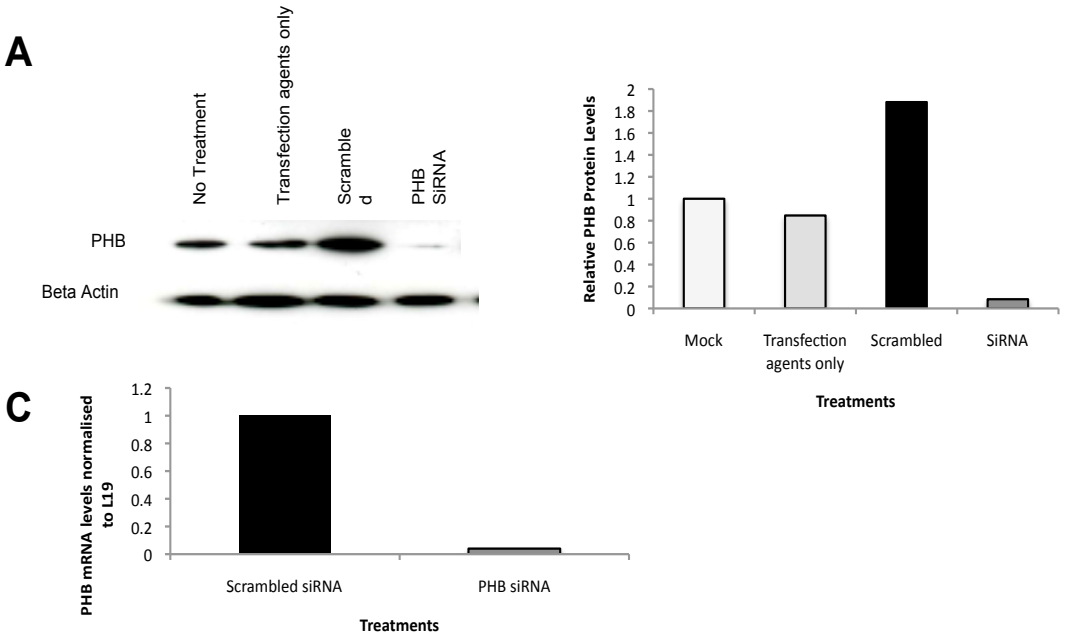

Figure 4.9: siRNA knockdown of PHB

(A) C42 cells were seeded in a 6 well plate then transiently transfected with siRNA against the PHB coding region or a scrambled control. The cells were harvested after 48 hours. The cell extracts were lysed and run on SDS-PAGE gel and transferred to a nitrocellulose membrane before being probed with an antibody against PHB and and Beta Actin. (A) The western blot of PHB and Beta actin acting as a loading control (B) the densitometry of relative PHB levels normalised to beta actin (C) qRTPCR analysis of PHB transcript levels in C42 cells transiently transfected with siRNA against PHB UTR. The PHB ct values are normalised to the ct values for L19.

Figure 4.11 shows that treating the only C4-2/TR/MAR4/siRNAPHB clone able to survive in selection media with 10nM doxycycline resulted in a reduction of the prohibitin protein levels of 60% and almost 80% at the mRNA transcript level (Figure 4.11 A, B & C).

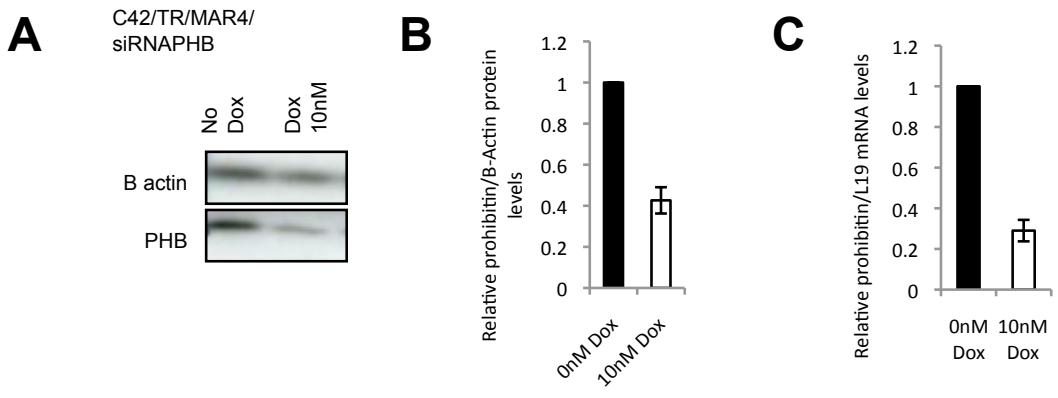

Figure 4.10: Confirmation of the stable integration of pcDNA/siRNA into C42/TR/MAR4

(A) Western blot analysis of the prohibitin protein expression levels in the C42/TR/MAR4/siRNAPHB clones relative to loading control B-Actin (B) Densitometry of the western blot of relative prohibitin levels to B-Actin, data shows the mean of three independent repeats (C) qRTPCR analysis of prohibitin transcript levels in the C42/TR/MAR4/siRNAPHB clones. The prohibitin ct values are normalised to the ct values of L19. Data shows the mean +/-SEM, n=3.

Two DU145/TR/MAR4/siRNAPHB clones survived the selection media and both showed knockdown at protein and mRNA levels (Figures 4.12 A, B and C). Clone two was used for future experiments as it showed a marginally better knockdown.

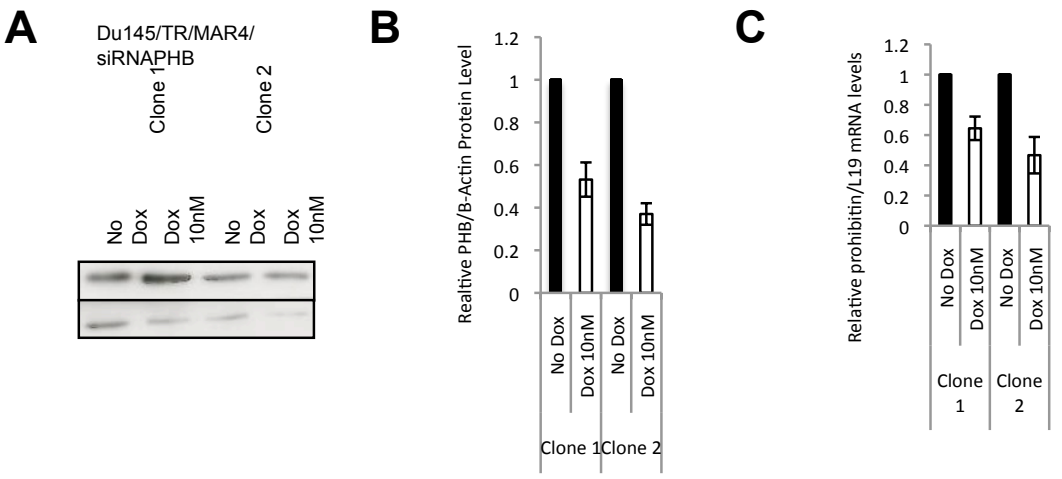

Figure 4.11: Confirmation of the stable integration of pcDNA/siRNA DU145/TR/MAR4

(A) Western blot analysis of the prohibitin protein expression levels in the DU145/TR/MAR4/siRNAPHB clones relative to loading control B-Actin (B) Densitometry of the western blot of relative prohibitin levels to B-Actin, data shows mean of 3 independent repeats (C) qRTPCR analysis of prohibitin transcript levels in the DU145/TR/MAR4/siRNAPHB clones. The prohibitin ct values are normalised to the ct values of L19.Data shows the mean +/-SEM, n=3.

4.1.3 Characterisation of the C4-2/TR/MAR4/PHBFlag Cell Line

The ability of the C4-2/TR/MAR4/PHBFlag cell line to express stably transfected prohibitin cDNA in response to treatment with Tetracycline was confirmed at protein level. An increase in both flag and prohibitin immunoreactivity in cell extract after treatment with 10nM doxycycline was seen (Figure 4.13 A and B). This was also confirmed at the RNA level using qRT-PCR, prohibitin showed an 8-fold increase following exposure to 10nM doxycycline.

To test our hypothesis that increasing cellular prohibitin levels would slow growth and proliferation, the cell line C4-2/TR/MAR4/PHBFlag was grown in full media and then treated with 10nM of doxycycline for 72 hours before FACS analysis of cell cycle was carried out. There was a significant increase in the percentage of cells in the G1 arrest phase of the cell cycle, indicating a shift towards decreased cell division in the cells expressing a higher level of prohibitin, and correspondingly a significant reduction in S and G2 phase (Figure 4.14 A and B). Proliferation was then

assessed using a sulphorhodamine B (SRB) assay. Parental C4-2/TR/MAR4 cells and C4-2/TR/MAR4/PHBFlag were seeded in equal numbers and grown in full medium. Twenty-four hours post-seeding, cells were treated with 10nM tetracycline to induce PHBFlag expression; SRB assays were performed at 0, 3 and 5 days following completion addition of treatment. The expression of PHBFlag decreased proliferation, although not to a statistically significant level (Figure 4.14 C and D). There has been a report in the literature that higher concentrations (greater than 1µg/ml or 2.25µM) of doxycycline can affect growth (Ahler, Sullivan et al. 2013). In order to determine if this was the case in the stable cell lines, I repeated the SRB assay in the C4-2/TR/MAR4 cell line. At a treatment concentration of 10nM there was no effect on growth (Figure 4.14 C).

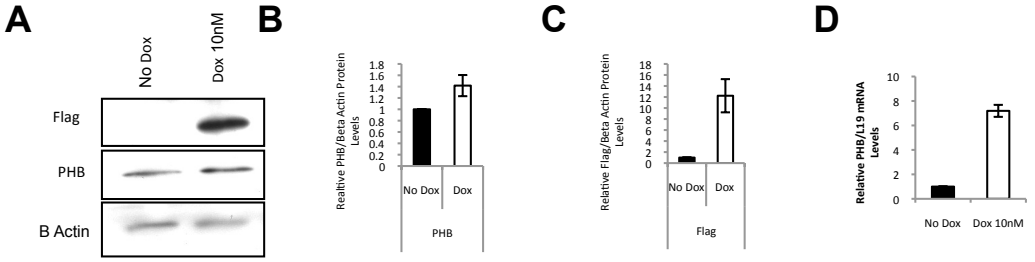

Figure 4.12: Confirmation of the stable integration of the Flag tag

(A) Western blot analysis demonstrating protein levels of PHB, flag and Beta-Actin in the stably transfected C42/TR/Mar4/PHBFlag cell (B) Graphical representation of the relative PHB levels before and after treatment with Doxycycline 10nM (C) Graphical representation of the relative flag levels before and after treatment with doxycyline (D) qRT-PCR data showing the relative increase in PHB mRNA following treatment of the cells with doxycyline. Data shows the mean +/-SEM, n=3

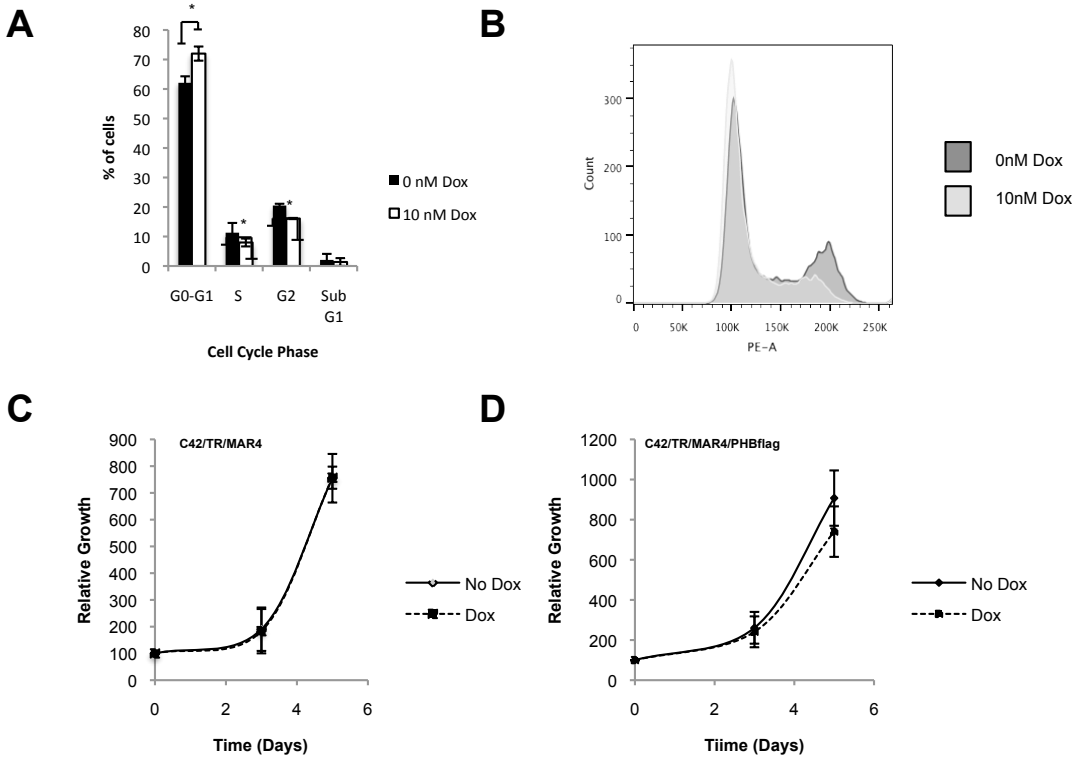

Figure 4.13: Characterisation of C42/TR/MAR4/PHBFlag

(A) C42/TR/MAR4/PHBFlag cells grown in the presence or absence of doxycycline for 72 hours then analysis with FACS. Experiment done in triplicate, points represent the mean ± SEM, * $p<0.05$ (T-Test) (B) Overlay histogram of a typical experiment from the data represented in A (C) C42/TR/Mar4 Cells or (D) C42/TR/Mar4/PHBflag cells treated and untreated with doxycycline (10 nM). SRB assays were performed at 0, 3 and 5 days post treatment. Points: mean relative absorbance ± SEM at 492nm for three independent experiments performed in 15 replicate wells per experiment +/- SEM, where absorbance at day 0 was set at 1 for all treatment conditions.

4.1.4 Characterisation of the C4-2/TR/MAR4/siRNAPHB Cell Line

It was confirmed that treatment with 10nM doxycycline could knockdown prohibitin at a protein and mRNA level in the C4-2/TR/MAR4/siRNAPHB cell line (see figures 4.15 A, B and C). In order to explore the hypothesis that knocking down prohibitin would led to increased proliferation as seen in the LNCaP prohibitin knockdown cell line (Dart, Spencer-Dene et al. 2009), the cells were grown in tetracycline-free medium and then treated with 10nM doxycycline. As can be seen in figure 4.16A and B there was a small decrease in the percentage of cells in G0/G1 arrest and a corresponding small increase in the percentage of cells in G2/M phase, indicating that there was a larger percentage of cells in active cell cycle when prohibitin was knocked down, although this did not reach significance. In addition, proliferation was assessed by growth assay and a small increase in proliferation could be seen, although it did not reach a statistically significant level (Figure 4.16 C).

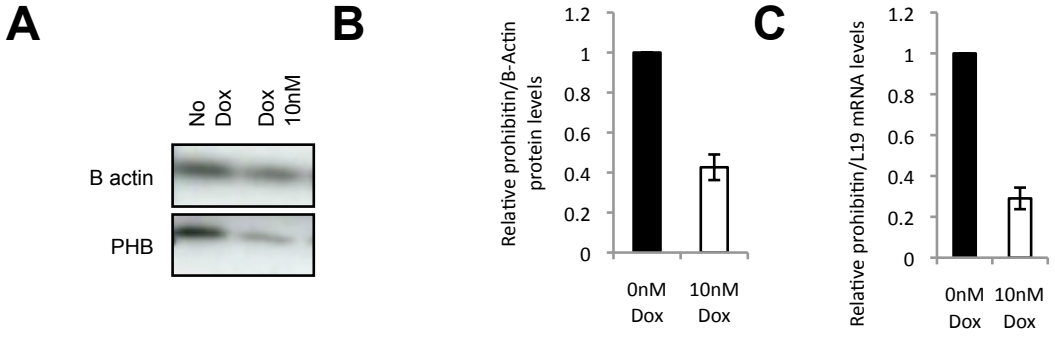

Figure 4.14: Confirmation of the C42/TR/Mar4/siRNAPHB cell line

(A) Western blot analysis demonstrating protein levels of PHB and Beta-Actin (B Actin) in the stably transfected C42/TR/Mar4/siRNAPHB cell line (B) Graphical representation of the relative PHB levels before and after treatment with Doxycycline 10nM, data is representative of 3 independent blots +/-SEM (C) qRT-PCR data showing the relative decrease in PHB mRNA following treatment of the cells with doxycyline. Data shows the mean +/-SEM, n=3.

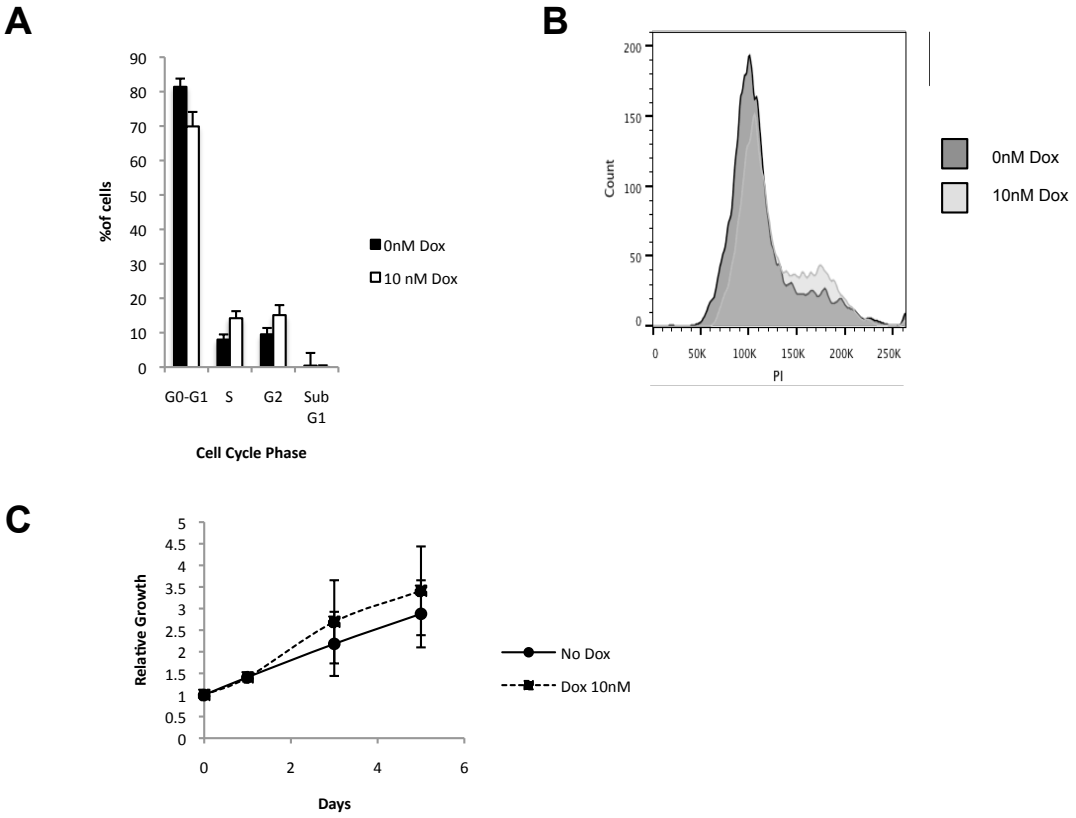

Figure 4.15: Characterisation of C42/TR/MAR4/siRNAPHB

(A) C42/TR/MAR4/siRNA cells grown in the presence or absence of doxycyline (10nM) for 72 hours then analysis with FACS. Experiment performed in triplicate, points represent the mean ± SEM, * $p<0.05$ (T-Test) (B) Overlay histogram of a representative experiment from the data represented in A (C) C42/TR/Mar4/siRNAPHB cells treated with 10nM doxycycline or equivalent volume of vehicle. SRB assays were performed at 0, 3 and 5 days post treatment. Points represent mean relative absorbance at 492nm for three independent experiments performed in 15 replicate wells per experiment +/- SEM, where absorbance at day 0 was set at 1 for all treatment conditions.

4.1.5 The overexpression of prohibitin in the DU145/TR/MAR4 Cell Line

As already discussed above, I was unable to stably incorporate the pcDNA4/PHBflag plasmid into the DU145/TR/MAR4 cell line. In order to investigate the effect of overexpression of prohibitin in this highly aggressive cell line I used transient transfection into the DU145/TR/MAR4 of the PSG5/PHB expression vector. Figure 4.17 A, B and C show that following transfection, the protein level of prohibitin was slightly raised relative to the loading control of Beta-Actin although not to a significant level. However, there was an approximately 45-fold increase of the prohibitin mRNA transcript. This marginal increase in prohibitin protein in this more aggressive cell line had no effect on the cell cycle and on proliferation, as seen in Figure 4.18 A, B and C.

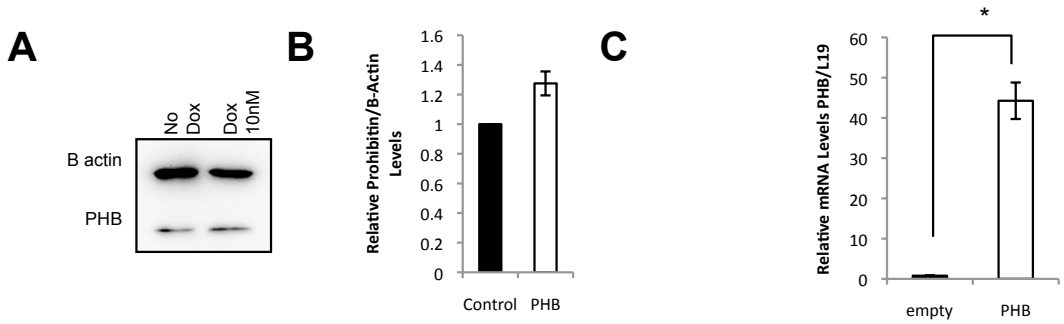

Figure 4.16: Confirmation of the DU145/TR/MAR4 cell line

(A) Western blot analysis demonstrating protein levels of PHB, flag and Beta-Actin (B Actin) in the transiently transfected DU145/TR/MAR4 cell line (B) Graphical representation of the mean relative PHB levels from 3 independent experiments (C) qRT-PCR data showing the relative increase in PHB mRNA following transfection with the PHB plasmid, data shows the mean +/-SEM, n=3.

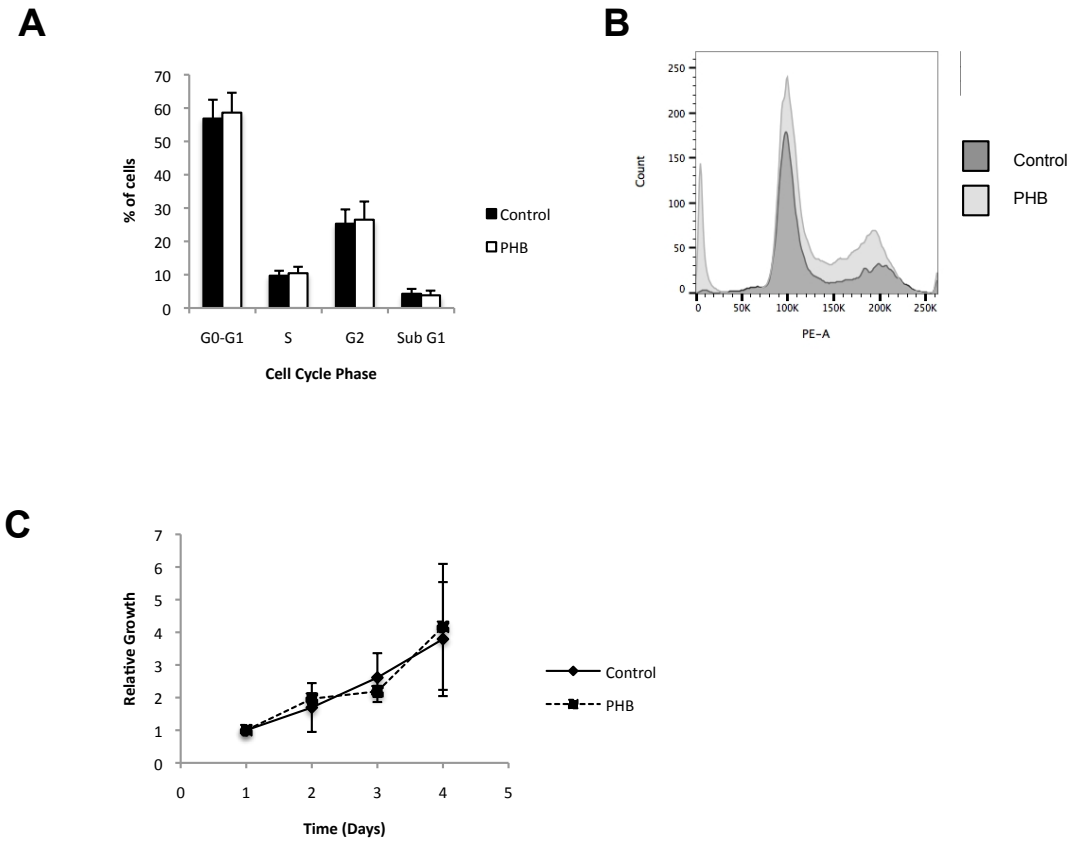

Figure 4.17: Characterisation of DU145/TR/MAR4

Transiently transfected with either the empty pSG5 plasmid (Empty) or the pSG5/PHB plasmid (A) DU145/TR/MAR4 cells transiently transfected with empty pSG5 plasmid (Control) or the pSG5/PHB plasmid then allowed to grow for 72 hours before being analysed by FACS. Experiment done in triplicate, points represent the mean +/-SEM (B) Overlay histogram of a typical experiment from the data represented in A (B) SRB assays were performed at 0, 3 and 5 days post treatment. Points: mean relative absorbance at 492nm for three independent experiments performed in 15 replicate wells per experiment +/- SEM, where absorbance at day 0 was set at 1 for all treatment conditions.

4.1.6 Characterisation of the DU145/TR/MAR4/siRNAPHB Cell Line

I confirmed the knockdown of prohibitin in the DU145/TR/MAR4/siRNAPHB cell line following treatment with doxycyline. Figures 4.19 A and B show that approximately 60% knockdown was achieved at the protein and mRNA level. This had a marginal effect on the cell cycle with a decrease in the percentage of cells in G0/G1 and conversely an increase in the G2/M phase (Figure 4.20). The effect on proliferation was again marginal and not significant but by day 5 there was an increase in the proliferation of cells in which prohibitin had been knocked down (Figure 4.20 C).

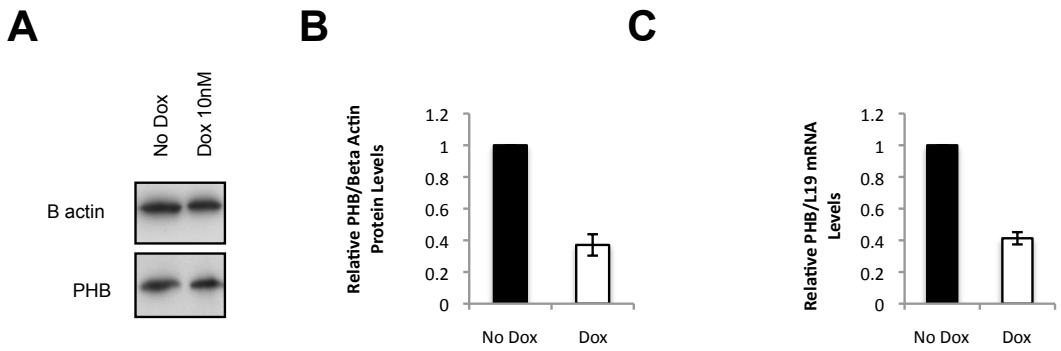

Figure 4.18: Confirmation of the DU145/TR/Mar4/siRNAPHB

(A) Western blot analysis demonstrating protein levels of PHB and Beta-Actin (B Actin) in the stably transfected DU145/TR/Mar4/siRNAPHB cell line (B) Graphical representation of the relative PHB levels before and after treatment with Doxycycline 10nM, data represents the mean of 3 independent experiments +/-SEM (C) qRT-PCR data showing the relative decrease in PHB mRNA following treatment of the cells with doxycyline. Data shows the mean +/-SEM, n=3.

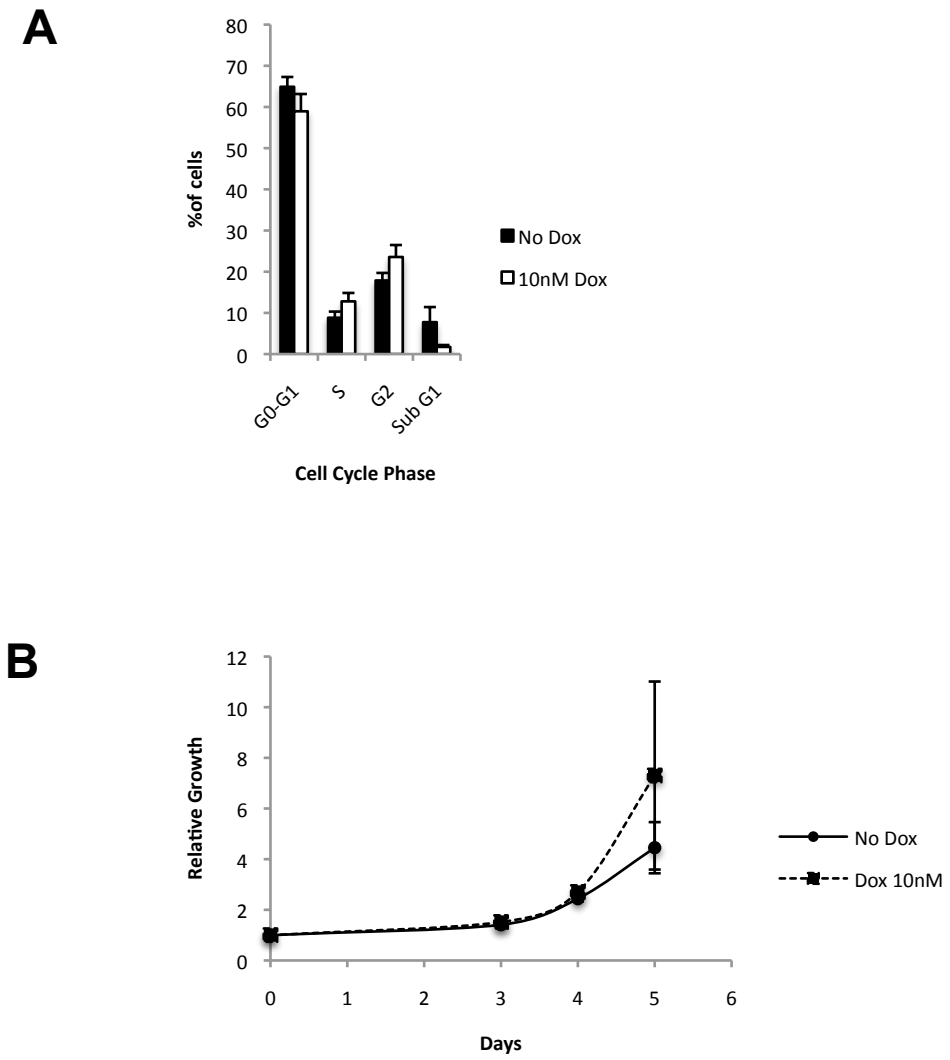

Figure 4.19: Characterisation of DU145/TR/MAR4/siRNAPHB

(A) DU145/TR/MAR4/siRNA cells grown with the presence or absence of doxycycline (10nM) then analysis with FACS Experiment done in triplicate, points represent the mean =/-SEM (B) DU145/TR/Mar4/siRNAPHB cells treated and untreated with doxycycline (10nM). SRB assays were performed at 0, 3 and 5 days post treatment. Points: mean relative absorbance at 492nm for three independent experiments performed in 15 replicate wells per experiment +/- SEM, where absorbance at day 0 was set at 1 for all treatment conditions.

4.1.7 The overexpression of prohibitin in the PC3 Cell Line

The hypothesis that overexpression of prohibitin may decrease proliferation and halt prostate cancer cells in G0/G1 is proven in the LNCaP cell line and supported by data from the C4-2 cell line, however the DU145 cell line did not show any changes to proliferation or cell cycle. To test whether this may be due DU145 cells being, traditionally, androgen insensitive and lacking functional AR, I performed the same experiments in the PC3 line which is also an aggressive prostate cancer cell line lacking AR. Figure 4.21 shows prohibitin protein level following transient transfection with the pSG5/PHB plasmid. There was a small increase in the prohibitin protein level, shown in figure 4.21A and B and a larger increase, approximately 7 fold, in the prohibitin mRNA transcript level. The overexpression of prohibitin had no effect on the cell cycle as can be seen in figures 4.22A and B. There was also no effect on proliferation as seen in figure 4.22C. There is a similar trend in the more aggressive cell lines, albeit not significant, in that there is a late effect on proliferation and a marginal increase in the percentage of cells in G0/G1 arrest.

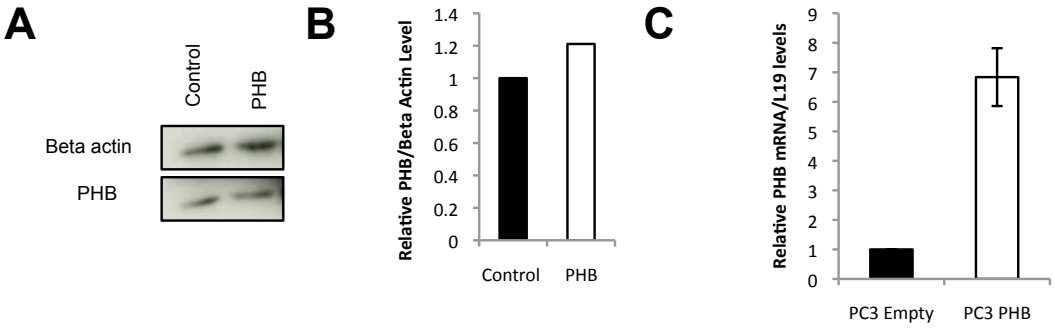

Figure 4.20: Transient transfection of PC3 cells with PSG5PHB

(A) Western blot analysis demonstrating protein levels of PHB, flag and Beta-Actin (B Actin) in the transiently transfected DU145/TR/MAR4 cell line (B) Graphical representation of the relative PHB levels, data represents the mean of 3 independent experiments +/-SEM (C) qRT-PCR data showing the relative increase in PHB mRNA following transfection with the PHB plasmid, data shows the mean +/-SEM, n=3.

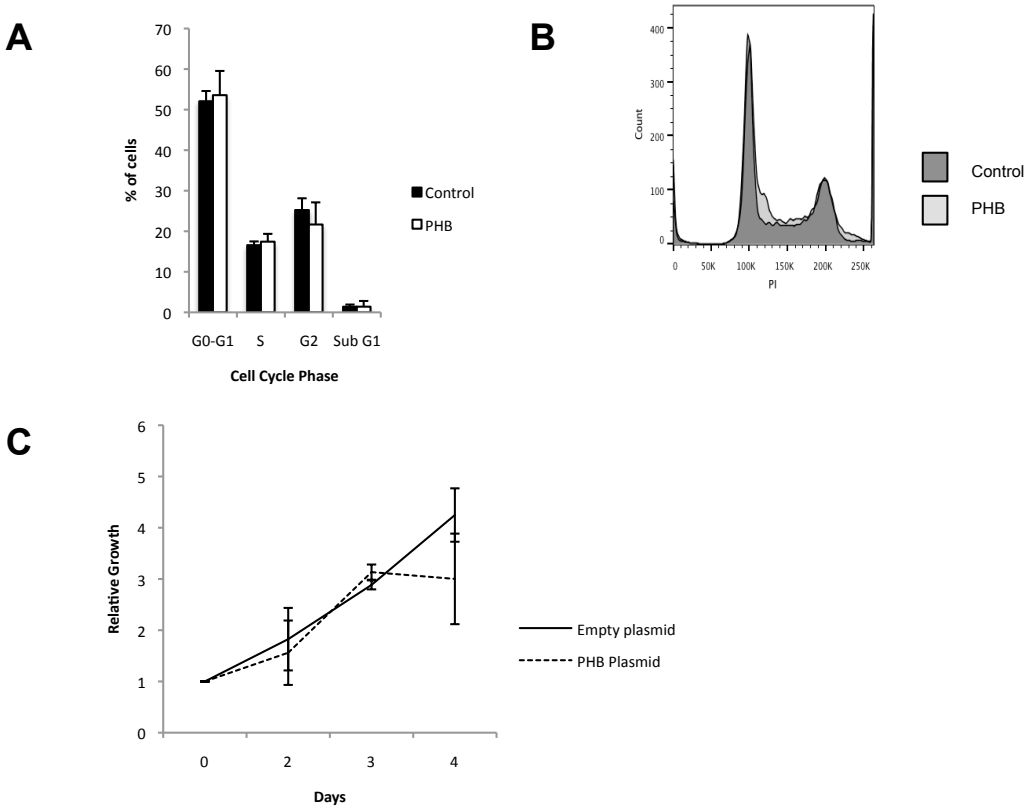

Figure 4.21: Characterisation of PC3 transiently transfected with the PHB plasmid

(A) PC3 cells transiently transfected with either the empty PSG5 plasmid or PSG5/PHB collected for analysis with FACS after 72 hours (B) Representative histogram of one of the three repeats (C) PC3 cells seeded in 96 well plates then transiently transfected with empty PSG5 plasmid or PSG5/PHB. SRB assays were performed at 0, 3 and 5 days post treatment. Points: mean relative absorbance at 492nm for three independent experiments performed in 15 replicate wells per experiment +/- SEM, where absorbance at day 0 was set at 1 for all treatment conditions.

4.2 Discussion

In previously published experiments, in the LNCaP cell line, overexpression of prohibitin led to G0/G1 arrest and the knockdown of prohibitin led to increased proliferation of the cell line (Gamble, Chotai et al. 2007). The aim was to create two pairs of prostate cancer cell lines, more aggressive than LNCaP, in which we could inducibly knockdown or ectopically overexpress prohibitin, respectively. In addition, an androgen receptor luciferase reporter construct was added to try and clarify the significance of the interaction between prohibitin and the androgen receptor. The C4-2 cell line was chosen as it was originally derived from the LNCaP cell line so bears a great genetic similarity; however, it was generated by co-cultures crossing with a bone stromal cell line (MS) in castrated mice so it is able to grow in an androgen deprived environment and has a faster doubling time and is able to metastasize *in vivo*.

Thus reflecting a later stage of prostate cancer where castration resistance has developed. Both the C4-2 prohibitin knockdown cell line and the overexpression cell line were successfully created. The second cell line chosen was DU145 as it is a well-characterised line that does not express the AR (although I found negligible levels in my cells Figure 3.2) and proliferates very efficiently in androgen-deprived media and metastasize readily *in vivo*. It was therefore used to reflect the end stage of the prostate cancer journey when the cancer is rapidly proliferating and will grow easily despite effective hormonal castration. In addition, using an AR-negative cell line gave us the advantage of potentially offering some clarity to the predominant mechanism by which prohibitin overexpression decreases proliferation. Although the DU145 prohibitin knockdown cell line was generated successfully I was unable to create a DU145 prohibitin overexpression cell line. Thus, these experiments had to be done using a transient transfection method.

4.2.1 Prohibitin influences cell cycle distribution and cellular proliferation in the C4-2 cell line

The effects of prohibitin manipulation were studied by FACS analysis of tetracycline-treated cells. In full serum medium, in which cells were cycling, prohibitin overexpression in C4-2 cells resulted in an accumulation at G0/G1 and a

subsequent reduction in S and G2/M phase. This implies that the increase in prohibitin prevented cell cycle entry, ie inhibited G1/S progression (Figure 4.12A). This is similar to the effect seen in the LNCaP cell line, although to a lesser degree. In LNCaP cells a significant decrease in the percentage of cells in S-phase (14% decreasing to 3%) was seen (Dart, Spencer-Dene et al. 2009); in the case of the C4-2 cell line, by contrast, the decrease was much more modest (8% decreasing to 6%).

The knockdown of prohibitin with the siRNA had the opposite effect to prohibitin overexpression but again proliferation was not significantly altered, with a small increase in the percentage of cells in S-phase (8% increasing to 14%). It is possible that because the cells were grown in full serum medium their growth was already maximal. This could be tested by studying their growth in sub-optimal conditions, such is in stripped media which has all growth stimulants removed.

The effect on proliferation was determined using an SRB assay on cells grown in full serum medium and treated with doxycyline to induce prohibitin overexpression. This led to a decrease in growth in those cells overexpressing prohibitin, although reproducible, the effect did not reach significance. In the C4-2 knockdown cell line the converse pattern was observed, with a small increase in proliferation, again these cells were grown in full medium and were therefore potentially growing at a maximal rate.

4.2.2 Prohibitin over expression does not influence cell cycle distribution or cellular proliferation in the most aggressive prostate cancer cell lines

To further clarify the effect of prohibitin manipulation in the most aggressive and AR-negative cell lines, DU145 and PC3 cells were transiently transfected with prohibitin expression vector and then studied by FACS analysis and SRB assay to determine cell cycle behaviour and proliferation respectively. Despite overexpressing prohibitin in these cell lines there was no change to cell cycle populations or to growth. However, given the very small increase in prohibitin protein achieved. It is unclear whether this is due to a lack of effect of prohibitin or insufficient prohibitin. This could be due to the fact that I was unable to establish stably transfected lines, and the efficiency of transfection is relatively low.

In the DU145 prohibitin knockdown cell line there was a small increase in the population in S-phase (9% to 12%) and there was a small increase in proliferation, although this did not reach significance.

Prohibitin is a cell-cycle regulatory protein, interacting with E2F to repress gene expression, and it is also reported to be a co-repressor of the AR (Wang, Nath et al. 1999, Wang, Hsu et al. 2005). The data above support the hypothesis that manipulation of prohibitin influences proliferation and cell cycling. Overexpression of prohibitin in the C4-2 cell line did lead to decreased proliferation and inhibition of cell cycle entry but to a lesser extent then that observed in the previous studies of the LNCaP cell line. C4-2 cells differ from LNCaPs in two major ways; firstly, they are less dependent on androgens for growth and secondly, they are more aggressive in nature with a faster doubling time and ability to metastasize. In addition, the C4-2 cell line has a lower endogenous level of prohibitin, as shown in the previous chapter. In the more aggressive cell lines (DU145 and PC3) overexpressing prohibitin had no effect at all. But knocking down prohibitin in the DU145 cell line had a similar effect to that in the C4-2 knockdown cell line. DU145 and PC3 cell lines do not express the AR so potentially some of this difference could be explained by prohibitin not being able to induce an anti-proliferative effect without its co-repressor role on the AR. Additionally, these results may indicate that the more aggressive cell lines have a mechanism for reducing prohibitin protein levels, as we know that prohibitin is not mutated in these cell lines but they do have less protein and mRNA expression so they may have other ways of silencing genes and downregulating the protein. As discussed in the introduction prohibitin binds and inhibits E2F via Rb and recruits BRG/BRM and other other genes all of which are commonly mutated in caner. A potential explatation for this result could be that there isn't a repressive Rb or functional BRG/BRM proteins for prohibitin to act upon. It should be noted that the prohibitin cassette that was being overexpressed in the plasmid was only the prohibitin coding region mRNA. The high levels of miR-27a in the more aggressive cell lines are unable to have an effect on the exogenous prohibitin so this cannot be the cause of the effect we see.

4.3 Summary of Chapter 4

In summary this chapter demonstrates evidence that over expressing prohibitin in the LNCaP and C4-2 cell line prevents cell cycle entry and decreases proliferation. Conversely the knockdown of prohibitin in the LNCaP and C4-2 cell lines increases the proportion of cells entering the cell cycle and increases proliferation. The effects are lesser in the more aggressive C4-2 cell line and in the most aggressive lines tested (DU145 and PC3) overexpression of prohibitin had no effect on cell cycle or proliferation. If time allowed it would be very interesting to explore why prohibitin overexpression has no effect on the more aggressive cell lines.

Chapter 5 Antisense oligonucleotide to miR-27a

My work so far had demonstrated lower prohibitin levels in the advanced stages of metastatic prostate cancer compared to benign prostate tissue. In addition, increasing prohibitin levels in hormone responsive cell lines decreased proliferation and cell cycle entry. Given that this inhibitory effect was seen in models of both hormone dependent (LNCaP) and castration reistant (C4-2) prostate cancer cell lines, we felt further investigaton of increasing prohibtin as a therapeutic strategy was warranted.

However, as discussed in the introduction, prohibitin is a 32kDa protein and a method of manipulating endogenous levels of the protein would be preferable to trying to deliver such a large protein into cells. MicroRNAs have shown tremendous potential as candidates for manipulating gene expression. Prohibitin is a *bona fide* target of miR-27a, which binds at the 3'UTR, triggering the prohibitin transcript for degradation and in turn lowering the protein level (Fletcher, Dart et al. 2012) and my recent work had shown that the levels of miR-27a inversely correlate with prohibitin levels across a panel of cell lines, supporting that this occurs *in vivo*. We hypothesised that by using an antisense oligonucleotide (ASO) that binds and blocks or degrades miR-27a we could reduce intra-tumoural levels of miR-27a, allowing the transcript of prohibitin to survive and be translated and in turn raise prohibitin protein levels, thereby inhibiting the cell cycle and abrogating growth of the tumour.

5.1 Results

5.1.1 ASO-27a decreases growth of prostate cancer cells *in vitro*

We hypothesized that an ASO designed to target miR-27a (ASO-27a) may result in inhibition of proliferation and may thus represent a novel therapeutic strategy for the treatment of prostate cancer. LNCaP cells were seeded in equal numbers in two dishes and once established bathed in androgen-depleted medium. The cells were transfected with ASO-27a or a scrambled non-targeting ASO (ASO-scram) in the presence or absence of mibolerone (a synthetic androgen). It was found that treatment of cells with mibolerone in the presence of ASO-scram gave a three-fold increase in cell number representing normal androgen-dependent proliferation (Figure 5.1A). In contrast, when cells were transfected with ASO-27a in the presence

of androgen the relative cell number increased by 1.5 fold, i.e only half compared to ASO-scram. This suggests that ASO-27a abrogates androgen-dependent growth of prostate cancer cells. These initial transfections were performed using an ASO manufactured by Dharmacon that would not be suitable for *in vivo* use as it lacked the stabilizing chemical modifications, such as the locked nucleic acid (LNA) modification. As described in my introduction this modification confers stability in circulation and aids penetration of the drug into tissues. To continue the work *in vivo* I used an ASO manufactured by Exiqon that was suitable for *in vivo* use (Krutzfeldt, Rajewsky et al. 2005, Lennox and Behlke 2010). Figure 5.1B shows that *in vitro* transfection of this ASO still abrogated growth of LNCaP cells albeit to a lesser degree than the Dharmacon version.

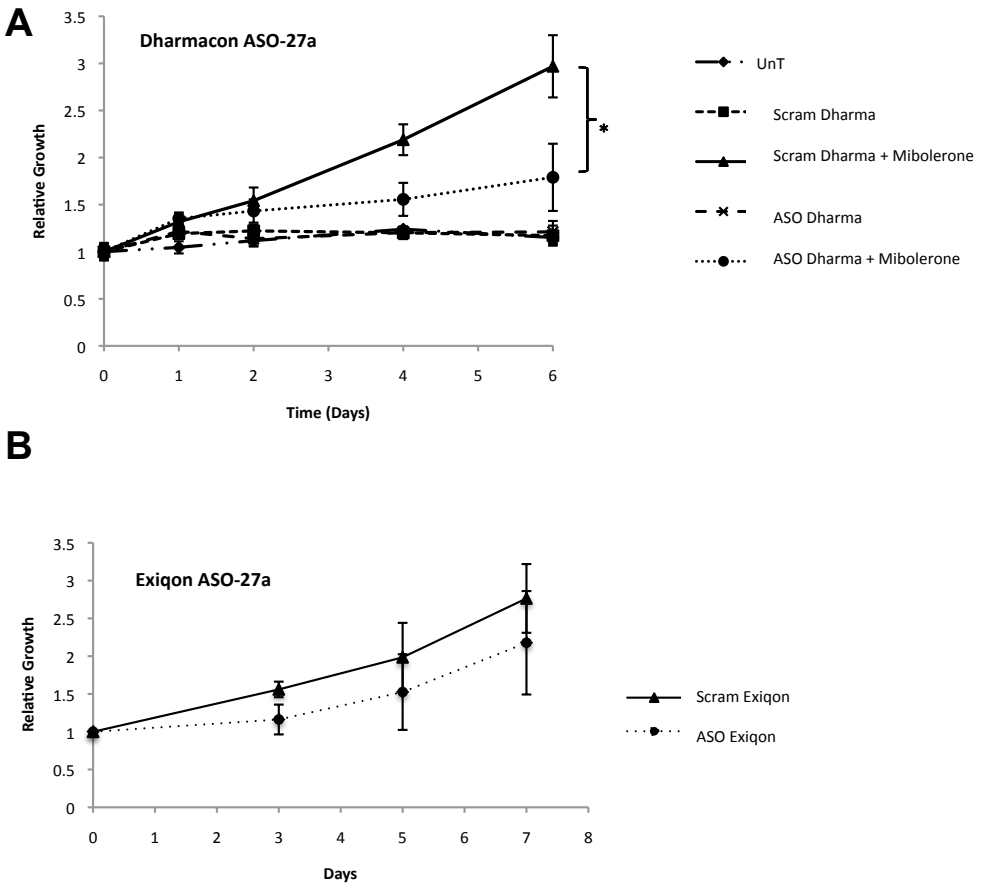

Figure 5.1: Assessing potential anti-proliferative effects of the anti-sense oligonucleotide (ASO) to miR-27a *in vitro*

(A) Sulphorhodamine B (SRB) growth assay of LNCaP cells grown in charcoal stripped media, transfected with miR27a ASO (Dharmacon) or a control scrambled ASO at a concentration of 50nM +/- 10nM mibolerone. SRB assays were performed at 0, 1, 2, 4 and 6 days post treatment. Data represent mean relative absorbance at 492nm for three independent experiments performed in six replicate wells per experiment +/- SEM, where absorbance at day 0 was set at 1 for all treatment conditions. *P <0.05. Data collected in collaboration with Dr Claire Fletcher (B) SRB growth assay of LNCaP/TR/MAR4 cells grown in full media, transfected with miR-27a ASO LNA stabilised for *in vivo* use (Exiqon). Data represents mean relative absorbance at 492nm for three independent experiments at 0, 3, 5 and 7 days post transfection +/- SEM, where absorbance at day 0 was set at 1 for all treatment conditions.

5.1.2 ASO-27a decreases growth of prostate cancer cells in vivo

Having demonstrated the anti-proliferative effects of ASO-27a *in vitro* I went on to test it in xenografts as this is a more physiologically relevant environment, Alwyn Dart had previously injected oligomiRs and could detect their presence 24 hours later in mouse serum. This demonstrates that the LNA configured ASO-27a demonstrates *in vivo* stability. Figure 5.2 A demonstrates the experimental plan. For establishment of xenografts, 8-week old male BALB/c strain nude mice were injected in the flanks with 10^6 LNCaP cells suspended in Matrigel. After 10 days, the tumours were measurable using calipers and were deemed established when the tumours reached a volume in the range of 100-200mm^3. At this point mice were separated into two treatment groups, namely the group to receive ASO-27a (4 mice, 8 potential tumours) and the group to receive the scrambled ASO (a non-targeting control) (4 mice, 8 potential tumours). A dose of 20ug/mouse of ASO-27a or ASO-scram were injected biweekly into the tail veins of mice. Before each injection animal weights were recorded and tumours were measured with calipers. The mice were monitored daily for signs of toxicity or ill effects. Mice were sacrificed either after 3 weeks of treatment or if they lost 20% of their starting weight. Serum was collected from mice at sacrifice and tumours dissected and divided into two, to be (a) fixed in paraformaldehyde for further immunohistochemical analysis of markers of cell cycle, mitosis and cell death and (b) flash frozen for subsequent RNA extraction and analysis of miR-27a targets. Other organs such as liver, kidneys and prostate were also collected to determine where ASO-27a is delivered *in vivo* and to allow a preliminary analysis of levels of ASO-27a sequestered in different tissues and to look for toxicity off target.

Figure 5.2 B shows the relative growth of the LNCaP xenografts in the two treatment groups. The LNCaP xenograft tumours treated with the ASO-27a had a slower growth trajectory when compared to ASO-scram, although the difference was not quite statistically significant ($p=0.052$) at the termination of the experiment. The experiment was terminated early at 15 days as a number of the mice in the scrambled group had lost a significant amount of weight necessitating termination on the basis of ethical treatment of animals.

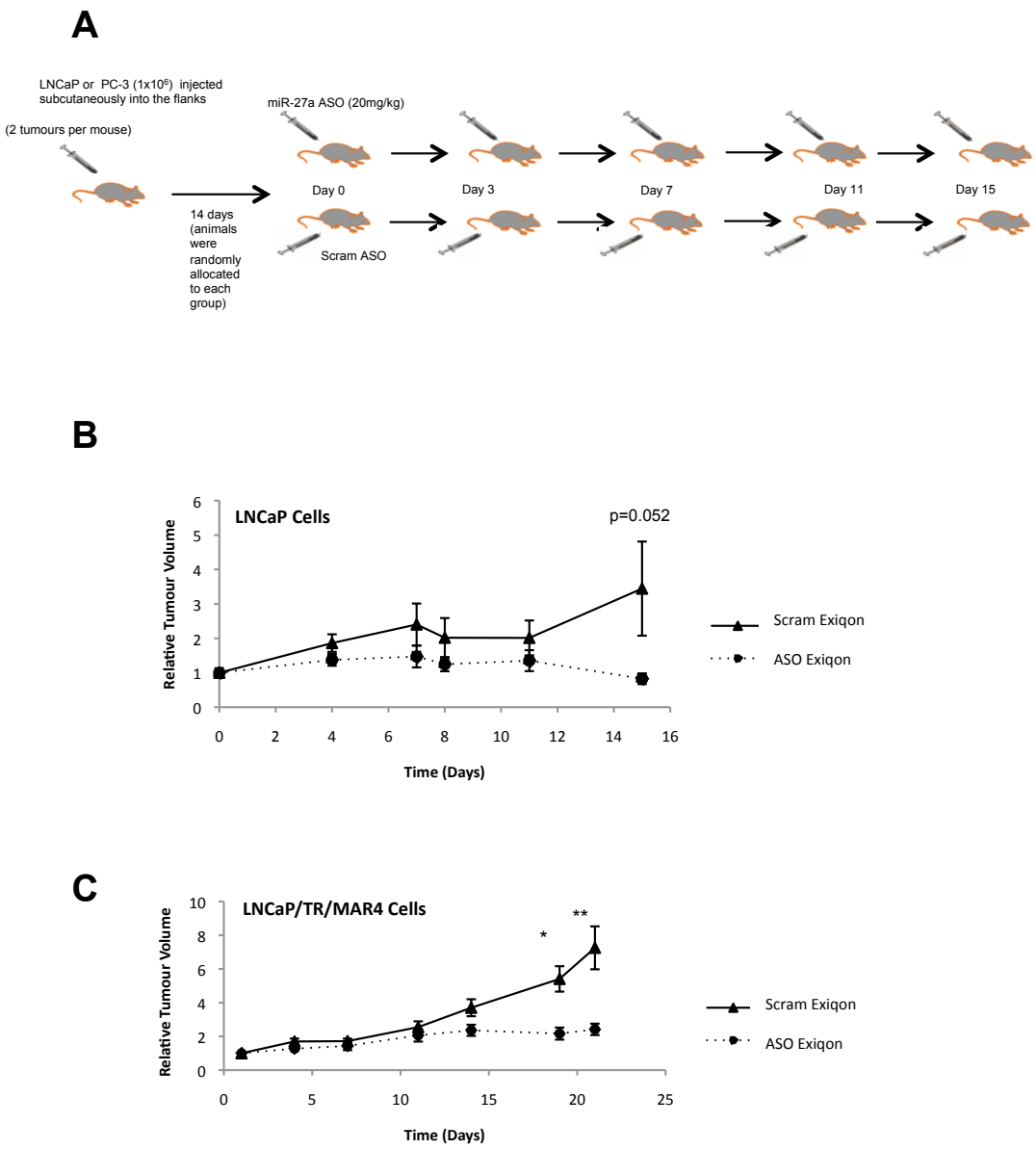

Figure 5.2: ASO miR-27a blocks prostate cancer proliferation *in vivo*

(A) Figure to demonstrate the experiment model (B) LNCaP cells were subcutaneously injected into the flanks of nude mice (n=8). Tumours were allowed to establish before the biweekly tail vein injection of the ASO-miR27a or the scrambled oligonucleotide (Commencing Day 0) . Tumour volume was measured prior to treatment on Days 0, 3, 7, 11 and 15 using calipers on the indicated days and relative tumour volume calculated. Data point represents mean ± SEM. T-Test p=0.052 at termination of the experiment (C) Experiment repeated with LNCaP/TR/MAR4 cell line, 8 mice in the ASO-miR-27a group and 8 mice in the scrambled oligonucleotide group. Tumour volume was measured prior to treatment on Days 0, 4, 7, 11, 14 18 and 21 using calipers on the indicated days and relative tumour volume calculated. Data point represents mean ± SEM (n=16). This experiment continued for 21 days. T-Test * P <0.05 ** P< 0.005

The experiment was repeated with a number of modifications: firstly, we used a larger number of animals in each group (8 in each, 16 potential tumours). Secondly the cell line used to create the xenografts was LNCaP/TR/MAR4, a stable LNCaP cell line generated in our lab, that contained an AR-driven luciferase reporter construct (Dart, Spencer-Dene et al. 2009). A similar protocol was followed with the addition of biweekly assessment of androgen-induced luciferase activity, detectable by light emission from live animals, imaged 8 minutes after intraperitoneal injection of D-luciferin using a Xenogen IVIS camera.

As shown in figure 5.2C the growth curves follow a similar pattern to the prior LNCaP experiment. In the second experiment, by day 18, the abrogation of growth induced by treatment with ASO-27a reached significance, indicating that the ASO to miR-27a reduced tumour growth, compared to a non-targeting oligonucleotide. The experiment was terminated on day 21 as planned. At termination there was a continued significant difference in growth between the xenografts treated with ASO-27a as opposed to the scrambled ASO (T-test P=0.005554).

5.1.3 ASO-27a reduces cancer related cachexia *in vivo*

To address effects of treatment on cancer related symptoms, specifically cachexia, the mice were weighed biweekly as an indicator of overall health and additionally if there were concerns with weight loss. At the termination of the experiment the mice in the scrambled ASO group had lost a mean of 9% of their body weight, in comparison the ASO-27a treatment group had lost significantly less weight (T-test P= 0.029507), a mean of just 2% of their baseline bodyweight (Figure 5.3).

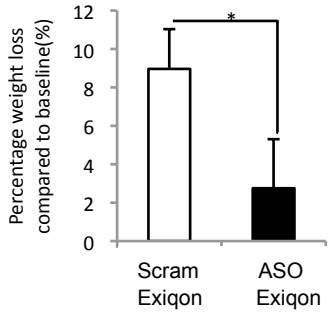

Figure 5.3: ASO miR-27a decreases cancer related weight loss *in vivo*

(A) The mice from the experiment described in Figure 9C were weighed biweekly throughout the experiment. The columns represent the mean weight loss for each group of mice at the termination of the experiment +/- SEM. *P<0.05.

5.1.4 ASO-27a lowers the levels of miR-27a within the xenograft tumours

It is still unclear whether the binding of the complementary ASO and miR triggers the miR for degradation or rather just sequesters the miR and in effect competes with the target mRNA to prevent transcriptional inhibition of miR:mRNA. As discussed, in the introduction, the chemical structure of the ASO can influence the outcome. High affinity ASOs such as LNAs promoting formation of a heteroduplex, but lower affinity oligonucleotides such as 2'-O-Me and cholesterol conjugated 2'-O-Me antagomirs promoting miR degradation (Davis, Propp et al. 2009, Torres, Fabani et al. 2011). In order to investigate this further, at the termination of the experiment the xenograft tumours were dissected, flash frozen, and then RNA was extracted. Using qRT-PCR and specific miR-27a Taqman probes the levels of miR-27a within the tumours was evaluated and normalized to the biological control U18. Figure 5.4 shows that the mean level of miR-27a in RNA extracted from the xenografts in the ASO-27a was reduced, although this did not reach significance (T-Test P=0.099103). While further mechanistic investigations are warranted, these data support the hypothesis that the generation of a duplex RNA when the ASO binds to the miR may be triggering it for degradation, which is not what we would necessarily expect with LNA technology (Torres, Fabani et al. 2011).

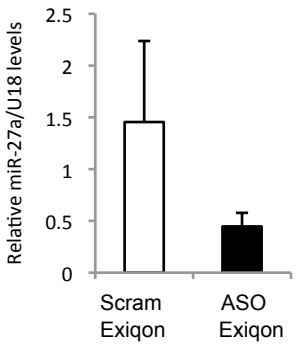

Figure 5.4: miR27a levels are lower in the xenografts from ASO-27a treated mice

At the termination of the experiment the xenografts were flash frozen and the RNA extracted. miR-27a levels were quantified using qRT-PCR and made relative to U18 as a control.

5.1.5 ASO-27a induces apoptosis but has little effect on proliferation *in vivo*

We initiated work on ASO-27a aiming to abrogate miR-27a signalling and thus increase levels of endogenous prohibitin, however, we were aware that miR-27a has 5,386 computationally predicted targets (TargetScan7, 2015) and may have produced the observed growth abrogation through a number of different pathways. As an initial study to try and elucidate the mechanisms of action of ASO-27a the xenograft tumours were fixed in paraformaldehyde and then stained for a proliferation marker (Ki67) and an apoptotic marker (Cleaved Caspase 3) (Figure 5.5). Surprisingly, there was no difference in Ki67 staining between the group treated with the scrambled oligonucleotide and the group treated with the ASO-27a. There was, however, a significant increase in caspase staining within the ASO-27a group indicating potentially that increased apoptosis, rather than decreased proliferation, may be the predominant mechanism via which growth of the xenografts was abrogated (T-test P=0.029962).

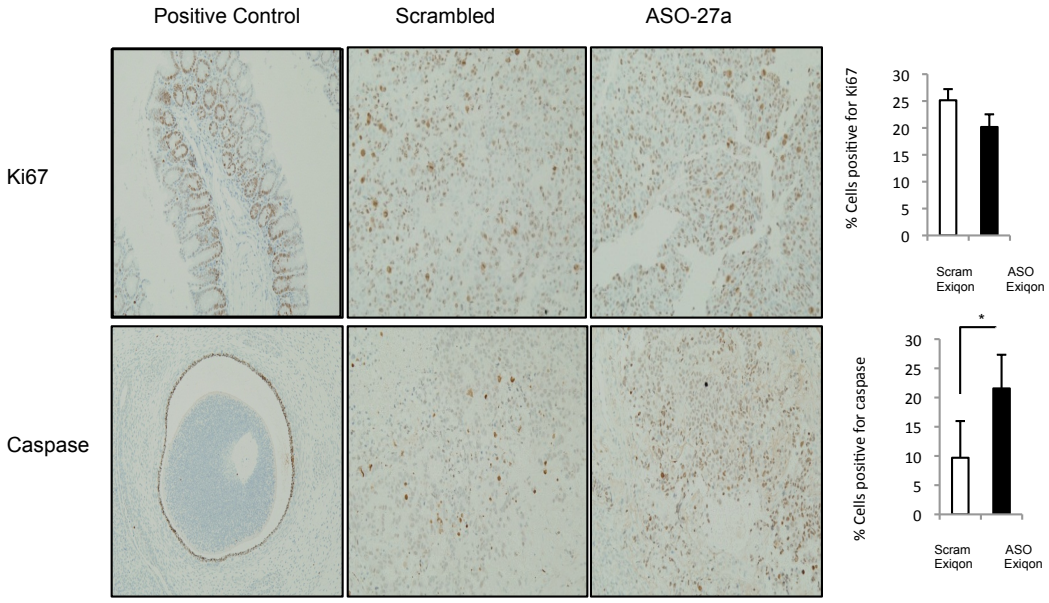

Figure 5.5: ASO-27a induces apoptosis but has little effect on proliferation *in vivo*

Ki67 (marker of proliferation) and caspase (marker of apoptosis) staining on representative tumour samples with their respective positive controls (The positive controls are from sections of human tonsil). Brown staining denotes expression, percentage of positively stained cells counted at 50 x magnification for quantification. The caspase was significantly lower in the ASO-27a group (* T Test P= 0.0299)

5.1.6 The anti-tumour effect of ASO-27a is partially mediated via the androgen receptor

Our hypothesis was that ASO-27a would have an anti-proliferative effect through increasing prohibitin protein levels thus repressing AR levels and promoting apoptosis. To explore this, we investigated the correlation between ASO-27a treatment and AR target genes via qRT-PCR as a surrogate for measuring AR activity *in vivo*. As shown in Figure 5.6 A, all four of the AR target genes tested were found to be expressed at lower levels in the ASO-27a treatment group, with TMPRSS2 reaching statistical significance (T-test P= 0.01502257). These data support the hypothesis that some of the mechanism of action may be through the AR. In addition, blood was collected from the mice at the termination of the experiment for serum extraction and an ELISA assay was conducted to elucidate the circulating

PSA levels within the mice. PSA levels were lower in the ASO-27a treatment group even when corrected for tumour volume; see Figure 5.6 B and C.

The cell line used in this experiment was stably transfected with an AR-driven luciferase reporter vector with a view to monitoring AR activity throughout the experiment using bioluminescent imaging. As can be seen from Figure 5.6 D the xenograft tumours all showed up clearly on bioluminescent imaging at the start of the intravenous injections. A luciferin kinetic study was done on the first three mice, whereby the bioluminescence was recorded every minute from seven minutes post injection of D-luciferin until twenty-seven minutes post injection to establish the optimal time for recording the bioluminescence. As can be seen in Figure 5.6 E the bioluminescence has a steady decline after 8-9 minutes post injection so this was chosen as our time point for imaging for the experiment.

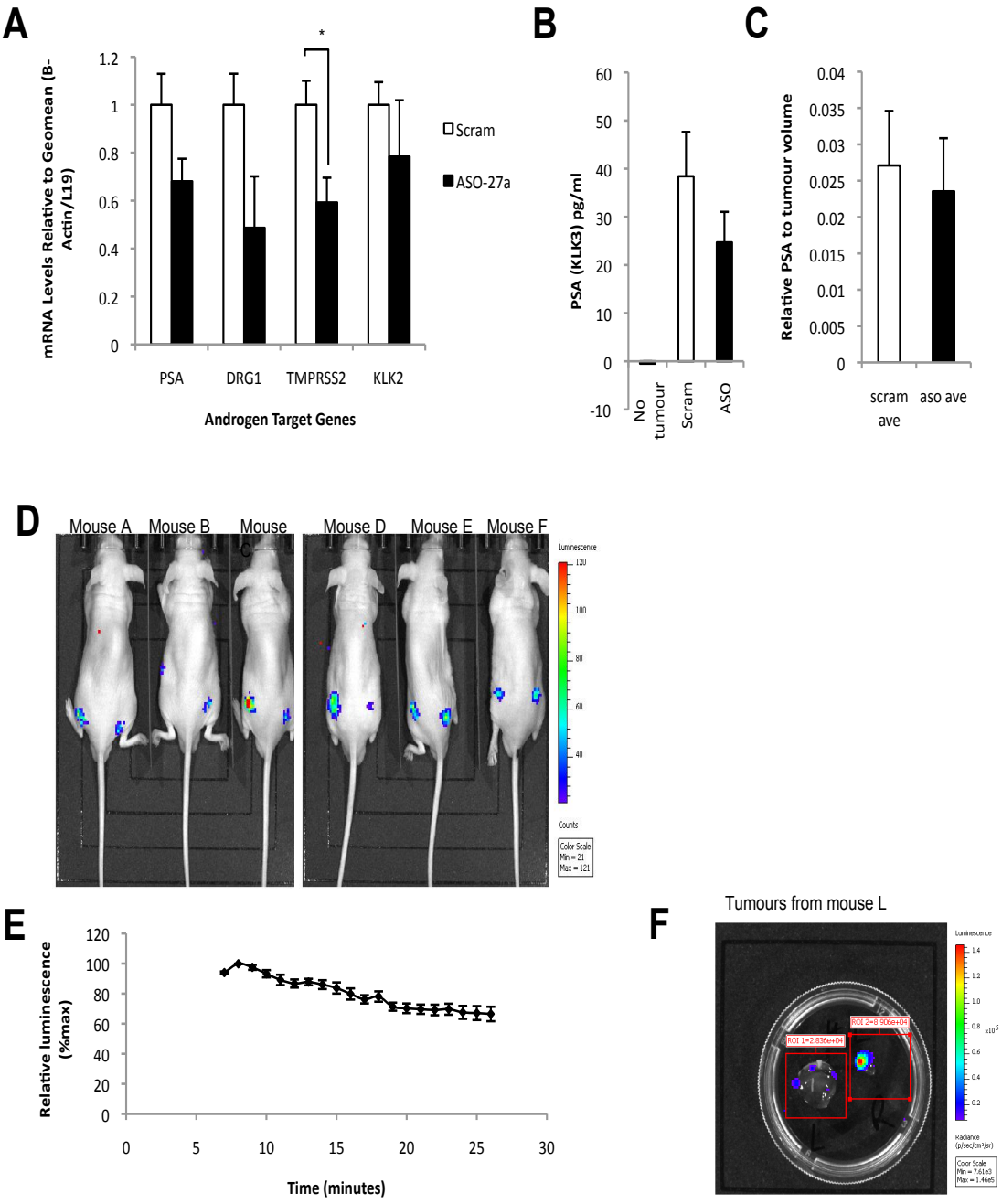
A
mRNA Levels Relative to Geomean (B-Actin/L19)
1.2
1
0.8
0.6
0.4
0.2
0
*
Scram
ASO-27a
PSA
DRG1
TMPRSS2
KLK2
Androgen Target Genes
B
PSA (KLK3) pg/ml
60
50
40
30
20
10
0
-10
No tumour
Scram
ASO
C
Relative PSA to tumour volume
0.04
0.035
0.03
0.025
0.02
0.015
0.01
0.005
0
scram ave
aso ave
D
Mouse A
Mouse B
Mouse
Mouse D
Mouse E
Mouse F
Luminescence
120
100
80
60
40
Counts
Color Scale
Min = 21
Max = 121
E
Relative luminescence (%max)
120
100
80
60
40
20
0
0
5
10
15
20
25
30
Time (minutes)
F
Tumours from mouse L
Luminescence
ROI 1=2.836e+04
ROI 2=6.905e+04
Radiance (p/sec/cm²/sr)
Color Scale
Min = 7.61e3
Max = 1.46e5

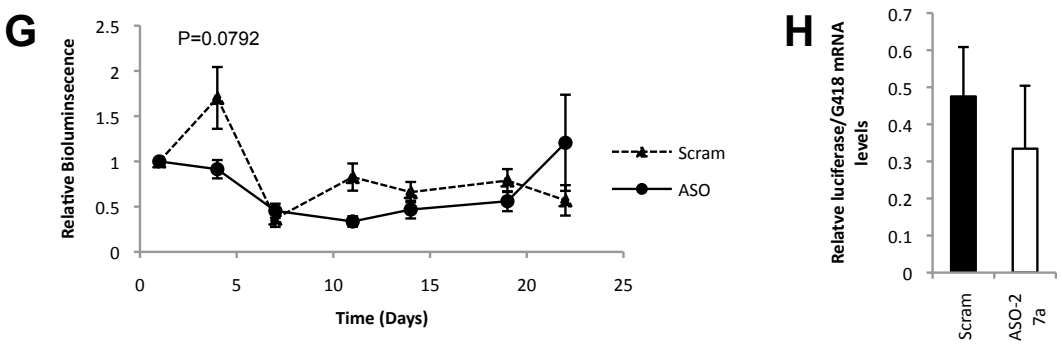

Figure 5.6: The antiproliferative effect of ASO-27a is partially mediated via the androgen receptor

(A) Androgen regulated genes were quantified from the tumour RNA via qRT-PCR and made relative to the geomean of Beta Actin and L19 (*P<0.005). (B) Blood was taken from the mice at the termination of the experiment , the serum was extracted and an ELISA assay conducted for the circulating PSA level. (C) As the mice had variable tumour burden the serum PSA levels are also displayed relative to the tumour volume at the end of the experiment. (D) The cell line used to generate the xenografts was stably transfected with an androgen receptor firefly luciferase reporter. Prior to the biweekly injection of the ASO-27a or scrambled ASO the mice received an intraperitoneal injection of luciferin and were then anaesthetised and imaged. (E) Luciferin kinetic study to determine the time post IP injection to record maximal luminescence (F) Tumours imaged ex-vivo at the end of the study, tumours are from mouse L that received ASO. (G) Quantification of the bioluminescence data obtained over the course of the experiment.(T-Test at Day 4 P= 0.079) (H) The luciferin gene was quantified using qRT-PCR made relative to G418 as an indicator of true stable cell line number.

Although the bioluminescence in the ASO-treated tumours was mostly lower than that in tumours treated with the scrambled, overall there was no real difference observed between the two groups in bioluminescence, as can be seen from Figure 5.6 G, and thus in turn it could be concluded that there was no change in AR signalling between the two groups. Initially, on the first data point at day 4, the data look promising and the difference between the two groups almost reaches statistical significance (T-Test P=0.0792). However, from that data point on there is no difference between the two groups. An example of the tumours *ex-vivo* at the end of the experiment can be seen in Figure 5.6F. This shows that by the end of the experiment the tumours were quite necrotic and haemorrhagic and the bioluminescent signal was not very strong despite the physical increase in size. At

the termination of the experiment the luciferase mRNA levels were assayed using qRT-PCR and made relative expression to the Geneticin (G418) resistance gene inserted in the stably transfected LNCaP cells, as such this will act as a more specific endogenous control marker for the number of LNCaP/TR/MAR4 cells. Figure 5.6 H shows that levels of luciferase were lower in the ASO-27a treated group although not to a significant degree, supporting the hypothesis that a degree of the mechanism of action is through suppression of AR activity.

5.1.7 ASO-27a reaches the prostate through intravenous tail vein injection

Northern blotting was performed on RNA extracted from various tissues of the xenograft mice, probing for the ASO-27a with a custom made probe from Exiqon. Ethidium bromide staining of total RNA was used as a loading control. It was found that the ASO-27a must circulate within the mouse as it could be detected in the liver, kidney and prostate tissue of the mice that received the injection of ASO-27a as well as the human xenograft tissue, nothing can be detected by the probe in RNA from the control group, see Figure 5.7.

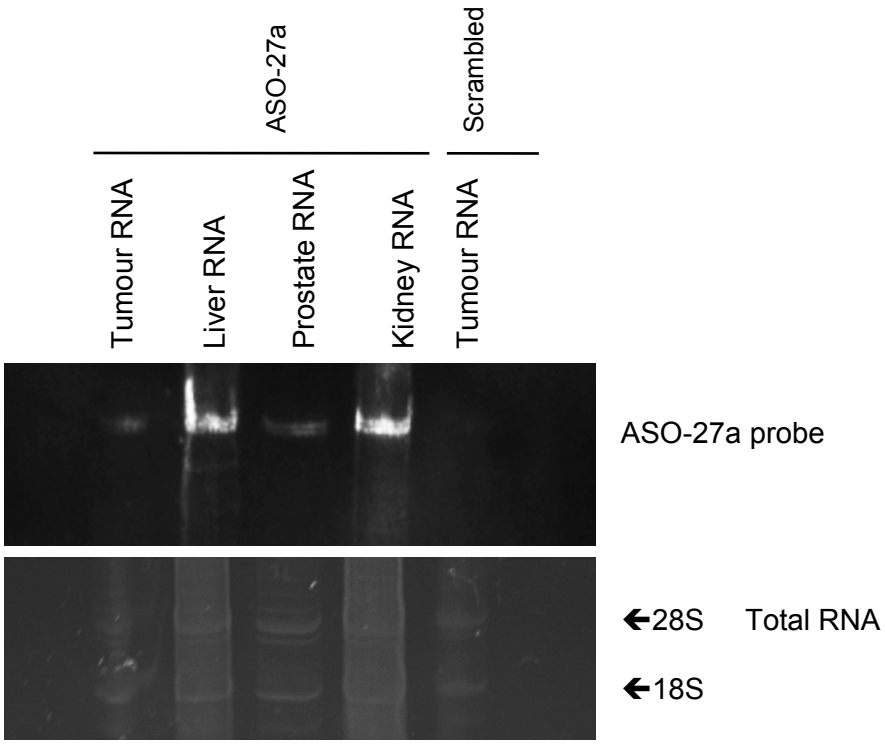

Figure 5.7: ASO-27a can be found in the tumour and three important organs following tail vein injection

Representative Northern blot of RNA extracted from the xenograft tumour, the liver, the kidney and the prostate of a mouse that received ASO-27a and RNA extracted from the xenograft tumour of a mouse that received the scrambled oligonucleotide. 10µg of total RNA was loaded and a custom designed probe to ASO-27a was used to determine presence of ASO-27a. Total RNA as visualized by staining with ethidium bromide and visualised under UV light to act as a loading control.

A Northern blot was also undertaken to confirm that the ASO-27a could be reliably found in the prostate of the mice that received the tail vein injection of the active oligonucleotide and not the mice that received the scrambled oligonucleotide. As can be seen in Figure 5.8 the ASO-27a can be reliably detected in the prostates of four of the mice that were injected with the active compound but not in the controls.

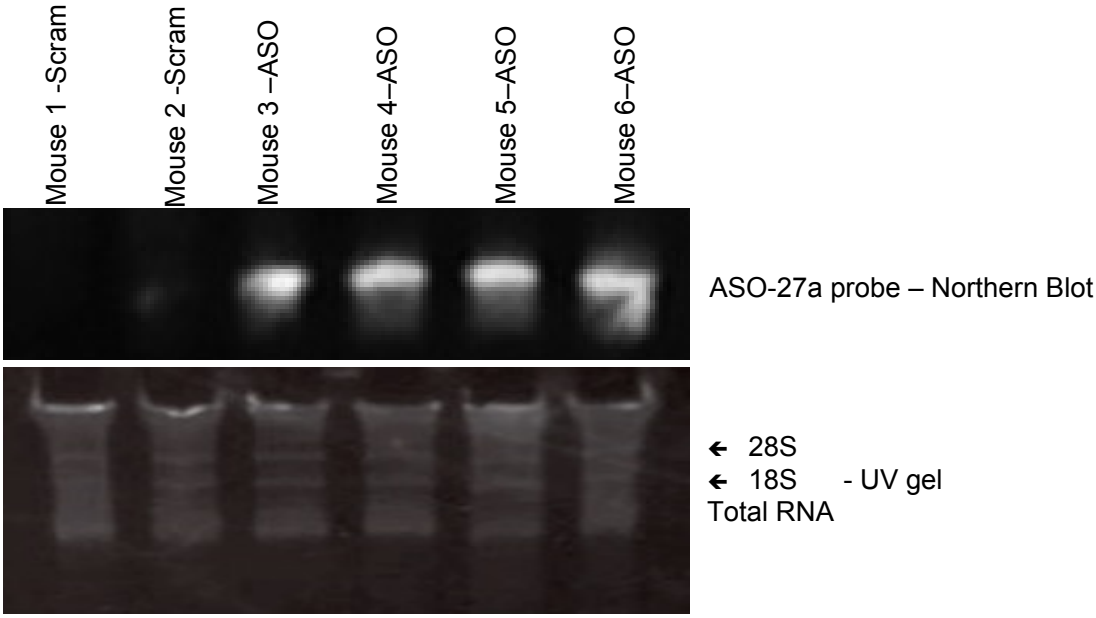

Figure 5.8: ASO-27a reaches the prostate after intravenous tail vein injection

Northern blot of RNA extracted from the prostates of the mice in both treatment groups at the termination of the experiment. 10µg of total RNA was loaded and a custom designed probe to ASO-27a was used to determine presence of ASO-27a. Total RNA as visualized by staining with ethidium bromide and visualised under UV light to act as a loading control.

5.1.8 mRNA quantification of validated miR-27a targets

In order to further elucidate the likely mechanism of action of ASO-27a a bioinformatics search was conducted using TargetScan7 which established that there are 5,386 predicted targets for miR-27a. The miRTarBase (http://mirtarbase.mbc.nctu.edu.tw/) was then used to establish the validated targets of miR-27a (Hsu, Tseng et al. 2014). The highest ranking genuine targets and those that were likely involved in the cancer pathways were chosen; these are highlighted in Table 1.3 in the introduction. Figure 5.9 displays the relative mRNA levels, as assayed by qPCR, of the selected panel of target genes between the two groups. Interestingly, prohibitin showed no difference between the two groups, however, the prohibitin UTR was marginally higher in the ASO-27a treatment group. The greatest differential expression with ASO-27a treatment were *EGFR, HIPK2, P53* and *RUNX1*. Expression of these was increased in the ASO-27a treated samples,

suggesting that they are indeed miR-27a targets in prostate cancer. *EGFR* and *HIPK2* were the only mRNAs to show a significantly higher level in the ASO-27a treatment group (*EGFR* T-test P=0.034748, *HIPK2* T-test P=0.02762).

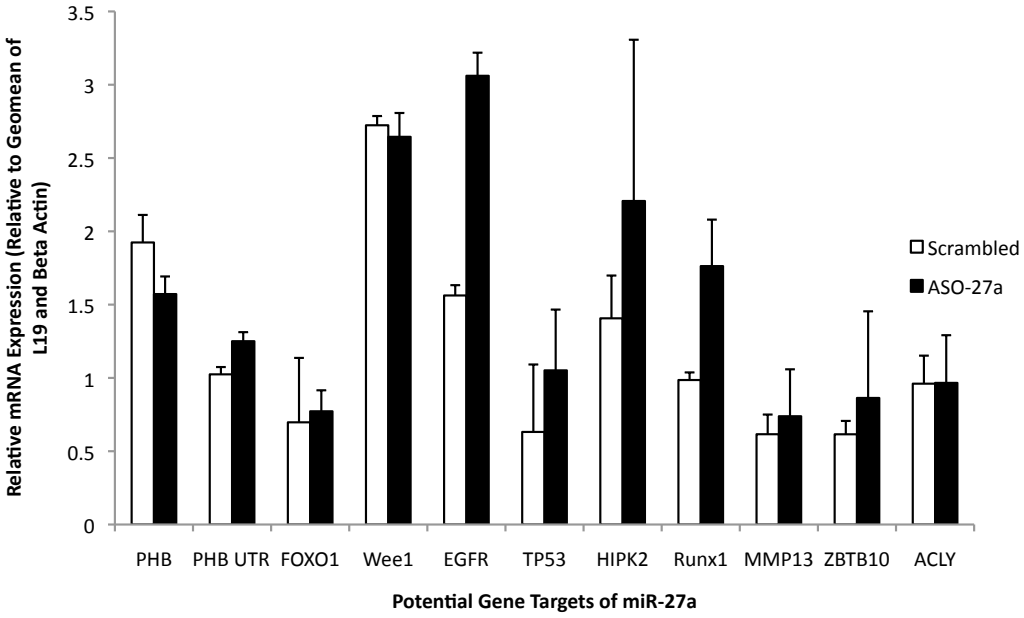

Figure 5.9: mRNA quantification of validated miR-27a targets

mRNA levels of predicted ASO-27a targets quantified from the RNA extracted from the xenograft tumours at the termination of the experiment, data normalised to a geomean of L19 and Beta Actin. Columns represent the mean +/- SEM (n=19 total, ASO = 10, Scram = 9 tumours). T Test *P<0.005

5.1.9 The pro-apoptotic ability of ASO-27a is less effective in aggressive and AR negative PC3 cells

As we hypothesized that a degree of the mechanism of action of ASO-27a was via the AR we thought it would be interesting to determine if the ASO would have similar effects in an AR negative cell line, such as PC3. In addition, PC3 is a very aggressive cell line that mirrors end-stage prostate cancer, in which few treatments are able to decrease growth. We injected $1x10^5$ PC3 cells into the flanks of SCID mice using the same experimental protocol described in Fig. 5.2 A.. In the PC3 xenografts the effect of ASO-27a on tumour volume was less pronounced and by the termination of the experiment at 24 days there was very little difference in the growth profiles of the ASO-27a and ASO-scrambled groups (Figure 5.10 A). As

already mentioned, the PC3 cell line is a highly aggressive line so any decrease in proliferation is important and potentially clinically relevant and some anti-proliferative activity was seen at days 8-14 (Figure 5.10 B).

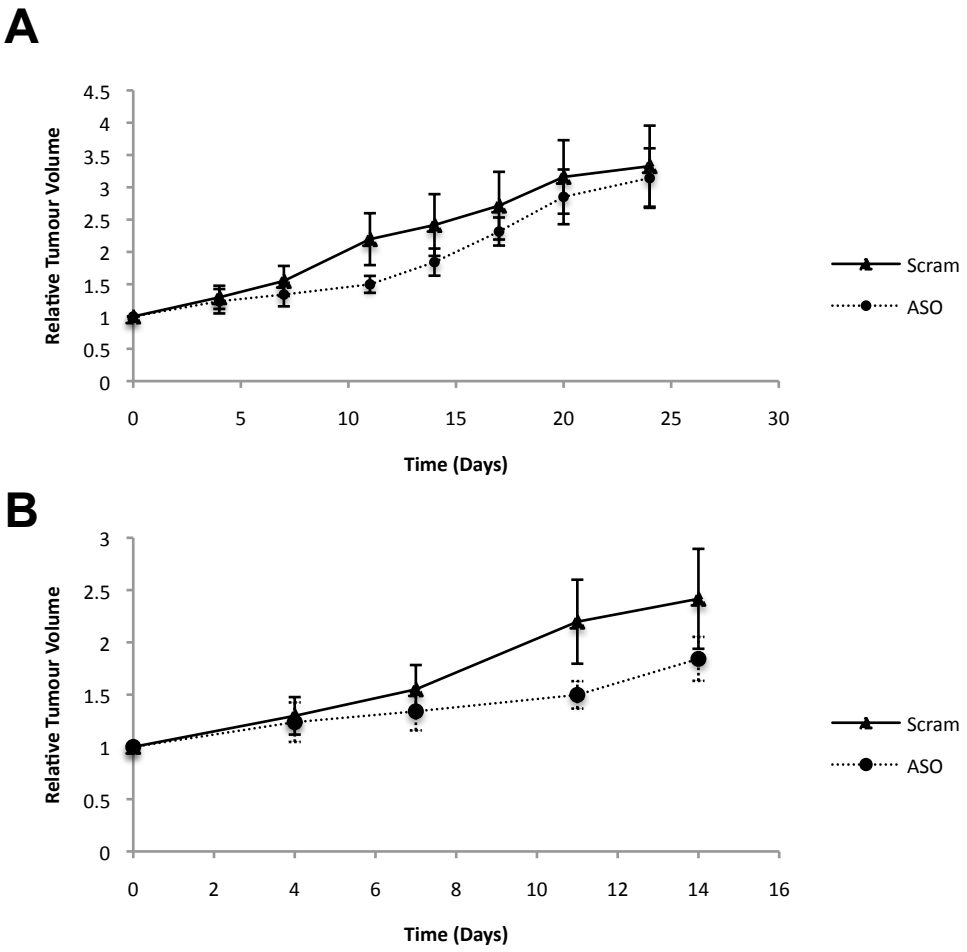

Figure 5.10: ASO-27a has a lesser anti-proliferative effect in aggressive and AR negative PC3 cells

(A) PC3 cells were subcutaneously injected into the flanks of nude mice. Tumours were allowed to establish before the biweekly tail vein injection of the ASO-miR27a or the scrambled oligonucleotide was commenced (Day 0) . Tumour volume was measured prior to treatment on Days 0, 3, 7, 11, 14, 18, 21 and 24 using calipers on the indicated days and relative tumour volume calculated. Data point represents mean ± SEM. (B) Data from days 0-14 expanded to demonstrate the separation of the two curves at 11 days.

5.1.10 RNA Sequencing – Whole data set analysis

While preliminary experiments to quantify candidate miR-27a target genes yielded interesting information, to get a global view of the miR-27a targets in a prostate cancer model we performed RNA-sequencing (RNAseq) analysis. We looked at RNA extracted from tumours dissected *ex vivo* from the mice receiving either treatment with the ASO or the scrambled oligonucleotide. RNAseq enables unbiased genome wide expression analysis with unprecedented accuracy and a broad range.

In order to do this I created a cDNA library of genes expressed in the tumours at the termination of the experiment. This entailed RNA extraction from the tumour samples (as described in materials and methods), assessment of RNA quality using a bioanalyser to determine the best samples to take forward. Samples that displayed low RIN scores were then purified. I used an Illumina Truseq kit to convert the RNA to cDNA. Then the relevant samples were then given to the MRC centre at Imperial to conduct the RNAseq on the Illumina HiSeq2500 sequencer. I sent a total of 12 cDNA libraries to be sequenced unfortuantly, one of the attempts was unsuccessful so only 6 samples were available for analysis in the end (3 from ASO treated tumours and 3 from scrambled olignonucleotide treated tumours).

A flow diagram of the methodology used to analyse RNA-seq data is shown in Figure 5.11. In brief the genes considered to have been differentially expressed to a significant extent (FDR<0.05) were uploaded into IPA (Ingenuity Systems, www.ingenuity.com) along with the gene identifiers and corresponding fold change values (log2 ratios). Each gene identifier was mapped to its corresponding gene object in the Ingenuity Pathways Knowledge Base (IPKB) and the list of genes was transformed into a set of relevant networks, focus genes and affected canonical pathways. The knowledge-base driven pathway analysis tool IPA was used in order to extract meaning from our long list of differentially expressed genes. Analysing the list of genes in this way allowed the grouping of molecules by the pathways that they are purported to be involved in and reduce the complexity to give us more explanatory power. This knowledge base comes from peer reviewed publications and is continuously updated.

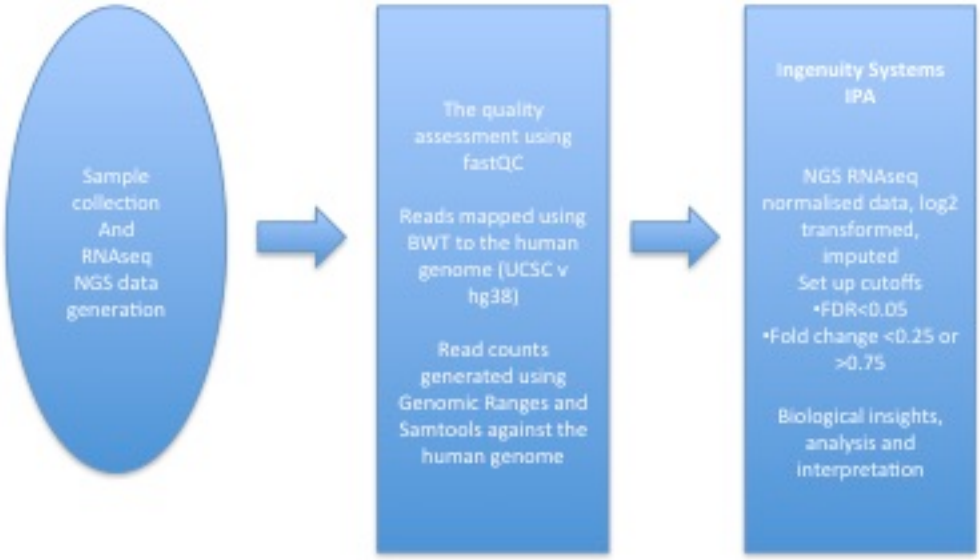

Abbreviations: RNAseq=RNA sequencing, NGS= next generation sequencing, BWT= Burrows wheeler Transformations, UCSC= University of California, Santa Cruz Genome Browser.

Figure 5.11: Flow diagram demonstrating the stages of data processing following the generation of the RNAseq data

Table 5.1 displays the 20 most differentially expressed genes and their representative log fold change. The genes showing the greatest degree of up-regulation are predominantly mitochondrial. The most up-regulated gene was mitochondrial encoded cytochrome c oxide (MT-CO1) this codes for the protein cytochrome C Oxidase 1(COX1) a subunit of respiratory complex IV in the electron transport chain of mitochondrial oxidative phosphorylation. MT-ND4 encodes for NADH dehydrogenase 4 part of the large enzyme complex known as complex 1, again necessary for oxidative phosphorylation. In fact the top 9 genes all code for proteins key to the electron transport chain and oxidative phosphorylation. In addition to these mitochondrial genes, HOXB13 is was also significantly up-regulated. HOXB13 is a highly conserved gene in the homeobox family that has been implicated in fetal skin development. A rare genetic variant has been linked to increased risk of prostate cancer (Ewing, Ray et al. 2012).

All ten of the most down-regulated genes encode for metallothionein genes, which code for cysteine rich, low molecular weight proteins localised to the membrane of the golgi apparatus.

Table 5-1: A table of the twenty most differentially expressed genes following treatment of the LNCaP xenografts with the scrambled and the ASO-27a

Upregulated Molecule	Expression	Downregulated Molecule	Expression
MT-CO1	↑18.210	MTICP	↓-18.188
MT-RNR2	↑17.175	MTIE	↓-16.906
MT-ND4	↑17.015	MTIJP	↓-16.741
MT-C03	↑16.981	MTIA	↓-16.537
MT-C02	↑16.812	MTIH	↓-15.703
MT-RNR1	↑14.961	MTIB	↓-15.564
MT-ND4L	↑14.433	MTIM	↓-15.557
MT-ND6	↑14.250	MTIG	↓-15.283
MT-ND3	↑14.218	MTIL	↓-14.629
HOXB13	↑12.945	MTIHL	↓-14.199

Canonical pathways analysis identified molecular pathways from the IPA library of canonical pathways (part of the IPKB) that were most significant to the data set. The significance of the association between the genes from the dataset and the canonical pathway (in the IPKB) was measured in two ways as described in IPA documentation: 1) A ratio was calculated of the number of genes from the dataset in a given pathway divided by the total number of molecules that make up the canonical pathway; 2) Fisher's exact test was used to calculate **a** p-value determining the probability that there is an association between the genes in the dataset and the canonical pathway that cannot be explained by chance alone. The canonical

pathways identified by this analysis can be seen in Figure 5.12. Given the dominance of mitochondrial genes maximally differentially regulated between the scrambled treated group when compared to the ASO-27a treated group, it is unsurprising that mitochondrial pathways feature heavily in the likely canonical pathways involved. Three other types of pathways were identified: firstly, folate metabolism with folate transformation, tetrahydrofolate salvage pathway and folate polyglutamylation. Secondly, cellular signalling appears to be affected as the EIF2 pathway, which is involved in translation as it modulates the binding of tRNA, and the 14-3-3 mediated signalling pathway are implicated.

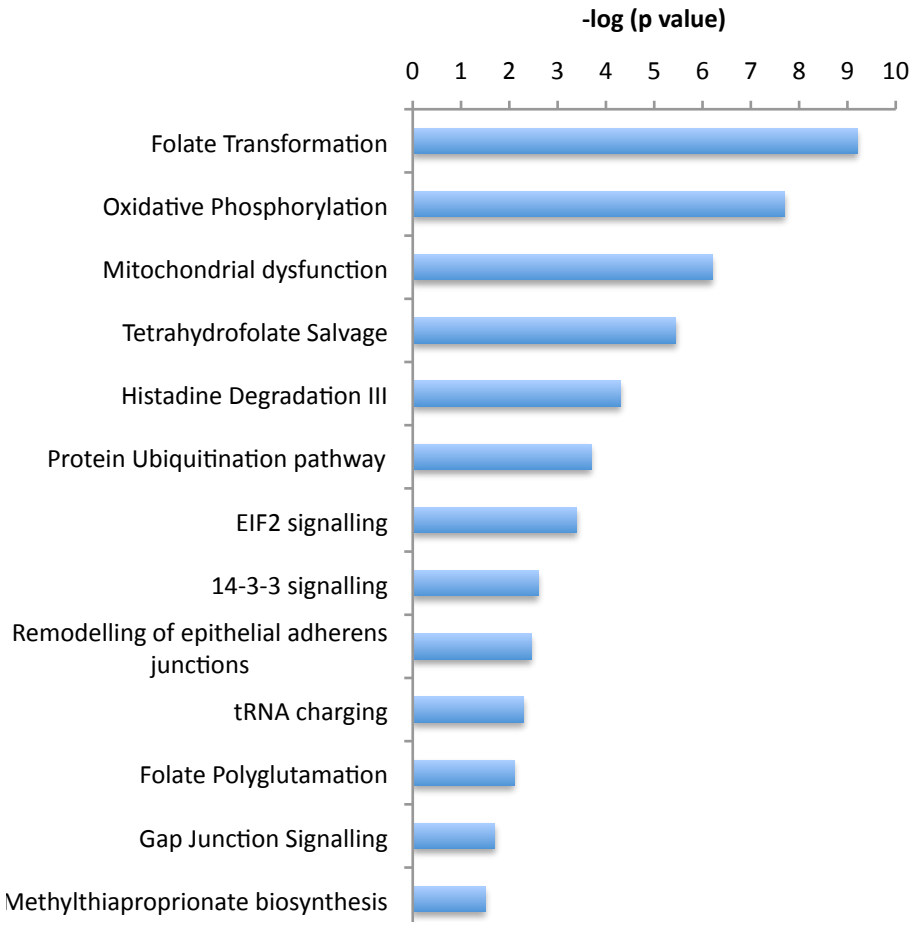

Figure 5.12: Canonical pathways indicated to be affected by ASO-27a treatment (analysis using Ingenuity software, Qiagen)

The bars represent the statistical likelihood that the number of members of the given pathway present within the selected differentially expressed genes are observed given the null hypothesis (Fisher's exact test (P value).

Network analysis was algorithmically generated by the IPA software, as can be seen in Figure 5.13 and 5.14. Two genes are considered to be connected if there is a path in the network between them. Highly-interconnected networks potentially represent significant biological function. In the graphical representation of a network, genes or gene products are represented as nodes, and the biological relationship between two nodes is represented as a line. All lines are supported by at least one reference as

stored in the IPKB. The intensity of the node colour indicates the degree of up- (red) or down- (green) regulation of a given gene. The network with the highest score is shown in Figure 5.13, this network had a score of 53 and contained 33 focus molecules. This network was highlighted as having a role in cell to cell signalling and inflammatory response. The network score is a guide to the relevance of the genes in relation to specific pathways identified in the software. The score is not an indication of the quality or biological relevance of the network; it simply calculates the approximate "fit" between each network and your Network Eligible Molecules.

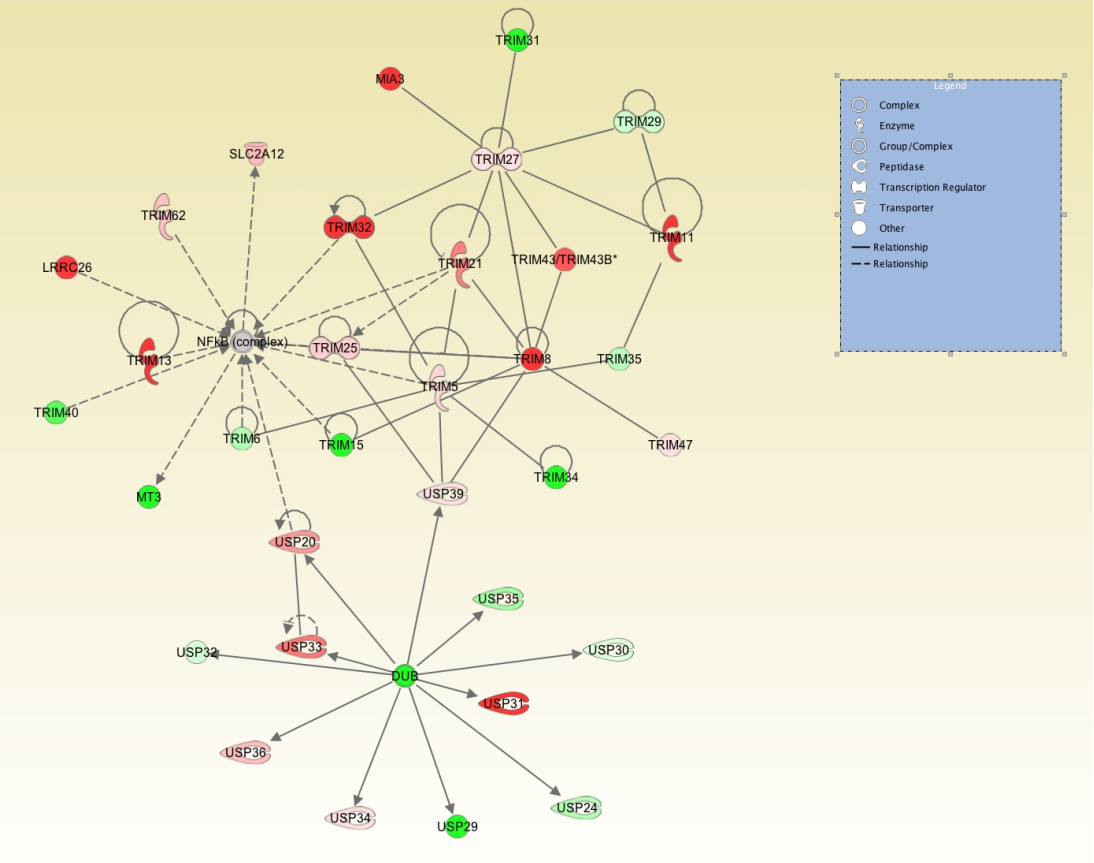

Figure 5.13: RNAseq Network Analysis (Ingenuity Software, Qiagen)

Top predicted network involvement of the differentially expressed genes following analysis with Inginuity software (IPA). This network is involved in cell to cell signaling and the inflammatory response

The second highest ranking network predicted by the IPA software is shown in Figure 5.14 and is described as being involved in cell death and cancer.

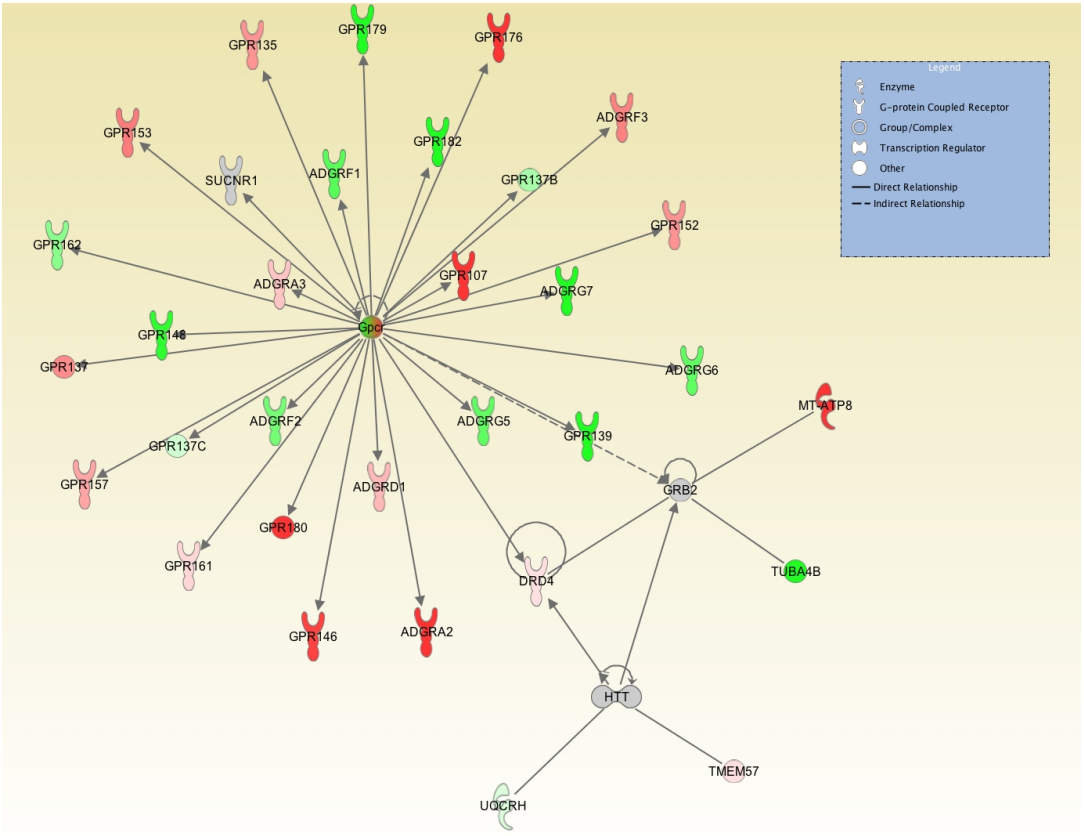

Figure 5.14: RNAseq Network Analysis (Ingenuity Software, Qiagen)

The second predicted network involvement of the differentially expressed genes following analysis with Inginuity software (IPA). This network is involved in cell death and cancer.

The RNAseq data was also analysed with Gene Set Enrichment Analysis (GSEA) software which uses a computational method to determine whether the set of genes identified shows a statistically significant difference between the two biological states (Subramanian, Tamayo et al. 2005). This analysis indicated similar pathways to be involved and corroborates the IPA analysis. The significant pathways highlight the effect on cellular protein metabolic processes, as well as mitochondrial pathways and signaling, see Figure 5.15. These heatmaps also visually demonstrate the extent of difference in expression levels of these particular genes between the two treatment groups.

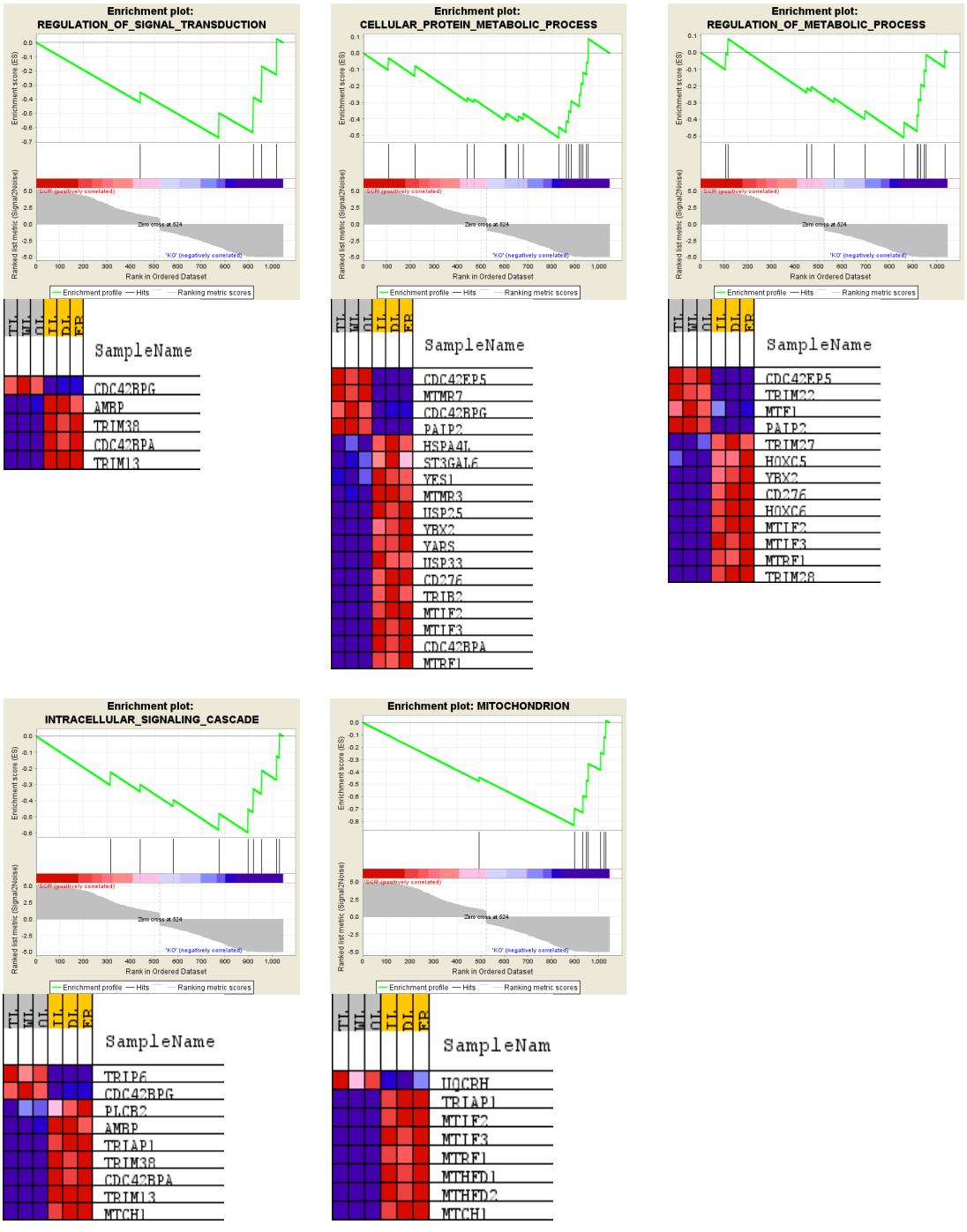

Figure 5.15: Gene enrichment plots generated (analysis with GSEA software)

The list of differentially expressed genes with an FDR >0.05 were up loaded to the GSEA software which sorts the genes into those biologically relevant to specific cellular pathways and processes. Data is displayed as gene enrichment plots and accompanying heat maps of the genes identified within that pathway.

Genes of interest established in the earlier parts of this project were identified and checked for differential expression between the two groups (scrambled versus ASO-27a treated). The predicted miR-27a target genes *PHB, FOX1, Wee1, EGFR, TP53*, *HIPK2, RUNX1, MMP13* were all plotted from the RNA seq data. There were no significant differences seen and the expected pattern of a rise in the ASO-27a group due to being direct targets of miR-27a was not seen across the panel, see Figure 5.16 A. The androgen regulated genes were also investigated within the data set and again no significant difference was seen as shown in Figure 5.16 B.

The LNCaP cell line used to create the xenograft tumours were stably transfected with a plasmid containing the luciferase reporter gene linked to the antibiotic resistance gene (G418). The expression levels of both of these were mined from the data. The level of G418 was used as a surrogate cell number marker, as its expression should be constant in the LNCaP cells. The variable luciferase (AR driven) gene count was made relative to the G418 to give an indication of any AR activity. There was no discernible difference as demonstrated in Figure 5.16 C.

The mice that received the ASO-27a were noted to have lost significantly less weight than their counterparts that received the scrambled oligonucleotide. We could extrapolate from this result that those that received the ASO-27a were less unwell than those that received the scrambled. We were unsure if this was due to the increased cancer burden causing related cachexia or cancer associated morbidity reducing their ability to feed. Genes known to be associated with cachexia were checked for differential expression within the data set, *EIF31, HGS, NUDC, POLMRT, TSC2, APCDD1*. There were no differences seen across this gene panel, see Figure 5.16 D.

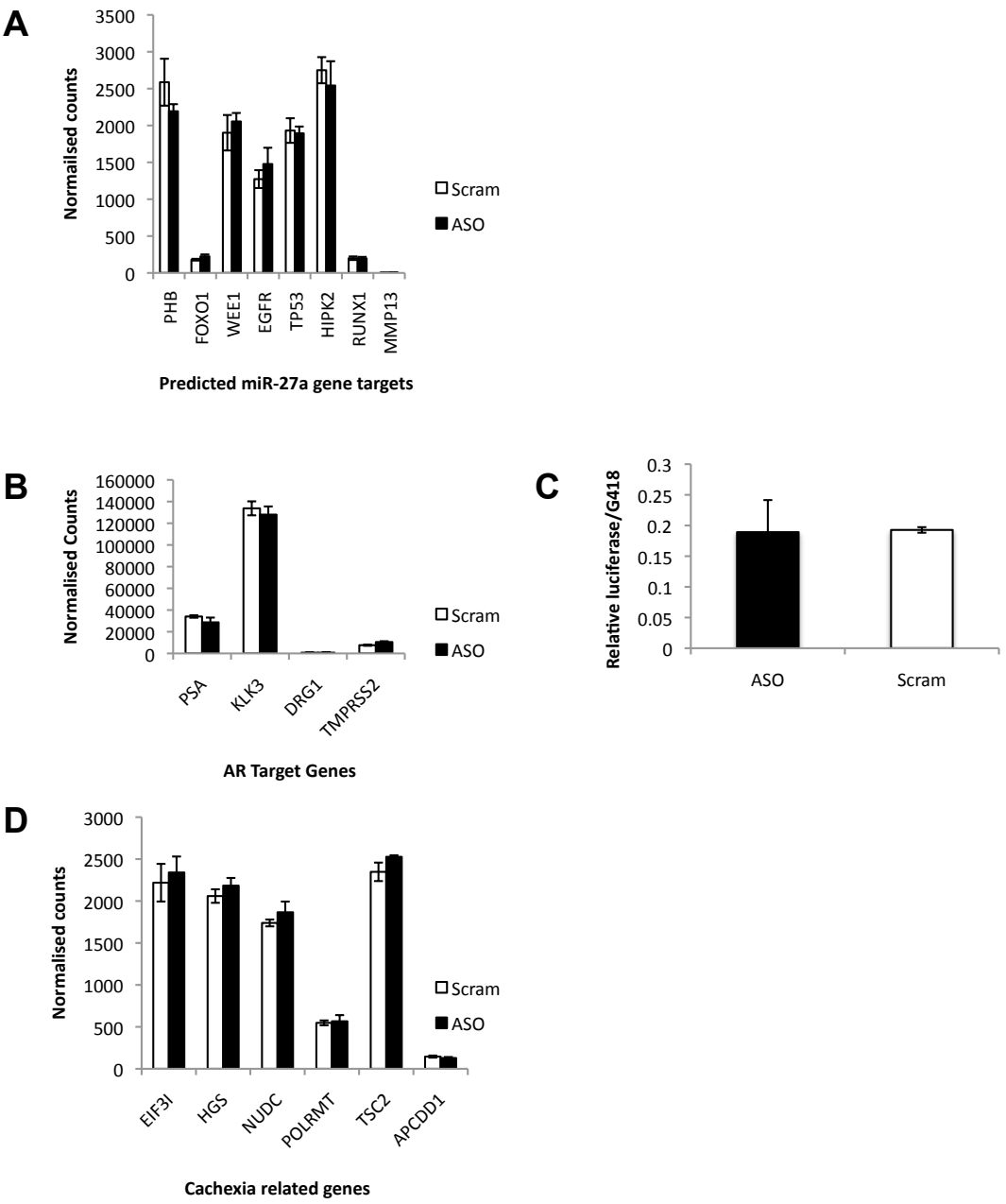

Figure 5.16: There is no effect seen in the predicted genes of interest.

Normalised gene expression counts generated from RNAseq, comparing RNA extracted from the animals injected with the scrambled oligonucleotide (scram n=3) and the miR-27a antisense oligomiR (ASO n=3). Data represents the mean +/- SEM. (A) Predicted miR-27a target genes. (B) Androgen regulated genes (C) Quantification of the luciferin gene relative to the G418 gene both stably transfected into the stable LNCaP cell line. (D) Cachexia related genes.

5.1.11 RNA Sequencing – miR Target Analysis

The set of differentially expressed genes (1046) were cross-referenced against the predicted miR-27a targets (3237) as generated by the online miR prediction tool TargetScan7, see Figure 5.17. We found 68 of the 1046 differentially expressed genes were predicted miR-27a targets (6.5%). As a random comparison predicted targets of two miRNAs (miR-423 and miR-191) were cross-referenced with our gene set and only 1.25% (13 genes) were found in overlap in the case of miR-423 and 1 gene in the case of miR-191 (data not shown).

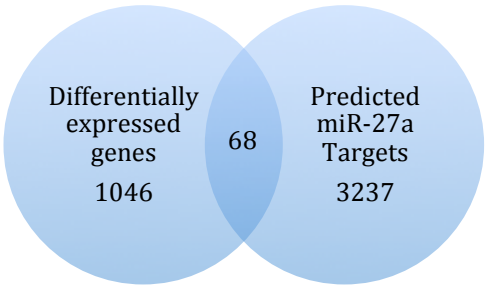

Figure 5.17: Venn diagram of the comparison of the differentially expressed genes from the RNAseq experiment crossed with predicted miR-27a target genes as identified by Targetscan7 software.

In addition we used mBISON software to analyse the differentially regulated gene list to look for the most common miR families that target this group of genes (Gebhardt, Reuter et al. 2014). The software looks at miR binding sites near the 3'UTR of genes and is powered using the TargetScan7 database. The family that includes miR-27a was fifth most common which is significant given that there are 1543 reported miRNA families, see Table 5.2 (Kamanu, Radovanovic et al. 2013).

Table 5-2: mBISON software analysis of miR binding sites within our list of differentially expressed genes

miR Family	Number of times the seed region was found in the 3'UTR of the genes with altered expression
miR-124/124ab/506	45
Let-7/98/4458/4500	36
miR-17/17-5p/20ab/20b-5p/93/106ab/427/518a-3p/519d	34
miR-137/137ab	32
miR-27abc/27a-3p	30
miR-200bc/429/548a	29
miR-30abcdef/30abe-5p/384-5p	29
miR-128/128ab	29
miR-96/507/1271	29
miR-15abc/16/16abc/195/322/424/497/1907	29

See Table 5.3 for a list of the 20 most differentially expressed genes also predicted to be targets of miR-27a, and their representative fold change.

Table 5-3: A table of the twenty most differentially expressed genes within the subset identified as being potential miR-27a targets

Upregulated Molecule	Expression	Downregulated Molecule	Expression
MT-ND4L	↑14.432	TRIM26BP	↓-10.797
TRIM 28	↑12.224	LRRC38	↓-9.087
TEX261	↑11.177	USP30-ASI	↓-6.513
GPR107	↑11.098	TNRC18PI	↓-10.797
TRIM 13	↑10.538	WDR78	↓-5.814
MTG2	↑10.526	GPR158-ASI	↓-5.299
MTHFR	↑10.078	TRIM55	↓-5.205
CDC42BPA	↑9.952	TBX20	↓-5.121
MTFRIL	↑9.861	ADG RG6	↓-4.604
MTPAP	↑9.664	ADG RG5	↓-4.552

The subset of 68 differentially expressed genes predicted to be targets of miR27a was analysed further by again employing IPA, GSEA, and other publically available datasets.The data set was uploaded to IPA and the most relevant genes investigated.

shows the most differentially expressed genes in this data subset. Again *MT-ND4L* the mitochondrial gene that codes for *NADH* is present in the up-regulated table. Other notable genes that are up-regulated are *TRIM28* and *TRIM13*, these are transcriptional mediators that can bind transcription factors.

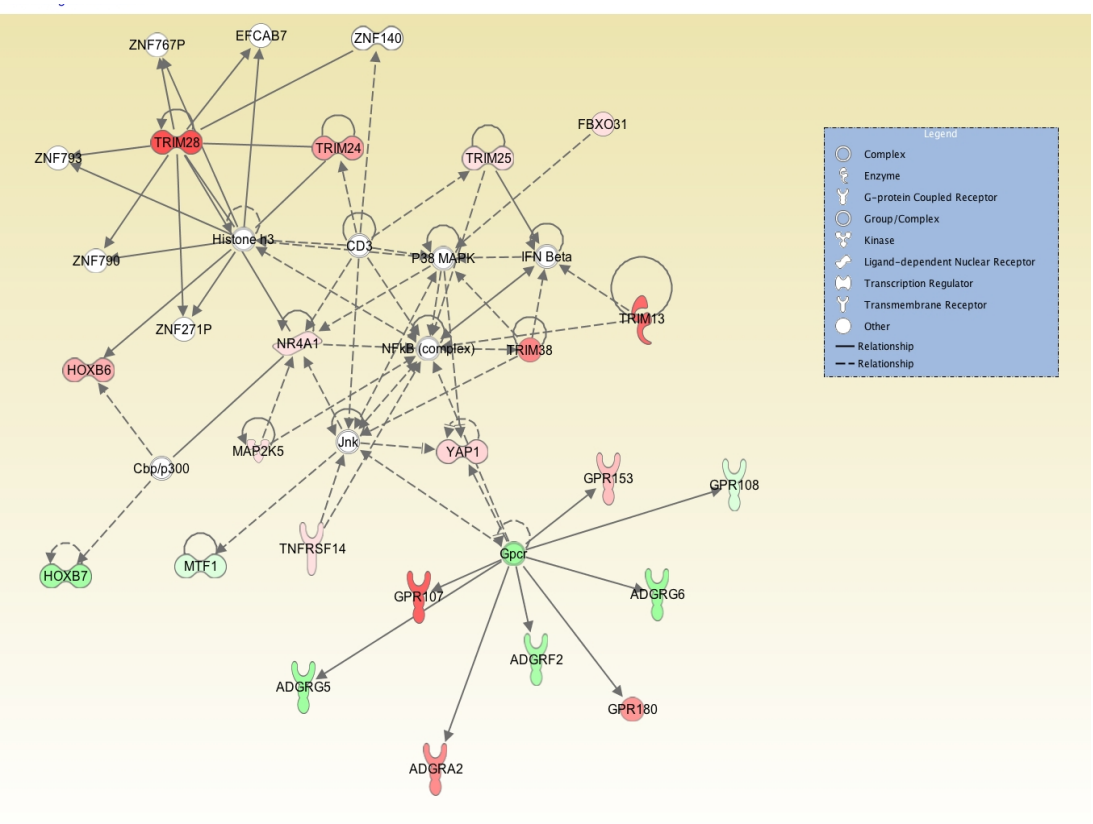

Figure 5.18: RNAseq Network Analysis (Inginuity Software, Qiagen)

IPA generated network analysis of the subset of genes identified to be differentially expressed and likely miR-27a targets. This pathway is involved in cell signaling.

As can be seen in Figure 5.18 the top network of this subset is relatively similar to that deducted from the whole gene set. When the data was analysed with GSEA the signal transduction pathway was again highlighted as being involved, see Figure 5.19.

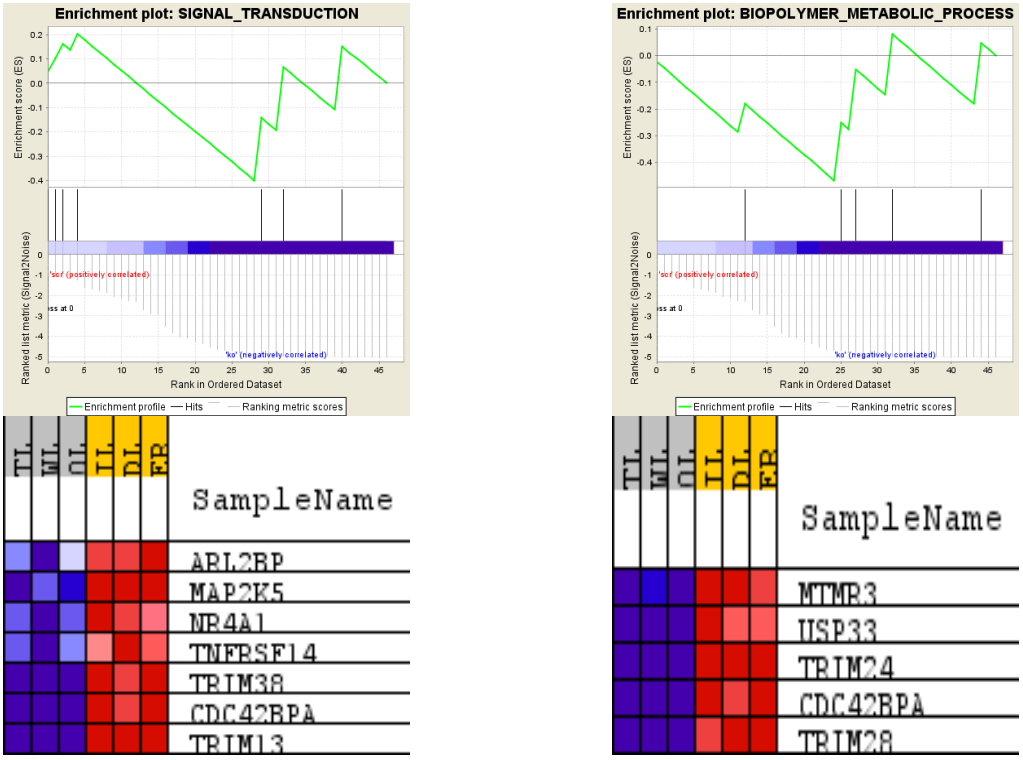

Figure 5.19: Gene enrichment plots generated (analysis with GSEA software)

The list of differentially expressed genes with an FDR >0.05 were up loaded to the GSEA software which sorts the genes into those biologically relevant to specific cellular pathways and processes. The data is displayed as gene enrichment plots and accompanying heat maps.

The 68 miR-27a regulated genes that were differentially expressed in the RNA-seq data were cross referenced with publicly available expression data sets from patient tissue using Galaxy (https://usegalaxy.org/). From the analysed data, heat maps were generated on non-log transformed data using Gene-E (broadinstitute). These data show that some of these genes exhibit expression changes upon disease progression. In a dataset from Varambally *et al.,* comprised of mRNA from benign, cancer, and metastatic prostate cancer, a number of the 68 genes were differentially expressed between disease states to a significant degrees (Fig. 5.20, (Shen, Ding et al. 2012)). Specifically, four genes that have significantly less expression in prostate cancer tissue compared to the benign tissue, namely *ARL2BP, CDC4-2BPA, COCH, MTFR1L*. Others appear to lose expression later in the disease process, at the metastatic stage, such as *YAP1* and *MTHFR,* which have significantly lower levels in the metastatic tissue. In contrast, *HOXB13* and *TMEM50B* were found to have significantly higher expression in metastatic prostate tissue. A further data set

published by Chandran *et al.* compares gene expression profiles from 24 metastatic samples obtained from 4 patients that had castrate resistant prostate cancer and 10 primary tumours, Figure 5.21 (Deng, Zhang et al. 2012). Some of the same genes had decreased expression in metastatic tissue across both datasets namely, *CDC4-2BPA, HOXB13*, *MTHFR, NR4A1* and *WDR70*. A third clinical data set was examined, published by Sun *et al*., it is a cohort of 79 patients that had radical prostatectomies for localised disease (Ziehr, Mahal et al. 2015). At five year follow up 39 of these patients had developed recurrent prostate cancer (defined by a rising PSA on three samples) and 40 of the patients were deemed to have non-recurrence with maintenance of an undetectable PSA. The gene expression data at prostatectomy was grouped by recurrence and the same gene set cross matched, Figure 5.22. Fewer genes were differentially expressed between these two datasets, however, two genes that were flagged in the last two clinical data sets were again significantly different in this study, namely *HOXB13* and *MTHFR*.

A

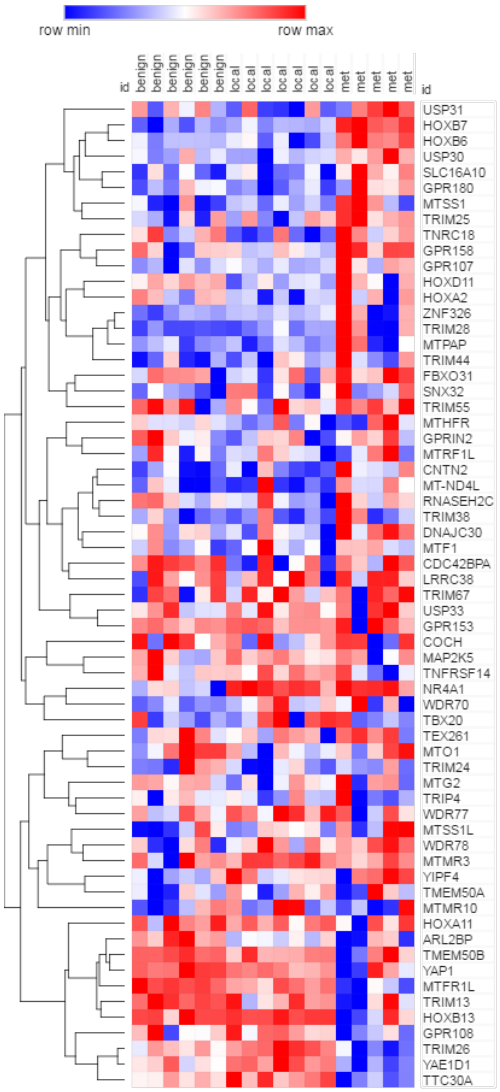

B

GSE3325	benign v local	local v met
ARL2BP	0.002073996	0.231666731
CDC42BPA	0.017936911	0.188886931
CNTN2	0.345929179	0.104054937
COCH	0.016661133	0.170121307
DNAJC30	0.500987646	0.1294956
FBXO31	0.272630833	0.077238338
GPR107	0.148875787	0.050586864
GPR108	0.325473109	0.003485022
GPR153	0.933658906	0.438161398
GPR158	0.360683665	0.002492467
GPR180	0.018477904	0.045193396
GPRIN2	0.170715436	0.183633979
HOXA11	0.356279324	0.573018176
HOXA2	0.022699642	0.088597467
HOXB13	0.608870317	0.004828481
HOXB6	0.999035854	0.005403938
HOXB7	0.078637301	0.000917446
HOXD11	0.000221848	0.124202997
LRRC38	0.872315978	0.441837716
MAP2K5	0.852261497	0.348482551
MTF1	0.342946455	0.807426607
MTFR1L	0.004883072	0.000222076
MTG2	0.800314245	0.859414256
MTHFR	0.661696468	0.013364164
MTMR10	0.265168929	0.53343215
MTMR3	0.172609295	0.086773905
MT-ND4L	0.940307789	0.144808999
MTO1	0.147658994	0.048239799
MTPAP	0.004523031	0.458155789
MTRF1L	0.290929457	0.28108855
MTSS1	0.324032178	0.001035722
MTSS1L	0.692767806	0.734303857
NR4A1	0.014733686	0.000234346
RNASEH2C	0.025756906	0.046965573
SLC16A10	0.318553718	0.083410856
SNX32	0.409616127	0.736493691
TBX20	0.162586464	0.247999049
TEX261	0.51502446	0.143112852
TMEM50A	0.539754985	0.065274776
TMEM50B	0.744494872	0.035411679
TNFRSF14	0.744879972	0.102915735
TNRC18	0.933921522	0.106788244
TRIM13	0.237472708	2.78551E-07
TRIM24	0.970589803	0.815860625
TRIM25	0.345621699	0.315606926
TRIM26	0.003214753	3.23594E-05
TRIM28	0.047848419	0.195689975
TRIM38	0.884997418	0.962454483
TRIM44	0.915616091	0.643619284
TRIM55	0.503929957	0.136117528
TRIM67	0.678805475	0.574410413
TRIP4	0.802636833	0.907634767
TTC30A	0.022177891	0.000630765
USP30	0.277896492	0.0040034
USP31	0.930287597	0.011137064
USP33	0.440462973	0.887924429
WDR70	0.020940529	0.669155107
WDR77	0.055103366	0.119490333
WDR78	0.12368138	0.237438938
YAE1D1	0.010387623	2.29093E-05
YAP1	0.00889538	0.000254013
YIPF4	0.011581448	0.006366949
ZNF326	0.211683414	0.393907664

Figure 5.20: Genes Identified by RNAseq Analysis are differentially expressed in progressive stages of prostate cancer

Data from GSE3325, mRNA from 15 patient prostate samples grouped by pathology, benign (n=5), local (localised prostate cancer) (n=5), met (metastatic prostate cancer) (n=5) analysed by microarray (A) The heat map was generated using the genes identified as differentially expressed between the ASO treated group and the scrambled treated group that are also predicted targets of miR-27a (Targetscan 7) the genes were ordered by unsupervised hierarchical clustering (B) Corresponding P values (two-tailed T-Test) yellow indicates a significant result.

A

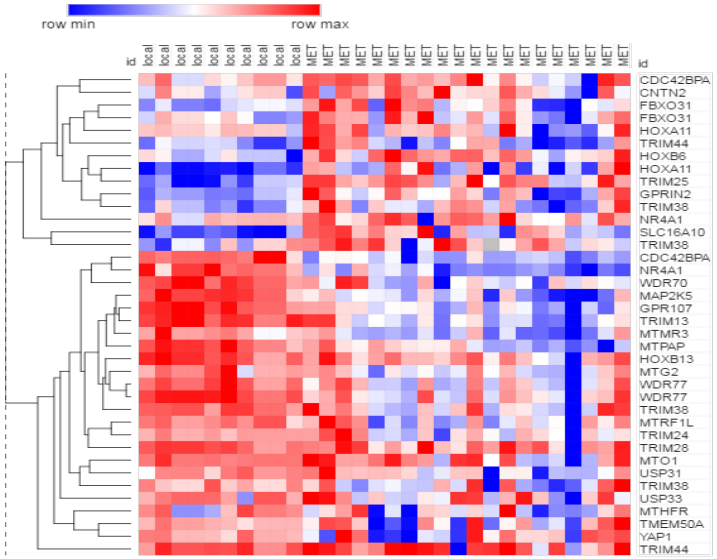

B

GSE6752	local v met
CDC42BPA	0.340158779
CDC42BPA	1.02579E-09
CNTN2	0.151455206
FBXO31	0.080052792
FBXO31	0.196576433
GPR107	7.82279E-08
GPRIN2	0.013723395
HOXA11	0.969848828
HOXA11	0.000545794
HOXB13	0.005504119
HOXB6	0.000150869
MAP2K5	5.19381E-07
MTG2	0.0024033
MTHFR	0.134756159
MTMR3	0.000133074
MTO1	0.168272295
MTPAP	6.2403E-06
MTRF1L	0.007661321
NR4A1	0.281999703
NR4A1	3.71863E-09
SLC16A10	5.58438E-05
TMEM50A	0.150879768
TRIM13	8.58533E-07
TRIM24	0.051728264
TRIM25	3.13341E-07
TRIM28	0.173645409
TRIM38	0.027351502
TRIM38	0.08129149
TRIM38	0.005074204
TRIM38	0.044110218
TRIM44	0.662465358
TRIM44	0.269401085
USP31	0.019638823
USP33	0.283553278
WDR70	3.68094E-05
WDR77	0.0004249
WDR77	4.79588E-05
YAP1	0.121985532

Figure 5.21: Genes Identified by RNAseq Analysis are differentially expressed in castrate resistant prostate cancer when compared to localised prostate cancer

Data from GSE6752, mRNA levels generated using affymetrix oligonucleotide array, 10 primary localised prostate tumours and 24 androgen-ablation resistant metastatic samples (A) The heat map was generated using the genes identified as differentially expressed between the ASO treated group and the scrambled treated group that are also predicted targets of miR-27a (Targetscan 7) the genes were ordered by unsupervised hierarchical clustering (B) Corresponding P values (two-tailed T-Test) yellow indicates a significant result.

A

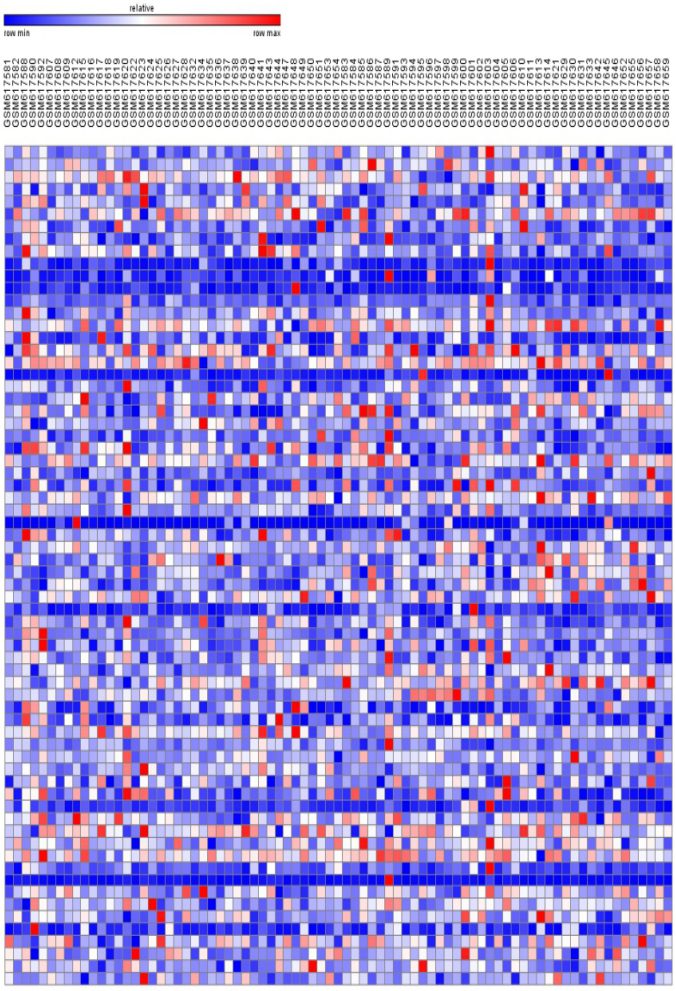

B

GSE25136	recurrent v non recurrent
ARL2BP	0.387182685
CDC42BPA	0.453362515
CNTN2	0.065838913
COCH	0.184252898
GPR107	0.115660314
GPR124	0.81970041
GPR153	0.479539166
GPRIN2	0.401214275
HOXA11	0.641368317
HOXA2	0.037028704
HOXB13	0.030378687
HOXB6	0.449738792
MAP2K5	0.567361444
MTHFR	0.017341164
MTMR3	0.360419643
MTO1	0.128269691
MTPAP	0.450413568
MTRF1L	0.386913579
MTSS1L	0.082117532
NR4A1	0.051580028
SLC16A10	0.999530102
TEX261	0.033385877
TMEM50A	0.770139777
TNFRSF14	0.435357873
TRIM13	0.670107727
TRIM24	0.438351288
TRIM25	0.105589004
TRIM28	0.126194307
TRIM38	0.258588168
TRIM44	0.164647101
TTC30A	0.982491197
USP33	0.578053915
WDR70	0.553821214
WDR77	0.668425119
YAP1	0.73506204

Figure 5.22: Genes Identified by RNAseq Analysis are differentially expressed in recurrent versus non recurrent prostate cancer

Data from GSE25136, data set from 79 patients with localised prostate cancer treated by radical prostatectomy, grouped by disease recurrence at 5 years post surgery, non-recurrent (n=40), recurrent (n=39) gene expression analysis generated using the Affymetrix human gene array (A) The heat map was generated using the genes identified as differentially expressed between the ASO treated group and the scrambled treated group that are also predicted targets of miR-27a (Targetscan 7) (B) Corresponding P values (two-tailed T-Test) yellow highlight indicate a significant result.

From this information I identified targets for qRT-PCR validation, *MTRF1*, MTHFR, *USP31* and *TRIM 13*. These were chosen as they were up-regulated in my main dataset, and they were also predicted targets of miR-27a based on Targetscan7 software.

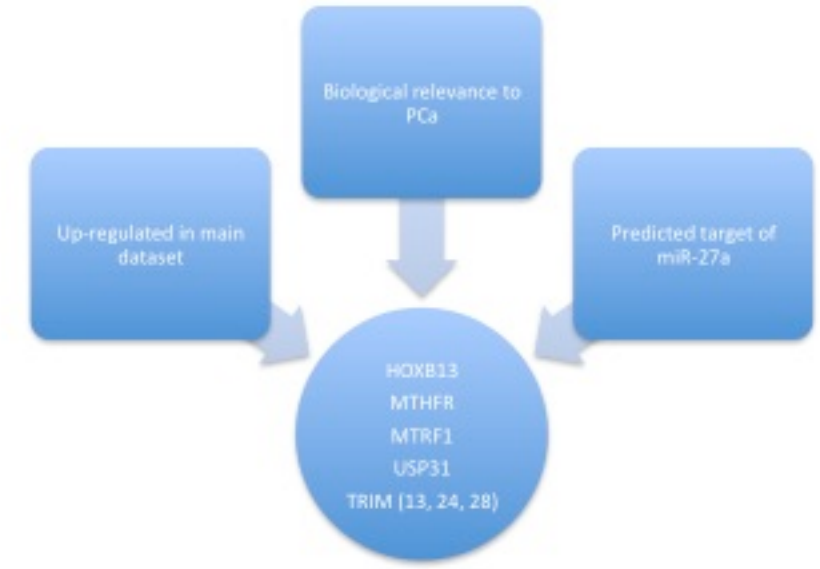

Figure 5.23: Diagram demonstrating the rationale for choosing which targets to validate by RT q-PCR

The mRNA transcript of the genes of interest was quantified from RNA extracted from the xenograft tumours of both mice that received the ASO-27a and those that received the scrambled oligonucleotide using qRT-PCR. As can be seen in Figure 5.24 the trend across the group was that the transcript was higher in the group that received the ASO-27a, as expected. However, none of these results reached significance. Unfortunately the HOXB13 primers did not work so I was unable to determine this result.

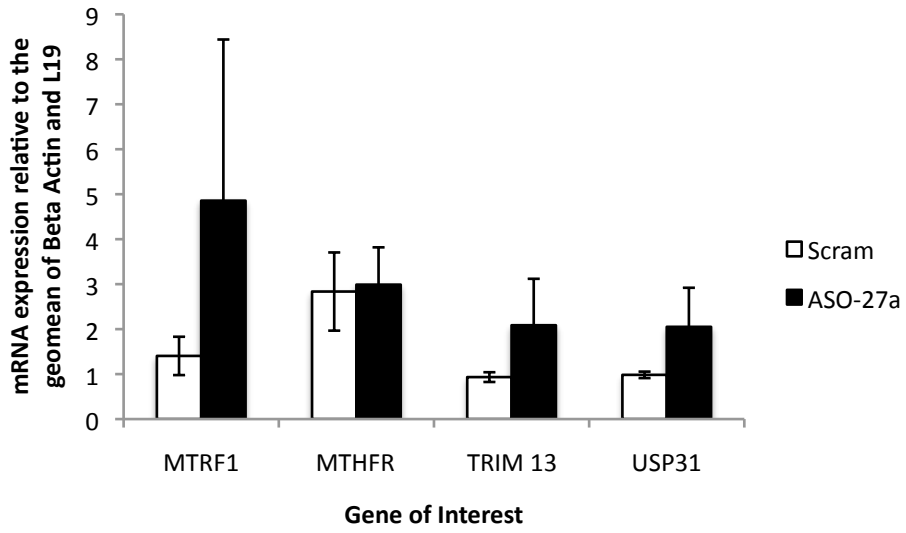

Figure 5.24: mRNA expression levels of the genes of interest

Levels of mRNA were quantified from the RNA extracted from the xenograft tumours at the termination of the experiment, data normalised to a geomean of L19 and Beta Actin. Columns represent the mean +/- SEM (ASO group n=7) (Scrambled group n=7)

5.2 Discussion

The major functional role of miRNAs is determined by the protein-coding mRNAs that they target. The majority of published data has focused on miRNAs exerting their effects via direct seeding to the 3'UTR, the canonical pathway. There are no mechanistic requirements that restrict miRNA action to only the 3'UTR region. There are published reports of miRNAs influencing gene expression via direct binding to DNA and they have been shown to bind to the 5'UTR, they have even been found to activate rather than inhibit gene expression in some instances, as discussed in my introduction. Thus, elucidating the biological function of a miRNA is challenging. Studies often use bioinformatic predictive software, such as Targetscan (Cambridge, MA, USA), miRanda (New York, NY, USA) and miRBase (Manchester, UK) to determine the putative targets for each miRNA (Enright, John et al. 2003, Kozomara and Griffiths-Jones 2014, Agarwal, Bell et al. 2015). Although these algorithms are a good starting point for the prediction of miRNA targets, ultimately functional experiments must be used to validate a gene target.

At a cell line level miR-27a has been associated with increased growth in a lung cancer cell line as well as two pancreatic cell lines and a breast cancer cell line (Liu, Tang et al. 2009, Wang, Li et al. 2011). MiR-27a has been identified as an oncomiR in several cancers, such as gastric and pancreatic, as discussed in the introduction. It has been labelled an oncomiR as it is predicted to target a number of cell cycle regulatory and tumour suppressor proteins including prohibitin. These proteins, as described in Table 1.3 in the introduction, can be grouped by their overlapping roles in cell cycle regulation, transcriptional repression and apoptosis. Studies exploring the levels of miR-27a in prostate cancer have been conflicting. This could be because miR-27a is androgen regulated and therefore hormonal treatments confound the results. Theoretically, miR-27a represents an exciting potential target for a novel therapy in prostate cancer.

Antisense oligonucleotides have been used successfully now in clinical trials - for example, ASO-122 to treat hepatitis C infection, as reviewed in Bandiera *et al* (Bandiera, Pfeffer et al. 2015). The ASO technology has considerable advantages

over currently available therapies. Low toxicity and few side effects would be anticipated while using ASOs because of their small size, potential for modification and high specificity (Saad, Hotte et al. 2011).

5.2.1 ASO-27a abrogates LNCaP growth both *in vitro* and *in vivo*

We confirmed in cells that ASO-27a decreases the level of miR-27a and that there is a corresponding increase in prohibitin expression. Transfection of LNCaP cells *in vitro* with ASO-27a in the presence of androgen led to a significant decrease in growth when compared to the ASO-scrambled control. Thus ASO-27a is able to abrogate androgen-dependent prostate cancer cell growth *in vitro* in part by increasing prohibitin protein levels, confirming the hypothesis that ASO-27a may be a potential therapeutic for prostate cancer. The anti-proliferative result was more marked when using the unmodified ASO-27a produced by Dharmacon but because we required a greater level of chemical stability for in-vivo work we used the ASO with less efficacy manufactured by Exiqon.

As discussed previously ASOs are highly target specific and very small so are unlikely to cause cellular toxicity. However, they have a multitude of different targets within different tissues, so the full extent of potential off-target effects is difficult to predict. Testing the ASO-27a in mice harbouring LNCaP tumour xenografts not only helps to investigate unwanted side effects but also to ensure that anti-proliferative effects of ASO-27a observed in cell lines are consistently observed in a more complex environment that in part approximates human prostate tumours. The first *in vivo* experiment showed the trend that tumour growth was lower in the group treated with ASO-27a but it did not quite reach significance and had to be terminated ahead of schedule. When the experiment was repeated the same growth pattern was observed and this time the experiment was able to run to completion and the difference in growth was found to be significant. ASO-27a significantly abrogates growth of LNCaP xenografts *in vivo*. The additional element of an androgen receptor activity luciferase reporter within the second xenograft experiment gave us the potential to determine some of the mechanism of action of the ASO-27a.

5.2.2 Preliminary data indicates that the ASO-27a was well tolerated and circulated widely with the mice

Importantly there were no signs of adverse effects in mice that received the ASO-27a. In fact these mice lost less weight than their counterparts that received the ASO-scram and none of them had to be culled early for humane reasons. These data support our hypothesis that the mice receiving the ASO-27a had less tumour burden. The reasons for this may be due to less cancer related cachexia, potentially due to the decreased tumour burden or it could be an off target effect of the treatment on cachexia related genes. It may also be that because of the increased tumour burden in the scrambled oligonucleotide group those mice felt less well and in turn ate less. Overall it does indicate that the mice in the group receiving the ASO-27a were healthier than their control counterparts. Further studies to explore the absorption, distribution, metabolism, excretion and toxicity (ADME-T) would need to be conducted if ASO-27a is to be pursued as a potential therapy.

The northern blots conducted on the mouse organs and on the tumour tissue demonstrate that following tail vein injection the ASO-27a is stable in circulation and able to be absorbed into the target tissues (Figures 5.7 and 5.8). From the very preliminary data (n=1) it does appear that there is more uptake of the ASO-27a in the kidneys and the liver than the prostate and the tumour. This is not unexpected as these are the waste organs of the body and receive a very large portion of the blood circulating volume. It had been my intention to further explore this with multiple repeats to establish ASO-27a levels in the respective tissues, however, this was limited by the amount of RNA required to conduct such experiments.

5.2.3 ASO-27a exerts its effects via apoptosis and some AR modulation

The data showed that those xenografts treated with ASO-27a had significant tumour growth suppression. Immunohistochemistry demonstrated no difference in the proliferative marker Ki67 on staining of the tumour tissue. However, we did see a statistically significant increase in the caspase marker, indicative of increased apoptosis in the ASO-27a group.

We aimed to try and further delineate the mechanism by which the growth suppression was achieved and following on from our initial data and the link between miR-27a and prohibitin we hypothesized that the AR may be involved. The data presented in Figure 5.6 alludes to the fact that it may, in part, play a role, but not to the extent at which we might have expected. We measured serum PSA levels post mortem and found lower levels in the serum of the mice receiving the treatment ASO-27a oligonucleotide, however this did not reach significance. This may reflect the higher tumour burden within scrambled oligonucleotide group rather than being a good indicator of higher AR activity. Indeed, when the PSA levels were made relative to the tumour volume the difference in the median between the two groups decreased further. However, complicating the mater is the fact that the measured tumour volume does not fully correlate to active tumour as they may well have had a dead centre (necrotic) no longer producing PSA and in addition the highly vascular tumours contained voluminous blood clots.

A second surrogate marker of AR activity that was measured was bioluminescence from the stably inserted AR luciferase reporter gene. Measurements of the bioluminescence were taken at biweekly intervals following injection of luciferin. Again we were expecting to see a difference in the bioluminescence reported from the model if AR activity was involved in the antiproliferative effects we observed. Unfortunately no difference was observed between the two groups and in addition the signal being reported actually decreased as the experiment went on despite tumour growth and therefore presumably increased numbers of cells expressing the AR reporter gene. This indicates that there were confounding variables that were impacting this data. As the tumours grew they became increasingly haemorrhagic, especially the larger tumours which were found in the scrambled oligonucleotide group. Coagulated blood is very dark in colour and this can absorb the luciferase signal. In addition, the centres of the larger tumours were often observed to be necrotic - this dead tissue would not be emitting any bioluminescent signal and also may have hindered delivery of the drug/substrate. In order to determine if the cells were still giving a bioluminescent signal that we were unable to read due to blood, the mRNA levels of the luciferase gene were determined from the mRNA extracted from the tumours at the completion of the experiment. As can be seen in Figure 5.6

H the trend was for less luciferase expression in the ASO-27a group but this did not reach significance. It may be more likely that the oxygen and ATP are required for the luciferin reaction were not reaching the tumour cells due to necrotic centres and poor vascularity. These factors probably all contributed to the lack of useful data obtained from the AR luciferase reporter in the xenografts.

We are also examined AR target genes for indications of secondary effects on AR signalling. The trend across all four target genes was that they were decreased in the mRNA from the tumours of the group treated with ASO-27a, but only in the case of *TMPRSS2* was this decrease significant.

The likelihood is that miRNAs act like cellular rheostats, fine-tuning target mRNA levels rather than acting as binary on/off switches. Thus the effect seen is dependent on the levels of endogenous mRNA targets for the miR in question within each tissue in question. For this reason looking at levels of expression at a singular time point, although it gives us indications as to mechanism of action, is unlikely to give us complete understanding. Thus, AR may play a role as well along with a number of other targets involved in apoptosis and or proliferation.

RT-qPCR analysis highlighted a significant increase in *EGFR* and *HIPK2* upon ASO-27a treatment (Figure 5.9). EGFRs, epidermal growth factor receptors, are a large group of receptor tyrosine kinases that play a wide role in cellular signalling and have been implicated in a large number of cancers, including lung, breast and head and neck (Ferguson, Berger et al. 2003). *EGFR* has been termed an oncogene in a number of cancers where it is has been found to be aberrantly overexpressed and this has led to the development of anticancer therapeutics directed against *EGFR*, including gefitinib and erlotinib for lung cancer, and cetuximab for colonic cancer (Raymond, Faivre et al. 2000, Paez, Janne et al. 2004, Mok, Wu et al. 2009, Van Cutsem, Kohne et al. 2009). The role of *EGFR* in prostate cancer is not well understood. However *EGFR* has been found to be frequently overexpressed and to correlate with disease relapse and poor outcome (Di Lorenzo, Tortora et al. 2002). Gefitinib and Erlotinib have been trialled in prostate cancer patients without advantage (Canil, Moore et al. 2005, Gravis, Bladou et al. 2008). The other mRNA

transcript found to be significantly raised was *HIPK2*, which is a nuclear serine-threonine kinase that regulates gene expression by phosphorylating transcription factors. It has recently been described as an AR regulator, and depletion of protein levels led to inhibition of AR-dependent gene expression and reduced proliferation of AR-expressing prostate cancer cells *in vitro* (Imberg-Kazdan, Ha et al. 2013). Thus like *EGFR*, elevation of this protein may be a problem for the long term scope of ASO-27a as a therapeutic. This could be explored further by immunostaining for the protein on xenograft tumour sections to determine if the rise in transcript level leads to an actual rise in the protein.

5.2.4 There is a potential, marginal response to ASO-27a in the AR negative, highly aggressive cell line PC3

In xenografts generated from the more aggressive PC3 cell line there was abrogation of growth in the ASO-27a cohort at 14 days but this effect was lost by the completion of the experiment at 24 days. PC3s are a very aggressive cell line that most accurately models castrate-resistant metastatic prostate cancer (CRPC) in patients that have very few viable therapeutic options. Any abrogation of growth in this cell line would certainly support the hypothesis that ASO-27a represents a putative therapeutic for advanced CRPC. The observation that the growth effect was lost towards the end of the experiment may be due to the fact that these cells grow despite not having the AR and therefore any mechanism acting via AR would have no effect. It is also possible that mechanisms of resistance are activated within the cell line - e.g. active export of ASO-27a from the cell or upregulation of endogenous miR-27a.

5.2.5 RNA sequencing indicates that apoptosis may be a key mechanism of action for ASO-27a

We conducted RNA sequencing from RNA extracted from 3 representative tumours from each treatment group in order to gain a greater understanding of how treatment with ASO-27a could be resulting in less tumour growth. 1046 genes were found to be differentially expressed between the two groups. The knowledge base driven pathway analysis tool IPA was used to try and draw biological meaning from the list

of genes. Nine of the ten most upregulated genes in the dataset coded for proteins key to the electron transport chain and oxidative phosphorylation. Unsurprisingly the software highlighted mitochondrial pathways as being significantly different between the two groups.

The expression level of prohibitin was not found to be different between the group treated with ASO-27a and the group treated with the scrambled oligonucleotide. However, we know that prohibitin and prohibitin2 form the holdase complex for the electron transfer chain proteins. Perhaps, although the transcript levels stay the same, the cellular location of the prohibitn and in turn its predominant role in the cell may be different. The prohibitin level could be lower in the mitochondria and thus have an effect on the electron transport chain but higher in the nucleus where it exerts its effect as a co-repressor of the AR, so the balance and total amount of prohibitin mRNA transcript is the same but the functionally different.

Another gene that was highly overexpressed following treatment with ASO-27a was *HOXB13* is a transcription factor belonging to the homeobox gene family. It has a role in foetal skin development and cutaneous regeneration (Davis, Murphy et al. 2009). *HOXB13* has been reported to be highly expressed in prostate tissue and has been implicated as a potential risk factor for prostate cancer. This potentially does not fit with our finding that it is raised by the treatment with ASO-27a, however, a paper published in 2012 by Ewing *et al.* showed a 10 to 20% fold increase in risk when men had a particular variant (G84) of *HOXB13* so it may be that the risk lies with the variant rather than the expression level (Ben, Li et al. 2013).

All of the ten most commonly downregulated genes coded for metallothioneins, which are proteins found on the membrane of the golgi apparatus. They have the capacity to bind heavy metals and are purported to have a role in protection against oxidative stress. The cysteine residues can capture harmful oxidative radicals like the superoxide and hydroxyl radicals (Zhou, Zeng et al. 2012, Zhou, Li et al. 2012). They are also purported to have a role in transcription factor regulation (Gu, Li et al. 2012).

In the canonical pathways analysis the 14-3-3 signalling pathway was identified as being significantly involved given the list of genes differentially expressed. The 14-3-3 pathway contains many regulatory molecules included in mitogenic signalling, apoptotic cell death and cell cycle control, for example *WEE1, P53, RAF1, JNK, MEK1* and *YAP,* some of which have already been flagged as potential miR-27a targets (*WEE1, P53, YAP*). Interestingly some of these targets (*P53, WEE1*) were checked directly from the RNAseq data and found not to be differentially expressed. *YAP1,* a predicted miR-27a target, was shown to be significantly higher in the RNA from the tumours treated with ASO-27a.

The network analysis demonstrated a large number of molecules involved in cell signalling and inflammation were affected by the treatment. I think this is to be expected given the amount of necrosis seen within the tumours that will have generated an inflammatory reaction. The second highest scoring IPA network was cell death and cancer, this supports the earlier immunohistochemistry staining that showed higher levels of apoptosis in the tumours treated with ASO-27a, Figure 5.5.

I mined the RNAseq data for the predicted miR-27a target genes that we had previously checked by qRT-PCR, including prohibitin. We had seen a significant rise in *EGFR* and *HIPK2* at mRNA level using qRT-pCR on all 19 tumours (Figure 5.9). Unfortunately these results were not validated in the RNAseq data (Figure 5.16 A). Potentially this may reflect the fact that the RNAseq was conducted on a subset of just 3 tumours from both treatment groups. In addition, the earlier small effect on the AR target genes was not validated nor was there any effect on the luciferase AR reporter. As discussed before the effect on the AR was never overwhelming and perhaps the small differences seen when the whole cohort of tumours were compared was lost when just a small subset was checked with the RNAseq.

Given that the mice receiving the ASO-27a lost significantly less weight then the mice receiving the scrambled ASO I mined the data looking specifically at cachexia related genes. Expresion of these were found not to differ between the two groups. This may indicate that the weight loss that was observed was not cancer related cachexia but rather cancer related morbidity.

5.2.6 RNA sequencing analysis of a subset of genes identified using miR predicitive software

To try and further interpret the RNAseq data I cross-referenced the list of genes differentially expressed between the two treatment groups against the list of predicted miR-27a targets according to miR predictive software Targetscan7. Only 6.5% of the differentially expressed genes were predicted miR-27a targets. These prediction tools, although a good starting point, are notoriously unreliable and must always be followed up with functional validation studies. It also could be that the remaining 90% of regulated but non-target genes are a secondary result of changes in the targeted genes. Reassuringly, similar genes were highlighted as having potential roles in the identified signalling pathways and gene enrichment plots.

The 68 genes that were differentially expressed and predicted miR-27a targets were cross-referenced against three publically available data sets. A large proportion of the genes found to be upregulated on treatment with ASO-27a also appear to be lower in metastatic tissue when compared to benign or even localized prostate cancer, notably *ARQBP, MTRF1, YAP1, MTHFR*. Extrapolating this result, it could be argued that these genes are lowered as part of the changes adapting a cell to be able to develop a metastatic phenotype. Given this, using ASO-27a to raise the levels of these genes could have potential for treatment and prevent development of this metastatic phenotype.

The third dataset, seen in Figure 5.22, demonstrated gene expression in prostate cancer recurrence. In this dataset fewer of the ASO-27a and miR-27a target genes came up as relevant, however, *HOXB13* and *MTHFR* were significantly lower in the tissue from recurrent prostate cancer.

DNA methylation has a role in carcinogenesis, as an important regulator of gene transcription. A variety of tumours are known to have alterations in DNA methylation. Both hypermethylation and hypomethylation have been recognised causes of oncogenesis. The role of dietary folate, *MTHFR* polymorphisms and the role of demethylating agents are being intensively investigated. The MTHFR enzyme regulates an irreversible reaction of 5,10-methyltetrahydrofolate to 5-

methyltetrahydrofolate. Insufficient DNA methylation can lead to genomic instability and activation of oncogenes. Folate-pathway gene polymorphisms have been implicated in several cancers and investigated inconclusively in relation to prostate cancer (Collin, Metcalfe et al. 2009). Lower levels of MTHFR expression in colorectal cancer samples has been linked to higher risk of relapse (Odin, Wettergren et al. 2006). Again could raising these genes with the ASO-27a potentially asisst in prevention of the recurrence of the prostate cancer.

5.2.7 QRT-PCR Validation of the RNA sequencing data

Given the discrepancy between the RNAseq data and the initial qRT-PCR results, validation was undertaken to try and confirm the RNAseq findings. The mRNA of four genes of interest (*MTRF1, MTHFR*, *TRIM13* and *USP13)* were quantified from the RNA extracted from tumours from both treatment groups. Although the results confirmed the same trend, i.e. upregulation in the ASO-27a, treated group none of them reached significance. This result may represent the fact that only a small subset (n=3 per group) were sent for RNA sequencing whereas a larger cohort were checked for expression levels via qRT-PCR (n=7 per group). However, even accounting for this when the subset used for RNAseq was looked at within the qRT-PCR data there was no significant difference found.

The limitations of this study include many related to the IPKB. It is a manually curated database that draws on the scientific literature, and the attribution of functions to gene sets is therefore somewhat subjective. As the literature evolves, so are the attributed pathways likely to evolve. The information in the IPKB, and the relations found in this study are not specific for prostate cancer. However, the analysis gives a good indication of relevant processes by drawing parallels with knowledge obtained from other organ systems and *in vitro* studies.

5.3 Summary of Chapter 5

In summary ASO-27a abrogates growth *in vitro* and *in vivo* in LNCaP cells. ASO-27a may do this via apoptotic pathways, as supported by the immunohistochemistry and RNAseq data. Targets shown to be upregulated following treatment with ASO-27a have been found to be lower in metastatic prostate cancer and recurrent prostate

cancer indicating potential clinical relevance of this as a treatment. Targets identified from the RNAseq data may be key in the response to this inhibitor, and/or may act as biomarkers that could be useful in measuring the response to future therapies based on it. Future work may include measuring levels of identified "targets" of the inhibitor in biopsy samples and serum from patients with prostate cancer.

There is a lot of potential for future work stemming from this study. There are many areas of this study that require clarification and completion that I would have liked to conduct had time allowed. It would be very helpful to confirm apoptosis as the predominant mode of action by doing *in vitro* apoptosis assays with the ASO-27a. This could be conducted using a florescent marker of caspase and flow cytometry, for example. As discussed earlier in order to take ASO-27a any further forward as a potential therapy ADME-T studies would need to be conducted.

It would be helpful to clarify the role of the identified target genes by overexpression of the genes in culture and monitoring for a similar effect on cell growth or cell number. I find it very interesting that USP31 and MTHFR as well as other post translational modifiying genes had increasing expression following treatment with ASO-27a. Yet tumour supressor genes that we were expecting to be raised by treatment were not affected at least at the transcriptional level.

It may also be interesting to investigate potential synergy between ASO-27a and other prostate cancer modulating drugs such as the chemotherapy docetaxel or the anti androgen Enzalutamide. Taxol resistant cell lines were found to have higher levels of miR-27a compared to the senistive parental cell lines. Could lowering the level using an ASO improve resistance to Taxol based chemotherapies . In another in vitro study in oesophageal cancer cell lowering miR-27a levels led to increased sensitivity to chemotherapy. Ultimately the ASO-27a produced a highly significant effect in decreasing growth of the LNCaP xenografts although the mechanism was not as predicted.

Chapter 6 Circulating miRNAs as Biomarkers for Prostate Cancer

The increasing rate of diagnosis of prostate cancer coupled with the lack of accurate biomarkers to distinguish indolent from aggressive disease, predict relapse, or aid with treatment stratification, make prostate cancer a growing clinical problem. MiRNAs have been proposed as potential biomarkers since their discovery, for a number of reasons: first, they are stable in circulation and even stable post collection; secondly, they have been shown to be dysregulated in cancer; thirdly, they are quantifiable. In addition, being able to assay these miRNAs in so-called liquid biopsies - such as serum, plasma or urine - is convenient due to their routine availability.

The major stumbling blocks in miRNA biomarker research have been normalization and reproducibility across studies. My work to date, showing some inverse correlation between prohibitin levels and aggression in a small panel of prostate cancer cell lines, supports the hypothesis that prohibitin levels may decrease with the advance of prostate cancer. I have also shown a corresponding increase in miR-27a levels with increasing aggressiveness of the cell lines and in metastatic tumours. My working hypothesis is that miR-27a is dysregulated in prostate cancer and indeed is higher in patients with advancing stages of the cancer. Whether the raised level is indicative of more aggressive disease or the levels rise as the cancer progresses is another question that would require further investigation. Thus, quantification of miR-27a could potentially aid in developing a biomarker of prostate cancer diagnosis or progression, or at the very least a biomarker to potentially identify patients who would benefit from treatment with ASO-27a or to monitor effects of treatment much like PSA is used.

Supporting this hypothesis are data from Dr Dart in our lab that were generated using the protocol I established and will describe in the following text: Dr Dart found a 3 fold higher level of miR-27a in mice with xenografted LNCaP tumours compared to healthy mice not bearing a xenograft (Figure 6.1A). This increase was even more marked in mice xenografted with PC3 tumours (Figure 6.1B), acting as proof-of-

principle that miR-27a levels can be measured from serum and that differences in level are seen in the presence of prostate cancer and higher grade prostate cancer.

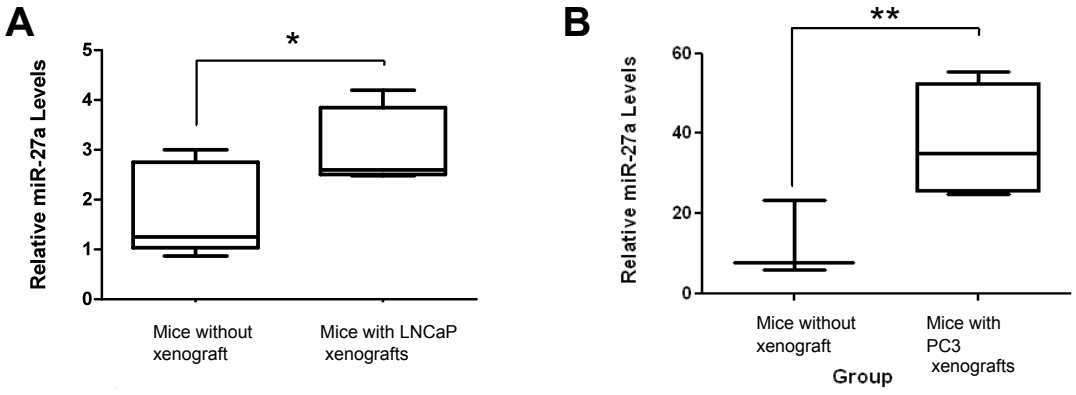

Figure 6.1: Mice with human prostate cancer cell lines have higher miR-27a levels, detectable in serum

(A) miR-27a levels quantified by qRT-PCR and normalised to spiked-in *Cel-miR-39-3p* from the serum of healthy mice and mice bearing LNCaP xenograft tumours. (B) miR-27a levels quantified by qRT-PCR and normalised to spike in *Cel-miR-39-3p* from the serum of healthy mice and mice bearing PC3 xenograft tumours. Data from Dr DA Dart.

6.1 Results

6.1.1 Assay Development

This work was started in 2011 when there was no published protocol or established methodology for miRNA extraction and quantification from liquid samples. The first published protocol was in 2012 and confirmed my early findings, which I will describe in this section. This first section of work was in refining the protocol using miR-27a as an exemplar. To establish a normal range for miR-27a levels in human serum, RNA was extracted from serum from 6 healthy volunteers and miR-27a was detected and quantified using specific Taqman qRT-PCR probes. Initially, the small RNAs U18, U16 and U423 were used to normalise the data as these had been used in many studies to normalize levels of miRNAs in tissues. However, it became clear that levels of these small RNAs differ between individuals' serum, unlike the case in tissue where they can be used as a 'housekeeping' small RNAs. This is demonstrated in Figure 6.2, showing that results varied significantly depending on which small RNA was used for the normalization. As there is no unified published known

'housekeeping' small RNA that can be used, different publications have used different methods of normalisation; chiefly absolute quantification using standard curves of the miR of interest and a spiked-in miRNA, normalising to a spiked in miRNA or a chosen potential miRNA or other small RNA, or a global average of miR expression across a large panel of miRNAs such as in a microarray experiment.

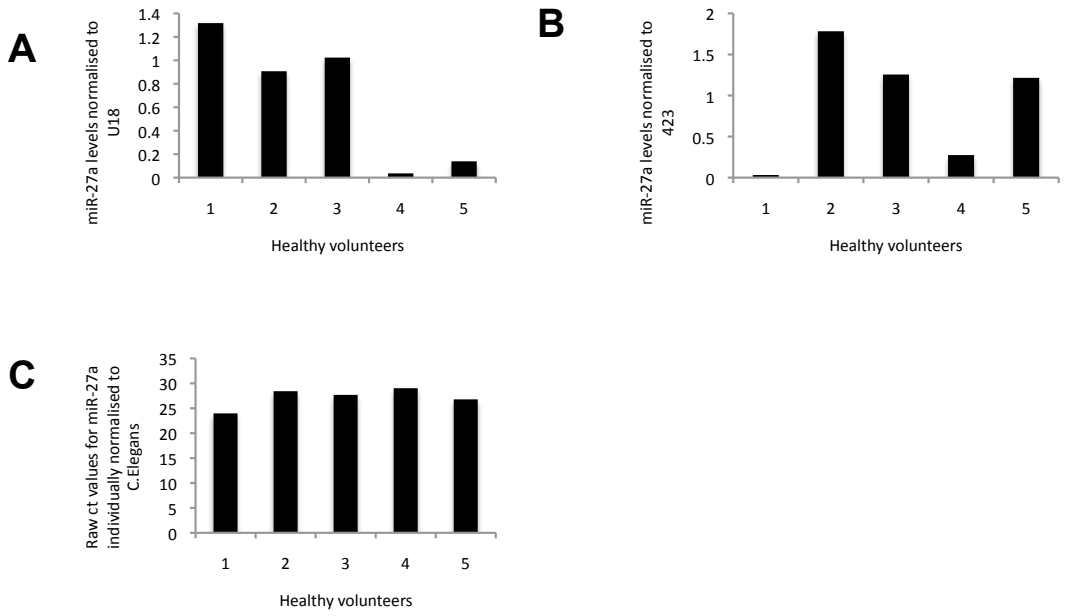

Figure 6.1: MiR-27a levels in human serum, exploring potential normalizing miRs

qRTPCR analysis of miR-27a levels in the serum of healthy volunteers (n=5) (A) shows miR-27a levels normalised to U18 a small RNA commonly used to normalise miRNAs extracted from tissue. (B) shows the same miR-27a levels normalised to small RNA 423 (C) miR-27a normalised to *Cel-miR-39* spike-in small RNA

In view of the fact that from literature search and pilot experiments I had been unable to identify a reliable candidate normalization miRNA, I decided to use absolute quantification. A standard curve of known dilutions of *Cel-miR-39-3p* was produced (Figure 6.3A & B), and a similar standard curve was produced using serial dilutions of a miR-27a mimic (Figure 6.4A). The lower limit of accurate quantification for each assay was designated based on the minimal number of copies input into an RT reaction that resulted in a Ct value within the linear range of the standard curve. A line was fitted to data from each dilution series using Ct values when within the linear range. The spiked-in Cel-MiR-39-3p was introduced to each serum sample

after the addition of the denaturing agent, so as to avoid degradation by the endogenous RNases. For each sample the Cel-miR-39 copy number was calculated using the method described above. This value was then used as a normalization value for the corresponding sample; see Materials and Methods section 2.25 for more detail.

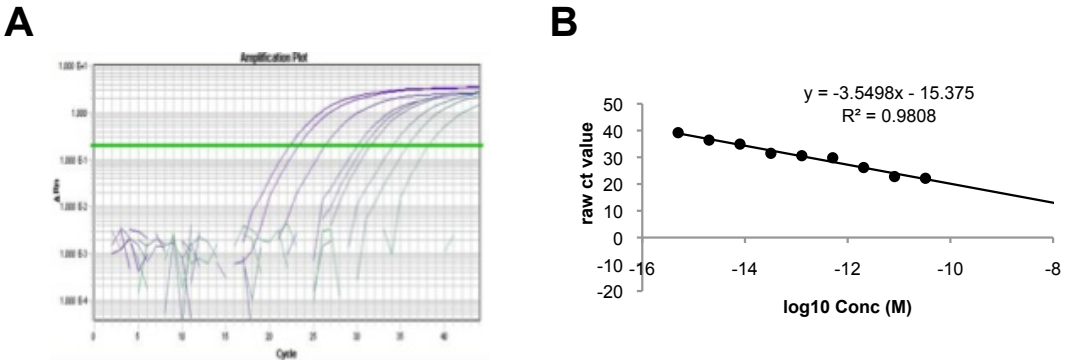

Figure 6.2: *C. elegans* Standard Curve

(A) Real time PCR fluorescent data from DNA amplified by qRTPCR showing product formation across 44 cycles representing *Cel-miR-39-3p* standard curve of RNA from 30pM to 0.1125fM in triplicate (B) Standard curve generated from A.

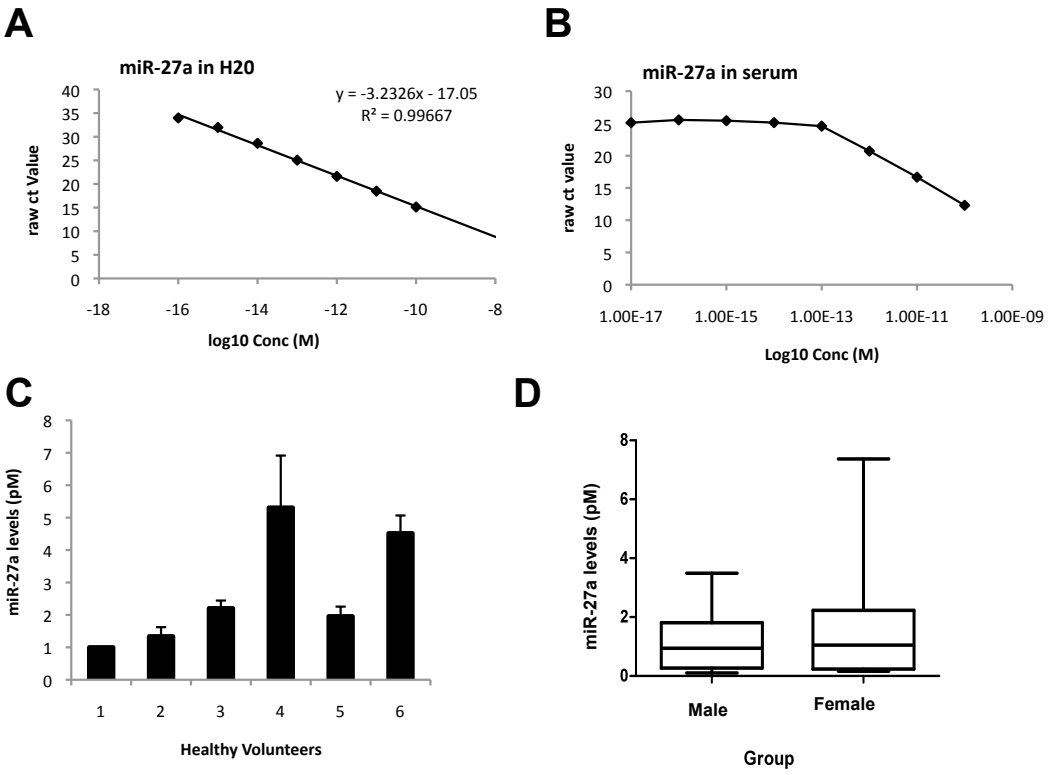

Figure 6.3: Establishing the protocol for miRNA extraction and quantification from blood

(A) Synthetic miR-27a mimic serially diluted in water and then quantified by qRT-PCR (B) Synthetic miR-27a mimic serially diluted in the serum of a healthy volunteer and then quantified by qRT-PCR, the dotted line represents the endogenous level of miR-27a in the serum sample (C) miR-27a levels in the serum of 6 healthy volunteers measured by qRT-PCR and analysed to give an absolute quantification using the data from the miR-27a and Cel-miR-39 standard curves. Data represents the mean from two independent samples from each healthy volunteer +/- SEM. (D) Pooled result of the healthy volunteers grouped by sex (males n=3, females n=3).

To confirm that miR-27a could be extracted and reliably detected by qRT-PCR a serial dilution of miR-27a mimic was spiked into pooled serum from healthy volunteers. As expected the miR-27a was detected in a linear fashion from the serum above a concentration of $1.00x10^{-13}$ M which is likely the endogenous level of miR-27a in this sample, confirming that the miR extraction, RT and qRT-PCR procedures were robust (Figure 6.4 B). Absolute concentrations of miR-27a were calculated for 6 healthy volunteers (Figure 6.4 C). There was no difference in miR levels between the male and female healthy volunteers (Figure 6.4 D).

Ultimately for any biomarker to become clinically useful the test needs to be cheap, reproducible, and robust. Importantly all of these criteria would have to be achievable within an NHS setting. Although in the best experimental settings we are able to control the circumstances of blood collection with a tight standard operating procedure (SOP), in the reality of the NHS this may not always be possible. The chief NHS variables are time from collection to separation of serum, choice of serum collection bottle, and temperature at which the serum is stored. In view of this a short time course experiment was conducted to ensure that the miRNAs are stable at 4°C within the serum, as is reported in the literature. We found that they are stable for at least 4 hours as shown in figure 6.5 A. Some variation was seen but only to approximately three fold which was much lower than the increases evident in the serum from patients with prostate cancer, which was significantly higher in the region of 40-60 fold (Figure 6.5 D). The maximum variation was after 8 hours and this length of time is very unlikely in a clinical scenario. It is also interesting that rather than degrading with time the level at 8 hours was slightly higher. Although the serum should be cell free it is theoretically possible that some cells remained and that the rise is due to cell lysis.

There are two types of serum collection bottles routinely used in NHS practice, the Becton Dickinson vacutainer red top silica coated tube (BD 367814) and the SST yellow top vacutainer tube (BD 367989). The chief difference is that the yellow tube has a gel layer that separates the clot from the serum following centrifugation. To determine if it would be possible to use serum collected in different bottles, serum was collected in each bottle type from 6 healthy volunteers. The levels of miR-27a were lower in the yellow tube serum collections and the pattern of expression was fairly similar except for in control 1, (Figure 6.5 B).

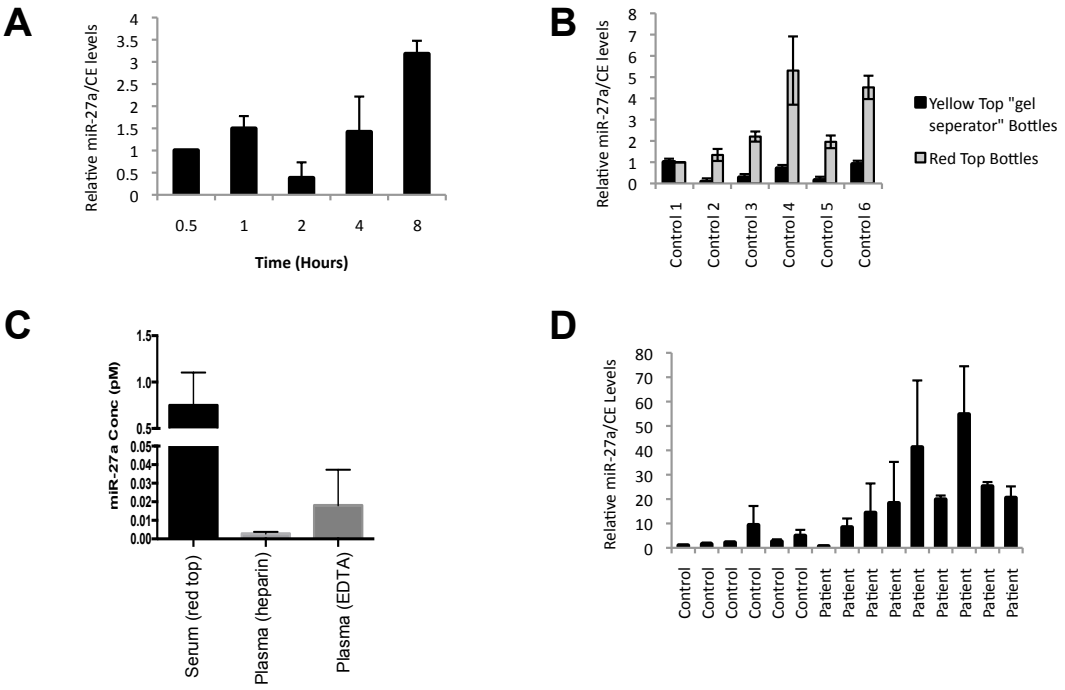

Figure 6.4: Controls to establish the protocol for miRNA extraction from blood and quantification

(A) Variation of miRNA levels from the same serum sample in aliquot and left at 4 degrees °C for extended times. Data represents the mean miR-27a level made relative to spiked in *Cel-miR-39* of three independent samples +/- SEM, then displayed relative to the value at 30 minutes (B) Comparison between the two most commonly used vacutainer bottles to collect serum. Columns in black represent serum collected from red top bottles, the grey columns represent serum collected in yellow top gel separator bottles. Data represents the mean miR-27a level made relative to spiked in *Cel-miR-39* of three independent samples +/- SEM (C) Comparison of miR-27a levels from serum collected in red top serum vacutainer bottle, plasma from a vacutainer bottle containing heparin and plasma in standard EDTA vacutainer bottle. Data represents the mean absolute miR-27a level of three independent samples +/- SEM (D) Triplicate technical repeats of extraction and quantification of miR-27a in control and patient serum. Data represents the mean miR-27a level made relative to spiked in *Cel-miR-39* of three independent samples +/- SEM

It is also possible to extract miRNAs from plasma as well as from serum and there is controversy in the literature as to whether the levels are comparable between the two. Three healthy volunteers had blood collected into three tubes, a red top silica coated tube to collect serum and then two types of plasma collection tubes, one containing

heparin as the anticoagulant agent and the other EDTA. The levels of miR-27a were found to be lower in the plasma collection compared to the collection from serum. Further, plasma collected using bottles containing heparin was unusable as the heparin interfered with the quantification at the qRT-PCR step resulting in an undetectable level of product (Figure 6.5 C). At this point the SOP was confirmed and all patient samples were then collected using the same SOP in the red top silica bottles. MiR-27a levels were quantified by qRT-PCR and normalized to the Cel-miR-39-3p spike-in and read against the standard curve to give absolute levels of the miRNA. Note a more detailed description can be found in the methods chapter 2.25. As can be seen in Figure 6.5 D there is generally a small variation across triplicate technical repeats; the widest variation is between the samples from people with higher levels of miRNAs.

6.1.2 miR-27a is found at higher levels in patients with active prostate cancer who are not on hormonal therapy

An initial pilot study of 15 prostate cancer patients was conducted: see Table 6.1 for patient characteristics. Blood was collected in the red top silica coated vacutainer tubes; it was allowed to clot for 30 minutes then centrifuged at 2,200g for 10 minutes, aliquoted and stored at -80°C. The levels of miR-27a were quantified using qRT-PCR and the data were normalised using the Cel-miR-39-3p spike-in and the standard curves for Cel-miR-39-3p and miR-27a. The patients, when compared to the healthy volunteers, had higher levels of miR-27a although this was not statistically significant (data not shown). However, when the patients whose cancer was in remission (PSA <0.1 for 3 sequential visits) were removed from the cohort there was a significantly higher level of miR-27a in the patients with active cancer (Figure 6.6 A, P=0.0062). In order to try and tease out any further correlations between miR-27a levels and prostate cancer we subdivided the cancer group into patients in remission or with active cancer (defined as having a rising PSA and/or clinical disease progression); this latter group was then subdivided by their treatment. As miR-27a is known to be androgen regulated we hypothesized that levels may be affected by hormonal therapies and so we would get a clearer picture in patients not receiving hormonal therapy. There was a statistically significant difference between the healthy volunteers and those patients with active cancer but off hormonal therapy

(P<0.0001). The patients with cancer in remission had a similar miR-27a level to the healthy volunteers. Those patients with active cancer but on a hormonal therapy (such as an anti-androgen e.g. bicalutamide) had higher levels than the healthy volunteers but these data did not reach significance (Figure 6.6 B).

Table 6-1: Table of patient characteristics for pilot study of miR-27a levels in prostate cancer patient's serum

	no. in group	Median PSA	PSA Range	Median Age	Age Range	Median miR-27a level	miR-27a Range
Healthy volunteers	6	n/a	n/a	34	27-40	2.16	0.92-17.1
Patients with Prostate Cancer	15	173.9	0.03-3224	75	68-88	2.83	0.75-74.49
Current Status:							
In remission	3	0.3	0.03-0.46	71	68-86	1.77	0.99-4.4
Active cancer off hormones	4	17.9	8.64-33.5	75	73-83	26.99	1.26-74.49
Active cancer on hormones	8	503.5	5.54-3224	75	70-88	1.91	0.75-27.52

Abbreviations no. = number, PSA = prostate specific antigen

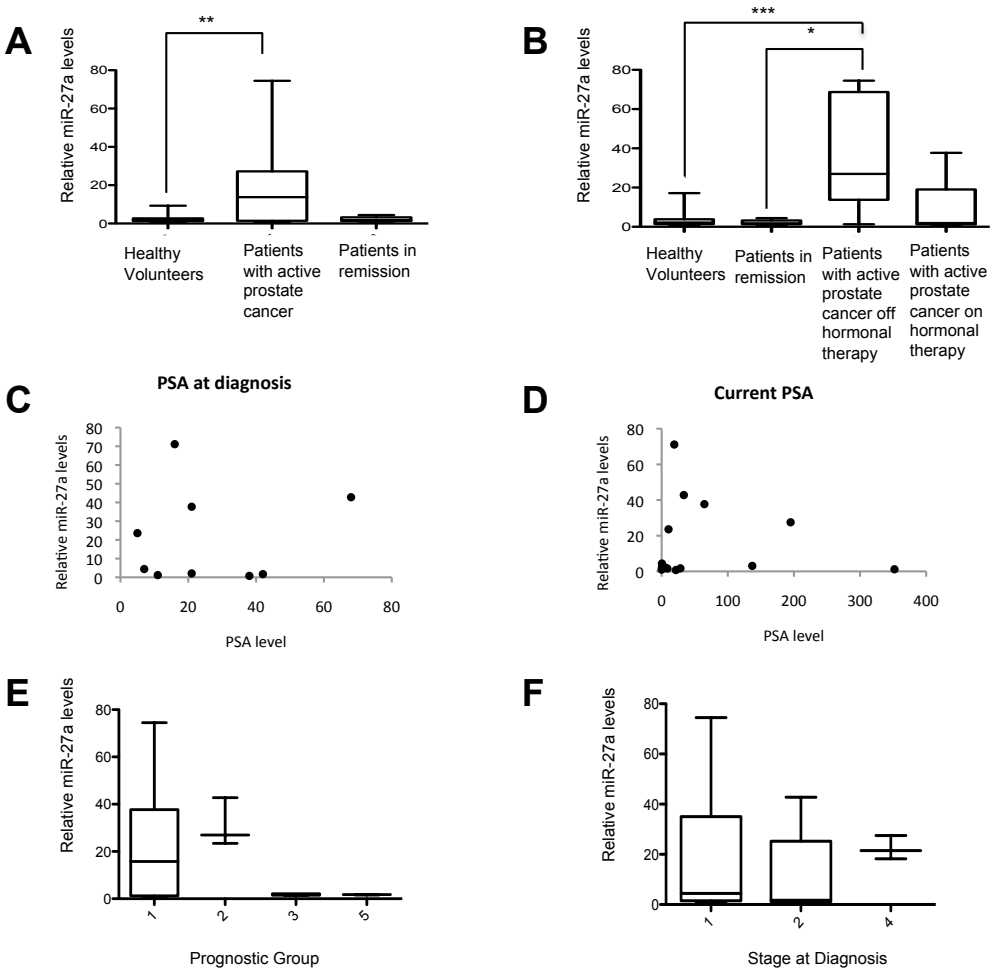

Figure 6.5: miR-27a levels in patients with prostate cancer, data from pilot study of 15 patients and 6 healthy volunteers

(A) miR27a levels comparing healthy volunteers (n=6) and patients with prostate cancer (n=15), Data represents the mean absolute miR-27a level made relative to a standard healthy volunteer sample +/- SEM ** T-test P=0.0062 (B) Cancer patient group broken down into those those in remission and then those with active cancer and then by the patients exposure to hormonal treatments. Data represents the mean absolute miR-27a level made relative to a standard healthy volunteer sample +/- SEM ** T-test P=0.0062 (* T-test P<0.0001, * T-test P=0.0099) (C) Patients serum PSA level at diagnosis plotted against the miR-27 level to determine any correlations (D) Serum PSA level at the time that the blood was taken for the miR-27a level (E) Patients relative miR027a level grouped by their prognostic score at diagnosis determined by their Gleason grade (1=<6, 2=7 (3+4), 3=7 (4+3), 4=8, 5=9) (F) Patients relative miR-27a level grouped by their prostate cancer stage at diagnosis.**

The current gold standard test for both prostate cancer diagnosis and management is the PSA test, although as discussed in the introduction it is far from perfect. MiR-27a levels were plotted against the patients PSA at diagnosis (Figure 6.6 C) and PSA level at the time of the blood sample (Figure 6.6 D) to determine if there was a relationship; no correlation was seen. The data were also plotted with the patients divided by their prognostic score, as determined from the pathological Gleason score, Figure 6.6 E. There appeared to be lower miR-27a levels in the more advanced prognostic groups (groups 3 and 4) which reflects the higher Gleason score of 7 and 8 respectively but these data did not reach statistical significance. Figure 6.6 F is the same miR-27a data plotted with the patients divided by the extent of their disease at diagnosis. Those with a stage 4 or metastatic disease had higher miR-27a levels on average, but this did not reach statistical significance.

6.1.3 A panel of miRNAs potentially dysregulated in prostate cancer

It is unlikely that any single miRNA will achieve the desired level of diagnostic or prognostic accuracy, as there is increasing evidence that miRNAs can be associated with several different types of tumour and physiological states. A miRNA panel or signature is more likely to hold promise as a biomarker, and in view of this we expanded our study to 5 miRNAs of interest. The miRNAs chosen are displayed in Table 6.2. At this time we also chose to change the technology we were using to quantify the miRs by qRT-PCR, moving from Taqman specific assays to LNA technology as this is a more sensitive and specific approach, and also so that we could perform a universal RT step, allowing us to probe for many miRs from each sample. As discussed before, although there are still no consensus endogenous control miRNAs, we included miR-124, miR-423 and miR-146a on the panel as putative control miRNAs as recommended by Exiqon. We also used 4 spike-in controls: uniSP2 and uniSP4 at the time of miRNA extraction, and cel-miR-39-3p and UniSP6 at the RT step as controls of our methodology. MiR assays were arranged on custom panels constructed by Exiqon and the panels themselves contained an interplate calibration assay.

Table 6-2: The miRNAs chosen for the Exiqon Panel

miRNA	Putative Role in Prostate Cancer	References
27a	Validated relationship with Prohibitin	(Liu, Tang et al. 2009)
141	Increased in the serum of men with prostate cancer	(Mitchell, Parkin et al. 2008, Gonzales, Fink et al. 2011, Cheng, Mitchell et al. 2013)
21	Increased in prostate cancer Increased in docetaxel resistance	(Yaman Agaoglu, Kovancilar et al. 2011, Zhang, Yang et al. 2011)
16	Putative control Increased in the serum of men with prostate cancer	(Lodes, Caraballo et al. 2009, Mahn, Heukamp et al. 2011)
195	Increased in prostate cancer	(Mahn, Heukamp et al. 2011)

Serum of a cohort of 28 patients that included the original 15 from the pilot study, was analysed for levels of 5 miRs of interest; see Table 6.3 for the patient characteristics. The patient samples were assigned a code JW1- JW44 in order of collection. As a first step of quality control each serum sample was checked for haemolysis by measuring miR-451 and miR-23a. As miR-451 is abundant in red blood cells a high miR-451 to miR-23a ratio indicates likely contamination with lysed red blood cells. These samples do not necessarily need to be excluded but they should be closely examined for signs that the miRNAs of interest have been influenced by the contamination. Not all miRNAs will be affected as they are not all endogenous in red blood cells. A sample with a miR 451:23a ratio above 7 is considered likely to have been haemolysed. As can be seen in Figure 6.7A, sample JW5 has a very high ratio and for this reason was excluded from further study. (Of

note, this sample would have been excluded regardless as the patient developed colorectal cancer and died shortly after the samples were collected). Sample JW1, JW6, JW10, and JW41 all show borderline levels and the miRNA results were examined for any potential outliers, but after consideration these samples remained in the study.

As previously discussed there is still no agreement on a standard miRNA to run as a internal control for circulating miRNAs. In view of this we ran 4 potential control miRNAs chosen on account of their use in publications as normalizing controls. Both geNorm and Normfinder algorithms run on the data set identified miR-423 as the most stably expressed reference gene for normalizing the RT-PCR data (data not shown). Thus the raw Ct values were normalized to miR-423.

In Figure 6.7 B the data is displayed from the 16 patients with active prostate cancer compared to the 6 healthy volunteer samples which make up the control group. The seven with cancer deemed to be in remission were excluded. There was no significant difference between the control group and the cancer patients over the miR panel overall. However, there was a trend that miRs-141, miR-16, miR-21 and miR-195 were raised in the serum of men with prostate cancer.

Table 6-3: Table of patient characteristics for follow up study using an Exiqon panel to determine the levels of 8 miRs in prostate cancer patient's serum

	no. in group	Median PSA ng/ul	PSA Range ng/ul	Median Age	Age Range
Patients with Prostate Cancer	23	12.8	0.03-3224	75	68-88
Healthy Volunteers	6	n/a	n/a	33	27-40
Current Status:					
In remission	7	0.25	0.01-1.7	70	64-76
Active cancer off hormones	7	19.1	1.51-64.6	79	74-83
Active cancer on hormones	9	71.8	7.58-3224	79	70-91

Abbreviations no.= number, PSA = prostate specific antigen

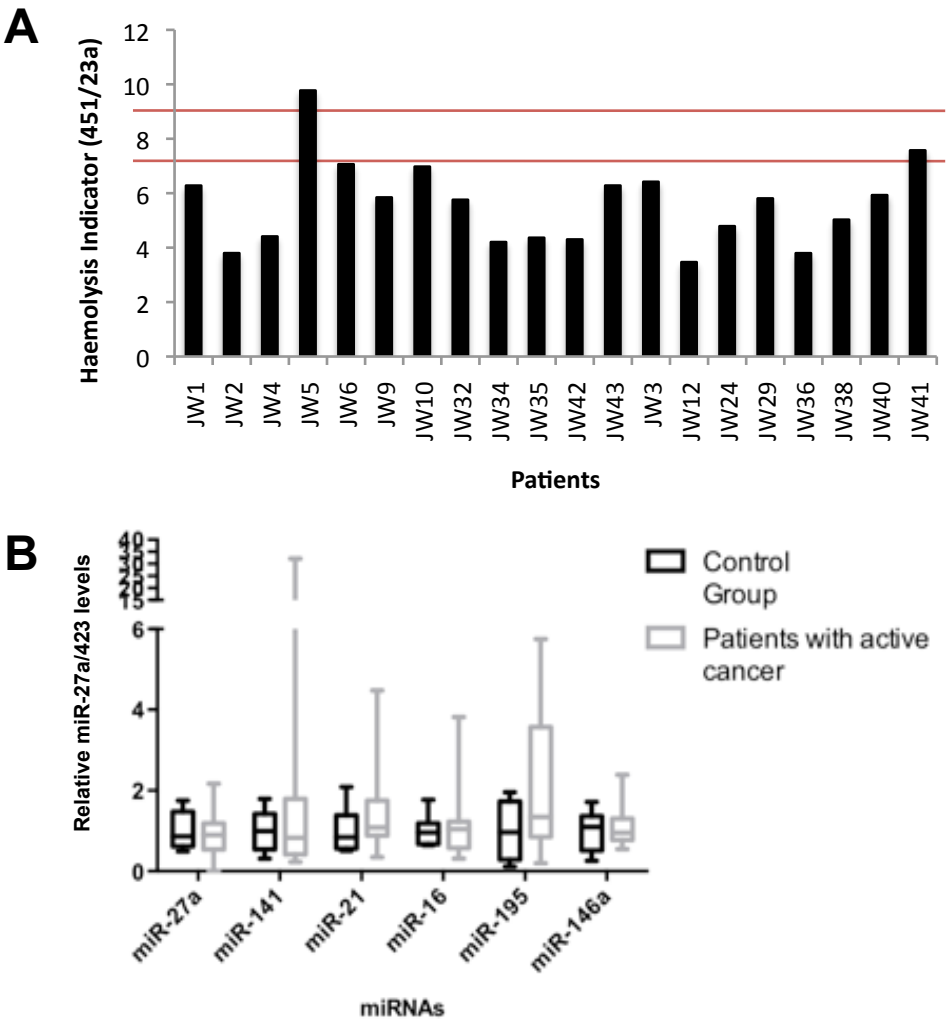

Figure 6.6: Data from a cohort of 7 healthy volunteers and 32 prostate cancer patients

(A) Checking the blood samples for indications of haemolysis miR-451 and miR-23a are quantified using qRT-PCR samples with relative high levels of miR-451 to miR-23a are likely to have had microscopic haemolysis as miR-451 is abundantly found in red blood cells, unlike miR-23a . The top red line indicates levels over 9 that are highly likely to be contaminated with red blood cells and have been excluded. Those between the red line with a ratio between 7 and 9 are possibly contaminated and must be reviewed and potentially excluded.(B) miRNAs quantified using qRT-PCR (Exiqon probes on a custom panel) and then normalised to miR-423. Data comparing the miRNAs of interest in both the control and cancer groups

In order to explore if a possible correlation between prostate cancer and miR level was being diluted in effect by the heterogeneous nature of the cohort we again subdivided the cancer group as before. The significant difference in miR-27a levels

between the control group and those patients with active cancer but not on hormonal therapy, initially seen in figure 6.6 A, was not observed in this data in Figure 6.8. In fact, there were no significant differences in expression levels between these different groups in any of the miRNAs assayed.

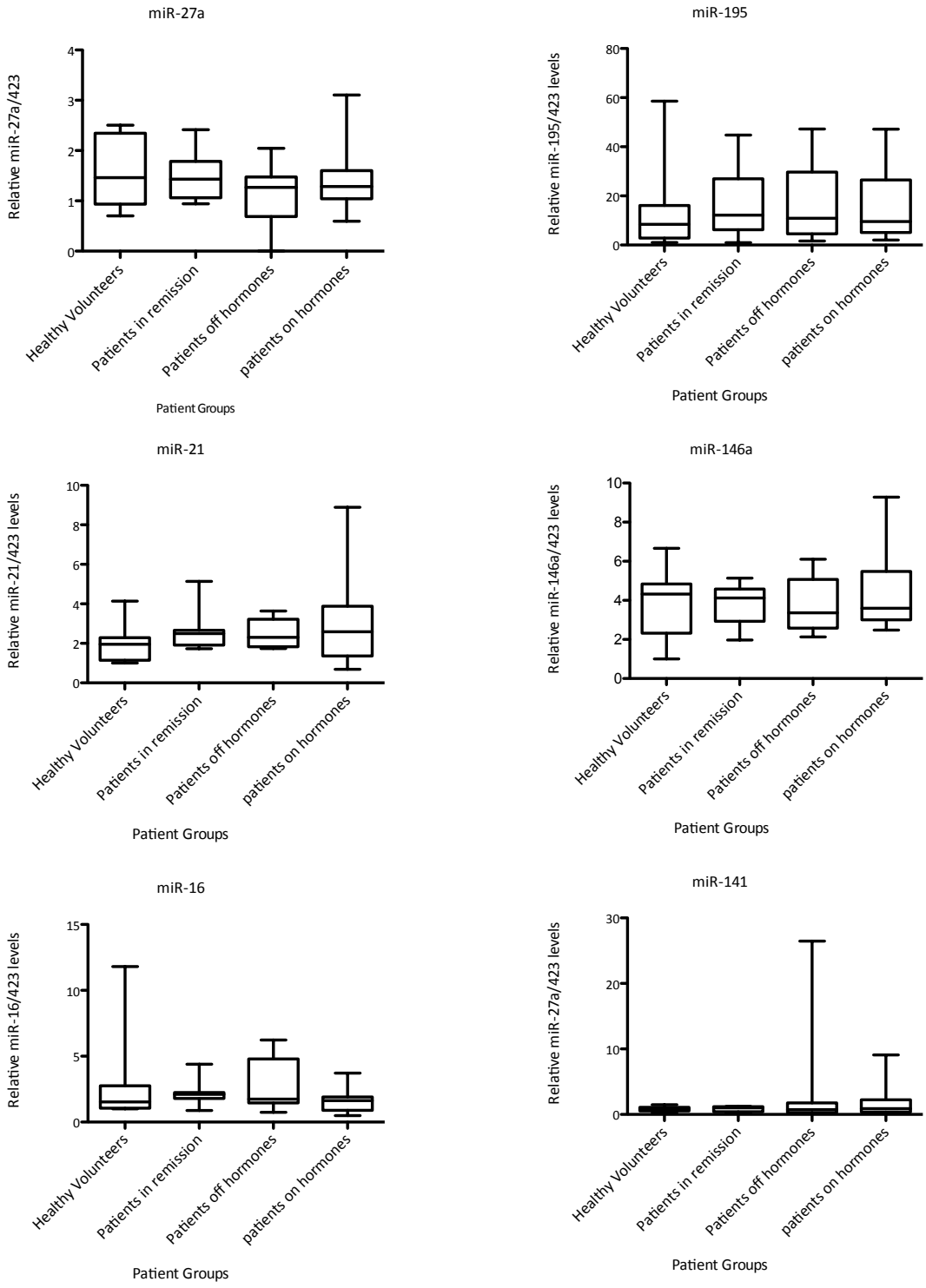

Figure 6.7: Data from a cohort of 7 healthy volunteers and 32 prostate cancer patients

miRNAs quantified using qRT-PCR (Exiqon probes on a custom panel) and then normalised to miR423. Data comparing the control group to the cancer group broken down by activity of the cancer and the exposure at the time of blood sampling to hormonal therapies

As discussed, the higher levels of miR-27a in the patients originally seen in our pilot Taqman study (Figure 6.6 A and B) were not present despite the pilot cohort of patients being included. To further explore this I plotted the data for miR-27a acquired using the Exiqon system against that using the Taqman system; Figure 6.9. As can be seen, the values are not similar and most importantly a similar pattern is not evident, thus even with the margins of variability there is a fundamental difference in these two systems and the data generated cannot be trusted.

To investigate this further I ran three different concentrations of cDNA (from the same sample), the first 10 fold above (1 in 5) the standard dilution used in the qRT-PCR, the standard dilution (1 in 50) and then 10 fold below (1 in 500), Figure 6.10. For the most of the miRNAs a dilution of 1 in 50 allows detection of the miRNA within the linear range of the assay. The assay for miR-27a does appear to be inhibited at the 1 in 5 dilution perhaps this is due to carry over of inhibiting products to the PCR reaction. Conversely miR-195 was beyond limits of the assay for detection at a dilution of 1 in 500. From this I have concluded that the miR-27a assay and miR-195 assay from Exiqon did not yield useable data, however the other miRNA assays are reliable.

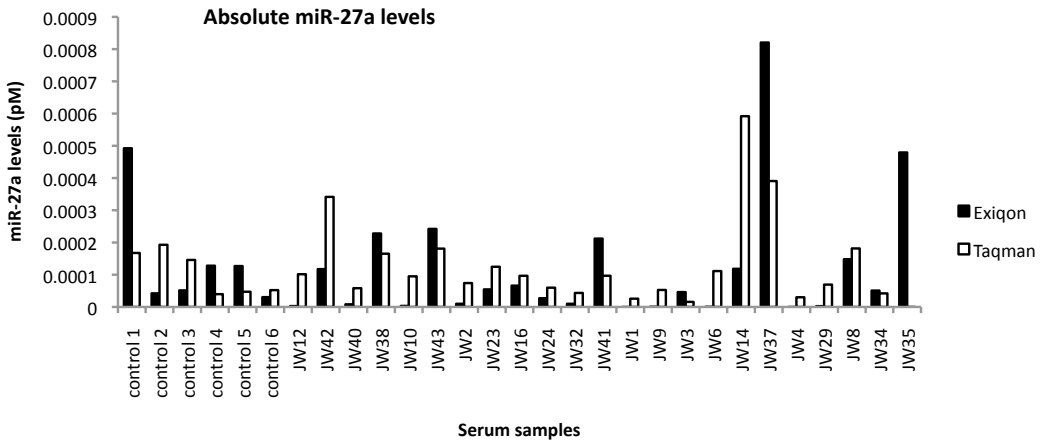

Figure 6.8: Comparison of data for samples tested by both the Taqman and the Exiqon system

Absolute miR-27a levels were quantified from the assay results using standard curves for spiked-in *C.elegans* in both systems.

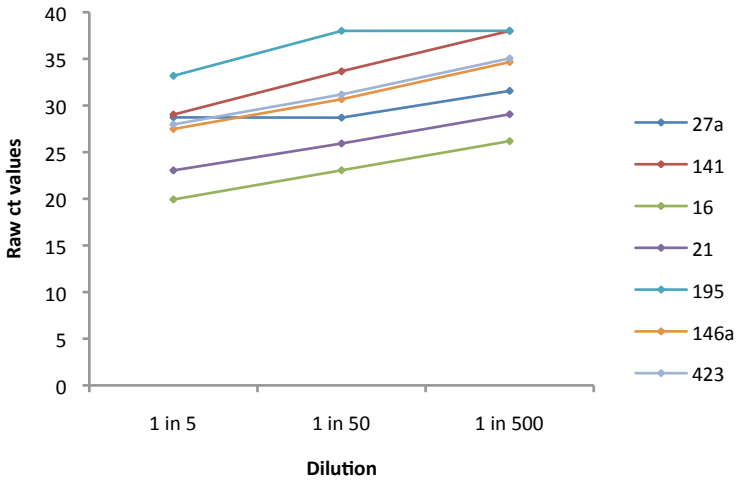

Figure 6.9: Dilution curve of miR panel assays (Exiqon)

cDNA from one healthy volunteer at three different concentrations quantified by qRT-PCR. Assays for miR-27a and miR-195 do not show the ability to pick up a large range of concentrations of miRNAs.

6.1.4 miR-146a is higher in patients whose cancer progresses after prostatectomy

One of our difficulties with these studies has been accessing serum samples from age- and sex-matched healthy controls. A second difficulty has been accessing and testing a large enough cancer patient population to detect a difference given the heterogenous nature of the treatments within the patient samples I collected. In view of these difficulties I designed a small study in which each patient acted as their own control. The patients' post operative serum miRNA levels were expressed relative to their baseline serum miRNA levels, thereby removing inter-patient variability and focusing on the removal of the prostate gland and the prostate cancer with the radical prostatectomy. A cohort of 4 newly diagnosed patients had serum samples taken on the day of their prostatectomy and then 6 weeks post operatively; see Table 6.4 for patient characteristics. These samples were analysed for their miRNA levels using the same Exiqon panel as established above. The patients' clinical outcome was

reviewed 1 year later and patients were divided into cohorts of those for whom surgery was adequate treatment and those patients that required further treatment in the form of radiotherapy or hormonal anti-cancer agents. The two cases that required further treatment had positive surgical margins on post-operative histopathological review and PSA levels that remained detectable. As can be seen in Figure 6.11 there was no difference across the miRNA panel with the exception of miR-146a. There was a fall in the level of miR146a post operatively in the patients cleared of prostate cancer whereas in those that required further treatment for residual prostate cancer the level went up 14 fold. These data are interesting but do not reach significance due to the small sample size (n=4).

Table 6-4: Table of patient characteristics for study of miRs pre and post prostatectomy

	PSA at diagnosis ng/ul	Tumour Stage (TNM)	Gleason Grade	Surgical Result	PSA 6 weeks post op Ng/ul
MW2	8.54	pT3aN0M0	3+4	Complete excision	0.01
MW3	6.16	pT2cN0M0	3+4	Complete excision	0.01
MW9	13.4	pT3aN0M0	3+3	Positive margins	0.03
MW10	25.3	pT2cN0M0	3+4	Positive margins	0.02

Samples labeled MW for Matt Winkler then assigned a number from 1-12 in order of collection
Abbreviations PSA = prostate specific antigen, TNM = TNM Tumour Classification of Malignant Tumours (a cancer staging system) p denotes staging was assigned during pathological examination of the surgical specimen, T describes the size of the primary tumour, N describes regional lymph node involvement, M describes distant metastasis.

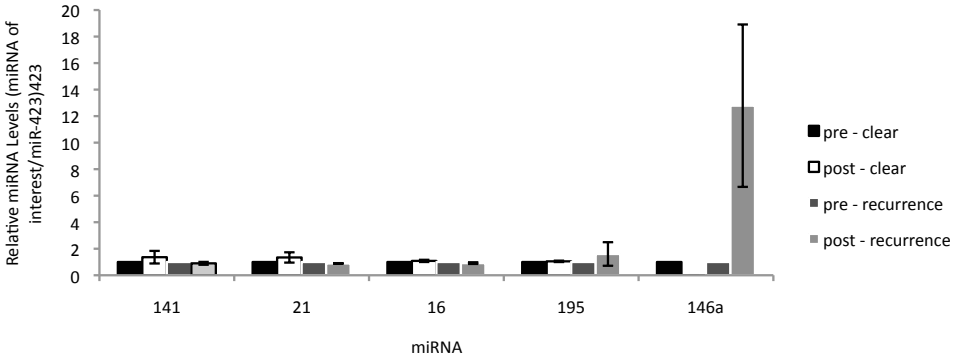

Figure 6.10: miR analysis pre- and post-prostatectomy

Cohort of 4 prostate cancer patients who gave samples pre- and post-prostatectomy. Two of the patients had successful prostatectomies and are clear of prostate cancer 2 years following the surgery. The other two patients had to have further anti-cancer therapy following the surgery due to biochemical recurrence. miRNAs quantified using qRT-PCR and samples pre- and post-surgery in those clear of cancer and those that recurred compared. The columns represent the means +/- the SEM.

6.1.5 miR-27a levels are higher in patients with active cancer not on hormonal therapy and in patients with metastatic disease

After ruling out the Exiqon panel for exploring miR-27a levels in prostate cancer a larger study was planned using the previous methodology of Taqman assays for qRT-PCR. Collecting serum from age-matched healthy control patients proved very difficult and having noted in the first study that patients in remission from prostate cancer (PSA <0.03 for three prior consecutive visits) had similar levels to the healthy controls (see Figure 6.6 B) we elected to use this group as the relative controls for this study. The patient characteristics are displayed in Table 6.5, there were 54 patient samples collected in total, 17 patients in remission, 18 with active cancer off hormonal therapy and 19 patients with active cancer on hormonal therapy. As can be seen in figure 6.12 A there was a trend towards higher relative miR-27a levels in the group of patients with active cancer off hormonal therapy with a median level of 26.99 compared to 1.77 for the group in remission; although this did not reach significance ($P = 0.32$), it is a similar trend to that seen in the first study (see Figure 6.6 B). When the patients with active cancer were then subdivided according to those known to have metastatic disease and those with advanced prostate cancer but not known to have metastasis there was a significant increase in the miR-27a levels in those with metastatic disease ($P = 0.03$), see Figure 6.12 B. Again the data were checked for potential correlations with PSA, of which there were none (see Figure 6.12 C and D). The data were plotted with the patients grouped according to prognostic level and miR-27a levels were higher in the higher Gleason grade cancers, Figure 6.12 E. This was the exact opposite pattern from that observed in the first smaller study. When the data were plotted with the patients grouped by stage there was a small non-significant increase in those patients diagnosed at stage 4 (Figure 6.12 F).

Table 6-5: Table of patient characteristics for the substantial study of miR-27a levels in prostate cancer patient's serum

	no. in group	Median PSA ng/ul	PSA Range ng/ul	Median Age	Age Range	Median miR-27a level	miR-27a Range
Patients with Prostate Cancer	54	173.9	0.03-3224	75	68-88	2.83	0.75-74.49
Current Status:							
In remission	17	0.3	0.03-0.46	71	68-86	1.77	0.99-4.4
Active cancer off hormones	18	17.9	8.64-33.5	75	73-83	26.99	1.26-74.49
Active cancer on hormones	19	503.5	5.54-3224	75	70-88	1.91	0.75-27.52

Abbreviations no.= number, PSA = prostate specific antigen

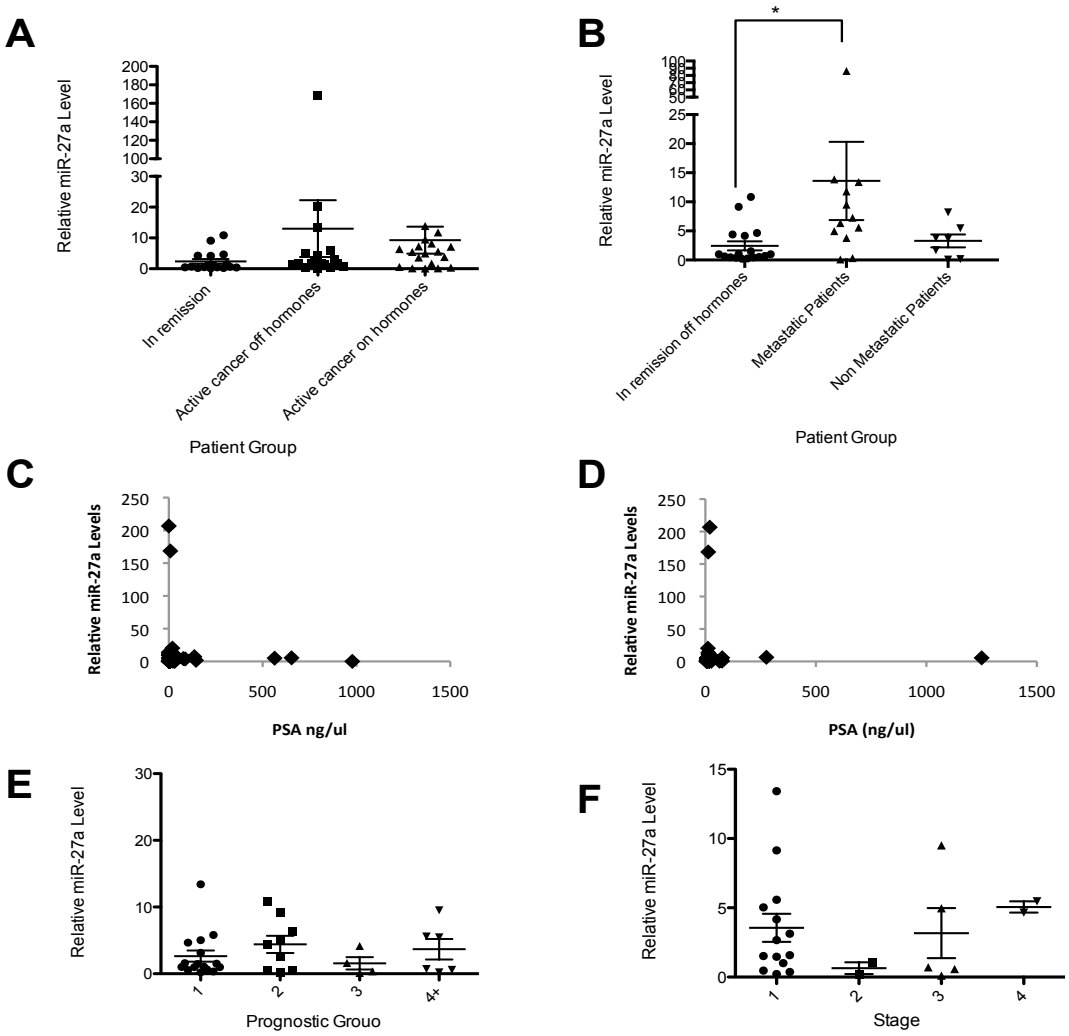

Figure 6.11: Substantial study of miR-27a levels in prostate cancer patients' serum

(A) miR-27a levels comparing patients with prostate cancer (n=54) divided into groups based on the extent of their disease at the time of the blood test and whether they are on hormonal based therapies. Data represents the mean absolute miR-27a level made relative to a the mean of the levels in the remission group +/- SEM (B) relative miR-27a comparing the patients in remission to those with metastatic disease, P=0.03. (C) Patients serum PSA level at diagnosis plotted against the miR-27a level (D) Serum PSA level at the the time of diagnosis plotted against relative miR-27a levels. (E) patients grouped by their prognostic score at diagnosis determined by their Gleason grade (1= Gleason <6, 2+7 (3+4), 3=&(4+3), 4+=8or9) (F) Patients grouped by their prostate cancer stage at diagnosis.

6.1.6 miR-27a levels are higher in the plasma of patients with metastatic prostate cancer

I was able to access some plasma samples from a small cohort of patients (n=8) with metastatic disease that were being investigated for another study. I ran a Taqman based qRT-PCR study to assess the miR-27a levels in this cohort and found a similar pattern to that seen in the serum samples – namely, that patients with metastatic disease have higher levels of miR-27a then the healthy controls but that it does not reach significance likely due to the small number of control samples (P = 0.063), see Figure 6.13.

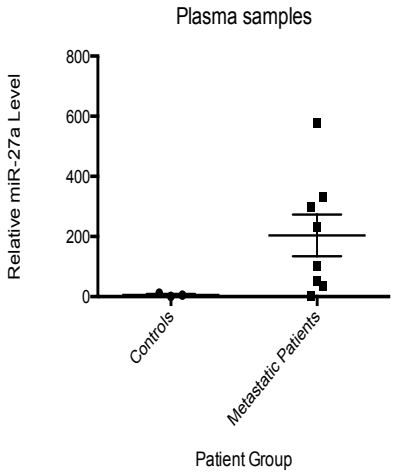

Figure 6.12: Small study of miR-27a in a cohort of patients with metastatic prostate cancer.

Healthy volunteers (n=3) Patients with metastatic prostate cancer (n=8). MiR-27a levels assayed using Taqman specific miR-27a probes and quantified using a standard curve. Data represents the mean absolute miR-27a level made relative to a the mean of the levels in the control group +/- SEM

6.1.7 A second attempt to establish a panel of miRNAs to act as biomarkers in prostate cancer

One of the major variables that appears to have affected my results, thus far, is the heterogeneous nature of the patient cohorts. We know that miR-27a is androgen-regulated and thus the levels are likely to be affected by hormonal therapies. As hormonal therapies are the backbone of prostate cancer treatment this may be altering any cancer-related changes I could potentially see. In addition, the clinical

situation wherein some of the patients had undergone prostatectomy and others retained intact prostates, is also likely to affect the miRNA differential. This is corroborated by the data in Figure 6.11 showing the alteration of miR-146a following prostatectomy but only in a sub group of patients. To investigate this, serum was collected from patients at the point of diagnosis of prostate cancer before any hormonal manipulation had begun and prior to any surgery. The serum was collected according to a strict SOP and stored at -80°C prior to miR analysis.

The serum miRNA profiles of 16 patients with prostate cancer (n=8 for localized disease and n=8 for metastatic disease) and 8 patients with proven biopsy negative prostates were investigated; see Table 6.6 for patient characteristics. The levels of 68 cancer-associated miRNAs were quantified using the Multiplex Circulating miRNA Assay at Abcam; see Appendix A for the table of miRs assayed. Three miRNAs were excluded as they did not reach detection threshold above background noise: miR-218-5p, miR-9-5p and miR-182-5p. The geNorm algorithm was applied to the data in order to select the three most appropriate miRNAs for normalization. These were identified as miR-106a-5p, miR-17-5p and miR-20-5p. For quality control haemolysis markers were also assayed (miR-451 and mR-23a); none of the samples required exclusion for haemolysis.

There were 14 miRNAs – let-7g-5p, miR-10-5p, miR-126-3p, miR-181b-5p, miR-21-5p, miR-22-3p, miR483-5p, miR-125b-5p, miR-195-5p, miR-210-3p, miR-378a-3p, miR-150-5p, miR-375 and miR-93-5p found at significantly different levels between the clinically different groups; see Figure 6.14 and Table 6.7. The patients with prostate cancer have higher circulating levels of all of these miRNAs except for miR-93-5p, expression of which was lower in the prostate cancer patients. Of note, miR-27a showed a trend towards higher levels in the serum samples taken from the metastatic patients when compared to those taken from the patients with localized prostate cancer. The data did not quite reach significance with a p value of 0.66 on the two-tailed T-Test. Initial analysis discounted any miR with a low signal intensity, defined as under 10, due to the potential that this was a false positive result. However, as some of these showed significant differences I have shown them in the figure.

Table 6-6: Table of patient characteristics for samples in the Abcam Firefly study

	no. in group	Medan PSA ng/ul	PSA range ng/ul	Median Age	Age range	Median combined Gleason Score
Benign Prostate samples	8	3.12	0.34-7.70	60	29-79	n/a
Localised Prostate cancer	8	9.01	4.6-15	64	60-81	7
Metastatic prostate cancer	8	567.25	40-1790	70	59-88	7

Abbreviations no.= number, PSA = prostate specific antigen

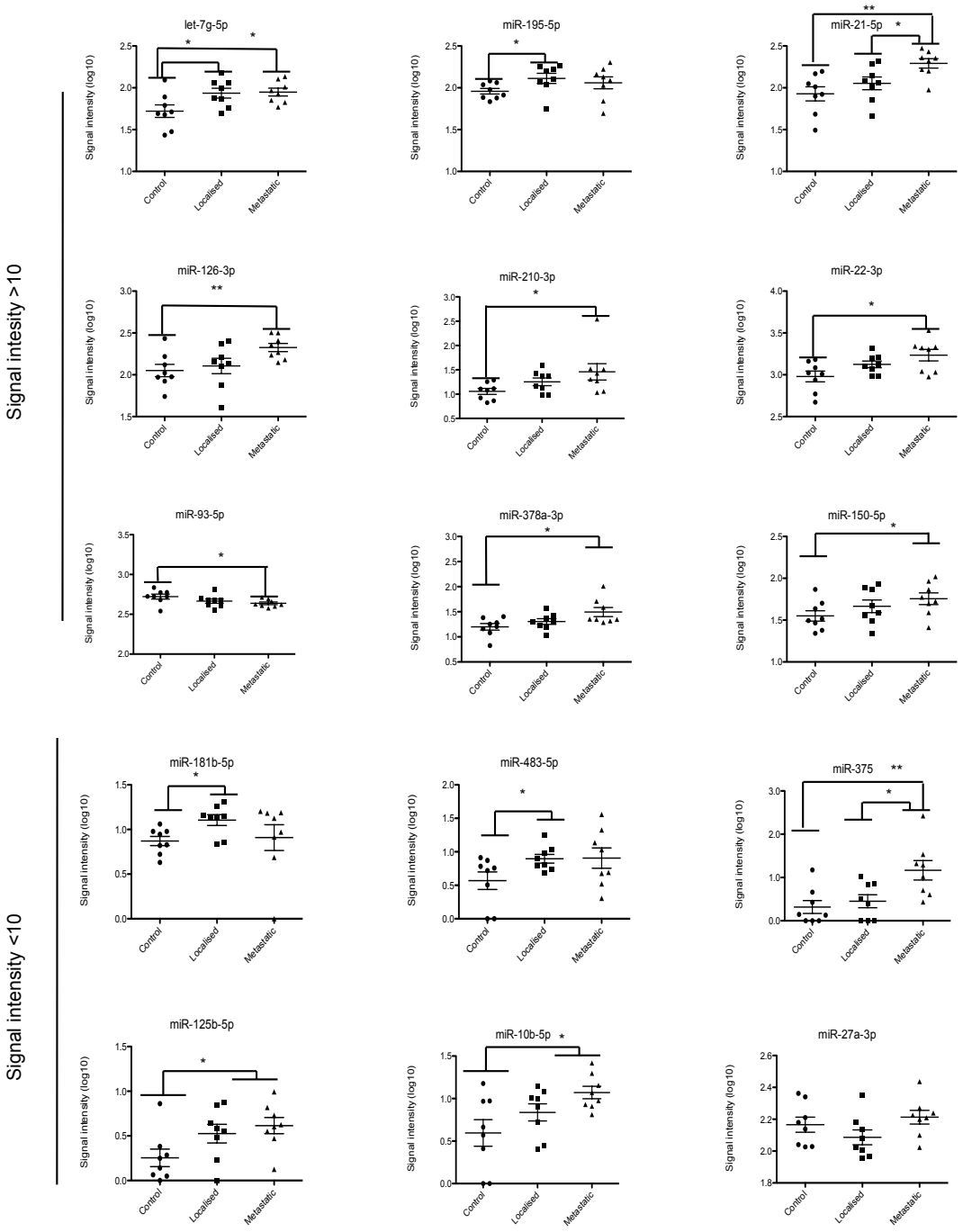

Figure 6.13: Scatter plot of miRNA expression in serum from three different PCA patient groups

Signals were normalised to the geometric average of miR-20a-5p, miR-17-5p and miR-106-5p. The bars represent mean +/- SEM. *p,0.05, **p,0.01 by the two-sample t-test. The top 9 plots had signal intensity on average over 10. The bottom 5 plots had lower signal intensity on average less than 10.

Table 6-7: Table of all the miRs on the firefly oncology panel and the associated P value when the groups were compared by T-Test. Green squares indicate significant results by the Two tailed T-Test P<0.05.

miRNA	p-value Control vs Localised	Control vs Metastatic	Localised vs Metastatic	miRNA	p-value Control vs Localised	Control vs Metastatic	Localised vs Metastatic
hsa-let-7d-5p	0.625	0.344	0.692	hsa-mir-200b-3p	0.334	0.334	0.785
hsa-let-7g-5p	0.041	0.022	0.869	hsa-mir-200c-3p	0.296	0.155	0.831
hsa-let-7i-5p	0.430	0.302	0.726	hsa-mir-205-5p	0.593	0.446	0.169
hsa-mir-103a-3p	0.593	0.191	0.514	hsa-mir-20a-5p	0.583	0.543	0.326
hsa-mir-106a-5p	0.978	0.564	0.622	hsa-mir-210-3p	0.070	0.041	0.289
hsa-mir-106b-5p	0.525	0.623	0.833	hsa-mir-21-5p	0.291	0.003	0.025
hsa-mir-107	0.339	0.487	0.836	hsa-mir-218-5p	0.334		0.334
hsa-mir-10b-5p	0.214	0.015	0.082	hsa-mir-221-3p	0.977	0.645	0.607
hsa-mir-122-5p	0.306	0.905	0.107	hsa-mir-222-3p	0.888	0.231	0.244
hsa-mir-125b-5p	0.079	0.017	0.526	hsa-mir-223-3p	0.878	0.804	0.869
hsa-mir-126-3p	0.649	0.008	0.053	hsa-mir-22-3p	0.075	0.017	0.190
hsa-mir-127-3p	0.623	0.920	0.567	hsa-mir-25-3p	0.981	0.929	0.886
hsa-mir-130a-3p	0.572	0.399	0.957	hsa-mir-26a-5p	0.795	0.176	0.408
hsa-mir-141-3p	0.475	0.193	0.355	hsa-mir-27a-3p	0.254	0.474	0.066
hsa-mir-145-5p	0.772	0.109	0.121	hsa-mir-29a-3p	0.847	0.255	0.215
hsa-mir-146a-5p	0.585	0.169	0.430	hsa-mir-29b-3p	0.327	0.150	0.493
hsa-mir-148a-3p	0.638	0.505	0.124	hsa-mir-29c-3p	0.673	0.160	0.298
hsa-mir-148b-3p	0.963	0.526	0.288	hsa-mir-320a	0.275	0.143	0.417
hsa-mir-150-5p	0.259	0.046	0.396	hsa-mir-335-5p	0.276	0.244	0.862
hsa-mir-151a-3p	0.253	0.296	0.937	hsa-mir-34a-5p	0.313	0.125	0.553
hsa-mir-155-5p	0.319	0.098	0.498	hsa-mir-34b-3p	0.187	0.108	0.886
hsa-mir-15b-5p	0.506	0.105	0.074	hsa-mir-375	0.536	0.007	0.019
hsa-mir-16-5p	0.520	0.476	0.099	hsa-mir-376c-3p	0.238	0.742	0.165
hsa-mir-17-5p	0.320	0.799	0.206	hsa-mir-378a-3p	0.243	0.019	0.097
hsa-mir-181a-5p	0.382	0.270	0.694	hsa-mir-409-3p	0.066	0.588	0.196
hsa-mir-181b-5p	0.011	0.805	0.231	hsa-mir-451a	0.149	0.103	0.806
hsa-mir-182-5p	0.334		0.334	hsa-mir-483-5p	0.042	0.114	0.950
hsa-mir-187-3p	0.090	0.150	0.454	hsa-mir-486-5p	0.205	0.430	0.513
hsa-mir-18a-5p	0.969	0.655	0.707	hsa-mir-574-3p	0.289	0.327	0.936
hsa-mir-192-5p	0.962	0.374	0.345	hsa-mir-625-3p	0.628	0.828	0.512
hsa-mir-195-5p	0.043	0.222	0.577	hsa-mir-652-3p	0.179	0.270	0.995
hsa-mir-199a-3p	0.618	0.191	0.516	hsa-mir-92a-3p	0.766	0.239	0.266
hsa-mir-199a-5p	0.209	0.355	0.709	hsa-mir-93-5p	0.188	0.031	0.401
hsa-mir-19a-3p	0.295	0.051	0.311				

Abbreviations vs = versus

Cluster analysis was performed on these data to generate the heatmap seen in Figure 6.15. Examining miR-21-5p and miR-195-5p (indicated by arrows), a general trend of increased expression with progressive cancer stage is evident, as seen in Figure 6.14. The heat maps also highlight that although miR-375 was technically significantly higher in the metastatic group when compared to the control group, this is likely due to an outlier sample 676. For miR-27a, the heatmap graphic demonstrates that, across the metastatic serum samples, miR-27a is consistently expressed at a higher level when compared to variable expression at a slightly lower level in the serum samples from the localized prostate cancer patient group.

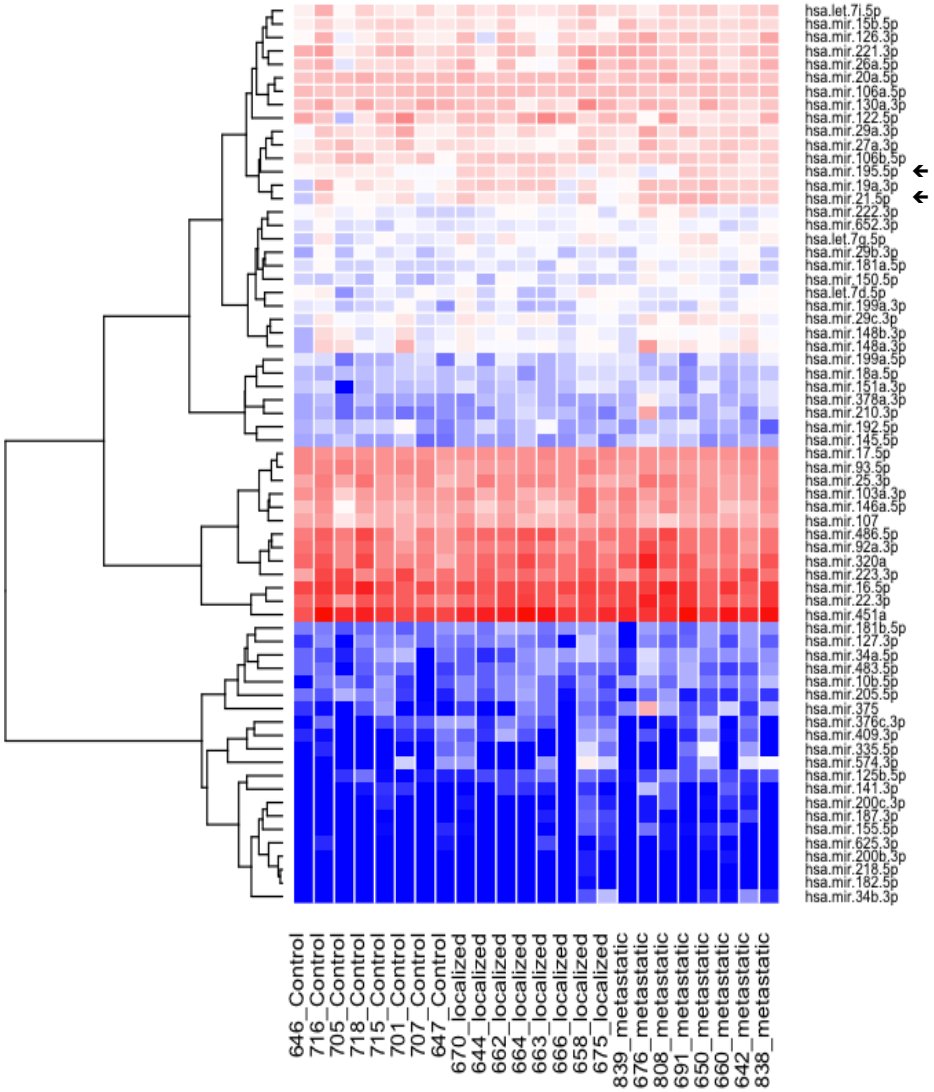

Figure 6.14: Heatmap displaying relative expression across the patient samples

Samples were assigned numbers in order of collection. For analysis the samples have been grouped by their classification status, the control group consists of serum from men with proven benign prostate disease, the localized group consists of serum from men with localized prostate cancer, the metastatic group consists of serum from men with metastatic prostate cancer. The arrows indicate miR-195 and miR-21.

6.1.8 MiR-210 is significantly higher in the patients with localized prostate cancer that developed recurrent disease during follow up

The group of miRNAs found to be significantly raised in the metastatic group of patients when compared to the control group could reflect a potential micrometastatic state in the serum of men with localised prostate cancer. Clinical information regarding disease status and treatment was recorded for all the patients in the study three years following diagnosis and sample collection. For the men in the group with localized prostate cancer, any evidence of biochemical relapse (PSA rise above baseline following definitive treatment) at three years was recorded and the group divided into those that relapsed and those that remained disease free at three years.

The group of miRNAs that had been found to be raised in the metastatic patients were then analysed across these two groups of patients (Figure 6.15). Both miR-210 and miR-375 showed higher levels in the patients that went onto have biochemical relapse following prostatectomy, however, only miR-210 was significantly raised (T test p= 0.02, two -tailed).

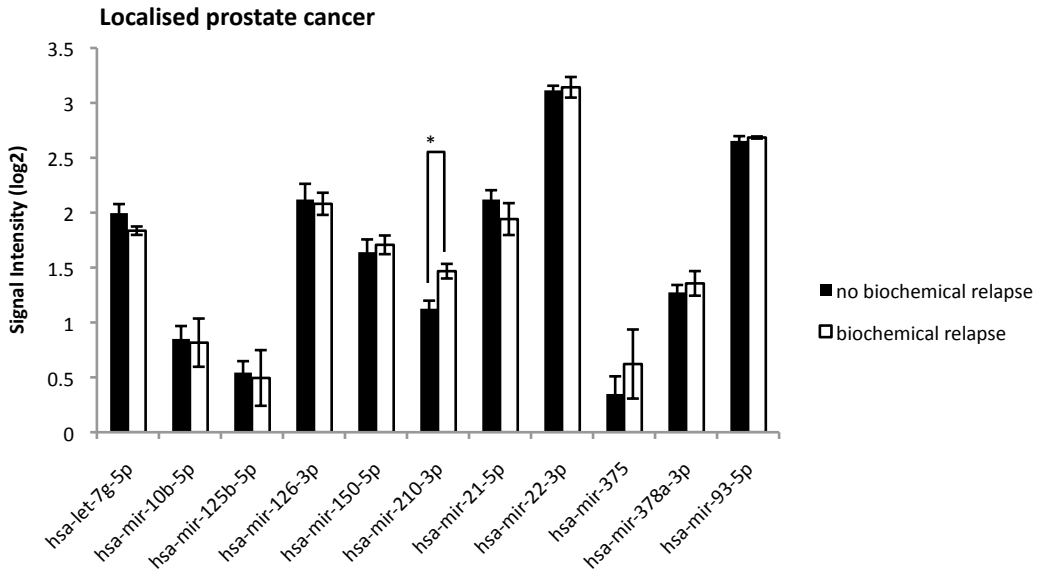

Figure 6.15: Bar chart of miRNA expression in the patients with localised prostate cancer divided into two groups by biochemical relapse 5 years later

The bars represent mean +/- SEM. *p<0.05 by the two sample T-Test.

6.1.9 Validation of the Abcam Firefly Study using an alternative platform

As previously discussed one of the major limitations of the work to date was reproducibility of results across two different technological platforms. In order to validate the results seen with the Abcam assay I repeated the same experiment using the Exiqon qRT-PCR platform for quantitating miRNAs using individual assays. The 14 miRNAs found to have a statistically significant difference in level between the benign (control) group and either of the groups with cancer were further investigated. MiR-27a was not included in the Exiqon panel as the result had not reached significance in the Abcam Firefly study and because of the problems I had previously had with Exiqon's miR-27a assay. RNA was extracted from the same 24 serum samples and reverse transcription performed and then qRT-PCR was performed on the resulting cDNA to quantify miRNA levels. The miRNAs of interested were then normalised to the same three reference miRNAs established in the Abcam Firefly study, miR-20a, miR17 and miR-106. The results were then made relative to the first sample in the control group.

In general the trends were the same with notably less significant results. Two miRNAs, let-7g and miR-22, were noticeably different between the two studies. In the Abcam Firefly study levels of both of these miRNAs were significantly and progressively higher in the localized cancer than the metastatic cancer groups. In the validation study the opposite result was observed, in fact let-7g was found to be significantly lower in the metastatic group compared to the benign cancer group, see Figure 6.17. The statistical significance of the differences between the groups was examined using a two tailed T-test and the summary of the comparison between the Abcam Firefly study and the Exiqon validation study can be found in Table 6.8.

MiRNAs 10b, 126, 150, 21, 378 had statistically significantly higher levels in the serum of men with prostate cancer across both studies. MiR-93 had significantly lower levels in the men with advanced prostate cancer across both studies. The most significant result across both studies was seen for miR-21. This is unsurprising as it is one of themiRNAs most widely cited as amplified in cancer in general.

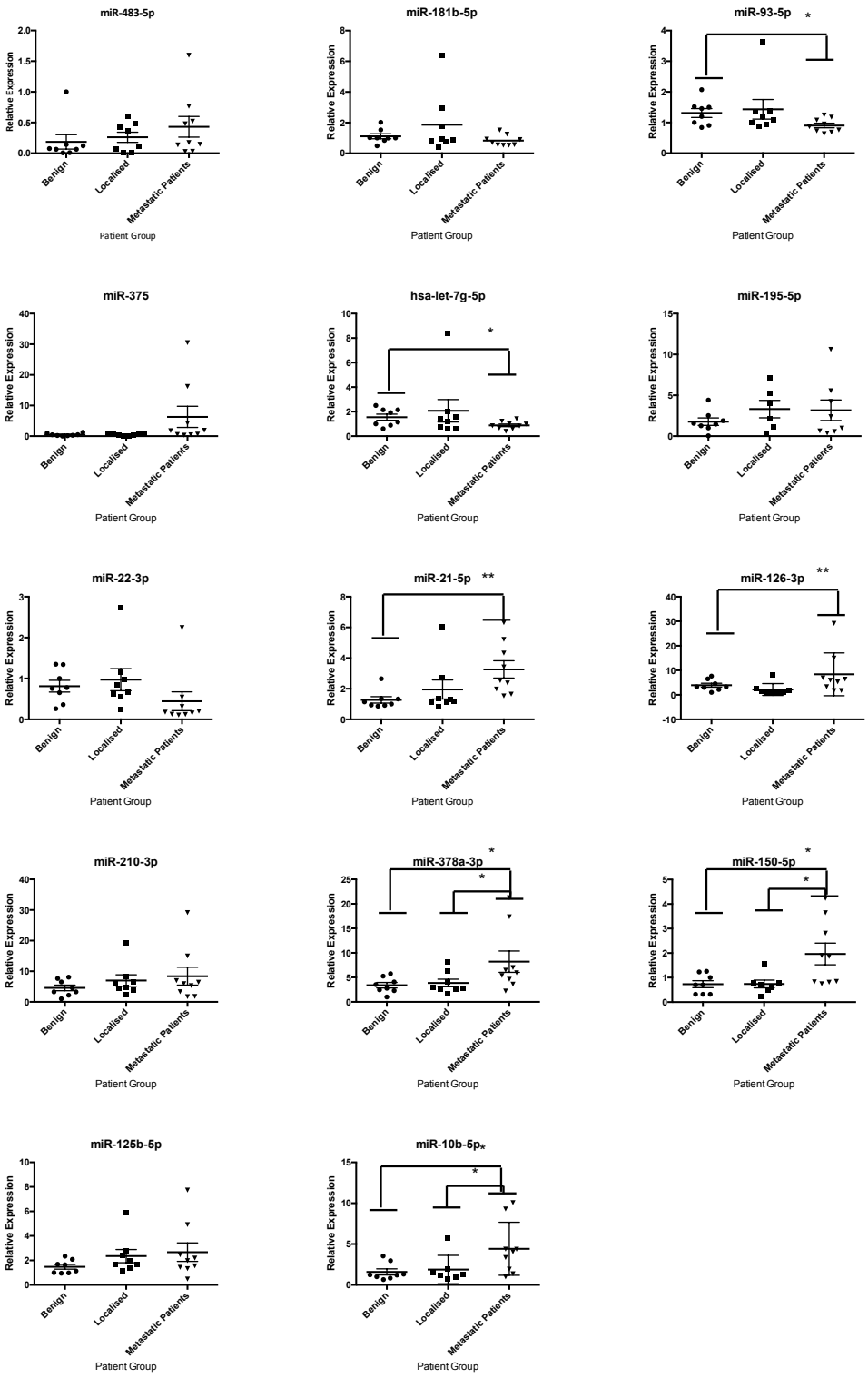

Figure 6.16: Verification of results of study displayed in figure 6.14 using Exiqon qPCR technology

Scatter plot of qPCR quantified miR levels were normalised to the geometric average of miR-20a-5p, miR-17-5p and miR-106-5p. The bars represent mean +/- SEM. *p,0.05, **p,0.01 by the two-sample t-test. Benign samples n=8, localised samples n=8, metastatic samples n=8.

Table 6-8: Table of the data trends from Figure 6.17 and P values of the signifcant miRs on the Abcam firefly panel and the Validation Exiqon Panel. P values calculated by two tailed T-Test.

		p-values of significant results from Abcam Firefly Study				p-values of significant results from Exiqon Validation study		
miRNA	Trend	Control vs Localised	Control vs Metastatic	Localised vs Metastatic	Trend	Control vs Localised	Control vs Metastatic	Localised vs Metastatic
hsa-let-7g-5p	↑	0.041	0.022		↓		0.02	
hsa-mir-10b-5p	↑		0.015		↑		0.01	0.041
hsa-mir-125b-5p	↑		0.017		↑			
hsa-mir-126-3p	↑		0.008		↑			0.035
hsa-mir-150-5p	↑		0.046		↑		0.0117	0.0173
hsa-mir-181b-5p	↑	0.011			↔			
hsa-mir-195-5p	↑	0.043			↑			
hsa-mir-210-3p	↑		0.041		↑			
hsa-mir-21-5p	↑		0.003	0.025	↑		0.003	
hsa-mir-22-3p	↑		0.017		↑			
hsa-mir-375	↑		0.007	0.019	↑			
hsa-mir-378a-3p	↑		0.019		↑		0.030	0.047
hsa-mir-483-5p	↑	0.042			↑			
hsa-mir-93-5p	↓		0.031		↓		0.02	

Further analysis of the data showed that three miRNAs showed statistically significant difference in levels between the serum of men with benign prostatic disease and those with any level of prostate cancer. Figure 6.18 demonstrates the spread of the miRNA levels to allow comparison of samples from patients with a beingn prostate and those with prostate cancer. MiR-21, which has been widely implicated as an oncomiR is shown to have a wide spread in the prostate cancer group when compared to the benign prostate group. All three of these miRNAs miR-21-5p, miR-126-3p and miR-150-5p were significantly raised in the serum of men with prostate cancer across both studies.

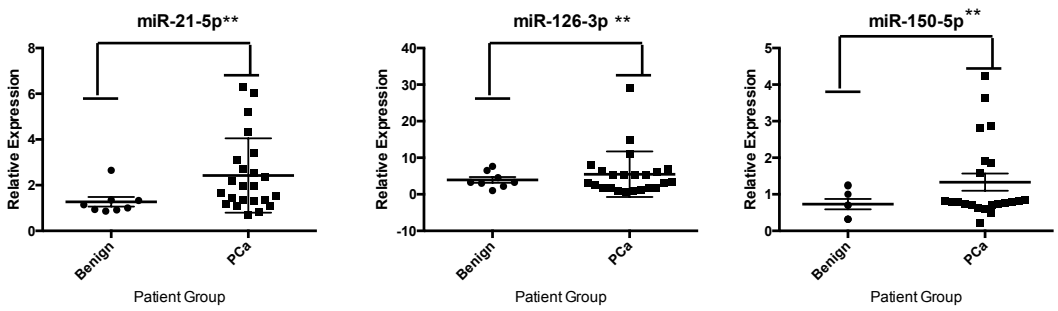

Figure 6.17: Verification of results of study displayed in figure 6.14 using Exiqon qPCR technology

Scatter plot of qPCR quantified miR levels were normalised to the geometric average of miR-20a-5p, miR-17-5p and miR-106-5p. The bars represent mean +/- SEM. *p,0.05, **p,0.01 by the two-sample t-test. Benign samples n=8, Prostate cancer samples (PCa) n=23.

6.2 Discussion

As discussed in the introduction there is an urgent need for new biomarkers for prostate cancer. Although the increased accesability and use of PSA testing is undoubtedly identifying more cases of prostate cancer that otherwise would have been missed, recent large multinational randomized prospective trials have shown no overall survival benefit (Schroder and Roobol 2009). In part this is because PSA testing identifies prostate cancer that would never have become clinically significant to the patient. It was to this end that I started working on the quantification of miRNAs in serum as a potential biomarker in prostate cancer.

Serum levels of miR-27a were significantly raised in mice bearing human prostate cancer xenografts when compared to serum levels from healthy mice. In addition the levels were higher in the serum of the animals bearing the more aggressive prosate cancer xenografts. The comparison is between mice bearing xenografts and mice without any human tissue and although the assay can detect and quantify both murine and human miR-27a, we can't be sure that the it is not the presence of the human tissue in the xenograft accounting for the changes in levels. My aim was to detect and quantify miR-27a and other miRs in human serum from patients with prostate cancer and compare it to control patients to explore serum miR-27a further.

It is not possible to know the origin of the circulating miRNAs found in blood, but it is hypothesized that due to the leaky nature of tumour vasculature and the fragile state of tumour cells in addition to their rapid rate of growth that the serum will in effect be enriched with the tumour miRNA population. In addition, it has been hypothesised that cancer cells actively secrete miRNAs. In support of this, circulating miRNA profiles in prostate cancer patients have been reported to reflect the miRNA profiles of their respective tumours (Brase, Johannes et al. 2011, Selth, Townley et al. 2012). The hypothesis follows that this enrichment of circulating miRNAs released by the tumours will create a differentiating pattern of miRNA expression between the blood of men with prostate cancer and those without. In addition, this differential expression of miRNAs could be coming in part from immune cell response to invasion damaging local tissues or the stromal tissues, or a combination of all of these. In the context of a biomarker these considerations are not

so critical so long as the biomarker is fit for purpose, i.e the result leads to accurate clarification of clinical status.

Accurately measuring circulating miRNAs has its challenges. There are no methods of controlling for a patient's individual physiological status, for example hydration. The RNA amount is so small, following extraction, that it is unable to be reliably measured with a nanodrop and thus we are unable to accurately put equivilent amounts of RNA into each reverse transcription reaction. There is also a lack of definitive control miRs for normalisation across studies. Further, there is also a lack of age matched healthy controls as most older men have some form of prostate abnormality. Thus the biomarker(s) we are looking for needs to be highly differentially expressed in order to overcome a number of confounding variables.

6.2.1 MiRNAs can be robustly quantified from serum and plasma

This work was started in 2011, before publication of established methodology for miRNA extraction and quantification. It became evident that miRNAs used as a biological normaliser for tissue miRNA quantification were not consistent in serum samples (Figure 6.2). However, by establishing a standard curve for a spiked-in synthetic miRNA and for our miRNA of interest we were able to convert the raw Ct values gained from RT-qPCR to absolute quantities of the miRNA of interest in the serum.

There was no difference in expression levels between males and females in the healthy volunteers, as shown in Figure 6.4. We know that miR-27a is androgen regulated and adult males have 7-8 fold higher circulating levels of testosterone then adult females (Torjesen and Sandnes 2004, Fletcher, Dart et al. 2012). The paper by Fletcher et.al, demonstrated that miR-27a is androgen regulated both directly with AR binding to the miRNA cluster promoter and post transcriptionally by accelerating primiR processing to the mature form. I would have potentially expected males to have a higher level given the androgen regulation, however, perhaps there are other factors that regulate miR-27a levels in addition (Fletcher, Dart et al. 2012).

Mitchell *et al.* established in 2008 that miRNAs are remarkably stable in blood and we confirmed that the miRNAs remain stable despite blood being left at room temperature for prolonged periods before processing (Figure 6.5 A) (Mitchell, Parkin et al. 2008). However, we did find that the type of serum collection bottle (i.e. the nature of the additives in the bottle) affected assay results therefore must be kept consistent across the study (Figure 6.5 B). In addition, we found that serum and plasma levels could not be directly compared (Figure 6.5 C). I have found at least one other study that uses serum and plasma interchangably as the miRNA source. Lin *et al*., were able to demonstrate a significant difference in miR levels in their patient cohorts despite the variations between sample types (Lin, Castillo et al. 2014). This was likely because the biological difference and patient sample size was large enough not to be affected by the small variation introduced by this technical discrepancy in the methodology. As can be seen in Figure 6.5 D, following a tight protocol and SOP resulted in consistent results across technical repeats (Tuck, Chan et al. 2009). The key features that require standardization were collection in standardized blood bottle, dividing the serum samples in to 1ml aliquots and freezing at -80°C so as to minimize freeze thaw cycles on subsequent testing. In addition all samples were thawed slowly on ice as there is some evidence that some miRNAs levels are affected differentially when thawed fast at 37°C (Farina, Wood et al. 2014).

Following the collection of serum from the first cohort of patients (Table 6.1) the serum was spun from the whole blood using the established SOP and then the miRNAs extracted and quantified with qRT-PCR using specific Taqman probes. Figure 6.6A demonstrates the significantly higher level of miR-27a found in the serum of patients with active prostate cancer. When the patient group was further divided into those patients on hormonal therapy, such as androgen deprivation treatments, and those not receiving any hormonal manipulation the difference became even more significant (Figure 6.6 B).

We know from previous work published from our laboratory that miR-27a is androgen-regulated so it could be interpreted that the hormonal therapies that lower androgen levels as treatment for the prostate cancer could be affecting the levels of

circulating miR-27a (Fletcher, Dart et al. 2012). When compared to our earlier mouse data (Figure 6.1) the fold ratios of miR-27a are a lot smaller in patients, perhaps because of the larger tumour to body mass ratio in mice. In addition 400µl of serum is a considerable amount of the mouse's total circulating blood volume. Potentially, any increases we might expect to see in humans could be diluted due to the fact that the patients have far smaller tumour to body mass ratio.

In view of the fact that patients whose prostate cancer is in remission had low miR-27a levels we wanted to determine whether there was a correlation or any relationship with PSA, as this is also very low in this group by definition. There was no correlation with circulating PSA level taken at the same time as the serum sample was taken for miR testing or with the PSA level at the time of diagnosis; Figures 6.6 C & D. This indicates that there is no correlation between PSA level and miR-27a level. With the hypothesis that miR-27a levels would increase with the progression of the prostate cancer we may have expected there to be a correlation between miR-27a and PSA. However, although PSA levels generally increase as prostate cancer progresses it is not a straightforward linear relationship. We are also still unclear as to whether the high miR-27a level seen in advanced cancer is due to it being a more aggressive cancer type or because of increased tumour burden. PSA is more reflective of tumour burden and does not reflect aggression of the prostate cancer.

To further explore this we looked for a correlation with prognostic score at diagnosis, which is gleaned from the patient's histological Gleason scores. There was no apparent correlation; see Figure 6.6 E. However, it must be noted that there were very small numbers of patients in the higher Gleason score groups. We also plotted miR-27a levels against stage at diagnosis, where there was a trend for the mean of the stage 4 metastatic cancer group to have a higher level, although this was not significant given the variation of levels seen with stage 1 disease; see Figure 6.6 F. As discussed above this could potentially be because increasing levels of miR-27a reflect the larger burden of disease found in stage 4 patients or that more aggressive tumours with metastatic potential have higher miR-27a levels.

6.2.2 MiRNA panel to establish a cohort of miRNAs to be used as biomarkers in prostate cancer

As mentioned earlier it was becoming increasingly obvious that no single miRNA was going to display sufficient differences to become a useful biomarker. With this in mind we changed platforms to the Exiqon system with which you can simultaneously and easily assay several miRNAs. The miRNA panel consisted of miR-27a, miR-141, miR-16, miR-21 and miR-195. We chose miR-141 as it has been widely published as being increased in prostate cancer (Mitchell, Parkin et al. 2008, Brase, Johannes et al. 2011, Nguyen, Xie et al. 2013); miR-16 is a putative prohibitin targeting miRNA, and has been shown to be increased in stage 4 prostate cancer (Watahiki, Wang et al. 2011) and on the converse side has been widely used as a control miRNA in the literature (Xiang, Zeng et al. 2014). MiR-21 was chosen as it has been reported to be increased in prostate cancer and able to predict resistance to docetaxol (Shen, Hruby et al. 2012, Hamilton, Rajapakshe et al. 2013, Lin, Castillo et al. 2014). MiR-195 is also a putative prohibitin-targeting miRNA and has been shown to be increased in prostate cancer compared to healthy controls (Mahn, Heukamp et al. 2011). When relative miR levels in the prostate cancer population (n=23) were compared to the healthy control group (n=6) there was no significant difference between the two groups even for miR-27a, where we had seen a difference in the previous experiment; compare Figure 6.7 B to 6.6 A. On closer examination of each of these miRs individually, even breaking patients down into groups as to their exposure to hormonal therapy, there was still no observed difference (Figure 6.8). This was a very unexpected result given our previous findings.

To explore this further I plotted relative miR-27a levels from both methodologies for the same patient samples; see Figure 6.9. Here it is quite evident that results are very different depending on which platform is used. This inconsistency in results between miRNA detection and measurement methods was highlighted in the miRQC paper by Mestdagh *et al,*: they used an analytical framework to compare the miRNA quantification platforms and published details of this in August 2014, unfortunately sometime after I completed this work (Mestdagh, Hartmann et al. 2014). However, at the time we were particularly concerned about the miR-27a results so we examined the panel more closely with a dilution curve of one healthy volunteer's serum. As

can be seen, the majority of the miRs are picked up at any of the dilutions and thus over a large range. However, the miR-27a assay gives a flat line result between the 1 in 5 and the 1 in 50 concentration and indicates that the reverse transcription step of the protocol was inhibited by chemical carryover from the RNA extraction; see Figure 6.10. In addition miR-195 was undetectable below a dilution of 1 in 50, this is likely because it is at a low concentration i.e below the detection limitin the blood. Given that we want to be able to test for all these miRs on the same panel we need a consistent starting concentration of cDNA that would yield accurate results for all the miRs.

6.2.3 MiRNA-146a is raised post prostatectomy in men with incomplete clearance of prostate cancer

There were some data of use gleaned from the Exiqon miRNA panels. The miRNA levels were measured in a small cohort of men newly diagnosed with localized prostate cancer (Gleason 6 or 7). These men had chosen to have a radical prostatectomy as definitive treatment. Their serum samples were collected immediately before prostatectomy and then six weeks post-operatively. These samples were analysed for miRNAs 141, 21, 16, 195 and 146a using the Exiqon platform. This small study was designed to try and give us some clarity regarding the relationship of these miRNAs to prostate cancer. The men could act as their own controls with and without their prostates and the prostate cancer. My expectation had been that we would see raised levels of the miRNAs associated with prostate cancer prior to the removal of the prostates that then fell post operatively, however, this pattern was not observed. The only changes of note were seen when the men were compared by outcome postoperatively. Two of the men went on to require further treatment as the margins of the pathological specimen were involved and their PSA levels did not become undetectable indicating the continued presence of prostate cancer tissue. As can be seen in Figure 6.11, miR-146a differs between the two groups. The levels of this miRNA went down post-operatively in the men whose operations were deemed successful and to have effectively eradicated their disease; in the other two men, who had residual prostate cancer, the levels actually went up. Unfortunately, these data do not reach significance due to the very small sample size but this is certainly an interesting result that requires further investigation. MiR-146a

is a mediator of inflammation, upregulated by tumour necrosis factor alpha and interleukin 1 (Sonkoly, Stahle et al. 2008). It has been found to dysregulate a number of targets in the cytokine response pathway and thus operate in a negative feedback loop as part of the innate immune system (Sheedy and O'Neill 2008). Perhaps the inflammatory response triggered by the incomplete dissection of the prostate cancer as opposed to complete extirpation has triggered a differential expression of this immunomodulating miRNA. Of course, given the small size, coincidental low grade infection, surgical damage, type of surgery and timing of blood sampling could potentially affect the results too.

6.2.4 MiRNA-27a is raised in the serum and plasma of patients with metastatic disease

Following from the relative lack of success with the Exiqon platform we returned to Taqman miR specific probes for further qRT-PCR miR analysis. A larger cohort of patients was collected to try and corroborate the findings of the first pilot study; Figure 6.6 B. Serum was collected from 54 patients with prostate cancer of all stages and prognostics groups (Table 6.4). In this larger cohort of patients the results were less dramatic and although miR-27a levels were highest again in the group of patients with active cancer not receiving any form of hormonal therapy, they did not reach significance; Figure 6.2 A. The highest levels of miR-27a were found in the patients who had metastatic disease (Figure 6.12 B); this again corroborated the earlier findings. Again there was no correlation between PSA level and miR-27a level; Figure 6.12 D & E. There was no clear difference in current miR-27a level and the patients' prognostic group at diagnosis; Figure 6.12 E. When the data is broken down by stage at diagnosis there is no clear difference.

Comparing the two Taqman based studies there is not a good correlation of the results. There are many stages within the extraction and quantification processes where there are confounding variabilities that I believe are affecting the reproducibility of this method. For example, there is no accurate method of quantifying the amount of total miRNA that is subjected to the reverse transcription reaction following extraction. In addition, accidental carry over of the denaturing agent can have a detrimental effect by inhibiting the reverse transcriptase enzyme. The miRQC paper published in August 2014 by Mestdaugh *et al.* investigated the

different technologies available for miRNA expression analysis, such as RT-qPCR, microarray, hybridization and sequencing (Mestdagh, Hartmann et al. 2014). They used an analytical framework to enable cross-platform evaluation and concluded that the different platforms tested have different detection rates, specificity and reproducibility. Specifically relevant to this work, they found that the Taqman platform had the lowest performing titration response which will undoubtedly be reducing the capacity to detect small expression changes in these low expression miRNAs (Mestdagh, Hartmann et al. 2014). They also found that the Taqman platform had the highest area left of the cumulative distribution curve score, which should decrease with increasing reproducibility (Mestdagh, Hartmann et al. 2014). From this study it would appear that Taqman assays are not the best platform on the market with which to quantify miRNAs from biofluids as it struggles to detect small expression changes and has poor reproducibility.

MiR-27a quantification was conducted on a small cohort of plasma samples that were collected for a different study. The men in this patient cohort all had advanced castrate-resistant disease that had progressed through the standard lines of treatment, most commonly prostatectomy or radical radiotherapy and then chemical castration with LHRH agonist once their cancer was found to have relapsed following initial treatment. Their disease had continued to progress despite castrate levels of testosterone. Their levels of circulating miR-27a were compared to healthy volunteers and were found to be significantly raised. This corroborates the findings in serum, as demonstrated in Figure 6.12 B. These gentleman are highly treated and should have castration levels of testoterone and yet still have high levels of miR-27a. This may reflect the switch to castration resistance or it may reflect the likely high burden if disease in these patients. To tease out the answer to this question, we could look at levels in stage 4 patients at diagnosis prior to hormonal intervention compared to this group of heavily pre-treated castration resitant patients.

6.2.5 MiRNAs are differentially expressed in the serum of patients with prostate cancer compared to age matched benign controls.

My results up to this point have suggested that miR-27a is raised in the serum of patients with metastatic prostate cancer but they have not been clear cut. One potential reason for this is that miRNAs are modulated by the treatments the patients

are receiving and that I have been working with a very heterogeneous cohort of patients i.e. some men still have their prostates others do not. Another confounding fact has been the lack of a true control group - having to use healthy volunteers that are not age-matched and in the early study not sex-matched. I set about finding a cleaner cohort of samples with a more appropriate control group of men of a similar age that had had negative prostate biopsies and low PSA levels. The samples for the men with prostate cancer were then taken at diagnosis prior to the commencement of any hormonal treatment and prior to the removal of the prostate. This gave me the best controlled cohort of serum samples for testing. Of note even in the controlled environment of the mouse study, where food, water, age, diet, tumour burden, tumour type and even genotype, collection method, timeare constant the error bars are still quite broad.

We still wanted to find a platform that would allow idenitification of a panel of miRs that could act as a biomarker in either diagnosis or prognosis. To this end we adopted a relatively new system from Abcam that uses fluorescent particles that bind to the specific miRNA targets and can then be quantified using a flow cytometer. One major advantage of this technology is that the circulating miRNAs can be quantified from the neat serum with no need for extraction or amplification, which can add bias to the results. In addition the probes are highly specific. This system correlates well with qRT-PCR and sequencing and is robust enough to detect as few as 1,000 copies of the miRNA per sample (Chapin, Appleyard et al. 2011, Chapin and Doyle 2011). As explained earlier we believe some of the variability in our results is due to the difficulties with quantifying inputs of RNA into the RT reaction when using traditional extraction methods such as Taqman and Exiqon, which is avoided when using the Abcam Firefly Technology.

We analysed 24 serum samples in total, from 8 men with benign prostate disease, 8 men with localized prostate cancer and 8 men with metastatic disease. The panel contained probes for 68 miRNAs, chosen for their links to oncological processes in the literature and including three potential normalisers; see Appendix A for the list of miRNAs and the relevant references. All samples were checked for microscopic haemolysis and none was found to have levels sufficient to require exclusion from

the study. Figure 6.14 shows the scatter plots of the most significantly altered miRNAs from this study. Thirteen miRNAs were found to have significantly raised levels between the control group and the groups with cancer. Of these, nine also had high signal levels (greater than ten) and were thus more likely to be true results. The other four significant results although interesting need to be interpreted with a degree of caution. There is a strong and significant inverse correlation between sensitivity and specificity when assaying a large number of miRNAs so this must be born in mind (Mestdagh, Hartmann et al. 2014). Unsurprisingly, the results for the majority of these miRNAs were most significantly different between the control group (age matched men with confirmed benign prostatic disease) and the group with metastatic disease, presumably reflecting the increased burden of disease or the more aggressive nature of prostate cancer that has metastasized.

In view of the previous conflicting results we endeavoured to try and validate the Abcam Firefly study findings using a different technological platform for miRNA quantification. I chose to use Exiqon as it performed robustly across the board compared to the other platforms in the miRQC study (Mestdagh, Hartmann et al. 2014). What was clear on comparison of the two sets of data was that the trends were largely the same. Fourteen miRNAs were tested and twelve of them followed the same trend. However, overall there were fewer significant differences in the Exiqon dataset. Potentially this could be because, in this technique (Exiqon) the RNA needs to be extracted from the serum and it is inevitable in this procedure to lose some of the miRNAs, so working with small levels and thus the differences between the miRNA levels could be reduced. Six miRNAs were significantly different levels in the serum of men with prostate cancer across both studies; miR-10b, miR-126, miR-150, miR-21, miR-378 were all raised and miR-93 was consistently lower.

The clearest potential biomarker was miR-21 as it was highly and significantly elevated in the serum from men with metastatic prostate cancer across both studies. To support this data, miR-21 has been shown to be over expressed in prostate cancer tissue in an array study when compared to benign prostate tissue (Volinia, Calin et al. 2006). Also, Zhang et al. have shown miR-21 to be elevated in the serum of men with metastatic castrate resistant prostate cancer and that it can potentially act as a

predictor for response to docetaxel chemotherapy (Zhang, Yang et al. 2011). In addition miR-21 has also repeatedly been shown to be elevated in the serum of patients with lung cancer, breast cancer and colorectal cancer (Asaga, Kuo et al. 2011, Wei, Gao et al. 2011, Wang and Zhang 2012). MiR-21 has been implicated as a potential oncomiR due to its role in counteracting the expression of PTEN and PDCD4 (Qi, Bart et al. 2009). As was discussed in the introduction, loss of PTEN expression is commonly found in prostate cancer and thought to play a key role in progression.

There has been no published link between prostate cancer and miR-10b to date, but miR-10b has been shown to be higher in the circulation of women with lymph node metastases from breast cancer (Chen, Cai et al. 2013). Its overexpression has been implicated in invasion and metastasis in models of breast cancer and it has been reported that expression in primary breast carcinomas correlates with clinical progression (Ma, Teruya-Feldstein et al. 2007). MiR-126 is a purported miRNA tumour suppressor reported to be involved in angiogenesis and vascular integrity (Meister and Schmidt 2010). It is, therefore, unexpected that in our results it is significantly higher in the serum of the men with prostate cancer. However, in another study it was reported to be found in lower levels in the circulation of patients with malignant mesothelioma (Tomasetti, Staffolani et al. 2012). Likewise miR-150 is also implicated to have a role in angiogenesis via modulation of VEGF (Liu, Zhao et al. 2013). High miR-150 expression in prostate cancer tissue was positively correlated with tumour recurrence or metastasis (Dezhong, Xiaoyi et al. 2015). High circulating levels have been associated with colorectal cancer progression (Aherne, Madden et al. 2015). Lastly miR-378 has been shown to be raised in the circulation of prostate cancer patients before and also in the blood of patients with gastric cancer (Liu, Zhu et al. 2012, Nguyen, Xie et al. 2013).

One miRNA miR-93-5p was found to have significantly lower levels in the cancer patients in both the Abcam Firefly study and the Exiqon validation study. This is contradictory to some published results by Hamilton *et al*, that on large data set analysis found that miR-93 was part of a large miRNA superfamily, expression of which was raised in cancerous tissue when compared to healthy tissue (Hamilton,

Rajapakshe et al. 2013). Subsequent to that study there has been another published result by Farina *et al*. suggesting that miR-93 is raised in the circulation of men with prostate cancer (Farina, Wood et al. 2014). There are notable reasons as to why we are getting conflicting results to those reported in the Farina paper. Firstly, their assay levels are not normalized to a set of endogenous miRNAs rather like my earlier work they are just normalised to spike in control miRNA. In addition, as we have discussed before the results are hard to compare across studies due to the effect of different SOPs on the quantity of miRNA found in the sample and lastly the fact that different platforms to date cannot be reliably compared.

6.2.6 MiRNA-210 can differentiate men who will go on to relapse following definitive treatment for localized prostate cancer

When the patient cohort with localized prostate cancer was followed up at three years and then divided by whether their cancer had relapsed, we found that miR-210 was significantly higher in those individuals who had relapsed, see Figure 6.16. MiR-210 has been shown to be elevated in the circulation of men with metastatic castrate resistant prostate cancer (Cheng, Mitchell et al. 2013). It was significantly elevated in the cohort of men in the study that had metastatic disease on diagnosis. This may indicate that the raised level is associated with the presence of micro metastatic disease and thus could potentially indicate miR-210 could be used as a prognostic biomarker. The fact that the patients in this study were treatment naïve helps us to tease apart metastatic disease from castration resistance which we were not able to do in the earlier studies where the samples had come from a more heterogenous populaton.

Prognostic biomarkers are used to predict disease progression in patients prior to treatment. These biomarkers are much needed in the clinic as it is estimated that 1 in 4 men treated for localized prostate cancer will relapse within 5 years. If these patients are correctly identified at diagnosis prior to relapse, adjuvant treatment could be administered to lower this risk. Currently this prognostic risk is calculated using PSA, Gleason score and stage of the disease at diagnosis such as the CAPRA score or the D'Amico score (Cooperberg, Moul et al. 2005). However, there is a degree of overtreatment within the current system as there is not a reliable way to determine those men with indolent cancer. It is unlikely that a single miRNA could give

prognostic information on its own. However, there is potential that miR-210 could add additional information to the prognostic scoring already done and indicate those patients who require adjuvant treatment at the time of definitive treatment: and thus gain improved outcomes.

My work has provided some evidence across multiple studies that circulating miR-27a levels are higher in metastatic disease. This fits with the fact that miR-27a is a reported oncomiR and although we know it to be androgen regulated we can extrapolate from our data that this regulation gets lost at some point in the progression of the prostate cancer. We have demonstrated that the levels of miR-27a are higher in AR negative cell lines and in the serum of men with castration resitant disease. A longitudinal study could show us whether miR-27a in conjunction with PSA or other miRNAs could be a biomarker of advancing disease and the AR response to therapy, aiding us in the decision of when to initiate further androgen blockade. There is also some evidence that miR-146a and miR-210 may be prognostic markers at diagnosis to indicate that men with localized prostate cancer may require further adjuvant treatment as they are at increased risk of having micro metastasis and therefore relapse with disease. This could be explored further with an expansion of the study comparing samples pre and post prostatectomy for the circulating levels of miR-146a and miR-210.

6.3 Summary of Chapter 6

I believe for a result to be of use it must be validated across two separate platforms. MiR-21 and miR-150 have been confirmed across two different technological platforms to be raised in the serum of men with prostate cancer. It also has been accepted as being a miRNA heavily implicated in cancer. As discussed before it is unlikely that one miRNA will ever be useful as a biomarker on its own in part due to the levels of dysregulation but also because the evidence so far indicates that they are not specific to individual cancer types. In summary the use of different SOPs, miRNA quantification platforms and a lack of standardized normalisation has given rise to a lack of reproducibility of results across different studies and delayed the progress of development of miRNAs as biomarkers. In the near future, it is necessary to develop a series of reference procedures for quantification for circulating

miRNAs. There is also an urgent need to evaluate the relationship between circulating miRNAs and established markers such as PSA, to aid the progression of miRNA testing out of the laboratory and into clinical use.

Chapter 7 Conclusions and Future Work

7.1 Critique of Methodology

The aim of chapter 3 was to ascertain the levels of prohibitin and miR-27a across a panel of prostate cancer cell lines. There are a number of critiques that can be levelled at this chapter. Firstly, the cell lines used were not consistent across all the experiments. RWPEI were potentially a very useful cell line as they represent benign prostate growth, unfortunately I did not do the orginal experiments with them and thus I only have data with regards to miR-27a and not prohibitin. In hindsight it would have been very useful to have repeated those early experiments using RWPEI as well. Secondly, it has to be acknowledged that the ranking of the cell lines in order of agressivity is subjective and fairly crude thus limiting the extent to which we can draw conclusions. Thirdly, the quality of my western blots was not good and ideally I should have pursued better quality blots. Lastly, as discussed in the viva this chapter does not demonstrate anything particularly novel or significant, however, it provides a thorough base for my future molecular biology techniques and work which was necessary to inform subsequent studies.

Chapter 4 aimed to establish a panel of cell lines that could stably express prohibitin or a prohibitin silencing sequence to allow the exploration of manipulaton of prohibitin on growth and the cell cycle. Again there are a number of critiques that can be explored in this chapter. Unfortuantely this work was increadibly time consuming due to the length of time needed to culture cells and then put them through selection to identify those that had stably incorporated the necessary element. I did obtain have the whole panel that I had aimed for as I was unsuccessful in creating the DU145 overexpression cell line and the PC3 overexpression cell line. This made it difficult to compare the data conclusively. The transiently transfected cell lines both showed high levels of prohibitin transcript, that then did not correspond with significant protein levels. In comparison the stably transfected cell lines had similar levels of transcript and protein expression, so would as anticpated be much more physiologically relevant models.

The in-vivo work was the main focus of this chapter 5. In hindsight I think the main critique of this work is that more should have been established in cell lines prior to working in-vivo, specifically in the PC3 cell lines. However, time, personnel and in vivo expertise constraints did not allow this. Having said that there are no concerns about the 3Rs (replacement, reduction and refinement) of animal welfare whch were optimised throughout. One issue tha would have benefitted from further otimisation/exploration is the use of intraperitoneal injections rather than intravenous as the difficulty of the intravenous technique led to variability between the doses delievered. In addition, the experiment could have been carried out in a blinded manner, to limit any subconscious bias. Technically, calipers are not the most robust measuring technique and it is disappointing that the bioluminescence protocol within the experiment did not work as this would have provided a surrogate marker of growth response that would not be subject to experimental bias. Lastly due to time limitations we have not looked in detail at the PC3 tumour cohort. The ASO-27a did not have a significant effect on growth, however, with more time and resources it would have been interesting to look at the mRNA target levels and repeat the immunohistochemitry in these tumours and to compare to the LNCaP tumour data.

Chapter 6 was much more clinically-based, and in hindsight could have been a project in its own right. This work suffered the most from the prolonged nature of my PhD as the science and techniques moved on significantly whilst I was working on it.. However despite the methodological limitations as already described in the chapter itself, specifically the lack of agreement between technological platforms, the last project was successful. The chief limitation may be that with the advent of MRI scanning, diagnosising prostate cancer more accurately with targeted biopsies, the need for a new prognostic biomarker may diminish. However, the future for miRNA based biomarkers is likely to be in logtitudinal studies offering predictive information in the era of the new treatments for prosate cancer. Finding a miRNA signature that corralates to the new imaging outputs would allow a less expensive and invasive way to follow treatment response.

7.2 Conclusions

The aim at the start of this PhD project was to establish the role of prohibitin in prostate cancer progression and elucidate its potential as a novel therapeutic target. I started with the hypothesis that increasing the level of prohibitin using an antisense inhibitor of miR-27a, ASO-27a would slow the growth of prostate cancer cells, as a cytostatic agent. In addition, that circulating levels of miRNAs, including miR-27a, may provide clinically useful biomarker information regarding diagnosis, prognosis, or prediction of response to treatment.

The first aim was to establish whether prohibitin levels are altered between the different prostate cancer cell lines and whether there is any correlation with parameters of aggression. The first chapter contains evidence that prohibitin is found at lower levels in the more aggressive cell lines and in the metastatic deposits of prostate cancer, thus establishing a link between lower levels of prohibitin and more aggressive phenotypes of prostate cancer. Conversely, cellular miR-27a levels were found to be higher in the more aggressive cell lines and in metastatic tissue. Prohibitin and miR-27a levels were found to be inversely correlated which supported data from Dr Fletcher, *et al*. that miR-27a does directly modify prohibitin levels *in vitro (Fletcher, Dart et al. 2012)*.

Given the above correlations, it remained to be established whether lower prohibitin is a driver of aggressive disease or simply a bystander effect. The second aim of the project was to investigate whether, by artificially increasing the prohibitin levels, we can slow cell/tumour growth in a range of cell line models and if this will affect the metastatic ability of the cells. I found that by increasing prohibitin levels in LNCaP and C42 cell lines there was a decrease in proliferation and entry to the cell cycle. However, in the more aggressive AR negative cell lines increasing prohibitin had little effect. This suggests that the more aggressive cell lines have a potential method of navigating the effects of increased prohibitin levels. Or that they have mechansisms of deactivating prohibitin that we cannot pick up on the western blot for example phosphorylation or methylation. Or lastly that the major pathway by which it has this affect in LNCaP is via the AR.

The third aim was to establish whether we can manipulate endogenous prohibitin using ASO to miR27a, and what effect this has on prostate cancer cell growth. I found that administration of ASO-27a abrogates growth in LNCaP cells both *in vitro* and *in vivo*. This is potentially achieved via an apoptotic pathway, but there is not a direct effect on prohibitin levels that we could observe. Many of the gene targets that were upregulated by the ASO-27a treatment were found to be present at lower levels in metastatic prostate cancer tissue implying that there would be clinical relevance to treatment with ASO-27a.

The fourth aim was to investigate whether circulating miR-27a found in the blood of prostate cancer patients is useful as a biomarker for diagnosing prostate cancer or as a biomarker of disease response or progression. I found that miR-27a is generally higher in the serum of men with metastatic prostate cancer but that on its own it would not be sufficient to distinguish the metastatic patients group. It could have potential as part of a wider screen of miRNAs to determine when control of the AR is lost on treatment before clinical progression of the disease. A panel of miRNAs consisting of miR-21, miR-10b, miR-126, miR-150, miR-378 and miR-93 could differentiate benign from metastatic disease and it would be interesting to explore this 6 miR signature further as potential diagnostic or predictive biomarker test.

In conclusion, I believe that my studies generated insufficient evidence to fully support the initial hypothesis that increasing the level of prohibitin using an ASO-27a would slow the growth of prostate cancer cells to a clinically relevant degree. However, individual elements of this hypothesis have proven to be true, namely that increasing prohibitin levels does slow the growth of AR positive prostate cancer cells *in vitro*. Secondly that ASO-27a does slow the growth of AR positive prostate cancer cells (and AR negative PC3 to some extent) *in vitro* and *in vivo*, albeit not via increasing prohibitin levels. There was sufficient evidence to confirm the second part of my initial hypothesis that circulating levels of miRNAs, including miR-27a, may provide clinically useful biomarker information regarding diagnosis, prognosis, or prediction of response to treatment.

7.3 Perspective and Future Work

There is a lot of potential for future work stemming from this ASO-27a *in vivo* study. There are many areas of this study that require clarification and completion that I would have liked to conduct had time allowed. Using a miRNA-based therapeutic offers a new paradigm for treating disease, as it utilizes the human genome for therapeutic purpose. MiRNAs are naturally occurring molecules that benefit from millions of years of evolutionary fine tuning of their function and there are likely to distinct advantages in applying miRNA therapeutics over conventional drugs. Specificity for a single mRNA is not the purpose, unlike targeted siRNA therapeutics, rather it is an advantage that one miRNA can target multiple downstream effectors within a pathway. Another advantage is that miRNAs are small in size and are therefore less antigenic than protein-coding gene replacement therapies. However, despite this great potential, there are marked challenges in bringing miRNA therapies from bench to bedside. Foremost of these is identification and validation of the pertinent miRNAs to cancer formation and progression. As in my study, oligonucleotides can be used to deliver the miRNA to the whole system, but virus-based constructs or nanoparticles are also being explored. However, a delivery system that targets the miRNA specifically to cancer cells, whether in the prostate or disseminated, would be preferable and is plausible. This may help limit the effect of perturbing miRNA levels of unintended mRNA targets. In addition another concern would be that the RNA-induced silencing complex (RISC) would become overwhelmed and inhibit the processing of other miRNAs key to normal cell function. These would have to be explored as part of the safety and toxicity assessment. Categorizing the off target gene effects of the specific miRNA therapeutic, the effect of general high levels of miRNAs on the liver and any potential toxicity associated with the chosen delivery system. Clearly ongoing clinical trials with miRNA therapeutics will be crucial to assessing their safety. Note the above are not specific to miR-27a but apply to all miR based therapies.

It would be helpful to confirm apoptosis as the predominant mode of action by doing *in vitro* apoptosis assays with the ASO-27a. Measuring levels of identified "targets" of the inhibitor in biopsy samples from patients with prostate cancer could establish potential biomarkers of ASO-27a efficacy. It would be valuable to clarify

the role of the identified target genes by overexpression of the genes in culture and monitoring for a similar effect on cell growth or cell number. In addition to see if there is a rescue effect *in vitro* with the addition of miR-27a after ASO-27a treatment. It may also be interesting to investigate the combination of ASO-27a and other prostate cancer modulating drugs such as the chemotherapy docetaxol or the anti androgen bicalutamide. In vitro stuides showed lowering miR-27a levels led to increased sensitivity to cancer. Prostate cancer is a heterogenous disease driven by complex molecular interactions. Its complexity also accounts for its reistance against many current therapies as targeting a single component may not be sufficient to disrupt these mechanisms.

With regards to the serum biomarkers work I believe that the use of different SOPs, miRNA quantification platforms and a lack of standardized normalisation has given rise to a lack of reproducibility of results across different studies and has delayed the progress of development of miRNAs as biomarkers. In the near future, it is necessary to develop a series of reference procedures for quantification for circulating miRNAs. There is also an urgent need to evaluate the relationship between circulating miRNAs and established markers such as PSA to aid the progression out of the laboratory and into clinical use. There may be value to combining the established markers with the new for improved sensitivity and specificity. As discussed before, it is unlikely that one miRNA will ever be useful as a biomarker on its own in part due to the levels of dysregulation but also because the evidence so far indicates that they are not specific to individual cancer types. However, there is sufficient evidence here with regards to the miRNAs identified that together they may illicit enough information to act as a biomarker panel and it would be very interesting to explore this with a bigger patient cohort.

Chapter 8 Appendix

8.1 List of miRNA Targets on the Abcam Firefly Assay

Target #	miRNA	miRbase 20 name	sequence	Identical in mouse?	One or more studies indicate disregulation in the disease or condition listed	References
1	let-7d-5p	hsa-let-7d-5p	agagguaguagguugcauaguu	YES	acute myeloid leukemia, multiple myeloma	PMID: 23391324, PMID: 24241494
2	let-7g-5p	hsa-let-7g-5p	ugagguaguaguuuguacaguu	YES	potential normalizer	
3	let-7i-5p	hsa-let-7i-5p	ugagguaguaguuugugcuguu	YES	potential normalizer	
4	miR-103a	hsa-miR-103a-3p	agcagcauuguacagggcuauga	YES	colon cancer, hepatocellular carcinoma	PMID: 24400111, PMID: 24583788
5	miR-106a	hsa-miR-106a-5p	aaaagugcuuacagugcagguag	YES	lung cancer, breast cancer, ovarian cancer, gastric cancer	PMID: 20801493, PMID: 21544802, PMID: 24366298, PMID: 20234369
6	miR-106b	hsa-miR-106b-5p	uaaagugcugacagugcagau	YES	gastric cancer (x2)	PMID: 23307259, PMID: 20234369
7	miR-107	hsa-miR-107	agcagcauuguacagggcuauca	YES	prostate cancer	PMID: 22240788
8	miR-10b-5p	hsa-miR-10b-5p	uacccuguagaaccgaauuugug	YES	breast cancer (x2), lung cancer	PMID: 23797906, PMID: 24440980, PMID: 21398193
9	miR-122	hsa-miR-122-5p	uggagugugacaaugguguuug	YES	hepatocellular carcinoma, lung adenocarcinoma, gastric cancer	PMID: 22105822, PMID: 24282590, PMID: 24481716
10	miR-125b	hsa-miR-125b-5p	ucccugagacccuaacuuguga	YES	hepatocellular carcinoma (x2), NSCLC (x2)	PMID: 24583788, PMID: 24595450, PMID: 22806310, PMID: 22983388
11	miR-126	hsa-miR-126-3p	ucguaccgugaguaauaaugcg	YES	breast cancer, NSCLC (x3), ovarian cancer (x2)	PMID: 20801493, PMID: 23342174, PMID: 21116241, PMID: 22009180, PMID: 18954897, PMID: 24366298
12	miR-127-3p	hsa-miR-127-3p	ucggauccgucugagcuuggcu	YES	breast cancer, ovarian cancer	PMID: 24194846, PMID: 18954897
13	miR-130a-3p	hsa-miR-130a-3p	cagugcaauguuaaaagggcau	YES	multiple myeloma, colorectal cancer	PMID: 24241494, PMID: 24304648
14	miR-141	hsa-miR-141-3p	uaacacugucugguaaagaugg	YES	prostate cancer (x2), colon cancer (x2), breast cancer, lung cancer	PMID: 22240788, PMID: 23377530, PMID: 21445232, PMID: 22952344, PMID: 23673725, PMID: 21398193
15	miR-145	hsa-miR-145-5p	guccaguuuucccaggaaucccu	YES	colorectal cancer (x2), breast cancer, prostate cancer, ovarian cancer (x2)	PMID: 24304648, PMID: 23301032, PMID: 22298119, PMID: 24157791, PMID: 22648208, PMID: 23542579
16	miR-146a	hsa-miR-146a-5p	ugagaacugaauuccauggguu	YES	breast cancer, NSCLC, ovarian cancer	PMID: 23898484, PMID: 24531034, PMID: 24366298
17	miR-148a	hsa-miR-148a-3p	ucagugcacuacagaacuuugu	YES	breast cancer, colon cancer (x2)	PMID: 21060830, PMID: 24400111, PMID: 23970420
18	miR-148b	hsa-miR-148b-3p	ucagugcaucacagaacuuugu	YES	breast cancer (x2)	PMID: 22927033, PMID: 24194846
19	miR-150	hsa-miR-150-5p	ucucccaacccuuguaccagug	YES	acute myeloid leukemia (x2), leukemia, ovarian cancer	PMID: 23437222, PMID: 23391324, PMID: 18348159, PMID: 24366298
20	miR-151	hsa-miR-151a-3p	cuagacugaagcuccuugagg	NO	breast cancer, gastric cancer	PMID: 21060830, PMID: 22956063
21	miR-155	hsa-miR-155-5p	uuaaugcuaaucgugauagggguu	NO	lymphoma, DLBCL (x2), leukemia, breast cancer (x5), NSCLC (x2), lung cancer (x2), esophageal cancer, pancreatic ductal adenocarcinoma, colon cancer, ovarian cancer	PMID: 22541087, PMID: 21987025, PMID: 18318758, PMID: 23821659, PMID: 20801493, PMID: 21544802, PMID: 23342174, PMID: 21060830, PMID: 21904633, PMID: 23372341, PMID: 22891887, PMID: 19723895, PMID: 24310813, PMID: 24440980, PMID: 23748853, PMID: 21398193, PMID: 18954897
22	miR-15b-5p	hsa-miR-15b-5p	uagcagcacaucauggguuaca	YES	prostate cancer, colorectal cancer (x3), NSCLC	PMID: 24646542, PMID: 24661838, PMID: 22389695, PMID: 23267864, PMID: 24022433
23	miR-16	hsa-miR-16-5p	uagcagcacguaaauauuggcg	YES	DLBCL, gastric cancer, lung cancer, ovarian cancer, hepatocellular carcinoma	PMID: 21987025, PMID: 24595006, PMID: 23774211, PMID: 24366298, PMID: 21278583

24	miR-17	hsa-miR-17-5p	caaagugcuuacagugcagguag	YES	NSCLC, colorectal cancer (x2), gastric cancer (x2), breast cancer, lung cancer, ovarian cancer	PMID: 21544802, PMID: 24646542, PMID: 22406928, PMID: 23748853, PMID: 23263848, PMID: 24366298, PMID: 20234369, PMID: 24022433
25	miR-181a	hsa-miR-181a-5p	aacauucaacgcugucggugagu	YES	breast cancer (x3)	PMID: 21060830, PMID: 22692639, PMID: 24498016
26	miR-181b-5p	hsa-miR-181b-5p	uaaggugcaucuagugcagauag	YES	ESCC, pancreatic cancer, gastric cancer, colorectal cancer	PMID: 23579215, PMID: 22045190, PMID: 24626859, PMID: 24649179
27	miR-182	hsa-miR-182-5p	aacauucauugcugucgguggguu	YES	acute meyloid leukemia, breast cancer, lung cancer (x2)	PMID: 23437222, PMID: 24498016, PMID: 24600991, PMID: 21920043
28	miR-187-3p	hsa-miR-187-3p	ucgugucuuguguugcagccgg	YES	lung cancer, breast cancer	PMID: 21904633, PMID: 24260062
29	miR-18a	hsa-miR-18a-5p	uaaggugcaucuagugcagauag	YES	breast cancer, renal cell carcinoma, colorectal cancer (x2)	PMID: 21060830, PMID: 23916610, PMID: 23673725, PMID: 23267864
30	miR-192	hsa-miR-192-5p	cugaccuaugaauugacagcc	YES	hepatocellular carcinoma, gastric cancer	PMID: 22105822, PMID: 24481716
31	miR-195	hsa-miR-195-5p	uagcagcacagaaauauuggc	YES	lung cancer, gastric cancer, colorectal cancer	PMID: 24282590, PMID: 23212612, PMID: 24022433
32	miR-199a	hsa-miR-199a-3p	acaguagucugcacauugguua	YES	breast cancer, gastric cancer (x2)	PMID: 20801493, PMID: 23733518, PMID: 22956063, PMID: 24161319
33	miR-199a-5p	hsa-miR-199a-5p	cccaguguucagacuaccuguuc	YES	NSCLC, hepatocellular carcinoma, osteosarcoma	PMID: 23342174, PMID: 21278583, PMID: 23269581
34	miR-19a	hsa-miR-19a-3p	ugugcaaaucuaugcaaaacuga	YES	breast cancer, colorectal cancer	PMID: 24416156, PMID: 23267864
35	miR-200b	hsa-miR-200b-3p	uaauacugccugguaaugauga	YES	prostate cancer, breast cancer, ovarian cancer	PMID: 24661838, PMID: 22952344, PMID: 23542579
36	miR-200c	hsa-miR-200c-3p	uaauacugccgguaaugaugga	YES	colorectal cancer, breast cancer, ovarian cancer, gastric cancer	PMID: 24649179, PMID: 22952344, PMID: 23542579, PMID: 22954417
37	miR-205	hsa-miR-205-5p	uccuucauuccaccggagucug	YES	ovarian cancer, breast cancer	PMID: 23372341, PMID: 24223734
38	miR-20a	hsa-miR-20a-5p	uaaagugcuuauagugcagguag	YES	gastric cancer (x3), NSCLC, colorectal cancer (x2), prostate cancer, esophageal cancer, ovarian cancer	PMID: 23307259, PMID: 23342174, PMID: 24304648, PMID: 22298119, PMID: 22406928, PMID: 22891887, PMID: 23673725, PMID: 24366298, PMID: 21112772
39	miR-21	hsa-miR-21-5p	uagcuuaucagacugauguuga	YES	lymphoma (x2), Hodgkin lymphoma, DLBCL, breast cancer (x3), NSCLC (x3), hepatocellular carcinoma (x2), prostate cancer, pancreatic ductal adenocarcinoma, colorectal cancer (x6), gastric cancer (x3), ESCC, lung cancer (x3), pancreatic cancer, ovarian cancer, osteosarcoma	PMID: 21602271, PMID: 22541087, PMID: 24222179, PMID: 24400911, PMID: 18318758, PMID: 20801493, PMID: 23756108, PMID: 22105822, PMID: 21116241, PMID: 22298119, PMID: 23898484, PMID: 19723895, PMID: 22868372, PMID: 23267156, PMID: 22860003, PMID: 22519435, PMID: 21864403, PMID: 21749846, PMID: 21627863, PMID: 21139804, PMID: 24423916, PMID: 24664585, PMID: 24440980, PMID: 22648208, PMID: 23970420, PMID: 23673725, PMID: 23625654, PMID: 22638884, PMID: 23774211, PMID: 21721011, PMID: 18954897, PMID: 20234369, PMID: 23269581
40	miR-210	hsa-miR-210-3p	cugugcgugugacagcggcuga	YES	lymphoma, DLBCL, NSCLC, pancreatic ductal adenocarcinoma, colon cancer, lung cancer, renal cell carcinoma, breast cancer	PMID: 22541087, PMID: 18318758, PMID: 21116241, PMID: 19723895, PMID: 24310813, PMID: 21864403, PMID: 24212760, PMID: 22952344
41	miR-218	hsa-miR-218-5p	uugugcuugaucuaaccaugu	YES	prostate cancer, gastric cancer	PMID: 24661838, PMID: 22860003
42	miR-22	hsa-miR-22-3p	aagcugccaguugaagaacugu	YES	lymphoma, NSCLC, gastric cacner, prostate cancer, pancreatic cancer, breast cancer	PMID: 21206010, PMID: 21544802, PMID: 23307259, PMID: 22298119, PMID: 23329235, PMID: 22156446

43	miR-221	hsa-miR-221-3p	agcuacauugucugcuggguuuc	YES	hepatocellular carcinoma, prostate cancer, NSCLC, ovarian cancer, gastric cancer	PMID: 24124720, PMID: 24583788, PMID: 22009180, PMID: 23569131, PMID: 22432036
44	miR-222	hsa-miR-222-3p	agcuacaucuggcuacugggu	YES	acute lymphoblastic leukemia, ESCC (x2), hepatocellular carcinoma (x2), NSCLC (x3), gastric cancer, breast cancer	PMID: 23484694, PMID: 24651474, PMID: 22105822, PMID: 23342174, PMID: 22860003, PMID: 24390317, PMID: 24531034, PMID: 24595450, PMID: 24440980, PMID: 22009180
45	miR-223	hsa-miR-223-3p	ugucaguuugucaaauacccca	YES	pancreatic cancer, breast cancer, ovarian cancer	PMID: 24578785, PMID: 24498016, PMID: 24366298
46	miR-25	hsa-miR-25-3p	cauugcacuugucucggucuga	YES	ESCC (x2), gastric cancer	PMID: 24651474, PMID: 24595006, PMID: 24390317
47	miR-26a	hsa-miR-26a-5p	uucaaguaauccaggauaggcu	YES	hepatocellular carcinoma, ovarian cancer (x2)	PMID: 22105822, PMID: 24466274, PMID: 23542579
48	miR-27a	hsa-miR-27a-3p	uucacaguggcuaaguuccgc	YES	NSCLC, hepatocellular carcinoma, gastric cancer	PMID: 21544802, PMID: 22105822, PMID: 21112772
49	miR-29a	hsa-miR-29a-3p	uagcaccaucugaaaucgguua	YES	colorectal cancer (x5), breast cancer, ovarian cancer	PMID: 19876917, PMID: 19201770, PMID: 24498016, PMID: 23673725, PMID: 23625654, PMID: 18954897, PMID: 23267864
50	miR-29b	hsa-miR-29b-3p	uagcaccauuugaaaucaguguu	YES	potential normalizer	
51	miR-29c	hsa-miR-29c-3p	uagcaccauuugaaaucgguua	YES	NSCLC (x2), mesothelioma, colorectal cancer	PMID: 21544802, PMID: 22617246, PMID: 24523873, PMID: 23970420
52	miR-320a	hsa-miR-320a	aaaagcuggguugagagggcga	YES	colon cancer	PMID: 24400111
53	miR-335	hsa-miR-335-5p	ucaagagcaauaacgaaaaaugu	YES	breast cancer, colorectal cancer	PMID: 20801493, PMID: 23267864
54	miR-34a	hsa-miR-34a-5p	uggcagugucuuagcugguugu	YES	multiple myeloma, DLBCL, breast cancer, colorectal cancer, gastric cancer	PMID: 21987025, PMID: 24241494, PMID: 23748853, PMID: 22648208, PMID: 21112772
55	miR-34b	hsa-miR-34b-3p	caaucacuaacuccacugccau	NO	osteosarcoma	PMID: 24063968
56	miR-375	hsa-miR-375	uuuguucguucggcucgcguga	YES	prostate cancer, ESCC (x2), pancreatic cancer (x2), NSCLC (x2), breast cancer	PMID: 22240788, PMID: 22519435, PMID: 23329235, PMID: 24390317, PMID: 24048453, PMID: 24404590, PMID: 24513341, PMID: 22952344
57	miR-376c	hsa-miR-376c-3p	aacauagaggaaauuccacgu	NO	breast cancer (x2), gastric cancer	PMID: 24194846, PMID: 22927033, PMID: 22432036
58	miR-378	hsa-miR-378a-3p	acuggacuuggagucagaaggc	NO	colorectal cancer, gastric cancer	PMID: 24423916, PMID: 22432036
59	miR-409	hsa-miR-409-3p	gaauguugcucggugaaccccu	YES	breast cancer (x2)	PMID: 24194846, PMID: 22927033
60	miR-451	hsa-miR-451a	aaaccguuaccauuacugaguu	YES	potential hemolysis marker, colon cancer, breast cancer, gastric cancer (x2)	PMID: 24400111, PMID: 23301032, PMID: 24595006, PMID: 22262318
61	miR-483-5p	hsa-miR-483-5p	aagacgggaggaaagaagggag	NO	ESCC, breast cancer, ovarian cancer	PMID: 24651474, PMID: 21060830, PMID: 24223734
62	miR-486	hsa-miR-486-5p	uccuguacugagcugccccgag	YES	potential hemolysis marker, NSCLC, gastric cancer (x2), lung cancer, breast cancer	PMID: 21116241, PMID: 24595006, PMID: 21864403, PMID: 22262318, PMID: 24498016
63	miR-574	hsa-miR-574-3p	cacgcucaugcacacacccaca	YES	prostate cancer, NSCLC, breat cancer	PMID: 22240788, PMID: 21258252, PMID: 21060830
64	miR-625-3p	hsa-miR-625-3p	gacuauagaacuuucccccuca	NO	mesothelioma, lung cancer	PMID: 22617246, PMID: 22675530
65	miR-652	hsa-miR-652-3p	aauggcgccacuaggguugug	YES	breast cancer (x2), colorectal cancer	PMID: 24194846, PMID: 24498016, PMID: 24022433
66	miR-9	hsa-miR-9-5p	ucuuugguuaucuagcuguauga	YES	endometrial carcinoma	PMID: 22987275
67	miR-92a	hsa-miR-92a-3p	uauugcacuugucccggccugu	NO	non-Hodgkin lymphoma, leukemia (x2), gastric cancer, colorectal cancer (x4), mesothelioma, endometrial carcinoma, ovarian cancer (x3)	PMID: 21383985, PMID: 19440243, PMID: 21182798, PMID: 24595006, PMID: 19876917, PMID: 22617246, PMID: 22987275, PMID: 22648208, PMID: 23673725, PMID: 23625654, PMID: 18954897, PMID: 23963852, PMID: 24366298

68	miR-93-5p	hsa-mir-93-5p	caaagugcuguucgugcagguag	YES	acute myeloid leukemia, NSCLC, breast cancer (x2), ovarian cancer	PMID: 23437222, PMID: 24523873, PMID: 24498016, PMID: 23748853, PMID: 18954897
69	x-control	x-control	x-control	N/A	internal reference	
70	blank	blank	none	N/A	internal reference	

Abbreviations: N/A = not applicable, NSCLC = Non small cell lung cancer, DLBCL = diffuse large B cell lymphoma, ESCC = oesophageal squamous cell cancer, PMID= The unique identifier number used by PubMed.
Green boxes indicate potential normalizers, blue boxes indicate haemolysis markers, purple boxes indicate internal reference,

8.2 Permissions for Figures used in this Thesis

NATURE PUBLISHING GROUP LICENSE TERMS AND CONDITIONS

Jul 14, 2016

This Agreement between Ailsa Sita ("You") and Nature Publishing Group ("Nature Publishing Group") consists of your license details and the terms and conditions provided by Nature Publishing Group and Copyright Clearance Center.

License Number	3792521336630
License date	Jan 19, 2016
Licensed Content Publisher	Nature Publishing Group
Licensed Content Publication	Nature Reviews Urology
Licensed Content Title	CYP17 inhibitors—abiraterone, C17,20-lyase inhibitors and multi-targeting agents
Licensed Content Author	Lina Yin, Qingzhong Hu
Licensed Content Date	Nov 26, 2013
Licensed Content Volume Number	11
Licensed Content Issue Number	1
Type of Use	reuse in a dissertation / thesis
Requestor type	academic/educational
Format	print and electronic
Portion	figures/tables/illustrations
Number of figures/tables/illustrations	1
High-res required	no
Figures	Figure 1
Author of this NPG article	no
Your reference number	
Title of your thesis / dissertation	The Role of Prohibitin and miR-27a in Prostate Cancer Progression and Therapy Response
Expected completion date	Mar 2016
Estimated size (number of pages)	200
Requestor Location	Ailsa Sita-Lumsden 80 Strathleven Road London, SW2 5LE United Kingdom Attn: Ailsa Sita-Lumsden
Billing Type	Invoice
Billing Address	Ailsa Sita-Lumsden 80 Strathleven Road London, United Kingdom SW2 5LE Attn: Ailsa Sita-Lumsden
Total	**0.00 GBP**
Total	**0.00 GBP**
Terms and Conditions	

Terms and Conditions for Permissions

Nature Publishing Group hereby grants you a non-exclusive license to reproduce this material for this purpose, and for no other use,subject to the conditions below:

NATURE PUBLISHING GROUP LICENSE TERMS AND CONDITIONS

Ju

This Agreement between Ailsa Sita ("You") and Nature Publishing Group ("Nature Publishing Group") consists of your license details and the terms and conditions pr Nature Publishing Group and Copyright Clearance Center.

License Number	3907690729055
License date	Jul 14, 2016
Licensed Content Publisher	Nature Publishing Group
Licensed Content Publication	Nature Reviews Drug Discovery
Licensed Content Title	RNA therapeutics: beyond RNA interference and antisense oligonucleotides
Licensed Content Author	Ryszard Kole, Adrian R. Krainer and Sidney Altman
Licensed Content Date	Jan 20, 2012
Licensed Content Volume Number	11
Licensed Content Issue Number	2
Type of Use	reuse in a dissertation / thesis
Requestor type	academic/educational
Format	print and electronic
Portion	figures/tables/illustrations
Number of figures/tables/illustrations	1
High-res required	no
Figures	2
Author of this NPG article	no
Your reference number	
Title of your thesis / dissertation	The Role of Prohibitin and miR-27a in Prostate Cancer Pro and Therapy Response
Expected completion date	Mar 2016
Estimated size (number of pages)	200
Requestor Location	Ailsa Sita-Lumsden 80 Strathleven Road London, SW2 5LE United Kingdom Attn: Ailsa Sita-Lumsden
Billing Type	Invoice
Billing Address	Ailsa Sita-Lumsden 80 Strathleven Road London, United Kingdom SW2 5LE Attn: Ailsa Sita-Lumsden

Print This Page

ELSEVIER LICENSE
TERMS AND CONDITIONS

Jul 18, 2016

This Agreement between Ailsa Sita ("You") and Elsevier ("Elsevier") consists of your license details and the terms and conditions provided by Elsevier and Copyright Clearance Center.

License Number	3911850809308
License date	Jul 18, 2016
Licensed Content Publisher	Elsevier
Licensed Content Publication	Trends in Molecular Medicine
Licensed Content Title	Prohibitin: a potential target for new therapeutics
Licensed Content Author	Suresh Mishra,Leigh C. Murphy,B.L. Gregoire Nyomba,Liam J. Murphy
Licensed Content Date	April 2005
Licensed Content Volume Number	11
Licensed Content Issue Number	4
Licensed Content Pages	6
Start Page	192
End Page	197
Type of Use	reuse in a thesis/dissertation
Portion	figures/tables/illustrations
Number of figures/tables/illustrations	1
Format	both print and electronic
Are you the author of this Elsevier article?	No
Will you be translating?	No
Order reference number	
Original figure numbers	1
Title of your thesis/dissertation	The Role of Prohibitin and miR-27a in Prostate Cancer Progression and Therapy Response
Expected completion date	Mar 2016
Estimated size (number of pages)	200
Elsevier VAT number	GB 494 6272 12
Requestor Location	Ailsa Sita-Lumsden 80 Strathleven Road London, SW2 5LE United Kingdom Attn: Ailsa Sita-Lumsden
Total	0.00 GBP
Terms and Conditions	

INTRODUCTION

NATURE PUBLISHING GROUP LICENSE TERMS AND CONDITIONS

Jul 18, 2016

This Agreement between Ailsa Sita ("You") and Nature Publishing Group ("Nature Publishing Group") consists of your license details and the terms and conditions provided by Nature Publishing Group and Copyright Clearance Center.

License Number	3911850927130
License date	Jul 18, 2016
Licensed Content Publisher	Nature Publishing Group
Licensed Content Publication	Nature Cell Biology
Licensed Content Title	Many roads to maturity: microRNA biogenesis pathways and their regulation
Licensed Content Author	Julia Winter,Stephanie Jung,Sarina Keller,Richard I. GregoryandSven Diederichs
Licensed Content Date	Mar 1, 2009
Licensed Content Volume Number	11
Licensed Content Issue Number	3
Type of Use	reuse in a dissertation / thesis
Requestor type	academic/educational
Format	print and electronic
Portion	figures/tables/illustrations
Number of figures/tables/illustrations	1
High-res required	no
Figures	1
Author of this NPG article	no
Your reference number	
Title of your thesis / dissertation	The Role of Prohibitin and miR-27a in Prostate Cancer Progression and Therapy Response
Expected completion date	Mar 2016
Estimated size (number of pages)	200
Requestor Location	Ailsa Sita-Lumsden 80 Strathleven Road London, SW2 5LE United Kingdom Attn: Ailsa Sita-Lumsden
Billing Type	Invoice
Billing Address	Ailsa Sita-Lumsden 80 Strathleven Road London, United Kingdom SW2 5LE Attn: Ailsa Sita-Lumsden
Total	0.00 GBP

Garite, Bibi

From: Ailsa Sita-Lumsden <a.sita-lumsden@ic.ac.uk>
Sent: Tuesday, January 19, 2016 10:20 AM
To: genesdev-feedback@highwire.stanford.edu
Subject: Seeking permission to use a figure in a thesis (Genes & Dev. Feedback Form)

Comments sent via GENES DEV. Feedback Page

TO: genesdev-feedback@highwire.stanford.edu
NAME: Ailsa Sita-Lumsden
EMAIL: a.sita-lumsden@ic.ac.uk
IP ADDRESSES: 88.105.51.85, 88.105.51.85
HOSTNAME: 88-105-51-85.dynamic.dsl.as9105.com
PREVIOUS PAGE: http://genesdev.cshlp.org/help/
BROWSER: Mozilla/5.0 (Macintosh; Intel Mac OS X 10_6_8) AppleWebKit/537.36 (KHTML, like Gecko) Chrome/47.0.2526.111 Safari/537.36, Genes & Dev.
PROMOTIONAL USE: Granted
SESSION ID: @mShoIZ2AmjyKRN924MkcQ

COMMENTS:
Dear Sir/Madam,

I am seeking permission to reproduce a figure from a published article.
Genes Dev. 2010 Sep 15; 24(18): 1967???2000.
doi: 10.1101/gad.1965810
Figure 1.
I would like to put this into my PhD thesis entitled The Role of Prohibitin and miR-27a in the Progression and Therapy of Prostate Cancer.

Thanks for your time,
Ailsa

Permission granted by the copyright owner, contingent upon the consent of the original author, provided complete credit is given to the original source and copyright date.
By Lauren Connell, Ph.D. 1/20/16
Date

COLD SPRING HARBOR LABORATORY PRESS

1

Chapter 9 References

Agarwal, V., G. W. Bell, J. W. Nam and D. P. Bartel (2015). "Predicting effective microRNA target sites in mammalian mRNAs." Elife **4**.

Aherne, S. T., S. F. Madden, D. J. Hughes, B. Pardini, A. Naccarati, M. Levy, P. Vodicka, P. Neary, P. Dowling and M. Clynes (2015). "Circulating miRNAs miR-34a and miR-150 associated with colorectal cancer progression." BMC Cancer **15**: 329.

Ahler, E., W. J. Sullivan, A. Cass, D. Braas, A. G. York, S. J. Bensinger, T. G. Graeber and H. R. Christofk (2013). "Doxycycline alters metabolism and proliferation of human cell lines." PLoS One **8**(5): e64561.

Alimirah, F., J. Chen, Z. Basrawala, H. Xin and D. Choubey (2006). "DU-145 and PC-3 human prostate cancer cell lines express androgen receptor: implications for the androgen receptor functions and regulation." FEBS Lett **580**(9): 2294-2300.

Ambs, S., R. L. Prueitt, M. Yi, R. S. Hudson, T. M. Howe, F. Petrocca, T. A. Wallace, C. G. Liu, S. Volinia, G. A. Calin, H. G. Yfantis, R. M. Stephens and C. M. Croce (2008). "Genomic profiling of microRNA and messenger RNA reveals deregulated microRNA expression in prostate cancer." Cancer Res **68**(15): 6162-6170.

Andriole, G. L., E. D. Crawford, R. L. Grubb, 3rd, S. S. Buys, D. Chia, T. R. Church, M. N. Fouad, E. P. Gelmann, P. A. Kvale, D. J. Reding, J. L. Weissfeld, L. A. Yokochi, B. O'Brien, J. D. Clapp, J. M. Rathmell, T. L. Riley, R. B. Hayes, B. S. Kramer, G. Izmirlian, A. B. Miller, P. F. Pinsky, P. C. Prorok, J. K. Gohagan and C. D. Berg (2009). "Mortality results from a randomized prostate-cancer screening trial." The New England journal of medicine **360**(13): 1310-1319.

Artal-Sanz, M. and N. Tavernarakis (2009). "Prohibitin couples diapause signalling to mitochondrial metabolism during ageing in C. elegans." Nature **461**(7265): 793-797.

Asaga, S., C. Kuo, T. Nguyen, M. Terpenning, A. E. Giuliano and D. S. Hoon (2011). "Direct serum assay for microRNA-21 concentrations in early and advanced breast cancer." Clin Chem **57**(1): 84-91.

Asaga, S., C. Kuo, T. Nguyen, M. Terpenning, A. E. Giuliano and D. S. Hoon (2011). "Direct serum assay for microRNA-21 concentrations in early and advanced breast cancer." Clinical chemistry **57**(1): 84-91.

Bandiera, S., S. Pfeffer, T. F. Baumert and M. B. Zeisel (2015). "miR-122--a key factor and therapeutic target in liver disease." J Hepatol **62**(2): 448-457.

Bao, B., S. Ali, D. Kong, S. H. Sarkar, Z. Wang, S. Banerjee, A. Aboukameel, S. Padhye, P. A. Philip and F. H. Sarkar (2011). "Anti-tumor activity of a novel compound-CDF is mediated by regulating miR-21, miR-200, and PTEN in pancreatic cancer." PLoS One **6**(3): e17850.

Bartel, D. P. (2009). "MicroRNAs: target recognition and regulatory functions." Cell **136**(2): 215-233.

Bassett, W. W., M. R. Cooperberg, N. Sadetsky, S. Silva, J. DuChane, D. J. Pasta, J. M. Chan, J. W. Anast, P. R. Carroll and C. J. Kane (2005). "Impact of obesity on prostate cancer recurrence after radical prostatectomy: data from CaPSURE." Urology **66**(5): 1060-1065.

Beck, A. M., J. W. Robinson and L. E. Carlson (2013). "Sexual values as the key to maintaining satisfying sex after prostate cancer treatment: the physical pleasure-relational intimacy model of sexual motivation." Arch Sex Behav **42**(8): 1637-1647.

Bello, D., M. M. Webber, H. K. Kleinman, D. D. Wartinger and J. S. Rhim (1997). "Androgen responsive adult human prostatic epithelial cell lines immortalized by human papillomavirus 18." Carcinogenesis **18**(6): 1215-1223.
Ben, Y. J., X. H. Li, Y. L. Yang, L. Li, J. P. Di, W. Y. Wang, R. F. Zhou, K. Xiao, M. Y. Zheng, Y. Tian and X. B. Xu (2013). "Dechlorane Plus and its dechlorinated analogs from an e-waste recycling center in maternal serum and breast milk of women in Wenling, China." Environ Pollut **173**: 176-181.
Ben-Ami, O., N. Pencovich, J. Lotem, D. Levanon and Y. Groner (2009). "A regulatory interplay between miR-27a and Runx1 during megakaryopoiesis." Proc Natl Acad Sci U S A **106**(1): 238-243.
Bernstein, E., S. Y. Kim, M. A. Carmell, E. P. Murchison, H. Alcorn, M. Z. Li, A. A. Mills, S. J. Elledge, K. V. Anderson and G. J. Hannon (2003). "Dicer is essential for mouse development." Nature genetics **35**(3): 215-217.
Boll, K., K. Reiche, K. Kasack, N. Morbt, A. K. Kretzschmar, J. M. Tomm, G. Verhaegh, J. Schalken, M. von Bergen, F. Horn and J. Hackermuller (2013). "MiR-130a, miR-203 and miR-205 jointly repress key oncogenic pathways and are downregulated in prostate carcinoma." Oncogene **32**(3): 277-285.
Bostwick, D. G., R. Montironi and I. A. Sesterhenn (2000). "Diagnosis of prostatic intraepithelial neoplasia: Prostate Working Group/consensus report." Scand J Urol Nephrol Suppl(205): 3-10.
Brase, J. C., M. Johannes, T. Schlomm, M. Falth, A. Haese, T. Steuber, T. Beissbarth, R. Kuner and H. Sultmann (2011). "Circulating miRNAs are correlated with tumor progression in prostate cancer." International journal of cancer. Journal international du cancer **128**(3): 608-616.
Brinkmann, A. O. and J. Trapman (2000). "Prostate cancer schemes for androgen escape." Nat Med **6**(6): 628-629.
Bryant, R. J., T. Pawlowski, J. W. Catto, G. Marsden, R. L. Vessella, B. Rhees, C. Kuslich, T. Visakorpi and F. C. Hamdy (2012). "Changes in circulating microRNA levels associated with prostate cancer." British journal of cancer **106**(4): 768-774.
Calin, G. A. and C. M. Croce (2006). "MicroRNA signatures in human cancers." Nat Rev Cancer **6**(11): 857-866.
Canil, C. M., M. J. Moore, E. Winquist, T. Baetz, M. Pollak, K. N. Chi, S. Berry, D. S. Ernst, L. Douglas, M. Brundage, B. Fisher, A. McKenna and L. Seymour (2005). "Randomized phase II study of two doses of gefitinib in hormone-refractory prostate cancer: a trial of the National Cancer Institute of Canada-Clinical Trials Group." J Clin Oncol **23**(3): 455-460.
Carlsbecker, A., J. Y. Lee, C. J. Roberts, J. Dettmer, S. Lehesranta, J. Zhou, O. Lindgren, M. A. Moreno-Risueno, A. Vaten, S. Thitamadee, A. Campilho, J. Sebastian, J. L. Bowman, Y. Helariutta and P. N. Benfey (2010). "Cell signalling by microRNA165/6 directs gene dose-dependent root cell fate." Nature **465**(7296): 316-321.
Chandra, R. V., S. Heinze, R. Dowling, C. Shadbolt, A. Costello and J. Pedersen (2007). "Endorectal magnetic resonance imaging staging of prostate cancer." ANZ J Surg **77**(10): 860-865.
Chandran, U. R., C. Ma, R. Dhir, M. Bisceglia, M. Lyons-Weiler, W. Liang, G. Michalopoulos, M. Becich and F. A. Monzon (2007). "Gene expression profiles of prostate cancer reveal involvement of multiple molecular pathways in the metastatic process." BMC Cancer **7**: 64.

Chapin, S. C., D. C. Appleyard, D. C. Pregibon and P. S. Doyle (2011). "Rapid microRNA profiling on encoded gel microparticles." Angew Chem Int Ed Engl **50**(10): 2289-2293.
Chapin, S. C. and P. S. Doyle (2011). "Ultrasensitive multiplexed microRNA quantification on encoded gel microparticles using rolling circle amplification." Anal Chem **83**(18): 7179-7185.
Chen, W., F. Cai, B. Zhang, Z. Barekati and X. Y. Zhong (2013). "The level of circulating miRNA-10b and miRNA-373 in detecting lymph node metastasis of breast cancer: potential biomarkers." Tumour biology : the journal of the International Society for Oncodevelopmental Biology and Medicine **34**(1): 455-462.
Chen, X., Y. Ba, L. Ma, X. Cai, Y. Yin, K. Wang, J. Guo, Y. Zhang, J. Chen, X. Guo, Q. Li, X. Li, W. Wang, J. Wang, X. Jiang, Y. Xiang, C. Xu, P. Zheng, J. Zhang, R. Li, H. Zhang, X. Shang, T. Gong, G. Ning, K. Zen and C. Y. Zhang (2008). "Characterization of microRNAs in serum: a novel class of biomarkers for diagnosis of cancer and other diseases." Cell Res **18**(10): 997-1006.
Chen, Y., P. Chi, S. Rockowitz, P. J. Iaquinta, T. Shamu, S. Shukla, D. Gao, I. Sirota, B. S. Carver, J. Wongvipat, H. I. Scher, D. Zheng and C. L. Sawyers (2013). "ETS factors reprogram the androgen receptor cistrome and prime prostate tumorigenesis in response to PTEN loss." Nat Med **19**(8): 1023-1029.
Cheng, H. H., P. S. Mitchell, E. M. Kroh, A. E. Dowell, L. Chery, J. Siddiqui, P. S. Nelson, R. L. Vessella, B. S. Knudsen, A. M. Chinnaiyan, K. J. Pienta, C. Morrissey and M. Tewari (2013). "Circulating microRNA profiling identifies a subset of metastatic prostate cancer patients with evidence of cancer-associated hypoxia." PLoS One **8**(7): e69239.
Chumbalkar, V. C., C. Subhashini, V. M. Dhople, C. S. Sundaram, M. V. Jagannadham, K. N. Kumar, P. N. Srinivas, R. Mythili, M. K. Rao, M. J. Kulkarni, S. Hegde, A. S. Hegde, C. Samual, V. Santosh, L. Singh and R. Sirdeshmukh (2005). "Differential protein expression in human gliomas and molecular insights." Proteomics **5**(4): 1167-1177.
Coates, P. J., D. J. Jamieson, K. Smart, A. R. Prescott and P. A. Hall (1997). "The prohibitin family of mitochondrial proteins regulate replicative lifespan." Curr Biol **7**(8): 607-610.
Coates, P. J., R. Nenutil, A. McGregor, S. M. Picksley, D. H. Crouch, P. A. Hall and E. G. Wright (2001). "Mammalian prohibitin proteins respond to mitochondrial stress and decrease during cellular senescence." Exp Cell Res **265**(2): 262-273.
Collin, S. M., C. Metcalfe, L. Zuccolo, S. J. Lewis, L. Chen, A. Cox, M. Davis, J. A. Lane, J. Donovan, G. D. Smith, D. E. Neal, F. C. Hamdy, J. Gudmundsson, P. Sulem, T. Rafnar, K. R. Benediktsdottir, R. A. Eeles, M. Guy, Z. Kote-Jarai, U. K. G. P. C. S. Group, J. Morrison, A. A. Al Olama, K. Stefansson, D. F. Easton and R. M. Martin (2009). "Association of folate-pathway gene polymorphisms with the risk of prostate cancer: a population-based nested case-control study, systematic review, and meta-analysis." Cancer Epidemiol Biomarkers Prev **18**(9): 2528-2539.
Connock, M., C. Hyde and D. Moore (2011). "Cautions regarding the fitting and interpretation of survival curves: examples from NICE single technology appraisals of drugs for cancer." Pharmacoeconomics **29**(10): 827-837.
Cooperberg, M. R., J. W. Moul and P. R. Carroll (2005). "The changing face of prostate cancer." J Clin Oncol **23**(32): 8146-8151.

Cortez, M. A., C. Bueso-Ramos, J. Ferdin, G. Lopez-Berestein, A. K. Sood and G. A. Calin (2011). "MicroRNAs in body fluids--the mix of hormones and biomarkers." Nature reviews. Clinical oncology **8**(8): 467-477.
CRUK. (2012). "Cancer Stats Report - Prostate Cancer UK." Cancer Research UK.
Dai, Y., D. Ngo, J. Jacob, L. W. Forman and D. V. Faller (2008). "Prohibitin and the SWI/SNF ATPase subunit BRG1 are required for effective androgen antagonist-mediated transcriptional repression of androgen receptor-regulated genes." Carcinogenesis **29**(9): 1725-1733.
Dart, D. A., B. Spencer-Dene, S. C. Gamble, J. Waxman and C. L. Bevan (2009). "Manipulating prohibitin levels provides evidence for an in vivo role in androgen regulation of prostate tumours." Endocr Relat Cancer **16**(4): 1157-1169.
Davis, A. P., C. G. Murphy, C. A. Saraceni-Richards, M. C. Rosenstein, T. C. Wiegers and C. J. Mattingly (2009). "Comparative Toxicogenomics Database: a knowledgebase and discovery tool for chemical-gene-disease networks." Nucleic Acids Res **37**(Database issue): D786-792.
Davis, B. M. and M. K. Waldor (2009). "High-throughput sequencing reveals suppressors of Vibrio cholerae rpoE mutations: one fewer porin is enough." Nucleic Acids Res **37**(17): 5757-5767.
Davis, M. E., J. E. Zuckerman, C. H. Choi, D. Seligson, A. Tolcher, C. A. Alabi, Y. Yen, J. D. Heidel and A. Ribas (2010). "Evidence of RNAi in humans from systemically administered siRNA via targeted nanoparticles." Nature **464**(7291): 1067-1070.
Davis, S., S. Propp, S. M. Freier, L. E. Jones, M. J. Serra, G. Kinberger, B. Bhat, E. E. Swayze, C. F. Bennett and C. Esau (2009). "Potent inhibition of microRNA in vivo without degradation." Nucleic Acids Res **37**(1): 70-77.
de Bono, J. S., S. Oudard, M. Ozguroglu, S. Hansen, J. P. Machiels, I. Kocak, G. Gravis, I. Bodrogi, M. J. Mackenzie, L. Shen, M. Roessner, S. Gupta and A. O. Sartor (2010). "Prednisone plus cabazitaxel or mitoxantrone for metastatic castration-resistant prostate cancer progressing after docetaxel treatment: a randomised open-label trial." Lancet **376**(9747): 1147-1154.
de la Taille, A., J. Irani, M. Graefen, F. Chun, T. de Reijke, P. Kil, P. Gontero, A. Mottaz and A. Haese (2011). "Clinical evaluation of the PCA3 assay in guiding initial biopsy decisions." J Urol **185**(6): 2119-2125.
Delage-Mourroux, R., P. G. Martini, I. Choi, D. M. Kraichely, J. Hoeksema and B. S. Katzenellenbogen (2000). "Analysis of estrogen receptor interaction with a repressor of estrogen receptor activity (REA) and the regulation of estrogen receptor transcriptional activity by REA." J Biol Chem **275**(46): 35848-35856.
Deng, B., J. Zhang, L. Zhang, Y. Jiang, J. Zhou, D. Fang, H. Zhang and H. Huang (2012). "Levels and profiles of PCDD/Fs, PCBs in mothers' milk in Shenzhen of China: estimation of breast-fed infants' intakes." Environ Int **42**: 47-52.
Dezhong, L., Z. Xiaoyi, L. Xianlian, Z. Hongyan, Z. Guohua, S. Bo, Z. Shenglei and Z. Lian (2015). "miR-150 is a factor of survival in prostate cancer patients." J BUON **20**(1): 173-179.
Di Lorenzo, G., G. Tortora, F. P. D'Armiento, G. De Rosa, S. Staibano, R. Autorino, M. D'Armiento, M. De Laurentiis, S. De Placido, G. Catalano, A. R. Bianco and F. Ciardiello (2002). "Expression of epidermal growth factor receptor correlates with disease relapse and progression to androgen-independence in human prostate cancer." Clin Cancer Res **8**(11): 3438-3444.

Dijkstra, S., A. R. Hamid, G. H. Leyten and J. A. Schalken (2012). "Personalized management in low-risk prostate cancer: the role of biomarkers." Prostate Cancer **2012**: 327104.
Eisenberg, M. S., R. J. Karnes, D. Kaushik, L. Rangel, E. J. Bergstralh and S. A. Boorjian (2013). "Risk stratification of patients with extraprostatic extension and negative lymph nodes at radical prostatectomy: identifying optimal candidates for adjuvant therapy." J Urol **190**(5): 1735-1741.
Enright, A. J., B. John, U. Gaul, T. Tuschl, C. Sander and D. S. Marks (2003). "MicroRNA targets in Drosophila." Genome Biol **5**(1): R1.
Ewing, C. M., A. M. Ray, E. M. Lange, K. A. Zuhlke, C. M. Robbins, W. D. Tembe, K. E. Wiley, S. D. Isaacs, D. Johng, Y. Wang, C. Bizon, G. Yan, M. Gielzak, A. W. Partin, V. Shanmugam, T. Izatt, S. Sinari, D. W. Craig, S. L. Zheng, P. C. Walsh, J. E. Montie, J. Xu, J. D. Carpten, W. B. Isaacs and K. A. Cooney (2012). "Germline mutations in HOXB13 and prostate-cancer risk." N Engl J Med **366**(2): 141-149.
Farina, N. H., M. E. Wood, S. D. Perrapato, C. S. Francklyn, G. S. Stein, J. L. Stein and J. B. Lian (2014). "Standardizing analysis of circulating microRNA: clinical and biological relevance." J Cell Biochem **115**(5): 805-811.
Farmer, P., J. Frenk, F. M. Knaul, L. N. Shulman, G. Alleyne, L. Armstrong, R. Atun, D. Blayney, L. Chen, R. Feachem, M. Gospodarowicz, J. Gralow, S. Gupta, A. Langer, J. Lob-Levyt, C. Neal, A. Mbewu, D. Mired, P. Piot, K. S. Reddy, J. D. Sachs, M. Sarhan and J. R. Seffrin (2010). "Expansion of cancer care and control in countries of low and middle income: a call to action." Lancet **376**(9747): 1186-1193.
Feng, J., A. Iwama, M. Satake and K. Kohu (2009). "MicroRNA-27 enhances differentiation of myeloblasts into granulocytes by post-transcriptionally downregulating Runx1." Br J Haematol **145**(3): 412-423.
Ferguson, K. M., M. B. Berger, J. M. Mendrola, H. S. Cho, D. J. Leahy and M. A. Lemmon (2003). "EGF activates its receptor by removing interactions that autoinhibit ectodomain dimerization." Mol Cell **11**(2): 507-517.
Fletcher, C. E., D. A. Dart, A. Sita-Lumsden, H. Cheng, P. S. Rennie and C. L. Bevan (2012). "Androgen-regulated processing of the oncomir MiR-27a, which targets Prohibitin in prostate cancer." Human molecular genetics **21**(14): 3112-3127.
Fletcher, C. E., D. A. Dart, A. Sita-Lumsden, H. Cheng, P. S. Rennie and C. L. Bevan (2012). "Androgen-regulated processing of the oncomir MiR-27a, which targets Prohibitin in prostate cancer." Human molecular genetics.
Fletcher, C. E., D. A. Dart, A. Sita-Lumsden, H. Cheng, P. S. Rennie and C. L. Bevan (2012). "Androgen-regulated processing of the oncomir miR-27a, which targets Prohibitin in prostate cancer." Hum Mol Genet **21**(14): 3112-3127.
Franzoni, A., M. Dima, M. D'Agostino, C. Puppin, D. Fabbro, C. D. Loreto, M. Pandolfi, E. Puxeddu, S. Moretti, M. Celano, R. Bruno, S. Filetti, D. Russo and G. Damante (2009). "Prohibitin is overexpressed in papillary thyroid carcinomas bearing the BRAF(V600E) mutation." Thyroid **19**(3): 247-255.
Fusaro, G., P. Dasgupta, S. Rastogi, B. Joshi and S. Chellappan (2003). "Prohibitin induces the transcriptional activity of p53 and is exported from the nucleus upon apoptotic signaling." J Biol Chem **278**(48): 47853-47861.
Fusaro, G., S. Wang and S. Chellappan (2002). "Differential regulation of Rb family proteins and prohibitin during camptothecin-induced apoptosis." Oncogene **21**(29): 4539-4548.
Gamble, S. C., D. Chotai, M. Odontiadis, D. A. Dart, G. N. Brooke, S. M. Powell, V. Reebye, A. Varela-Carver, Y. Kawano, J. Waxman and C. L. Bevan (2007).

"Prohibitin, a protein downregulated by androgens, represses androgen receptor activity." Oncogene **26**(12): 1757-1768.
Gamble, S. C., M. Odontiadis, J. Waxman, J. A. Westbrook, M. J. Dunn, R. Wait, E. W. Lam and C. L. Bevan (2004). "Androgens target prohibitin to regulate proliferation of prostate cancer cells." Oncogene **23**(17): 2996-3004.
Ganeswaran, D., C. Sweeney, F. Yousif, S. Lang, C. Goodman and G. Nabi (2014). "Population-based linkage of health records to detect urological complications and hospitalisation following transrectal ultrasound-guided biopsies in men suspected of prostate cancer." World J Urol **32**(2): 309-315.
Gebhardt, M. L., S. Reuter, R. Mrowka and M. A. Andrade-Navarro (2014). "Similarity in targets with REST points to neural and glioblastoma related miRNAs." Nucleic Acids Res **42**(9): 5436-5446.
Gilbert, S. M., M. G. Sanda, R. L. Dunn, T. K. Greenfield, L. Hembroff, E. Klein, C. S. Saigal, L. Pisters, J. Michalski, H. M. Sandler, M. S. Litwin and J. T. Wei (2014). "Satisfaction with information used to choose prostate cancer treatment." J Urol **191**(5): 1265-1271.
Gonzales, J. C., L. M. Fink, O. B. Goodman, Jr., J. T. Symanowski, N. J. Vogelzang and D. C. Ward (2011). "Comparison of circulating MicroRNA 141 to circulating tumor cells, lactate dehydrogenase, and prostate-specific antigen for determining treatment response in patients with metastatic prostate cancer." Clinical genitourinary cancer **9**(1): 39-45.
Gottlieb, B., M. Trifiro, R. Lumbroso and L. Pinsky (1997). "The androgen receptor gene mutations database." Nucleic Acids Res **25**(1): 158-162.
Gravis, G., F. Bladou, N. Salem, A. Goncalves, B. Esterni, J. Walz, S. Bagattini, M. Marcy, S. Brunelle and P. Viens (2008). "Results from a monocentric phase II trial of erlotinib in patients with metastatic prostate cancer." Ann Oncol **19**(9): 1624-1628.
Grimson, A., K. K. Farh, W. K. Johnston, P. Garrett-Engele, L. P. Lim and D. P. Bartel (2007). "MicroRNA targeting specificity in mammals: determinants beyond seed pairing." Mol Cell **27**(1): 91-105.
Gu, Y., M. Li, T. Wang, Y. Liang, Z. Zhong, X. Wang, Q. Zhou, L. Chen, Q. Lang, Z. He, X. Chen, J. Gong, X. Gao, X. Li and X. Lv (2012). "Lactation-related microRNA expression profiles of porcine breast milk exosomes." PLoS One **7**(8): e43691.
Gupta, S. (2010). "Effect of development assistance on domestic health expenditures." Lancet **376**(9741): 593-594; author reply 592-593.
Hahn, N. M., C. T. Yiannoutsos, K. Kirkpatrick, J. Sharma and C. J. Sweeney (2014). "Failure to suppress markers of bone turnover on first-line hormone therapy for metastatic prostate cancer is associated with shorter time to skeletal-related event." Clinical genitourinary cancer **12**(1): 33-40 e34.
Hamilton, M. P., K. Rajapakshe, S. M. Hartig, B. Reva, M. D. McLellan, C. Kandoth, L. Ding, T. I. Zack, P. H. Gunaratne, D. A. Wheeler, C. Coarfa and S. E. McGuire (2013). "Identification of a pan-cancer oncogenic microRNA superfamily anchored by a central core seed motif." Nat Commun **4**: 2730.
Haussecker, D. and M. A. Kay (2010). "miR-122 continues to blaze the trail for microRNA therapeutics." Molecular therapy : the journal of the American Society of Gene Therapy **18**(2): 240-242.

He, B., Q. Feng, A. Mukherjee, D. M. Lonard, F. J. DeMayo, B. S. Katzenellenbogen, J. P. Lydon and B. W. O'Malley (2008). "A repressive role for prohibitin in estrogen signaling." Mol Endocrinol **22**(2): 344-360.
Heinlein, C. A. and C. Chang (2004). "Androgen receptor in prostate cancer." Endocr Rev **25**(2): 276-308.
Heneghan, H. M., N. Miller and M. J. Kerin (2010). "MiRNAs as biomarkers and therapeutic targets in cancer." Current opinion in pharmacology **10**(5): 543-550.
Horoszewicz, J. S., S. S. Leong, T. M. Chu, Z. L. Wajsman, M. Friedman, L. Papsidero, U. Kim, L. S. Chai, S. Kakati, S. K. Arya and A. A. Sandberg (1980). "The LNCaP cell line--a new model for studies on human prostatic carcinoma." Prog Clin Biol Res **37**: 115-132.
Horoszewicz, J. S., S. S. Leong, E. Kawinski, J. P. Karr, H. Rosenthal, T. M. Chu, E. A. Mirand and G. P. Murphy (1983). "LNCaP model of human prostatic carcinoma." Cancer Res **43**(4): 1809-1818.
Hoskin, P., O. Sartor, J. M. O'Sullivan, D. C. Johannessen, S. I. Helle, J. Logue, D. Bottomley, S. Nilsson, N. J. Vogelzang, F. Fang, M. Wahba, A. K. Aksnes and C. Parker (2014). "Efficacy and safety of radium-223 dichloride in patients with castration-resistant prostate cancer and symptomatic bone metastases, with or without previous docetaxel use: a prespecified subgroup analysis from the randomised, double-blind, phase 3 ALSYMPCA trial." Lancet Oncol **15**(12): 1397-1406.
Howlader N, N. A., Krapcho M, Garshell J, Miller D, Altekruse SF, Kosary CL, Yu M, Ruhl J, Tatalovich Z, Mariotto A, Lewis DR, Chen HS, Feuer EJ, Cronin KA (eds). (2014). "SEER Cancer Statistics Review, 1975-2011,." September 10, 2014., from http://seer.cancer.gov/csr/1975_2011/.
Hsiao, A. F., M. D. Wong, M. F. Miller, A. H. Ambs, M. S. Goldstein, A. Smith, R. Ballard-Barbash, L. S. Becerra, E. M. Cheng and N. S. Wenger (2008). "Role of religiosity and spirituality in complementary and alternative medicine use among cancer survivors in California." Integr Cancer Ther **7**(3): 139-146.
Hsu, S. D., Y. T. Tseng, S. Shrestha, Y. L. Lin, A. Khaleel, C. H. Chou, C. F. Chu, H. Y. Huang, C. M. Lin, S. Y. Ho, T. Y. Jian, F. M. Lin, T. H. Chang, S. L. Weng, K. W. Liao, I. E. Liao, C. C. Liu and H. D. Huang (2014). "miRTarBase update 2014: an information resource for experimentally validated miRNA-target interactions." Nucleic Acids Res **42**(Database issue): D78-85.
Hyun, D. H., S. Jeong, J. W. Lee, B. J. Jeong, S. T. Ryu, C. K. Lee, M. S. Kim, K. S. Kwon, D. H. Lee, P. S. Kim, H. G. Kim, Y. W. Shin and Y. S. Kim (2003). "[Usefulness of endoscopic mucosal resection for curative treatment of early gastric cancer]." Korean J Gastroenterol **42**(6): 453-460.
Iguchi, H., N. Kosaka and T. Ochiya (2010). "Secretory microRNAs as a versatile communication tool." Communicative & integrative biology **3**(5): 478-481.
Imberg-Kazdan, K., S. Ha, A. Greenfield, C. S. Poultney, R. Bonneau, S. K. Logan and M. J. Garabedian (2013). "A genome-wide RNA interference screen identifies new regulators of androgen receptor function in prostate cancer cells." Genome Res **23**(4): 581-591.
Isakoff, M. S., C. G. Sansam, P. Tamayo, A. Subramanian, J. A. Evans, C. M. Fillmore, X. Wang, J. A. Biegel, S. L. Pomeroy, J. P. Mesirov and C. W. Roberts (2005). "Inactivation of the Snf5 tumor suppressor stimulates cell cycle progression and cooperates with p53 loss in oncogenic transformation." Proc Natl Acad Sci U S A **102**(49): 17745-17750.

Italiano, A., C. Ortholan, S. Oudard, D. Pouessel, G. Gravis, P. Beuzeboc, E. Bompas, A. Flechon, F. Joly, J. M. Ferrero and K. Fizazi (2009). "Docetaxel-based chemotherapy in elderly patients (age 75 and older) with castration-resistant prostate cancer." Eur Urol **55**(6): 1368-1375.
James, N. D., M. R. Sydes, N. W. Clarke, M. D. Mason, D. P. Dearnaley, M. R. Spears, A. W. Ritchie, C. C. Parker, J. M. Russell, G. Attard, J. de Bono, W. Cross, R. J. Jones, G. Thalmann, C. Amos, D. Matheson, R. Millman, M. Alzouebi, S. Beesley, A. J. Birtle, S. Brock, R. Cathomas, P. Chakraborti, S. Chowdhury, A. Cook, T. Elliott, J. Gale, S. Gibbs, J. D. Graham, J. Hetherington, R. Hughes, R. Laing, F. McKinna, D. B. McLaren, J. M. O'Sullivan, O. Parikh, C. Peedell, A. Protheroe, A. J. Robinson, N. Srihari, R. Srinivasan, J. Staffurth, S. Sundar, S. Tolan, D. Tsang, J. Wagstaff and M. K. Parmar (2015). "Addition of docetaxel, zoledronic acid, or both to first-line long-term hormone therapy in prostate cancer (STAMPEDE): survival results from an adaptive, multiarm, multistage, platform randomised controlled trial." Lancet.
Janik, P., P. Briand and N. R. Hartmann (1975). "The effect of estrone-progesterone treatment on cell proliferation kinetics of hormone-dependent GR mouse mammary tumors." Cancer Res **35**(12): 3698-3704.
Jansen, F. H., M. Roobol, G. Jenster, F. H. Schroder and C. H. Bangma (2009). "Screening for prostate cancer in 2008 II: the importance of molecular subforms of prostate-specific antigen and tissue kallikreins." Eur Urol **55**(3): 563-574.
Jemal, A., R. Siegel, J. Xu and E. Ward (2010). "Cancer statistics, 2010." CA Cancer J Clin **60**(5): 277-300.
Jupe, E. R., X. T. Liu, J. L. Kiehlbauch, J. K. McClung and R. T. Dell'Orco (1996). "Prohibitin in breast cancer cell lines: loss of antiproliferative activity is linked to 3' untranslated region mutations." Cell growth & differentiation : the molecular biology journal of the American Association for Cancer Research **7**(7): 871-878.
Kaighn, M. E., J. F. Lechner, K. S. Narayan and L. W. Jones (1978). "Prostate carcinoma: tissue culture cell lines." Natl Cancer Inst Monogr(49): 17-21.
Kamanu, T. K., A. Radovanovic, J. A. Archer and V. B. Bajic (2013). "Exploration of miRNA families for hypotheses generation." Sci Rep **3**: 2940.
Kane, C. J., W. W. Bassett, N. Sadetsky, S. Silva, K. Wallace, D. J. Pasta, M. R. Cooperberg, J. M. Chan and P. R. Carroll (2005). "Obesity and prostate cancer clinical risk factors at presentation: data from CaPSURE." J Urol **173**(3): 732-736.
Kang, X., L. Zhang, J. Sun, Z. Ni, Y. Ma, X. Chen, X. Sheng and T. Chen (2008). "Prohibitin: a potential biomarker for tissue-based detection of gastric cancer." J Gastroenterol **43**(8): 618-625.
Kantoff, P. W., C. S. Higano, N. D. Shore, E. R. Berger, E. J. Small, D. F. Penson, C. H. Redfern, A. C. Ferrari, R. Dreicer, R. B. Sims, Y. Xu, M. W. Frohlich and P. F. Schellhammer (2010). "Sipuleucel-T immunotherapy for castration-resistant prostate cancer." N Engl J Med **363**(5): 411-422.
Kasashima, K., M. Sumitani, M. Satoh and H. Endo (2008). "Human prohibitin 1 maintains the organization and stability of the mitochondrial nucleoids." Exp Cell Res **314**(5): 988-996.
Kelavkar, U. P., N. S. Harya, J. Hutzley, D. J. Bacich, F. A. Monzon, U. Chandran, R. Dhir and D. S. O'Keefe (2007). "DNA methylation paradigm shift: 15-lipoxygenase-1 upregulation in prostatic intraepithelial neoplasia and prostate cancer by atypical promoter hypermethylation." Prostaglandins Other Lipid Mediat **82**(1-4): 185-197.

Kent, W. J., C. W. Sugnet, T. S. Furey, K. M. Roskin, T. H. Pringle, A. M. Zahler and D. Haussler (2002). "The human genome browser at UCSC." Genome Res **12**(6): 996-1006.
Khorasanizadeh, S. and F. Rastinejad (2001). "Nuclear-receptor interactions on DNA-response elements." Trends Biochem Sci **26**(6): 384-390.
Kolonin, M. G., P. K. Saha, L. Chan, R. Pasqualini and W. Arap (2004). "Reversal of obesity by targeted ablation of adipose tissue." Nat Med **10**(6): 625-632.
Korenchuk, S., J. E. Lehr, M. C. L, Y. G. Lee, S. Whitney, R. Vessella, D. L. Lin and K. J. Pienta (2001). "VCaP, a cell-based model system of human prostate cancer." In Vivo **15**(2): 163-168.
Kozomara, A. and S. Griffiths-Jones (2014). "miRBase: annotating high confidence microRNAs using deep sequencing data." Nucleic Acids Res **42**(Database issue): D68-73.
Kroh, E. M., R. K. Parkin, P. S. Mitchell and M. Tewari (2010). "Analysis of circulating microRNA biomarkers in plasma and serum using quantitative reverse transcription-PCR (qRT-PCR)." Methods **50**(4): 298-301.
Krutzfeldt, J., N. Rajewsky, R. Braich, K. G. Rajeev, T. Tuschl, M. Manoharan and M. Stoffel (2005). "Silencing of microRNAs in vivo with 'antagomirs'." Nature **438**(7068): 685-689.
Lai, E. C. (2004). "Predicting and validating microRNA targets." Genome Biol **5**(9): 115.
Lawrie, C. H., S. Gal, H. M. Dunlop, B. Pushkaran, A. P. Liggins, K. Pulford, A. H. Banham, F. Pezzella, J. Boultwood, J. S. Wainscoat, C. S. Hatton and A. L. Harris (2008). "Detection of elevated levels of tumour-associated microRNAs in serum of patients with diffuse large B-cell lymphoma." British journal of haematology **141**(5): 672-675.
Lee, R. C., R. L. Feinbaum and V. Ambros (1993). "The C. elegans heterochronic gene lin-4 encodes small RNAs with antisense complementarity to lin-14." Cell **75**(5): 843-854.
Lee, Y. G., S. Korenchuk, J. Lehr, S. Whitney, R. Vessela and K. J. Pienta (2001). "Establishment and characterization of a new human prostatic cancer cell line: DuCaP." In Vivo **15**(2): 157-162.
Lennox, K. A. and M. A. Behlke (2010). "A direct comparison of anti-microRNA oligonucleotide potency." Pharm Res **27**(9): 1788-1799.
Li, H. and R. Durbin (2009). "Fast and accurate short read alignment with Burrows-Wheeler transform." Bioinformatics **25**(14): 1754-1760.
Li, X., S. U. Mertens-Talcott, S. Zhang, K. Kim, J. Ball and S. Safe (2010). "MicroRNA-27a Indirectly Regulates Estrogen Receptor {alpha} Expression and Hormone Responsiveness in MCF-7 Breast Cancer Cells." Endocrinology **151**(6): 2462-2473.
Lin, H. M., L. Castillo, K. L. Mahon, K. Chiam, B. Y. Lee, Q. Nguyen, M. J. Boyer, M. R. Stockler, N. Pavlakis, G. Marx, G. Mallesara, H. Gurney, S. J. Clark, A. Swarbrick, R. J. Daly and L. G. Horvath (2014). "Circulating microRNAs are associated with docetaxel chemotherapy outcome in castration-resistant prostate cancer." Br J Cancer **110**(10): 2462-2471.
Lin, K., R. Lipsitz, T. Miller and S. Janakiraman (2008). "Benefits and harms of prostate-specific antigen screening for prostate cancer: an evidence update for the U.S. Preventive Services Task Force." Ann Intern Med **149**(3): 192-199.

Liu, D., Y. Lin, T. Kang, B. Huang, W. Xu, M. Garcia-Barrio, M. Olatinwo, R. Matthews, Y. E. Chen and W. E. Thompson (2012). "Mitochondrial dysfunction and adipogenic reduction by prohibitin silencing in 3T3-L1 cells." PLoS One **7**(3): e34315.
Liu, H., L. Zhu, B. Liu, L. Yang, X. Meng, W. Zhang, Y. Ma and H. Xiao (2012). "Genome-wide microRNA profiles identify miR-378 as a serum biomarker for early detection of gastric cancer." Cancer Lett **316**(2): 196-203.
Liu, T., H. Tang, Y. Lang, M. Liu and X. Li (2009). "MicroRNA-27a functions as an oncogene in gastric adenocarcinoma by targeting prohibitin." Cancer Lett **273**(2): 233-242.
Liu, X. H., A. Kirschenbaum, K. Yu, S. Yao and A. C. Levine (2005). "Cyclooxygenase-2 suppresses hypoxia-induced apoptosis via a combination of direct and indirect inhibition of p53 activity in a human prostate cancer cell line." J Biol Chem **280**(5): 3817-3823.
Liu, Y., L. Zhao, D. Li, Y. Yin, C. Y. Zhang, J. Li and Y. Zhang (2013). "Microvesicle-delivery miR-150 promotes tumorigenesis by up-regulating VEGF, and the neutralization of miR-150 attenuate tumor development." Protein Cell **4**(12): 932-941.
Lodes, M. J., M. Caraballo, D. Suciu, S. Munro, A. Kumar and B. Anderson (2009). "Detection of cancer with serum miRNAs on an oligonucleotide microarray." PLoS One **4**(7): e6229.
Lu, Y., C. D. Darne, I. C. Tan, G. Wu, N. Wilganowski, H. Robinson, A. Azhdarinia, B. Zhu, J. C. Rasmussen and E. M. Sevick-Muraca (2013). "In vivo imaging of orthotopic prostate cancer with far-red gene reporter fluorescence tomography and in vivo and ex vivo validation." J Biomed Opt **18**(10): 101305.
Lu, Y., J. Zhang, J. Dai, L. A. Dehne, A. Mizokami, Z. Yao and E. T. Keller (2004). "Osteoblasts induce prostate cancer proliferation and PSA expression through interleukin-6-mediated activation of the androgen receptor." Clin Exp Metastasis **21**(5): 399-408.
Ma, L., J. Teruya-Feldstein and R. A. Weinberg (2007). "Tumour invasion and metastasis initiated by microRNA-10b in breast cancer." Nature **449**(7163): 682-688.
Mahal, B. A., A. A. Aizer, D. R. Ziehr, A. S. Hyatt, T. K. Choueiri, J. C. Hu, K. E. Hoffman, C. J. Sweeney, C. J. Beard, A. V. D'Amico, N. E. Martin, S. P. Kim, Q. D. Trinh and P. L. Nguyen (2014). "Racial disparities in prostate cancer-specific mortality in men with low-risk prostate cancer." Clinical genitourinary cancer **12**(5): e189-195.
Mahal, B. A., A. A. Aizer, D. R. Ziehr, A. S. Hyatt, J. D. Sammon, M. Schmid, T. K. Choueiri, J. C. Hu, C. J. Sweeney, C. J. Beard, A. V. D'Amico, N. E. Martin, S. P. Kim, Q. D. Trinh and P. L. Nguyen (2014). "Trends in disparate treatment of African American men with localized prostate cancer across National Comprehensive Cancer Network risk groups." Urology **84**(2): 386-392.
Mahn, R., L. C. Heukamp, S. Rogenhofer, A. von Ruecker, S. C. Muller and J. Ellinger (2011). "Circulating microRNAs (miRNA) in serum of patients with prostate cancer." Urology **77**(5): 1265 e1269-1216.
Manjeshwar, S., D. E. Branam, M. R. Lerner, D. J. Brackett and E. R. Jupe (2003). "Tumor suppression by the prohibitin gene 3'untranslated region RNA in human breast cancer." Cancer Res **63**(17): 5251-5256.
May, M., N. Knoll, M. Siegsmund, D. Fahlenkamp, H. Vogler, B. Hoschke and O. Gralla (2007). "Validity of the CAPRA score to predict biochemical recurrence-free

survival after radical prostatectomy. Results from a european multicenter survey of 1,296 patients." J Urol **178**(5): 1957-1962; discussion 1962.
McClung, J. K., R. L. King, L. S. Walker, D. B. Danner, M. J. Nuell, C. A. Stewart and R. T. Dell'Orco (1992). "Expression of prohibitin, an antiproliferative protein." Experimental gerontology **27**(4): 413-417.
McGrath, M. J., L. C. Binge, A. Sriratana, H. Wang, P. A. Robinson, D. Pook, C. G. Fedele, S. Brown, J. M. Dyson, D. L. Cottle, B. S. Cowling, B. Niranjan, G. P. Risbridger and C. A. Mitchell (2013). "Regulation of the transcriptional coactivator FHL2 licenses activation of the androgen receptor in castrate-resistant prostate cancer." Cancer Res **73**(16): 5066-5079.
McIntosh, H. (1997). "Why do African-American men suffer more prostate cancer?" J Natl Cancer Inst **89**(3): 188-189.
McKenna, N. J., R. B. Lanz and B. W. O'Malley (1999). "Nuclear receptor coregulators: cellular and molecular biology." Endocr Rev **20**(3): 321-344.
McKenna, N. J., J. Xu, Z. Nawaz, S. Y. Tsai, M. J. Tsai and B. W. O'Malley (1999). "Nuclear receptor coactivators: multiple enzymes, multiple complexes, multiple functions." J Steroid Biochem Mol Biol **69**(1-6): 3-12.
Meister, J. and M. H. Schmidt (2010). "miR-126 and miR-126*: new players in cancer." ScientificWorldJournal **10**: 2090-2100.
Meltzer, P. S. (2005). "Cancer genomics: small RNAs with big impacts." Nature **435**(7043): 745-746.
Mestdagh, P., N. Hartmann, L. Baeriswyl, D. Andreasen, N. Bernard, C. Chen, D. Cheo, P. D'Andrade, M. DeMayo, L. Dennis, S. Derveaux, Y. Feng, S. Fulmer-Smentek, B. Gerstmayer, J. Gouffon, C. Grimley, E. Lader, K. Y. Lee, S. Luo, P. Mouritzen, A. Narayanan, S. Patel, S. Peiffer, S. Ruberg, G. Schroth, D. Schuster, J. M. Shaffer, E. J. Shelton, S. Silveria, U. Ulmanella, V. Veeramachaneni, F. Staedtler, T. Peters, T. Guettouche, L. Wong and J. Vandesompele (2014). "Evaluation of quantitative miRNA expression platforms in the microRNA quality control (miRQC) study." Nat Methods **11**(8): 809-815.
Mishra, S., S. Moulik and L. J. Murphy (2007). "Prohibitin binds to C3 and enhances complement activation." Mol Immunol **44**(8): 1897-1902.
Mishra, S., L. C. Murphy, B. L. Nyomba and L. J. Murphy (2005). "Prohibitin: a potential target for new therapeutics." Trends Mol Med **11**(4): 192-197.
Mitchell, D. M., R. Swindell, T. Elliott, J. P. Wylie, C. M. Taylor and J. P. Logue (2008). "Analysis of prostate-specific antigen bounce after I(125) permanent seed implant for localised prostate cancer." Radiotherapy and oncology : journal of the European Society for Therapeutic Radiology and Oncology **88**(1): 102-107.
Mitchell, P. S., R. K. Parkin, E. M. Kroh, B. R. Fritz, S. K. Wyman, E. L. Pogosova-Agadjanyan, A. Peterson, J. Noteboom, K. C. O'Briant, A. Allen, D. W. Lin, N. Urban, C. W. Drescher, B. S. Knudsen, D. L. Stirewalt, R. Gentleman, R. L. Vessella, P. S. Nelson, D. B. Martin and M. Tewari (2008). "Circulating microRNAs as stable blood-based markers for cancer detection." Proceedings of the National Academy of Sciences of the United States of America **105**(30): 10513-10518.
Mitchell, P. S., R. K. Parkin, E. M. Kroh, B. R. Fritz, S. K. Wyman, E. L. Pogosova-Agadjanyan, A. Peterson, J. Noteboom, K. C. O'Briant, A. Allen, D. W. Lin, N. Urban, C. W. Drescher, B. S. Knudsen, D. L. Stirewalt, R. Gentleman, R. L. Vessella, P. S. Nelson, D. B. Martin and M. Tewari (2008). "Circulating microRNAs as stable blood-based markers for cancer detection." Proc Natl Acad Sci U S A **105**(30): 10513-10518.

Mitry, E., A. Lievre, J. B. Bachet and P. Rougier (2009). "Irinotecan as palliative chemotherapy for metastatic colorectal cancer: evolving tactics following initial treatment." Int J Colorectal Dis **24**(6): 605-612.
Mok, T. S., Y. L. Wu, S. Thongprasert, C. H. Yang, D. T. Chu, N. Saijo, P. Sunpaweravong, B. Han, B. Margono, Y. Ichinose, Y. Nishiwaki, Y. Ohe, J. J. Yang, B. Chewaskulyong, H. Jiang, E. L. Duffield, C. L. Watkins, A. A. Armour and M. Fukuoka (2009). "Gefitinib or carboplatin-paclitaxel in pulmonary adenocarcinoma." N Engl J Med **361**(10): 947-957.
Molife, L. R., G. Attard, P. C. Fong, V. Karavasilis, A. H. Reid, S. Patterson, C. E. Riggs, Jr., C. Higano, W. M. Stadler, W. McCulloch, D. Dearnaley, C. Parker and J. S. de Bono (2010). "Phase II, two-stage, single-arm trial of the histone deacetylase inhibitor (HDACi) romidepsin in metastatic castration-resistant prostate cancer (CRPC)." Ann Oncol **21**(1): 109-113.
Moltzahn, F., A. B. Olshen, L. Baehner, A. Peek, L. Fong, H. Stoppler, J. Simko, J. F. Hilton, P. Carroll and R. Blelloch (2011). "Microfluidic-based multiplex qRT-PCR identifies diagnostic and prognostic microRNA signatures in the sera of prostate cancer patients." Cancer research **71**(2): 550-560.
Montironi, R., L. Cheng, A. Lopez-Beltran, R. Mazzucchelli, M. Scarpelli and P. H. Bartels (2009). "Decision support systems for morphology-based diagnosis and prognosis of prostate neoplasms: a methodological approach." Cancer **115**(13 Suppl): 3068-3077.
Mootha, V. K., P. Lepage, K. Miller, J. Bunkenborg, M. Reich, M. Hjerrild, T. Delmonte, A. Villeneuve, R. Sladek, F. Xu, G. A. Mitchell, C. Morin, M. Mann, T. J. Hudson, B. Robinson, J. D. Rioux and E. S. Lander (2003). "Identification of a gene causing human cytochrome c oxidase deficiency by integrative genomics." Proc Natl Acad Sci U S A **100**(2): 605-610.
Nana-Sinkam, S. P. and C. M. Croce (2011). "MicroRNAs as therapeutic targets in cancer." Transl Res **157**(4): 216-225.
Nana-Sinkam, S. P. and C. M. Croce (2011). "Non-coding RNAs in cancer initiation and progression and as novel biomarkers." Mol Oncol **5**(6): 483-491.
Nguyen, H. C., W. Xie, M. Yang, C. L. Hsieh, S. Drouin, G. S. Lee and P. W. Kantoff (2013). "Expression differences of circulating microRNAs in metastatic castration resistant prostate cancer and low-risk, localized prostate cancer." Prostate **73**(4): 346-354.
Nijtmans, L. G., S. M. Artal, L. A. Grivell and P. J. Coates (2002). "The mitochondrial PHB complex: roles in mitochondrial respiratory complex assembly, ageing and degenerative disease." Cellular and molecular life sciences : CMLS **59**(1): 143-155.
Nijtmans, L. G., L. de Jong, M. Artal Sanz, P. J. Coates, J. A. Berden, J. W. Back, A. O. Muijsers, H. van der Spek and L. A. Grivell (2000). "Prohibitins act as a membrane-bound chaperone for the stabilization of mitochondrial proteins." EMBO J **19**(11): 2444-2451.
Nishi, H., K. Ono, T. Horie, K. Nagao, M. Kinoshita, Y. Kuwabara, S. Watanabe, T. Takaya, Y. Tamaki, R. Takanabe-Mori, H. Wada, K. Hasegawa, Y. Iwanaga, T. Kawamura, T. Kita and T. Kimura (2011). "MicroRNA-27a regulates beta cardiac myosin heavy chain gene expression by targeting thyroid hormone receptor beta1 in neonatal rat ventricular myocytes." Mol Cell Biol **31**(4): 744-755.

O'Hair, D., M. M. Villagran, E. Wittenberg, K. Brown, M. Ferguson, H. T. Hall and T. Doty (2003). "Cancer survivorship and agency model: implications for patient choice, decision making, and influence." Health Commun **15**(2): 193-202.
Odin, E., Y. Wettergren, G. Carlsson, P. V. Danenberg, A. Termini, R. Willen and B. Gustavsson (2006). "Expression and clinical significance of methylenetetrahydrofolate reductase in patients with colorectal cancer." Clin Colorectal Cancer **5**(5): 344-349.
Oh, W. K. (2002). "Secondary hormonal therapies in the treatment of prostate cancer." Urology **60**(3 Suppl 1): 87-92; discussion 93.
Osborne, J. R., D. A. Green, D. E. Spratt, S. Lyashchenko, S. B. Fareedy, B. D. Robinson, B. J. Beattie, M. Jain, J. S. Lewis, P. Christos, S. M. Larson, N. H. Bander and D. S. Scherr (2014). "A prospective pilot study of (89)Zr-J591/prostate specific membrane antigen positron emission tomography in men with localized prostate cancer undergoing radical prostatectomy." J Urol **191**(5): 1439-1445.
Paez, J. G., P. A. Janne, J. C. Lee, S. Tracy, H. Greulich, S. Gabriel, P. Herman, F. J. Kaye, N. Lindeman, T. J. Boggon, K. Naoki, H. Sasaki, Y. Fujii, M. J. Eck, W. R. Sellers, B. E. Johnson and M. Meyerson (2004). "EGFR mutations in lung cancer: correlation with clinical response to gefitinib therapy." Science **304**(5676): 1497-1500.
Parekh, D. J., D. P. Ankerst, B. A. Higgins, J. Hernandez, E. Canby-Hagino, T. Brand, D. A. Troyer, R. J. Leach and I. M. Thompson (2006). "External validation of the Prostate Cancer Prevention Trial risk calculator in a screened population." Urology **68**(6): 1152-1155.
Parr, R. L., J. Mills, A. Harbottle, J. M. Creed, G. Crewdson, B. Reguly and F. S. Guimont (2013). "Mitochondria, prostate cancer, and biopsy sampling error." Discov Med **15**(83): 213-220.
Perlmutter, M. A. and H. Lepor (2007). "Androgen deprivation therapy in the treatment of advanced prostate cancer." Rev Urol **9 Suppl 1**: S3-8.
Pierorazio, P. M., P. C. Walsh, A. W. Partin and J. I. Epstein (2013). "Prognostic Gleason grade grouping: data based on the modified Gleason scoring system." BJU Int **111**(5): 753-760.
Pigati, L., S. C. Yaddanapudi, R. Iyengar, D. J. Kim, S. A. Hearn, D. Danforth, M. L. Hastings and D. M. Duelli (2010). "Selective release of microRNA species from normal and malignant mammary epithelial cells." PLoS One **5**(10): e13515.
Porkka, K. P., M. J. Pfeiffer, K. K. Waltering, R. L. Vessella, T. L. Tammela and T. Visakorpi (2007). "MicroRNA expression profiling in prostate cancer." Cancer Res **67**(13): 6130-6135.
Portal, M. M. (2011). "MicroRNA-27a regulates basal transcription by targeting the p44 subunit of general transcription factor IIH." Proc Natl Acad Sci U S A **108**(21): 8686-8691.
Puttini, S., R. W. van Zwieten, D. Saugy, M. Lekka, F. Hogger, D. Ley, A. J. Kulik and N. Mermod (2013). "MAR-mediated integration of plasmid vectors for in vivo gene transfer and regulation." BMC Mol Biol **14**: 26.
Pyfferoen, L., P. Mestdagh, K. Vergote, N. De Cabooter, J. Vandesompele, B. N. Lambrecht and K. Y. Vermaelen (2014). "Lung tumours reprogram pulmonary dendritic cell immunogenicity at the microRNA level." Int J Cancer **135**(12): 2868-2877.
Qi, L., J. Bart, L. P. Tan, I. Platteel, T. Sluis, S. Huitema, G. Harms, L. Fu, H. Hollema and A. Berg (2009). "Expression of miR-21 and its targets (PTEN, PDCD4,

TM1) in flat epithelial atypia of the breast in relation to ductal carcinoma in situ and invasive carcinoma." BMC Cancer **9**: 163.
Rajalingam, K., C. Wunder, V. Brinkmann, Y. Churin, M. Hekman, C. Sievers, U. R. Rapp and T. Rudel (2005). "Prohibitin is required for Ras-induced Raf-MEK-ERK activation and epithelial cell migration." Nat Cell Biol **7**(8): 837-843.
Raoul, J. L., J. L. Van Laethem, M. Peeters, C. Brezault, F. Husseini, L. Cals, J. Nippgen, A. H. Loos and P. Rougier (2009). "Cetuximab in combination with irinotecan/5-fluorouracil/folinic acid (FOLFIRI) in the initial treatment of metastatic colorectal cancer: a multicentre two-part phase I/II study." BMC Cancer **9**: 112.
Rastinejad, F., T. Perlmann, R. M. Evans and P. B. Sigler (1995). "Structural determinants of nuclear receptor assembly on DNA direct repeats." Nature **375**(6528): 203-211.
Ray, H. N., V. K. Mootha and A. A. Boxwala (2003). "Building an application framework for integrative genomics." AMIA Annu Symp Proc: 981.
Raymond, E., S. Faivre and J. P. Armand (2000). "Epidermal growth factor receptor tyrosine kinase as a target for anticancer therapy." Drugs **60 Suppl 1**: 15-23; discussion 41-12.
Ren, H. Z., J. S. Wang, P. Wang, G. Q. Pan, J. F. Wen, H. Fu and X. Z. Shan (2010). "Increased expression of prohibitin and its relationship with poor prognosis in esophageal squamous cell carcinoma." Pathol Oncol Res **16**(4): 515-522.
Rhim, J. S., M. M. Webber, D. Bello, M. S. Lee, P. Arnstein, L. S. Chen and G. Jay (1994). "Stepwise immortalization and transformation of adult human prostate epithelial cells by a combination of HPV-18 and v-Ki-ras." Proc Natl Acad Sci U S A **91**(25): 11874-11878.
Robinson, K., J. Creed, B. Reguly, C. Powell, R. Wittock, D. Klein, A. Maggrah, L. Klotz, R. L. Parr and G. D. Dakubo (2010). "Accurate prediction of repeat prostate biopsy outcomes by a mitochondrial DNA deletion assay." Prostate Cancer Prostatic Dis **13**(2): 126-131.
Robinson, M. D., D. J. McCarthy and G. K. Smyth (2010). "edgeR: a Bioconductor package for differential expression analysis of digital gene expression data." Bioinformatics **26**(1): 139-140.
Ryan, C. J., M. R. Smith, K. Fizazi, F. Saad, P. F. Mulders, C. N. Sternberg, K. Miller, C. J. Logothetis, N. D. Shore, E. J. Small, J. Carles, T. W. Flaig, M. E. Taplin, C. S. Higano, P. de Souza, J. S. de Bono, T. W. Griffin, P. De Porre, M. K. Yu, Y. C. Park, J. Li, T. Kheoh, V. Naini, A. Molina and D. E. Rathkopf (2015). "Abiraterone acetate plus prednisone versus placebo plus prednisone in chemotherapy-naive men with metastatic castration-resistant prostate cancer (COU-AA-302): final overall survival analysis of a randomised, double-blind, placebo-controlled phase 3 study." Lancet Oncol **16**(2): 152-160.
Ryu, J. W., H. J. Kim, Y. S. Lee, N. H. Myong, C. H. Hwang, G. S. Lee and H. C. Yom (2003). "The proteomics approach to find biomarkers in gastric cancer." J Korean Med Sci **18**(4): 505-509.
Saad, F., S. Hotte, S. North, B. Eigl, K. Chi, P. Czaykowski, L. Wood, M. Pollak, S. Berry, J. B. Lattouf, S. D. Mukherjee, M. Gleave and E. Winquist (2011). "Randomized phase II trial of Custirsen (OGX-011) in combination with docetaxel or mitoxantrone as second-line therapy in patients with metastatic castrate-resistant prostate cancer progressing after first-line docetaxel: CUOG trial P-06c." Clinical cancer research : an official journal of the American Association for Cancer Research **17**(17): 5765-5773.

Salami, S. S., F. Schmidt, B. Laxman, M. M. Regan, D. S. Rickman, D. Scherr, G. Bueti, J. Siddiqui, S. A. Tomlins, J. T. Wei, A. M. Chinnaiyan, M. A. Rubin and M. G. Sanda (2013). "Combining urinary detection of TMPRSS2:ERG and PCA3 with serum PSA to predict diagnosis of prostate cancer." Urologic oncology **31**(5): 566-571.
Sato, T., H. Saito, J. Swensen, A. Olifant, C. Wood, D. Danner, T. Sakamoto, K. Takita, F. Kasumi, Y. Miki and et al. (1992). "The human prohibitin gene located on chromosome 17q21 is mutated in sporadic breast cancer." Cancer Res **52**(6): 1643-1646.
Schaar, D. G., D. J. Medina, D. F. Moore, R. K. Strair and Y. Ting (2009). "miR-320 targets transferrin receptor 1 (CD71) and inhibits cell proliferation." Exp Hematol **37**(2): 245-255.
Scher, H. I., K. Fizazi, F. Saad, M. E. Taplin, C. N. Sternberg, K. Miller, R. de Wit, P. Mulders, K. N. Chi, N. D. Shore, A. J. Armstrong, T. W. Flaig, A. Flechon, P. Mainwaring, M. Fleming, J. D. Hainsworth, M. Hirmand, B. Selby, L. Seely and J. S. de Bono (2012). "Increased survival with enzalutamide in prostate cancer after chemotherapy." N Engl J Med **367**(13): 1187-1197.
Schleicher, M., B. R. Shepherd, Y. Suarez, C. Fernandez-Hernando, J. Yu, Y. Pan, L. M. Acevedo, G. S. Shadel and W. C. Sessa (2008). "Prohibitin-1 maintains the angiogenic capacity of endothelial cells by regulating mitochondrial function and senescence." J Cell Biol **180**(1): 101-112.
Schroder, F. H. (2008). "Progress in understanding androgen-independent prostate cancer (AIPC): a review of potential endocrine-mediated mechanisms." Eur Urol **53**(6): 1129-1137.
Schroder, F. H. (2009). "Review of diagnostic markers for prostate cancer." Recent Results Cancer Res **181**: 173-182.
Schroder, F. H., J. Hugosson, M. J. Roobol, T. L. Tammela, S. Ciatto, V. Nelen, M. Kwiatkowski, M. Lujan, H. Lilja, M. Zappa, L. J. Denis, F. Recker, A. Berenguer, L. Maattanen, C. H. Bangma, G. Aus, A. Villers, X. Rebillard, T. van der Kwast, B. G. Blijenberg, S. M. Moss, H. J. de Koning and A. Auvinen (2009). "Screening and prostate-cancer mortality in a randomized European study." N Engl J Med **360**(13): 1320-1328.
Schroder, F. H. and M. J. Roobol (2009). "Defining the optimal prostate-specific antigen threshold for the diagnosis of prostate cancer." Current opinion in urology **19**(3): 227-231.
Selth, L. A., S. Townley, J. L. Gillis, A. M. Ochnik, K. Murti, R. J. Macfarlane, K. N. Chi, V. R. Marshall, W. D. Tilley and L. M. Butler (2012). "Discovery of circulating microRNAs associated with human prostate cancer using a mouse model of disease." International journal of cancer. Journal international du cancer **131**(3): 652-661.
Shang, Y., M. Myers and M. Brown (2002). "Formation of the androgen receptor transcription complex." Mol Cell **9**(3): 601-610.
Sheedy, F. J. and L. A. O'Neill (2008). "Adding fuel to fire: microRNAs as a new class of mediators of inflammation." Ann Rheum Dis **67 Suppl 3**: iii50-55.
Shen, H., G. Ding, Y. Wu, G. Pan, X. Zhou, J. Han, J. Li and S. Wen (2012). "Polychlorinated dibenzo-p-dioxins/furans (PCDD/Fs), polychlorinated biphenyls (PCBs), and polybrominated diphenyl ethers (PBDEs) in breast milk from Zhejiang, China." Environ Int **42**: 84-90.

Shen, J., G. W. Hruby, J. M. McKiernan, I. Gurvich, M. J. Lipsky, M. C. Benson and R. M. Santella (2012). "Dysregulation of circulating microRNAs and prediction of aggressive prostate cancer." The Prostate.
Shen, M. M. and C. Abate-Shen (2010). "Molecular genetics of prostate cancer: new prospects for old challenges." Genes Dev **24**(18): 1967-2000.
Siegel, R., D. Naishadham and A. Jemal (2012). "Cancer statistics, 2012." CA Cancer J Clin **62**(1): 10-29.
Smith, M. R., F. Saad, R. Coleman, N. Shore, K. Fizazi, B. Tombal, K. Miller, P. Sieber, L. Karsh, R. Damiao, T. L. Tammela, B. Egerdie, H. Van Poppel, J. Chin, J. Morote, F. Gomez-Veiga, T. Borkowski, Z. Ye, A. Kupic, R. Dansey and C. Goessl (2012). "Denosumab and bone-metastasis-free survival in men with castration-resistant prostate cancer: results of a phase 3, randomised, placebo-controlled trial." Lancet **379**(9810): 39-46.
Sobel, R. E. and M. D. Sadar (2005). "Cell lines used in prostate cancer research: a compendium of old and new lines--part 1." J Urol **173**(2): 342-359.
Sobel, R. E. and M. D. Sadar (2005). "Cell lines used in prostate cancer research: a compendium of old and new lines--part 2." J Urol **173**(2): 360-372.
Sonkoly, E., M. Stahle and A. Pivarcsi (2008). "MicroRNAs and immunity: novel players in the regulation of normal immune function and inflammation." Semin Cancer Biol **18**(2): 131-140.
Stone, K. R., D. D. Mickey, H. Wunderli, G. H. Mickey and D. F. Paulson (1978). "Isolation of a human prostate carcinoma cell line (DU 145)." Int J Cancer **21**(3): 274-281.
Subramanian, A., P. Tamayo, V. K. Mootha, S. Mukherjee, B. L. Ebert, M. A. Gillette, A. Paulovich, S. L. Pomeroy, T. R. Golub, E. S. Lander and J. P. Mesirov (2005). "Gene set enrichment analysis: a knowledge-based approach for interpreting genome-wide expression profiles." Proc Natl Acad Sci U S A **102**(43): 15545-15550.
Subramanian, C., A. W. Opipari, Jr., X. Bian, V. P. Castle and R. P. Kwok (2005). "Ku70 acetylation mediates neuroblastoma cell death induced by histone deacetylase inhibitors." Proc Natl Acad Sci U S A **102**(13): 4842-4847.
Sun, Q., H. Gu, Y. Zeng, Y. Xia, Y. Wang, Y. Jing, L. Yang and B. Wang (2010). "Hsa-mir-27a genetic variant contributes to gastric cancer susceptibility through affecting miR-27a and target gene expression." Cancer Sci **101**(10): 2241-2247.
Sweeney, C. J., Y. H. Chen, M. Carducci, G. Liu, D. F. Jarrard, M. Eisenberger, Y. N. Wong, N. Hahn, M. Kohli, M. M. Cooney, R. Dreicer, N. J. Vogelzang, J. Picus, D. Shevrin, M. Hussain, J. A. Garcia and R. S. DiPaola (2015). "Chemohormonal Therapy in Metastatic Hormone-Sensitive Prostate Cancer." N Engl J Med **373**(8): 737-746.
Szafranska-Schwarzbach, A. E., A. T. Adai, L. S. Lee, D. L. Conwell and B. F. Andruss (2011). "Development of a miRNA-based diagnostic assay for pancreatic ductal adenocarcinoma." Expert review of molecular diagnostics **11**(3): 249-257.
Tardif, G., D. Hum, J. P. Pelletier, N. Duval and J. Martel-Pelletier (2009). "Regulation of the IGFBP-5 and MMP-13 genes by the microRNAs miR-140 and miR-27a in human osteoarthritic chondrocytes." BMC Musculoskelet Disord **10**: 148.
Taylor, D. D. and C. Gercel-Taylor (2008). "MicroRNA signatures of tumor-derived exosomes as diagnostic biomarkers of ovarian cancer." Gynecol Oncol **110**(1): 13-21.

Terashima, M., K. M. Kim, T. Adachi, P. J. Nielsen, M. Reth, G. Kohler and M. C. Lamers (1994). "The IgM antigen receptor of B lymphocytes is associated with prohibitin and a prohibitin-related protein." EMBO J **13**(16): 3782-3792.
Thalmann, G. N., P. E. Anezinis, S. M. Chang, H. E. Zhau, E. E. Kim, V. L. Hopwood, S. Pathak, A. C. von Eschenbach and L. W. Chung (1994). "Androgen-independent cancer progression and bone metastasis in the LNCaP model of human prostate cancer." Cancer Res **54**(10): 2577-2581.
Theiss, A. L., R. D. Idell, S. Srinivasan, J. M. Klapproth, D. P. Jones, D. Merlin and S. V. Sitaraman (2007). "Prohibitin protects against oxidative stress in intestinal epithelial cells." FASEB J **21**(1): 197-206.
Theiss, A. L. and S. V. Sitaraman (2011). "The role and therapeutic potential of prohibitin in disease." Biochim Biophys Acta **1813**(6): 1137-1143.
Thompson, I. M., D. P. Ankerst, C. Chi, P. J. Goodman, C. M. Tangen, M. S. Lucia, Z. Feng, H. L. Parnes and C. A. Coltman, Jr. (2006). "Assessing prostate cancer risk: results from the Prostate Cancer Prevention Trial." J Natl Cancer Inst **98**(8): 529-534.
Thompson, I. M., C. Chi, D. P. Ankerst, P. J. Goodman, C. M. Tangen, S. M. Lippman, M. S. Lucia, H. L. Parnes and C. A. Coltman, Jr. (2006). "Effect of finasteride on the sensitivity of PSA for detecting prostate cancer." J Natl Cancer Inst **98**(16): 1128-1133.
Tomasetti, M., S. Staffolani, L. Nocchi, J. Neuzil, E. Strafella, N. Manzella, L. Mariotti, M. Bracci, M. Valentino, M. Amati and L. Santarelli (2012). "Clinical significance of circulating miR-126 quantification in malignant mesothelioma patients." Clin Biochem **45**(7-8): 575-581.
Tomlins, S. A., S. M. Aubin, J. Siddiqui, R. J. Lonigro, L. Sefton-Miller, S. Miick, S. Williamsen, P. Hodge, J. Meinke, A. Blase, Y. Penabella, J. R. Day, R. Varambally, B. Han, D. Wood, L. Wang, M. G. Sanda, M. A. Rubin, D. R. Rhodes, B. Hollenbeck, K. Sakamoto, J. L. Silberstein, Y. Fradet, J. B. Amberson, S. Meyers, N. Palanisamy, H. Rittenhouse, J. T. Wei, J. Groskopf and A. M. Chinnaiyan (2011). "Urine TMPRSS2:ERG fusion transcript stratifies prostate cancer risk in men with elevated serum PSA." Sci Transl Med **3**(94): 94ra72.
Tong, A. W., P. Fulgham, C. Jay, P. Chen, I. Khalil, S. Liu, N. Senzer, A. C. Eklund, J. Han and J. Nemunaitis (2009). "MicroRNA profile analysis of human prostate cancers." Cancer Gene Ther **16**(3): 206-216.
Torjesen, P. A. and L. Sandnes (2004). "Serum testosterone in women as measured by an automated immunoassay and a RIA." Clin Chem **50**(3): 678; author reply 678-679.
Torres, A. G., M. M. Fabani, E. Vigorito and M. J. Gait (2011). "MicroRNA fate upon targeting with anti-miRNA oligonucleotides as revealed by an improved Northern-blot-based method for miRNA detection." RNA **17**(5): 933-943.
Tsai, H. W., N. H. Chow, C. P. Lin, S. H. Chan, C. Y. Chou and C. L. Ho (2006). "The significance of prohibitin and c-Met/hepatocyte growth factor receptor in the progression of cervical adenocarcinoma." Hum Pathol **37**(2): 198-204.
Tuck, M. K., D. W. Chan, D. Chia, A. K. Godwin, W. E. Grizzle, K. E. Krueger, W. Rom, M. Sanda, L. Sorbara, S. Stass, W. Wang and D. E. Brenner (2009). "Standard operating procedures for serum and plasma collection: early detection research network consensus statement standard operating procedure integration working group." J Proteome Res **8**(1): 113-117.

Van Cutsem, E., C. H. Kohne, E. Hitre, J. Zaluski, C. R. Chang Chien, A. Makhson, G. D'Haens, T. Pinter, R. Lim, G. Bodoky, J. K. Roh, G. Folprecht, P. Ruff, C. Stroh, S. Tejpar, M. Schlichting, J. Nippgen and P. Rougier (2009). "Cetuximab and chemotherapy as initial treatment for metastatic colorectal cancer." N Engl J Med **360**(14): 1408-1417.
van den Bergh, R. C., S. Roemeling, M. J. Roobol, G. Aus, J. Hugosson, A. S. Rannikko, T. L. Tammela, C. H. Bangma and F. H. Schroder (2009). "Gleason score 7 screen-detected prostate cancers initially managed expectantly: outcomes in 50 men." BJU Int **103**(11): 1472-1477.
Veldscholte, J., C. Ris-Stalpers, G. G. Kuiper, G. Jenster, C. Berrevoets, E. Claassen, H. C. van Rooij, J. Trapman, A. O. Brinkmann and E. Mulder (1990). "A mutation in the ligand binding domain of the androgen receptor of human LNCaP cells affects steroid binding characteristics and response to anti-androgens." Biochem Biophys Res Commun **173**(2): 534-540.
Vessal, M., S. Mishra, S. Moulik and L. J. Murphy (2006). "Prohibitin attenuates insulin-stimulated glucose and fatty acid oxidation in adipose tissue by inhibition of pyruvate carboxylase." FEBS J **273**(3): 568-576.
Volinia, S., G. A. Calin, C. G. Liu, S. Ambs, A. Cimmino, F. Petrocca, R. Visone, M. Iorio, C. Roldo, M. Ferracin, R. L. Prueitt, N. Yanaihara, G. Lanza, A. Scarpa, A. Vecchione, M. Negrini, C. C. Harris and C. M. Croce (2006). "A microRNA expression signature of human solid tumors defines cancer gene targets." Proc Natl Acad Sci U S A **103**(7): 2257-2261.
Wang, B. and Q. Zhang (2012). "The expression and clinical significance of circulating microRNA-21 in serum of five solid tumors." J Cancer Res Clin Oncol **138**(10): 1659-1666.
Wang, L., C. L. Hsu and C. Chang (2005). "Androgen receptor corepressors: an overview." Prostate **63**(2): 117-130.
Wang, Q., D. C. Li, Z. F. Li, C. X. Liu, Y. M. Xiao, B. Zhang, X. D. Li, J. Zhao, L. P. Chen, X. M. Xing, S. F. Tang, Y. C. Lin, Y. D. Lai, P. Yang, J. L. Zeng, Q. Xiao, X. W. Zeng, Z. N. Lin, Z. X. Zhuang, S. M. Zhuang and W. Chen (2011). "Upregulation of miR-27a contributes to the malignant transformation of human bronchial epithelial cells induced by SV40 small T antigen." Oncogene **30**(36): 3875-3886.
Wang, S., N. Nath, M. Adlam and S. Chellappan (1999). "Prohibitin, a potential tumor suppressor, interacts with RB and regulates E2F function." Oncogene **18**(23): 3501-3510.
Wang, S., B. Zhang and D. V. Faller (2002). "Prohibitin requires Brg-1 and Brm for the repression of E2F and cell growth." EMBO J **21**(12): 3019-3028.
Wang, S., B. Zhang and D. V. Faller (2004). "BRG1/BRM and prohibitin are required for growth suppression by estrogen antagonists." EMBO J **23**(11): 2293-2303.
Watahiki, A., Y. Wang, J. Morris, K. Dennis, H. M. O'Dwyer, M. Gleave and P. W. Gout (2011). "MicroRNAs associated with metastatic prostate cancer." PLoS One **6**(9): e24950.
Wei, J., W. Gao, C. J. Zhu, Y. Q. Liu, Z. Mei, T. Cheng and Y. Q. Shu (2011). "Identification of plasma microRNA-21 as a biomarker for early detection and chemosensitivity of non-small cell lung cancer." Chin J Cancer **30**(6): 407-414.

Winter, J., S. Jung, S. Keller, R. I. Gregory and S. Diederichs (2009). "Many roads to maturity: microRNA biogenesis pathways and their regulation." Nat Cell Biol **11**(3): 228-234.
Workman, P., E. O. Aboagye, F. Balkwill, A. Balmain, G. Bruder, D. J. Chaplin, J. A. Double, J. Everitt, D. A. Farningham, M. J. Glennie, L. R. Kelland, V. Robinson, I. J. Stratford, G. M. Tozer, S. Watson, S. R. Wedge and S. A. Eccles (2010). "Guidelines for the welfare and use of animals in cancer research." Br J Cancer **102**(11): 1555-1577.
Wu, H. C., J. T. Hsieh, M. E. Gleave, N. M. Brown, S. Pathak and L. W. Chung (1994). "Derivation of androgen-independent human LNCaP prostatic cancer cell sublines: role of bone stromal cells." Int J Cancer **57**(3): 406-412.
Wu, T. F., H. Wu, Y. W. Wang, T. Y. Chang, S. H. Chan, Y. P. Lin, H. S. Liu and N. H. Chow (2007). "Prohibitin in the pathogenesis of transitional cell bladder cancer." Anticancer Res **27**(2): 895-900.
Xiang, M., Y. Zeng, R. Yang, H. Xu, Z. Chen, J. Zhong, H. Xie, Y. Xu and X. Zeng (2014). "U6 is not a suitable endogenous control for the quantification of circulating microRNAs." Biochem Biophys Res Commun **454**(1): 210-214.
Yaman Agaoglu, F., M. Kovancilar, Y. Dizdar, E. Darendeliler, S. Holdenrieder, N. Dalay and U. Gezer (2011). "Investigation of miR-21, miR-141, and miR-221 in blood circulation of patients with prostate cancer." Tumour biology : the journal of the International Society for Oncodevelopmental Biology and Medicine **32**(3): 583-588.
Yin, L. and Q. Hu (2014). "CYP17 inhibitors--abiraterone, C17,20-lyase inhibitors and multi-targeting agents." Nat Rev Urol **11**(1): 32-42.
Yu, Y. P., D. Landsittel, L. Jing, J. Nelson, B. Ren, L. Liu, C. McDonald, R. Thomas, R. Dhir, S. Finkelstein, G. Michalopoulos, M. Becich and J. H. Luo (2004). "Gene expression alterations in prostate cancer predicting tumor aggression and preceding development of malignancy." J Clin Oncol **22**(14): 2790-2799.
Zhang, H. L., L. F. Yang, Y. Zhu, X. D. Yao, S. L. Zhang, B. Dai, Y. P. Zhu, Y. J. Shen, G. H. Shi and D. W. Ye (2011). "Serum miRNA-21: elevated levels in patients with metastatic hormone-refractory prostate cancer and potential predictive factor for the efficacy of docetaxel-based chemotherapy." The Prostate **71**(3): 326-331.
Zhang, W., S. Ambati, M. A. Della-Fera, Y. H. Choi, C. A. Baile and T. M. Andacht (2011). "Leptin modulated changes in adipose tissue protein expression in ob/ob mice." Obesity (Silver Spring) **19**(2): 255-261.
Zhang, Z., S. Liu, R. Shi and G. Zhao (2011). "miR-27 promotes human gastric cancer cell metastasis by inducing epithelial-to-mesenchymal transition." Cancer Genet **204**(9): 486-491.
Zhou, J., X. Zeng, K. Zheng, X. Zhu, L. Ma, Q. Xu, X. Zhang, Y. Yu, G. Sheng and J. Fu (2012). "Musks and organochlorine pesticides in breast milk from Shanghai, China: levels, temporal trends and exposure assessment." Ecotoxicol Environ Saf **84**: 325-333.
Zhou, L., B. Yin, Y. Liu, Y. Hong, C. Zhang and J. Fan (2012). "Mechanism and function of decreased FOXO1 in renal cell carcinoma." J Surg Oncol **105**(8): 841-847.
Zhou, Q., M. Li, X. Wang, Q. Li, T. Wang, Q. Zhu, X. Zhou, X. Gao and X. Li (2012). "Immune-related microRNAs are abundant in breast milk exosomes." Int J Biol Sci **8**(1): 118-123.

Ziehr, D. R., B. A. Mahal, A. A. Aizer, A. S. Hyatt, C. J. Beard, A. V. D'Amico, T. K. Choueiri, A. Elfiky, C. S. Lathan, N. E. Martin, C. J. Sweeney, Q. D. Trinh and P. L. Nguyen (2015). "Income inequality and treatment of African American men with high-risk prostate cancer." Urologic oncology **33**(1): 18 e17-13.